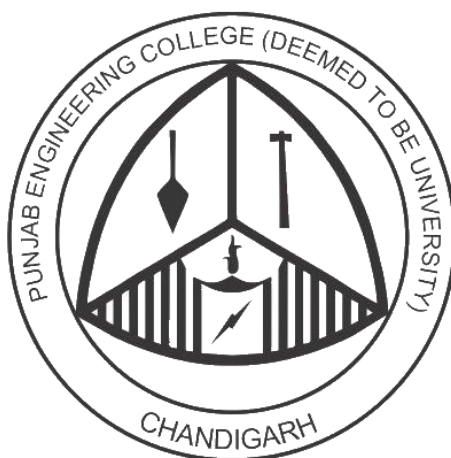


*Capstone Project Design Report on*

# Design and Analysis of Propellers for Slow-Flyer Quadcopters

**Department of Mechanical Engineering  
Punjab Engineering College (PEC), Chandigarh**



**Submitted by:**

1.	Aman Aloon	<b>16107012</b>
2.	Ashutosh Mukherjee	<b>16107042</b>
3.	Samarth Kakkar	<b>16107045</b>
4.	Aman Kumar	<b>16107056</b>
5.	Bikramjit Singh Sidhu	<b>16107066</b>
6.	Aayush Rampal	<b>16107068</b>

---

**Project Guide**

(Dr. V.P Singh)

## **DECLARATION**

We hereby certify that the work which is being presented in the major project entitled **Design and Analysis of Propellers for Slow-Flyer Quadcopters** in the partial fulfilment of the requirements for the award of the **Bachelor of Engineering** and submitted in the **Department of Mechanical Engineering** of the PEC University of Technology, Chandigarh, is an authentic record of our own work carried out during the period from **Jan 2020** to **May 2020** under the Supervision of Dr. V. P. Singh, Department of Mechanical Engineering.

Date: 30 May, 2020

This is to certify that the above statement made by the candidate is correct to the best of our knowledge.

Dr. V. P. Singh

Department of Mechanical Engineering

PEC University of Technology

Chandigarh – 160012, India

## **ACKNOWLEDGEMENT**

We deem it a pleasure to acknowledge our sense of gratitude to our project guide Dr. V. P. Singh under whom we have carried out the project work. His incisive and objective guidance and timely advice encouraged us with constant flow of energy to continue the work.

We shall remain grateful to Dr. Dheeraj Sanghi, Director, Punjab Engineering College, for providing us with a strong academic atmosphere by enforcing strict discipline to do the project work with utmost concentration and dedication.

We would like to express my sincere gratitude to the group members with whom fruitful discussions resulted in the successful completion of the project.

Finally, we must say that no height is ever achieved without some sacrifices made at some end and it is here where we owe our special debt to our parents and friends for showing their generous love and care throughout the entire period of time.

## TABLE OF CONTENTS

DECLARATION .....	II
ACKNOWLEDGEMENT .....	III
ABSTRACT.....	XIX
CHAPTER 1: Theoretical Formulation Of Propellers.....	1
1.1 Introduction .....	1
1.2 Propeller Geometry .....	1
1.3 Geometric Propeller Pitch .....	2
1.4 Pitch Angle or Geometric Pitch .....	2
1.5 Blade Element Theory.....	4
CHAPTER 2: Objectives And Details Of The Propeller Design .....	7
2.1 Shifting the efficiency curve towards left: .....	7
2.2 Ways of shifting the propeller efficiency curves to the left: .....	8
2.3 Theoretical basis for the relation between decreased pitch and increased efficiency for lower advance ratios:.....	9
CHAPTER 3: Tools Used And Design Process .....	11
3.1 QMIL:.....	11
3.2 QPROP:.....	16
3.3 PROPELLER DESIGN PROCESS .....	18
3.4 1 <sup>st</sup> Design Point: .....	20
3.5 2 <sup>nd</sup> Design Point: .....	21
3.6 3 <sup>rd</sup> Design Point:.....	24
CHAPTER 4: Airfoils Used And Their Aerodynamic Analysis .....	27
4.1 Eppeler 63: .....	28
4.2 Clark Y: .....	30
4.3 ARAD-10: .....	31

4.4 S7055.....	33
4.5. BE 50:.....	35
4.6 MH22 (7.2%): .....	36
4.7 MH30 (7.84%): .....	38
4.8 MH32 (8.7%): .....	40
4.9 MH43 (8.5%): .....	42
4.10 MH64 (8.59%): .....	43
<b>Chapter 5: 1<sup>st</sup> Design Point .....</b>	<b>46</b>
5.1 Propeller with ARAD-10 airfoil.....	46
5.2 Propeller with BE 50 airfoil .....	49
5.3 Propeller with Eppeler 63 Airfoil:.....	52
5.4 Propeller with CLARK Y Airfoil:.....	55
5.5 Propeller with MH22 (7.2%) airfoil:.....	58
5.6 Propeller with MH30 (7.84%) airfoil:.....	62
5.7 Propeller with MH32 (8.7%) airfoil:.....	65
5.8 Propeller with MH43 (8.5%) airfoil:.....	69
5.9 Propeller with MH64 (8.59%) airfoil:.....	72
5.10 Propeller with S7055 airfoil: .....	76
5.11 General Observations Regarding First Design Point: .....	79
5.12 Main Take Aways From The First Design Point .....	81
<b>CHAPTER 6: 2<sup>ND</sup> DESIGN POINT.....</b>	<b>82</b>
6.1 Explanation of the parameter modifications .....	82
1). Propeller with ARAD-10 airfoil: .....	83
2). Propeller with BE 50 airfoil:.....	85
3). Propeller with Eppeler 63 airfoil: .....	87
4). Propeller with CLARK Y airfoil: .....	89
5). Propeller with MH22 (7.2%) airfoil: .....	91

6). Propeller with MH30 (7.84%) airfoil: .....	93
7). Propeller with MH32 (8.7%) airfoil: .....	95
8). Propeller with MH43 (8.5%) airfoil: .....	97
9). Propeller with MH64 (8.59%) airfoil: .....	99
10). Propeller with S7055 airfoil:.....	101
6.2 General Observations From 2 <sup>nd</sup> Design Point:.....	103
<b>CHAPTER 7: 3<sup>rd</sup> Design Point .....</b>	<b>106</b>
1). Propeller with ARAD-10 airfoil: .....	106
2). Propeller with BE50 airfoil:.....	107
3). Propeller with Eppeler 63 airfoil: .....	108
4). Propeller with CLARK Y airfoil: .....	109
5). Propeller with MH22 (7.2%) airfoil: .....	110
6). Propeller with MH30 (7.84%) airfoil: .....	111
7). Propeller with MH32 (8.7%) airfoil: .....	112
8). Propeller with MH43 (8.5%) airfoil: .....	113
9). Propeller with MH64 (8.59%) airfoil: .....	114
10). Propeller with S7055 airfoil:.....	115
7.1 General Observations From 3 <sup>rd</sup> Design Point .....	116
<b>CHAPTER 8: Chosen Design Point and Further Modification of Design .....</b>	<b>118</b>
8.1 Thin tip propellers .....	118
1). ARAD-10 Propeller:.....	118
2). BE50 Propeller:.....	121
3) MH32 (8.7%) propeller:.....	123
8.2 Comparison of thin tip propellers: .....	126
8.3 Further Advantage of the final propeller design: .....	128
<b>CHAPTER 9: Final Propeller Design .....</b>	<b>130</b>
9.1 Geometry .....	130

9.2 CAD of the propeller.....	133
9.3 Pitch of the propeller:.....	136
<b>CHAPTER 10: Obtaining Formal Aerodynamic Performance Of The Propeller Using Computational Fluid Dynamics .....</b>	<b>137</b>
10.1 Introduction .....	137
10.2 Governing Equations.....	137
10.3 Meshing and its requirements .....	138
10.3.1 Choosing the Correct Mesh .....	138
10.3.2 Consequences of over-refined mesh.....	139
10.3.3 Comparison of Cell Types .....	140
10.4 Mesh Quality .....	141
10.4.1 Volume Based Approach.....	141
10.4.2. Angle Based approach.....	142
10.4.3 Equiangle Skewness .....	142
10.5 General Guidelines in Quality.....	144
10.5.1 Objectives of a perfect mesh .....	144
10.5.2 Sizing .....	145
10.5.3 Biasing .....	145
10.5.4 Behaviour.....	145
10.5.6 Sphere of Influence.....	146
10.5.7 Body of influence .....	146
10.5.8 Mapped Face Meshing.....	146
10.6 Turbulence Modelling .....	146
10.6.1 Introduction .....	146
10.6.2 Boussinesq Approach .....	147
10.7 Spalart Allmaras Model .....	148
10.7.1 Transport equation:.....	149

10.8 K-Epsilon Model .....	150
10.9 K-Omega Model.....	152
10.10 K-Kl-Omega Model .....	153
10.11 Transition SST Model .....	154
10.12 CFD Best Practices.....	155
10.12.1 Domain Selection .....	155
10.13 Turbulence Definition .....	159
10.14 Solver Settings.....	159
10.14.1 Initialization.....	159
10.14.2 External Flows.....	160
10.14.3 Internal rotary flows .....	160
10.15 CFD Analysis for 8x3.8 APC Propeller.....	160
10.15.1 Introduction .....	160
10.15.3 Geometry .....	161
10.15.4 Mesh .....	162
10.16 Moving Reference Frame (MRF) Approach.....	163
Results .....	166
Inferences And Conclusions.....	166
Conclusions and Inferences.....	169
CHAPTER 11: Strength Of The Propeller.....	170
REFERENCES .....	173

## LIST OF FIGURES

Figure 1 Fundamental Formulation of Propeller Rotation.....	3
Figure 2 Velocity Triangles formed underneath a propeller section .....	4
Figure 3 Thrust and Resisting torque formation in a propeller.....	5
Figure 4 Section-wise division of a propeller blade .....	6
Figure 5 General performance curves of a propeller .....	7
Figure 6 Lift and Drag polar curve fitments for calculating airfoil specific aerodynamic variables .....	12
Figure 7 Sample input file for QMIL.....	14
Figure 8 Sample output from QMIL.....	15
Figure 9 Sample detailed output from QMIL .....	16
Figure 10 Sample motor input file for QPROP .....	17
Figure 11 Sample output from QPROP .....	18
Figure 12 QPROP input file for APC 11x4.7 .....	19
Figure 13 QMIL input file for ARAD-10 .....	46
Figure 14 QMIL input file for BE 50.....	49
Figure 15 QMIL input file for Eppeler 63 .....	52
Figure 16 QMIL input file for CLARK Y .....	55
Figure 17 QMIL input file for MH22 (7.2%) .....	58
Figure 18 QMIL input file for MH30 (7.84%) .....	62
Figure 19 QMIL input file for MH32 (8.7%) .....	65
Figure 20 QMIL input file for MH43 (8.5%) .....	69
Figure 21 QMIL input file for MH64 (8.59%) .....	72
Figure 22 QMIL input file for S7055 .....	76
Figure 23 QMIL input file for ARAD-10 .....	83
Figure 24 QMIL input file for BE50.....	85
Figure 25 QMIL input file for Eppeler 63 .....	87
Figure 26 QMIL input file for CLARK Y .....	89
Figure 27 QMIL input file for MH22 (7.2%) .....	91
Figure 28 QMIL input file for MH30 (7.84%) .....	93
Figure 29 QMIL input file for MH32 (8.7%) .....	95
Figure 30 QMIL input file for MH43 (8.5%) .....	97
Figure 31 QMIL input file for MH64 (8.59%) .....	99

Figure 32 QMIL input file for S7055 .....	101
Figure 33 Orthogonal view of the propeller CAD .....	133
Figure 34 Top view of the propeller CAD.....	133
Figure 35 Top view of the propeller and propeller dimensions.....	134
Figure 36 Section AA (at the middle of the propeller blade) .....	134
Figure 37 Section BB (at the root of the propeller blade).....	135
Figure 38 Section CC (at the tip of the propeller blade).....	135
Figure 39 Side profile of the propeller.....	135
Figure 40 General procedure for any computer simulation .....	137
Figure 41 Types of cells used in mesh.....	139
Figure 42 Polyhedral Mesh.....	141
Figure 43 Volume based approach .....	142
Figure 44 Angle based approach.....	142
Figure 45 Smoothness.....	143
Figure 46 Aspect ratio.....	143
Figure 47 Mechanism of turbulence .....	148
Figure 48 Guidelines for domain sizing.....	156
Figure 49 Factors to be considered for convergence in decreasing order of priority .....	157
Figure 50 Geometry used for MRF.....	161
Figure 51 Propeller Mesh.....	162
Figure 52 Boundary Layer Mesh for Propeller Section.....	162
Figure 53 Sectional View of Complete Mesh.....	163
Figure 54 Complete Mesh Orthogonal View .....	163
Figure 55 Pressure contours.....	164
Figure 56 Velocity contours front view .....	164
Figure 57 Velocity contours side view .....	165
Figure 58 Streamlines Result .....	165
Figure 59 Propeller rotation .....	166
Figure 60 Meshed model of the propeller.....	170
Figure 61 Model setup for the propeller in static structural workbench in ANSYS.....	171
Figure 62 Imported CFD thrust load on the propeller .....	171
Figure 63 Von-Mises stress distribution in the propeller .....	171

## LIST OF TABLES

Table 1 Modified Chord length distribution for 2nd design point.....	23
Table 2 Modified chord length distribution for 3rd design point .....	25
Table 3 Selected airfoils and their thicknesses .....	27
Table 4 Aerodynamic variable values for Eppeler 63 .....	29
Table 5 Aerodynamic variable values for Clark Y .....	31
Table 6 Aerodynamic variable values for ARAD-10 .....	33
Table 7 Aerodynamic variable values for S7055.....	34
Table 8 Aerodynamic variable values for BE50.....	36
Table 9 Aerodynamic variable values for MH22 (7.2%) .....	38
Table 10 Aerodynamic variable values for MH30 (7.84%) .....	39
Table 11 Aerodynamic variable values for MH32 (8.7%) .....	41
Table 12 Aerodynamic variable values for MH43 (8.5%) .....	43
Table 13 Aerodynamic variable values for MH64 (8.59%) .....	45
Table 14 1st design point parameters.....	46
Table 15 QMIL generated propeller geometry for ARAD-10.....	47
Table 16 QMIL generated propeller geometry for BE 50 .....	50
Table 17 QMIL generated propeller geometry for Eppeler 63 .....	53
Table 18 QMIL generated propeller geometry for CLARK Y .....	56
Table 19 QMIL generated propeller geometry for MH22 (7.2%) .....	59
Table 20 QMIL generated propeller geometry for MH30 (7.84%) .....	63
Table 21 QMIL generated propeller geometry for MH32 (8.7%) .....	66
Table 22 QMIL generated propeller geometry for MH43 (8.5%) .....	70
Table 23 QMIL generated propeller geometry for MH64 (8.59%) .....	73
Table 24 QMIL generated propeller geometry for S7055 .....	77
Table 25 Summary of aerodynamic performance characteristics at 1st design point.....	79
Table 26 Comparison of thrust and propeller efficiency between the 1st design point and APC 11x4.7.....	80
Table 27 Comparison of thrust and propeller efficiency between the 1st design point and APC 11x4.7.....	80
Table 28 2nd design point parameters .....	82

Table 29 Summary of aerodynamic performance characteristics at 2nd Design Point .....	103
Table 30 1). Comparison of propeller efficiency and thrust between 2nd Design point and APC 11x4.7.....	104
Table 31 2). Comparison of propeller efficiency and thrust between 2nd Design point and APC 11x4.7.....	104
Table 32 Summary of aerodynamic characteristics for 3rd Design point .....	116
Table 33 1). Thrust and propeller efficiency comparison between 3rd design point and APC 11x4.7.....	117
Table 34 2). Thrust and propeller efficiency comparison between 3rd design point and APC 11x4.7.....	117
Table 35 Airfoils eligible to be used as thin tip airfoils for the propeller made of ARAD-10 .....	119
Table 36 1). Thrust and Propeller efficiency comparison between all possible thin tip ARAD- 10 propellers and the pure ARAD-10 propeller.....	120
Table 37 2). Thrust and Propeller efficiency comparison between all possible thin tip ARAD- 10 propellers and the pure ARAD-10 propeller.....	121
Table 38 Airfoils eligible to be used as thin tip airfoils for the propeller made of BE50.....	122
Table 39 Thurst and propeller efficiency comparision between Eppeler 63 and MH22 (7.2%) thin .....	123
Table 40 Airfoils eligible to be used as thin tip airfoils for the propeller made of MH32 (8.7%) .....	124
Table 41 1). Thrust and Propeller efficiency comparison between the thin tip propellers for MH32 (8.7%) and the propeller made purely of MH32 (8.7%) .....	125
Table 42 2). Thrust and Propeller efficiency comparison between the thin tip propellers for MH32 (8.7%) and the propeller made purely of MH32 (8.7%) .....	125
Table 43 Thrust and propeller efficiency comparison between ARAD10 + BE50 BE50 MH32 (8.7%) + E63 .....	127
Table 44 Electrical power consumption comparison between the final selected propeller and APC 11x4.7.....	129
Table 45 Quadcopter flight time comparison between the final selected propeller and APC 11x4.7.....	129
Table 46 Propeller geometry of the final selected propeller.....	131
Table 47 Comparison of Cell Types .....	140
Table 48 5 General Guidelines in Quality .....	144

Table 49 Reference Chart for Turbulence Models (Validated by ANSYS Expert) .....	158
Table 50 Solver settings of the CFD model.....	159
Table 51 Comparison of thrust and torque values between the CFD data and the wind tunnel data of APC 8x3.8.....	166
Table 52 CFD aerodynamic data for APC 11x4.7 .....	167
Table 53 CFD aerodynamic data for the final selected propeller .....	168
Table 54Material mechanical properties for ABS Plastic.....	170

## LIST OF GRAPHS

Graph 1 Efficiency curve comparison between APC 11x4.7 Slow flyer and APC 11x5 Sport 8	8
Graph 2 Drag Polar comparison for varying Reynolds Number .....	13
Graph 3 Efficiency curve of APC 11x4.7 .....	20
Graph 4 Thrust curve of APC 11x4.7 .....	20
Graph 5 Modified chord length distribution for 2nd design point.....	23
Graph 6 Modified chord length distribution for 3rd design point .....	26
Graph 7 Eppeler 63 lift polar curve fitment.....	28
Graph 8 Eppler 63 drag polar curve fitment .....	28
Graph 9 Clark Y lift polar curve fitment .....	30
Graph 10 Clark Y drag polar curve fitment .....	30
Graph 11 ARAD-10 lift polar curve fitment.....	31
Graph 12 ARAD-10 drag polar curve fitment .....	32
Graph 13 S7055 lift polar curve fitment .....	33
Graph 14 S7055 drag polar curve fitment.....	33
Graph 15 BE50 lift polar curve fitment .....	35
Graph 16 BE50 drag polar curve fitment.....	35
Graph 17 MH22 (7.2%) lift polar curve fitment.....	36
Graph 18 MH22 (7.2%) drag polar curve fitment .....	37
Graph 19 MH30 (7.84%) lift polar curve fitment.....	38
Graph 20 MH30 (7.84%) drag polar curve fitment .....	38
Graph 21 MH32 (8.7%) lift polar curve fitment.....	40
Graph 22 MH32 (8.7%) drag polar curve fitment .....	40
Graph 23 MH43 (8.5%) lift polar curve fitment.....	42
Graph 24 MH43 (8.5%) drag polar curve fitment .....	42
Graph 25 MH64 (8.59%) lift polar curve fitment.....	43
Graph 26 MH64 (8.59%) drag polar curve fitment .....	44
Graph 27 QMIL generated chord distribution for ARAD-10 .....	48
Graph 28 QMIL generated pitch angle distribution for ARAD-10 .....	48
Graph 29 Propeller efficiency curve comparison between ARAD-10 and APC 11x4.7 .....	48
Graph 30 Thrust curve comparison between ARAD-10 and APC 11x4.7 .....	49
Graph 31 QMIL generated chord length distribution for BE 50 .....	51
Graph 32 QMIL generated pitch angle distribution for BE 50.....	51

Graph 33 Propeller efficiency curve comparison between BE 50 and APC 11x4.7 .....	51
Graph 34 Thrust curve comparison between BE 50 and APC 11x4.7.....	52
Graph 35 QMIL generated chord length distribution for Eppeler 63 .....	54
Graph 36 QMIL generated pitch angle distribution for Eppeler 63.....	54
Graph 37 Efficiency curve comparison between Eppeler 63 and APC 11x4.7 .....	54
Graph 38 Thrust curve comparison between Eppeler 63 and APC 11x4.7 .....	55
Graph 39 QMIL generated chord length distribution for CLARK Y .....	57
Graph 40 QMIL generated pitch angle distribution for CLARK Y.....	57
Graph 41 Efficiency curve comparison between CLARK Y and APC 11x4.7 .....	57
Graph 42 Thrust curve comparison between CLARK Y and APC 11x4.7 .....	58
Graph 43 QMIL generated chord length distribution for MH22 (7.2%) .....	60
Graph 44 QMIL generated pitch angle distribution for MH22 (7.2%).....	60
Graph 45 Efficiency curve comparison between MH22 (7.2%) and APC 11x4.7 .....	61
Graph 46 Thrust curve comparison between MH22 (7.2%) and APC 11x4.7 .....	61
Graph 47 QMIL generated chord length distribution for MH30 (7.84%) .....	63
Graph 48 QMIL generated pitch angle distribution for MH30 (7.84%).....	64
Graph 49 Efficiency curve comparison between MH30 (7.84%) and APC 11x4.7 .....	64
Graph 50 Thrust curve comparison between MH30 (7.84%) and APC 11x4.7 .....	65
Graph 51QMIL generated chord length distribution for MH32 (8.7%) .....	67
Graph 52 QMIL generated pitch angle distribution for MH32 (8.7%).....	67
Graph 53 Efficiency curve comparison between MH32 (8.7%) and APC 11x4.7 .....	68
Graph 54 Thrust curve comparison between MH32 (8.7%) and APC 11x4.7 .....	68
Graph 55 QMIL generated chord length distribution for MH43 (8.5%) .....	70
Graph 56 QMIL generated pitch angle distribution for MH43 (8.5%).....	71
Graph 57 Efficiency curve comparison between MH43 (8.5%) and APC 11x4.7 .....	71
Graph 58 Thrust curve comparison between MH43 (8.5%) and APC 11x4.7 .....	72
Graph 59 QMIL generated chord length distribution for MH64 (8.59%) .....	74
Graph 60 QMIL generated pitch angle distribution for MH64 (8.59%).....	74
Graph 61 Efficiency curve comparison between MH64 (8.59%) and APC 11x4.7 .....	75
Graph 62 Thrust curve comparison between MH64 (8.59%) and APC 11x4.7 .....	75
Graph 63 QMIL generated chord length distribution for S7055 .....	77
Graph 64 QMIL generated pitch angle distribution for S7055.....	78
Graph 65 Efficiency curve comparison between S7055 and APC 11x4.7 .....	78
Graph 66 Thrust curve comparison between S7055 and APC 11x4.7 .....	79

Graph 67 QMIL generated pitch angle distribution for ARAD-10 .....	83
Graph 68 Efficiency curve comparison between ARAD-10 and APC 11x4.7.....	84
Graph 69 Thrust curve comparison between ARAD-10 and APC 11x4.7 .....	84
Graph 70 QMIL generated pitch angle distribution for BE50.....	85
Graph 71 Efficiency curve comparison between BE50 and APC 11x4.7 .....	86
Graph 72 Thrust curve comparison between BE50 and APC 11x4.7.....	86
Graph 73 QMIL generated pitch angle distribution for Eppeler 63.....	87
Graph 74 Efficiency curve comparison between Eppeler 63 and APC 11x4.7 .....	88
Graph 75 Thrust curve comparison between Eppeler 63 and APC 11x4.7 .....	88
Graph 76 QMIL generated pitch angle distribution for CLARK Y.....	89
Graph 77 Efficiency curve comparison between CLARK Y and APC 11x4.7 .....	90
Graph 78 Thrust curve comparison between CLARK Y and APC 11x4.7 .....	90
Graph 79 QMIL generated pitch angle distribution for MH22 (7.2%).....	91
Graph 80 Efficiency curve comparison between MH22 (7.2%) and APC 11x4.7 .....	92
Graph 81 Thrust curve comparison for MH22 (7.2%) and APC 11x4.7 .....	92
Graph 82 QMIL generated pitch angle distribution for MH30 (7.84%).....	93
Graph 83 Efficiency curve comparison between MH30 (7.84%) and APC 11x4.7 .....	94
Graph 84 Thrust curve comparison between MH30 (7.84%) and APC 11x4.7 .....	94
Graph 85 QMIL generated pitch angle distribution for MH32 (8.7%).....	95
Graph 86 Efficiency curve comparison between MH32 (8.7%) and APC 11x4.7 .....	96
Graph 87 Thrust curve comparison between MH32 (8.7%) and APC 11x4.7 .....	96
Graph 88 QMIL generated pitch angle distribution for MH43 (8.5%).....	97
Graph 89 Efficiency curve comparison between MH43 (8.59%) and APC 11x4.7 .....	98
Graph 90 Thrust curve comparison between MH43 (8.5%) and APC 11x4.7 .....	98
Graph 91 QMIL generated pitch angle distribution for MH64 (8.59%).....	99
Graph 92 Efficiency curve comparison between MH64 (8.59%) and APC 11x4.7 .....	100
Graph 93 Thrust curve comparison between MH64 (8.59%) and APC 11x4.7 .....	100
Graph 94 QMIL generated pitch angle distribution for S7055.....	101
Graph 95 Efficiency curve comparison between S7055 and APC 11x4.7 .....	102
Graph 96 Thrust curve comparison between S7055 and APC 11x4.7 .....	102
Graph 97 Efficiency curve comparison for BE50, ARAD-10, MH32 (8.7%) and APC 11x4.7 .....	105
Graph 98 Thrust curve comparison for BE50, ARAD-10, MH32 (8.7%) and APC 11x4.7.105	
Graph 99 Efficiency curve comparison between ARAD-10 and APC 11x4.7.....	106

Graph 100 Thrust curve comparison between ARAD-10 and APC 11x4.7 .....	107
Graph 101 Efficiency curve comparison between BE50 and APC 11x4.7 .....	107
Graph 102 Thrust curve comparison between BE50 and APC 11x4.7.....	108
Graph 103 Efficiency curve comparison between Eppeler 63 and APC 11x4.7 .....	108
Graph 104 Thrust curve comparison between Eppeler 63 and APC 11x4.7 .....	109
Graph 105 Efficiency curve comparison between CLARK Y and APC 11x4.7 .....	109
Graph 106 Thrust curve comparison between CLARK Y and APC 11x4.7 .....	110
Graph 107 Efficiency curve comparison between MH22 (7.2%) and APC 11x4.7 .....	110
Graph 108 Thrust curve comparison between MH22 (7.2%) and APC 11x4.7 .....	111
Graph 109 Efficiency curve comparison between MH30 (7.84%) and APC 11x4.7 .....	111
Graph 110 Thrust curve comparison between MH30 (7.84%) and APC 11x4.7 .....	112
Graph 111 Efficiency curve comparison between MH32 (8.7%) and APC 11x4.7 .....	112
Graph 112 Thrust curve comparison between MH32 (8.7%) and APC 11x4.7 .....	113
Graph 113 Efficiency curve comparison between MH43 (8.5%) and APC 11x4.7 .....	113
Graph 114 Thrust curve comparison between MH43 (8.5%) and APC 11x4.7 .....	114
Graph 115 Efficiency curve comparison between MH64 (8.59%) and APC 11x4.7 .....	114
Graph 116 Thrust curve comparison between MH64 (8.59%) and APC 11x4.7 .....	115
Graph 117 Efficiency curve comparison between S7055 and APC 11x4.7 .....	115
Graph 118 Thrust curve comparison between S7055 and APC 11x4.7 .....	116
Graph 119 Efficiency curve comparison between all the possible thin tip propellers made of ARAD-10.....	119
Graph 120 Thrust curve comparison between all the possible thin tip propellers made of ARAD- 10.....	120
Graph 121 Efficiency curve comparison between all the possible thin tip propellers made of BE50 .....	122
Graph 122 Thrust curve comparison between all the possible thin tip propellers made of BE50 .....	122
Graph 123 Efficiency curve comparison between all the possible thin tip propellers for MH32 (8.7%).....	124
Graph 124 Thrust curve comparison between all the possible thin tip propellers for MH32 (8.7%).....	124
Graph 125 Efficiency curve comparison between the three selected thin tip propellers and APC 11x4.7.....	126

Graph 126 Thrust curve comparison between the three selected thin tip propellers and APC 11x4.7.....	127
Graph 127 Thrust comparison between the selected propeller at 4700 RPM and APC 11x4.7 at 5000 RPM .....	128
Graph 128 Chord length distribution of the final selected propeller .....	131
Graph 129 Pitch angle distribution of the final selected propeller .....	131
Graph 130 Efficiency curve of the final selected propeller .....	132
Graph 131 Thrust curve of the final selected propeller .....	132
Graph 132: Comparison of the efficiency data extracted from CFD for the final selected propeller and APC 11x4.7.....	168
Graph 133: Comparison of the thrust data extracted from CFD for the final selected propeller and APC 11X4.7 .....	169

## **ABSTRACT**

Propellers to be used on slow flying quadcopters should have high propeller efficiencies for low velocities, the cruise range for such quad-copters being 2 m/s – 6 m/s. APC 11x4.7 is one such propeller which is a market standard for slow flying applications. The main aim of this project is to make a propeller design showing better propeller efficiencies than APC 11x4.7 and comparable thrusts in the cruise range of 2m/s to 6m/s. 10 industry standard airfoils have been used as propeller sections and 1<sup>st</sup> order tool QMIL has been used to generate propeller geometry on the basis of airfoil characteristics and flight conditions while first order tool QPROP has been used to calculate the propeller performance characteristics on the generated QMIL geometry. A total of 3 design points, varying on the basis of flight conditions and chord length distribution along the propeller blade have been compared from which the design point giving the most desirable propeller performance i.e. propeller efficiencies significantly higher than APC 11x4.7 and comparable thrust to APC 11x4.7 in the cruise range, has been chosen as the final design point. For the chosen design point, all the propellers made of each airfoil have been compared and 3 propellers showing the most desirable performance have been chosen. Then, the concept of thin tip propellers has been used to further modify the design of the 3 propellers chosen in hopes of an improvement in the design performance. The thin tip propeller which shows the best performance in the cruise range has been chosen as the final propeller. Once the propeller has been decided, its formal aerodynamic performance is calculated with the help of CFD, a 2<sup>nd</sup> order tool. For comparison, CFD of APC 11x4.7 is also carried out and the CFD results of both the propellers is calculated. Once the CFD has been carried out, the thrust load generated on the propeller is imported into a ANSYS static structural workbench where finite element analysis is carried out to find the strength of the propeller and if it is able to bear the bending load arising from the thrust over its surface and the centrifugal stresses arising from its rotational motion.

# CHAPTER 1: Theoretical Formulation Of Propellers

## 1.1 Introduction

A **propeller** is a mechanical device that converts mechanical energy into a force, which we call thrust, and is used to propel the vehicle to which it is attached.

A propeller blade is made up of **airfoils** which are fundamentally created to produce **lift & drag**.

Propellers provide a very efficient means of generating thrust by giving a relatively large mass of matter a modest acceleration.

Generally, the larger the acceleration, the greater is the amount of chemical energy (fuel) that must be converted into mechanical energy. Thus, the generation of thrust using a propeller consumes far less fuel than any other method, making it the most efficient propulsive option currently available for airplanes.

The thrust generated by the propeller is the consequence of a complex interaction between the forward motion of the propeller, its rotational speed, and geometry.

Two important theories that can be used to calculate propeller thrust; the **Disc momentum theory** and the so-called **blade-element theory**. The latter, while much more complicated to use, **allows the power required to rotate the propeller to be estimated**.

## 1.2 Propeller Geometry

The **spinner** is an aerodynamically shaped cover, whose **purpose is to reduce the drag of the hub of the propeller** and to protect it from the elements.

The **planform** of the propeller blade **has a profound impact on the magnitude of the thrust force** created, as well as at what “cost.” What constitutes “cost” is the amount of power required to rotate it, as well as side effects such as noise.

The blade planform, along with geometric properties such as twist and airfoil camber, is of crucial importance Propeller geometry to optimize a propeller.

### **1.3 Geometric Propeller Pitch**

The **distance it would cover in one full revolution** is called the geometric pitch or pitch distance,  $P_D$ , of the propeller. It is commonly **specified in terms of inches of pitch**. Thus a propeller designated as a 42-inch pitch prop would move 42 inches forward in one revolution (using the metal screw through wood analogy). The **angle the helix makes to the rotation plane is called the geometric pitch angle and is denoted by beta.**

Pitch angle:

$$P_D = 2\pi r_r \tan \beta_r$$

$P_D$  = pitch distance of the propeller

$r_r$  = radial distance of the representative section of the propeller, a section whose properties are often the average representation of the properties of the whole propeller. Usually, the representative section of the propeller lies between 60%-70% of the blade length.

$\beta_r$  = Pitch angle of the representative section

Angle formed between the rotation plane and a tangent to the blade tip helix at each blade station is less than the geometric pitch angle. This angle is called the *flow angle*.

$$\tan \phi = \frac{V_0}{\omega r}$$

Where  $V_0$  is the linear forward speed of the aircraft or the air and  $\omega r$  is the rotational velocity of the blade section.

### **1.4 Pitch Angle or Geometric Pitch**

In order for the propeller **to generate thrust** in a forward direction its chord line **must form a positive angle-of-attack to the relative wind** as it moves about its rotation axis.

## Fundamental Relationships of Propeller Rotation

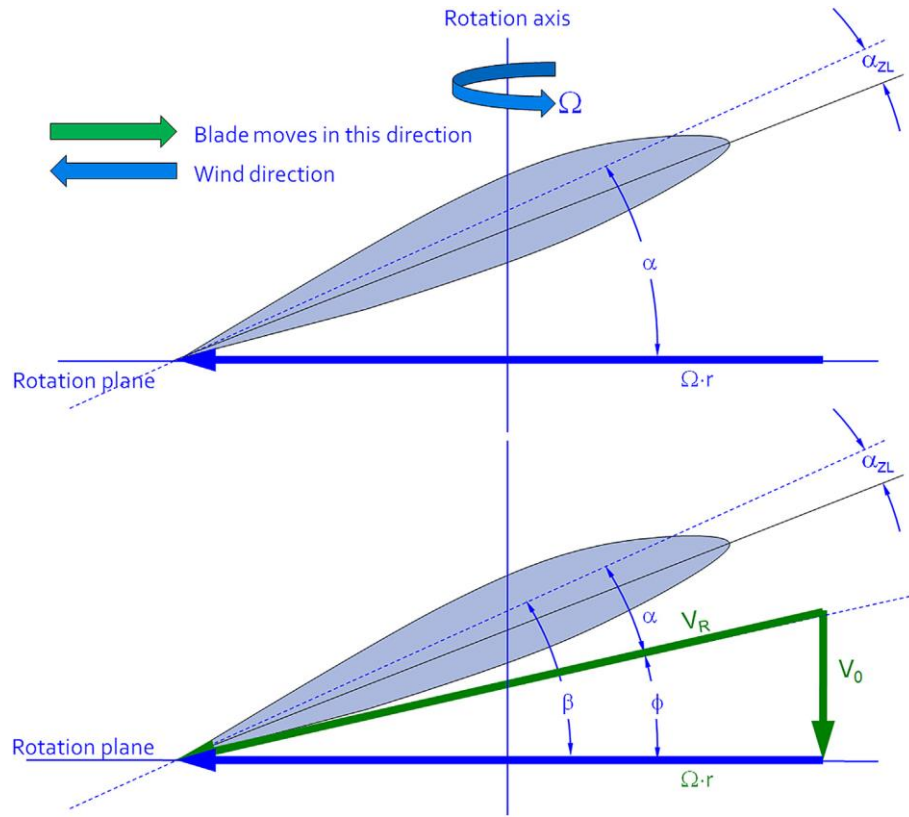


*Figure 1 Fundamental Formulation of Propeller Rotation*

The upper one shows the blade airfoil at a zero-forward airspeed (static condition, e.g. airplane sitting on ground at rest prior to T-O). The thick vector indicates the oncoming airflow seen by an imaginary observer on the blade. The angle  $\beta$  is the pitch angle, whereas the AOA is represented by  $\alpha$  as usual.

Propeller rotational speed:

$$V_{ROT} = \omega * r$$

The angle of attack is the angle between the blade's chord line and the rotation plane.

**The angle of attack changes with forward airspeed,  $V_0$ .** AOA is the function of Blade element, Geometric Pitch (Blade Setting), effective pitch angle. The variation should be within the characteristic property of the chosen aerofoil, beyond the maximum and minimum limits, it has non-aerodynamic motion which is of no use or in other words, the aerofoil becomes ineffective.

To maintain the best AOA for each Blade Element, Pitch setting is required to be varied from hub to tip which gives rise to the twist.

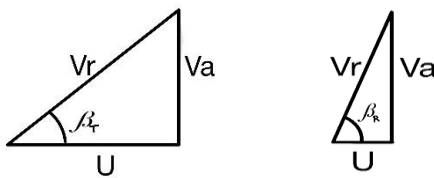


*Figure 2 Velocity Triangles formed underneath a propeller section*

As pitch angle at root is larger than that at the tip and also the effective pitch angle or helix angle would also show similar comparison, thus the pitch setting needs to be varied from hub to tip to maintain the best angle of attack for each blade element.

### **1.5 Blade Element Theory**

The blade element theory (BET) attempts to estimate the thrust of a propeller by dividing each blade into a number of segments, called blade elements. The theory treats each element as an independent two-dimensional air foil, which allows the aerodynamic forces to be calculated based on the local flow conditions at the element. Then, once the aerodynamic properties have been determined, they are summed up to evaluate the properties of the complete propeller.

An accurate depiction of the propeller is realized by the BET only through an estimation of the so-called propeller-induced velocity, which changes the AOA seen by the blade elements. This is caused by the fact that the airspeed inside the propeller stream tube moves faster than the surrounding air. One way of modelling this effect is to use the momentum theory to describe the induced velocity inside the stream tube.

Primary reasons for the method's popularity in propeller design.

It can account for varying blade geometry, change in the air foil's chord, angle-of-pitch, and aerodynamic characteristics.

It allows torque to be estimated, which allows the designer to determine the power required to swing it.

It also allows important non-linearities, such as that of a standard lift curve, to be modelled.

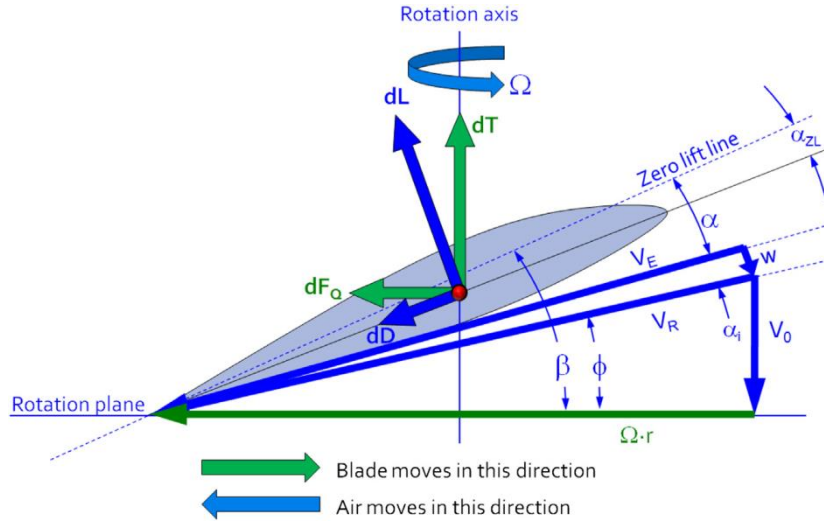


*Figure 3 Thrust and Resisting torque formation in a propeller*

$r$  = arbitrary distance from hub to blade element

$V_0$  = forward airspeed of the airplane

$V_E$  = effective resultant velocity

$V_R$  = resultant velocity

$w$  = elemental induced velocity; due to flow in the stream tube being faster than the far-field airspeed

$U$  = angular velocity of the propeller

$\alpha$  = elemental angle-of-attack

$\alpha_i$  = induced angle-of-attack that results from the induced velocity of air

$\alpha_{ZL}$  = airfoil's zero lift angle

$\beta$  = pitch angle, which is defined as the angle between the rotation plane and the zero lift line of the blade element airfoil

$\phi$  = helix angle

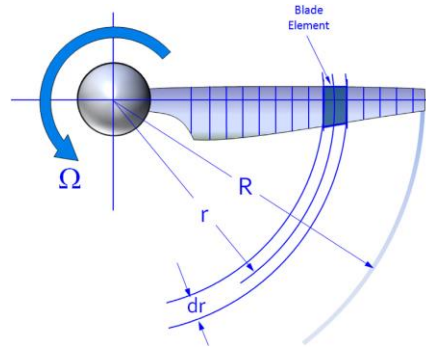


Figure 4 Section-wise division of a propeller blade

Differential thrust:

$$dT = dL \cos(\phi) - dD \sin(\phi)$$

Differential torque:

$$dQ = rdL \sin(\phi) + r \cdot dD \cos(\phi)$$

This allows us to calculate thrust and torque by integrating these differentials with limits as radius of Hub to the final radius.

Propeller efficiency:

The propeller efficiency is the measure of the work done by the propeller on the air compared to the input mechanical energy provided by the motor output shaft.

$$\eta = \frac{T \cdot v_0}{Q \cdot \omega}$$

Advance Ratio:

The advance ratio of the propeller is given by:

$$J = \frac{v_0}{nD}$$

Where n = Rotational speed of the propeller in revolutions per second

D = diameter of the propeller.

## CHAPTER 2: Objectives And Details Of The Propeller Design

The main objective of this capstone project will be to design a propeller which ensures good aerodynamic performance along with saving of electrical power for slow flyer quadcopters. The target quadcopters for which the propeller is being designed usually have a cruise speed of about 2 m/s (7.2 km/hr) to 6 m/s (21.6 km/hr) and may go up to a maximum speed of 10 m/s (36 km/hr).

The propeller will be designed as an alternative to the APC 11x4.7 (Propeller diameter = 11 inches, Propeller Pitch = 4.7 inches) slow flyer electric propeller which is one of the most popular slow flyers propellers available in the market. Through our design, we wish to achieve better propeller efficiency for comparable thrust in the cruise range of the drone.

Since we are not designing the propeller for a particular drone, there is no design constraint on the propeller thrust produced although the thrust achieved by the propeller should be close (and preferably higher than) to the thrust produced by APC 11x4.7 Propeller in the cruise range.

The only design constraint we have is the propeller diameter which is 11 inches as we need to compare our propeller with the APC 11x4.7.

### ***2.1 Shifting the efficiency curve towards left:***

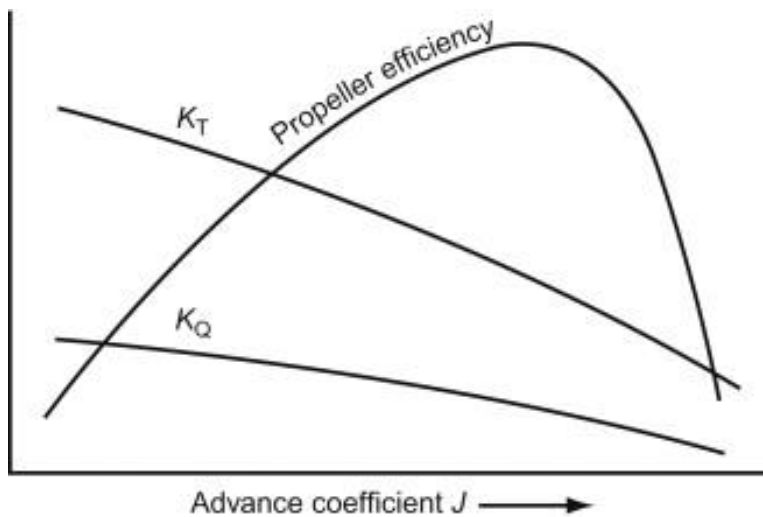
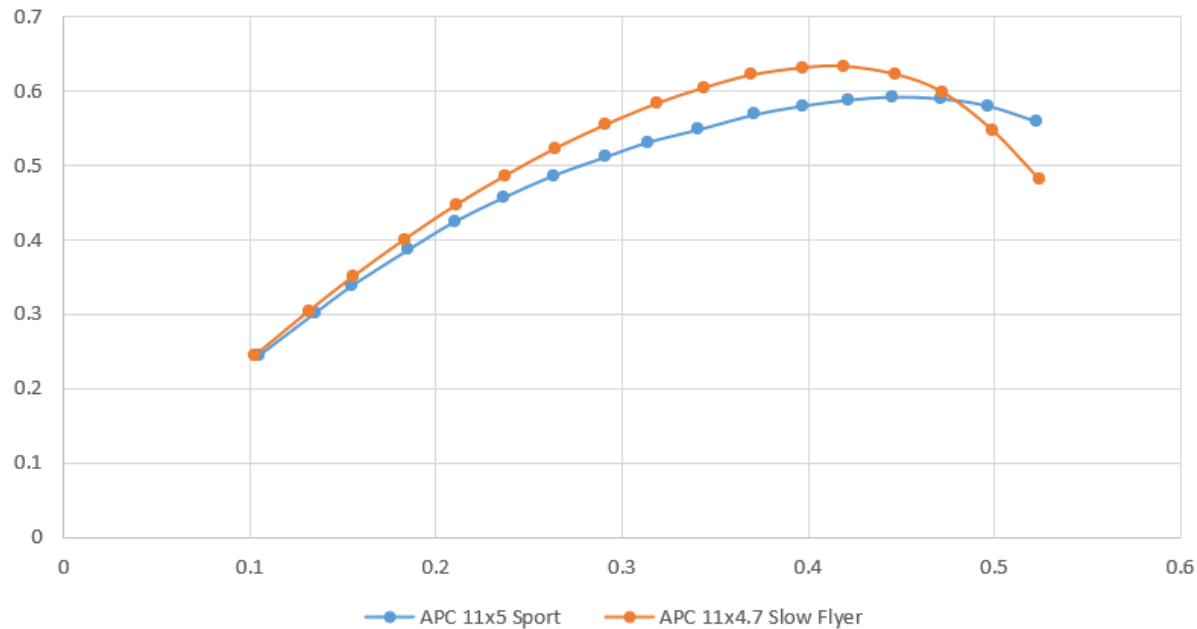


*Figure 5 General performance curves of a propeller*

As seen in the efficiency variation with the advance ratio above, the propeller efficiency reaches a maximum value for a particular advance ratio and then drops down as advance ratio is increased. Designing a propeller for slow flyer quadcopters requires the efficiency plot to be

shifted to the left side i.e. the propeller efficiency increases for lower advance ratios and thus lower quadcopter speeds (assuming constant propeller rotational velocity).

For illustrating this we can take the experimental performance curves of two propellers: one meant for slow flying purposes (APC 11x4.7) and the other meant for moderate to fast flying purposes



*Graph 1 Efficiency curve comparison between APC 11x4.7 Slow flyer and APC 11x5 Sport*

As seen above, the APC 11x5 Sport (for moderate to fast flying applications) has a peak in efficiency which comes at an advance ratio higher than the advance ratio at which the efficiency of the APC 11x4.7 peaks. In essence, the efficiency plot of the APC 11x4.7 is to more to the left as compared to the APC 11x5 sport. In most of the cases, the efficiency curves which are to the left tend to have higher efficiencies in the cruise range advance ratios (0.086 to 0.258) as is seen in the above plot.

## **2.2 Ways of shifting the propeller efficiency curves to the left:**

**1). Decreasing the ratio of propeller pitch by propeller diameter:** the pitch by diameter ratio can be decreased by either decreasing the propeller pitch or by increasing the propeller diameter. Since the diameter of the propeller is a design constraint, we are interested in only

decreasing the propeller pitch. As explained in the previous chapter, the propeller pitch is directly related to the pitch angle of the representative section of the blade (75% of the blade length). Further the pitch angle is the summation of the angle of attack of the relative wind and the flow angle (or the actual pitch angle). We also know that the flow angle is directly proportional to the forward linear velocity of the air/or the quadcopter.

### ***2.3 Theoretical basis for the relation between decreased pitch and increased efficiency for lower advance ratios:***

A propeller achieves maximum efficiency when the angle of attack of the relative wind has reached its optimum value. At the optimum angle of attack, for a particular airfoil, we get the maximum lift and the minimum drag. Since the angle of attacks of all the sections of the propeller lie close to each other, thus at the optimum angle of attack for one airfoil section, all the other sections too will have maximum lift and minimum drag and thus the propeller will be at its maximum efficiency.

Now, if we decrease the pitch, the pitch angle also gets decreased and as per the relation between the pitch angle, angle of attack and the flow angle, we observe that the optimum angle of attack is achieved at a lower flow angle and thus a lower velocity. For example, suppose the optimum angle of attack is  $4^\circ$  and the pitch angle at a particular section is  $20^\circ$ . In that case, the flow angle required to achieve optimum angle of attack is  $16^\circ$ . Now if the pitch angle at the same section is reduced to  $10^\circ$ , then the flow angle required to achieve optimum angle of attack will be  $6^\circ$  and since the flow angle is directly proportional to the forward linear velocity which in turn is directly proportional to the advance ratio, the peak efficiency will be achieved at a much lower advance ratio. Furthermore, we can observe that in the case of the decreased pitch, we get angles of attack much closer to the optimum value (and thus higher propeller efficiency) for low velocities which also explains why the plots which are shifted to the left often tend to have higher propeller efficiencies for low advance ratios (or low velocities). It is worth noting that this behaviour is consistent only for propellers having the same airfoil i.e. there may exist propellers which have higher pitch but higher low velocity efficiency, which just means that the propellers being compared have different airfoils.

**2). *Changing airfoil:*** Different airfoils have different optimum angle of attacks depending on their geometry and the airfoils which have higher optimum angles of attack will help in achieving higher efficiencies at lower velocities. However, the effect changing airfoils have on the efficiency curve is less significant than the pitch of the propeller thus it's a secondary step for shifting the efficiency curve towards the left.

Propellers can have either only one airfoil or multiple ones. For example, the APC 11x4.7 has the airfoil E63 for the majority of its blade length and then has CLARK Y at its tip. Most of the propellers tend to be thin tip propellers i.e. having a thinner airfoil near the tip. This is primarily due to the fact that low airfoils tend to have less profile drag (skin frictions drag, form drag. Pressure drag) as compared to thicker airfoils and thus are more efficient in high velocity conditions, considering the velocity of air near the tip is the highest and that drag forces increase for higher velocities. Changing or adding airfoils to the propeller can decrease or increase the efficiency depending on the airfoil performance and its optimum angle of attack.

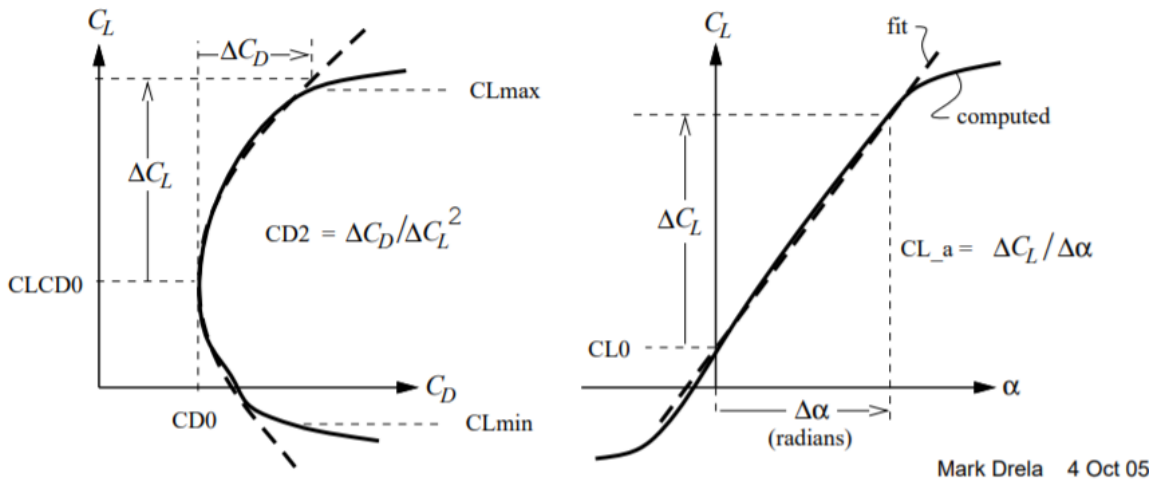
## **CHAPTER 3: Tools Used And Design Process**

The propeller is designed using the first order tools QMIL and QPROP, solvers developed by Mark Drela of Massachusetts Institute of Technology back in 2005. The solver employs the Vortex theory where it calculates the performance of the propeller on the basis of the necessary conditions in the trailing vortex system shed by the propeller blades which are then used to calculate the circulation on the propeller blades which can be used to determine the physical characteristics of the propeller like the chord length and the number of blades. QPROP treats the propeller blades as rotating wings by considering the propeller blade as a lift producing surface with a circulation associated with the bound vorticity and a vortex sheet that is shed continuously from the trailing edges of all the sections. QMIL uses the minimum induced loss theory to determine the geometric properties of the propeller like the chord length and the pitch distribution along the blade length. Unfortunately, the rigorous mathematics employed by both the vortex theory and the minimum induced loss theory are beyond the scope of this thesis.

### ***3.1 QMIL:***

QMIL is the primary tool used for developing a propeller geometry on the basis of flight conditions of the propeller and the airfoil properties of the airfoil. The first step for using QMIL is identifying the airfoils which will be used in the propeller and extracting their aerodynamic data (lift and drag polars) at the required Reynold's number. The aerodynamic data can be generated using XFOIL where the airfoil coordinate file needs to be uploaded. XFOIL employs the vortex panel method where the airfoil shape is captured using series of panels and at the middle of each panel there is a control point where the flow's normal velocity is equal to zero. The vortex at the control point of each panel is considered and the strengths of all the vortices are found. The strength of all the vortices help us to find the circulation which further helps in calculating the lift generated by the airfoil.

XFOIL converges for a particular range of angles of attack, usually starting from stall point for negative angle of attack up to a little over the maximum lift coefficient angle ending just before the stall point for positive angle of attack. After obtaining the lift and drag polars of the airfoils, a linear curve fit needs to be added to the lift polar and a parabolic fit curve needs to be added to the drag polar and the following aerodynamic variables need to be found out:



Mark Drela 4 Oct 05

*Figure 6Lift and Drag polar curve fitments for calculating airfoil specific aerodynamic variables*

**NOTE:** The lift polar needs to be truncated in such a way that the truncated part has a good value of coefficient of determination ( $R^2$ ) for the linear fit curve.

The aerodynamic variables for each airfoil are given as:

$CD_0$ : Profile drag of the airfoil (minimum drag produced)

$CL_{LCD0}$ : Coefficient of lift corresponding to the profile drag

$CL_a$ : Slope of the linear fit curve on the lift polar

$CL_0$ : Coefficient of lift corresponding to zero angle of attack

$CL_{max}$ : Maximum lift coefficient corresponding to the entire lift polar

$CL_{min}$ : Minimum lift coefficient corresponding to the truncated lift polar

$\Delta C_L$ : Difference between the maximum/minimum lift coefficient of the truncated lift polar and the coefficient of lift corresponding to zero angle of attack.

$\Delta C_D$ : Difference between the drag coefficient corresponding to the maximum/minimum lift coefficient of the truncated lift polar and the profile drag.

$$CD2 = \Delta C_D / (\Delta C_L)^2$$

The variables  $CD2$ ,  $\Delta C_L$ ,  $\Delta C_D$  have separate upper and lower values, upper values considered if  $C_L > CL_{LCD0}$  and lower values considered if  $C_L < CL_{LCD0}$ .

Two other important variables to be considered are:

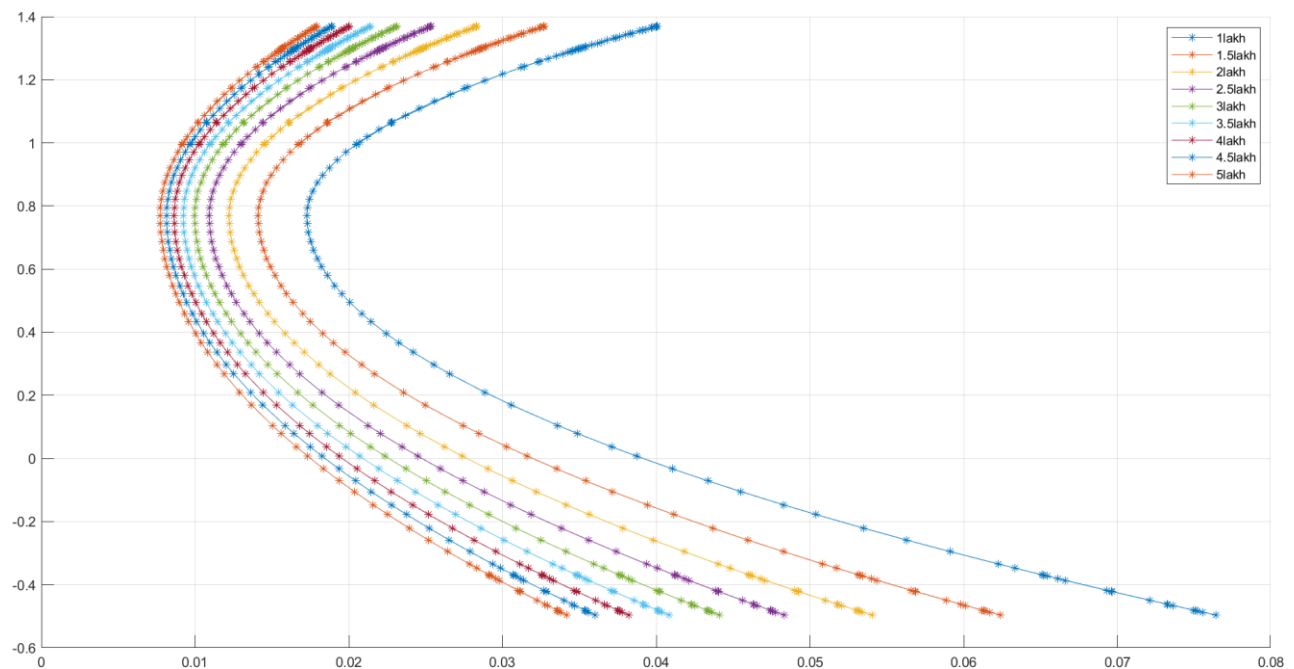
$Re_{ref}$ : The intended operational Reynolds number

$Re_{exp}$ : an exponential factor for ensuring consistent aerodynamic performance for varying Reynolds number.  $Re_{exp}$  is a very useful factor which ensures that there is no drop in the aerodynamic performance of the airfoil in case the Reynolds number of the surroundings surpass the intended operational Reynolds number.

The drag of any airfoil varying with the lift coefficient and the Reynolds number is given by:

$$C_D = [CD_0 + CD_2(C_L - CLCD_0)^2] \cdot \{Re/Re_{ref}\}^{Re_{exp}}$$

By setting a particular value of  $Re_{exp}$ , we want to get similar values of  $C_D$  for the same lift at a different Reynolds number than  $Re_{ref}$ . Suppose,  $Re_{ref}$  is equal to 100000 and the actual Re is above 100000 up to 500000. If we set  $Re_{exp}$  as -0.5 and plot the function in MATLAB for a particular set of lift coefficient values, we get the following:



*Graph 2 Drag Polar comparison for varying Reynolds Number*

The above figure shows how all the drag polars for all the Reynolds numbers are pretty close to each other and such kind of airfoil performance is desired. For almost all slow flyer applications,  $Re_{exp} = -0.5$  is an industry standard.

After all the airfoil specific aerodynamic variables are calculated, they are input in a QMIL input file, a .mil file which contains the aerodynamic information of the airfoil being used as

well as the operational conditions for the propeller. We have to decide the cruise speed the propeller should be designed for and the rotational speed of the propeller motor. The QMIL input file also asks for the coefficient of lift distribution along the blade length. Default input file ask for the lift coefficient values at the root (radial distance = 0), at the centre (radial distance = half of the blade length) and at the tip (radial distance = blade length).

```

Template prop

2           ! Nblades

0.0000  6.2832    ! CL0      CL_a
-0.8000  1.2000    ! CLmin    CLmax

0.01000   0.008  0.006  0.40  ! CD0      CD2u    CD2l    CLCD0
1500000.0 -0.500          ! REref    REexp

0.0  0.5  1.0  ! XIdes   (r/R locations where design cl is specified)
0.6  0.5  0.4  ! CLdes   (specified cl)

0.05    ! hub radius(m)
1.50    ! tip radius(m)
8.00    ! speed(m/s)
240.0   ! rpm

0.0     ! Thrust(N)  ( 0 if power specified )
500.0   ! Power(W)   ( 0 if thrust specified )

0  0.0  ! Ldes   [ KQdes ]
# 30    ! Nout    number of output stations (optional)

```

*Figure 7 Sample input file for QMIL*

We also have to input the radius of the propeller and its hub along with the tentative thrust value that the propeller should generate. Alternatively, instead of the tentative thrust, we can also mention the power which should be utilised in rotating the power.

In the above input file, Ldes refers to the theory being used for designing the propeller geometry: if Ldes = 0, then minimum induced loss method is used to design the chord length distribution and the pitch angle distribution along the blade length. If Ldes = 1, then the minimum total loss method is used for designing the propeller geometry but this method is quite unreliable thus is not preferred. Ldes = 2 is used for designing wind turbine blades.

Once the QMIL file has been created, QMIL is run in a terminal/command window with the help of the following command:

qmil <qmil input file name> <output text file for propeller geometry>

Following is a sample QMIL ouput:

```

Template prop

      2      ! Nblades

      0.0000  6.2832    ! CL0     CL_a
     -0.8000  1.2000    ! CLmin   CLmax

      0.01000  0.00800  0.00600  0.4000    ! CD0     CD2u   CD2l   CLCD0
     150000.0  -0.500          ! REref   REexp

      1.0000  1.0000  1.0000    ! Rfac    Cfac   Bfac
      0.0000  0.0000  0.0000    ! Radd    Cadd   Badd

#      r           c           beta
      0.86250E-01  0.83189E-01  81.1978
      0.15875       0.14500       70.3563
      0.23125       0.19038       61.0978
      0.30375       0.21721       53.4627
      0.37625       0.22900       47.2539
      0.44875       0.23069       42.2076
      0.52125       0.22633       38.0776
      0.59375       0.21863       34.6624
      0.66625       0.20923       31.8050
      0.73875       0.19901       29.3862
      0.81125       0.18842       27.3155
      0.88375       0.17765       25.5241
      0.95625       0.16667       23.9592
      1.0288        0.15535       22.5802
      1.1012        0.14345       21.3549
      1.1738        0.13059       20.2583
      1.2462        0.11620       19.2701
      1.3188        0.99320E-01  18.3741
      1.3912        0.77971E-01  17.5570
      1.4638        0.45712E-01  16.8081
      1.5000        0.25491E-01  16.4592

```

*Figure 8 Sample output from QMIL*

In the output file the radial distance of each section is given along with the corresponding chord length and the pitch angle. A more elaborated version of the results is also provided by QMIL which provides with the information of the flow angles at each section, the lift and drag at each section, the induced efficiency and the elemental propeller efficiency at each section and the elemental thrust and torques at each section.

r/R	phi	c/R	beta	CL	CD	Mach	Re	adw_local	effi	effp	eff	T_c	Q_c
0.057	75.83	0.0555	81.20	0.588	0.01829	0.024	47445.	0.2278	0.9316	0.8701	0.8106	0.01764	0.01942
0.106	65.08	0.0967	70.36	0.579	0.01330	0.026	89174.	0.2278	0.9316	0.9405	0.8762	0.03344	0.03527
0.154	55.91	0.1269	61.10	0.569	0.01101	0.029	129483.	0.2278	0.9316	0.9589	0.8933	0.05208	0.05425
0.202	48.36	0.1448	53.46	0.559	0.00972	0.033	165198.	0.2278	0.9316	0.9655	0.8995	0.07547	0.07819
0.251	42.24	0.1527	47.25	0.550	0.00893	0.036	195086.	0.2278	0.9316	0.9680	0.9017	0.10447	0.10795
0.299	37.29	0.1538	42.21	0.540	0.00840	0.041	219400.	0.2278	0.9316	0.9684	0.9021	0.13941	0.14386
0.347	33.25	0.1509	38.08	0.531	0.00803	0.045	238972.	0.2278	0.9316	0.9677	0.9015	0.18025	0.18593
0.396	29.92	0.1458	34.66	0.521	0.00776	0.050	254647.	0.2278	0.9316	0.9664	0.9003	0.22681	0.23400
0.444	27.15	0.1395	31.81	0.511	0.00757	0.055	267104.	0.2278	0.9316	0.9646	0.8986	0.27880	0.28782
0.492	24.82	0.1327	29.39	0.501	0.00742	0.059	276787.	0.2278	0.9316	0.9624	0.8965	0.33586	0.34705
0.541	22.84	0.1256	27.32	0.492	0.00732	0.064	283926.	0.2278	0.9316	0.9598	0.8942	0.39759	0.41136
0.589	21.14	0.1184	25.52	0.482	0.00725	0.069	288542.	0.2278	0.9316	0.9570	0.8915	0.46357	0.48035
0.637	19.66	0.1111	23.96	0.473	0.00722	0.074	290461.	0.2278	0.9316	0.9538	0.8885	0.53337	0.55367
0.686	18.37	0.1036	22.58	0.463	0.00722	0.080	289289.	0.2278	0.9316	0.9502	0.8852	0.60653	0.63095
0.734	17.24	0.0956	21.35	0.453	0.00728	0.085	284364.	0.2278	0.9316	0.9460	0.8813	0.68260	0.71186
0.782	16.23	0.0871	20.26	0.444	0.00740	0.090	274647.	0.2278	0.9316	0.9412	0.8768	0.76113	0.79613
0.831	15.33	0.0775	19.27	0.434	0.00762	0.095	258480.	0.2278	0.9316	0.9352	0.8713	0.84164	0.88364
0.879	14.53	0.0662	18.37	0.424	0.00803	0.100	233019.	0.2278	0.9316	0.9274	0.8639	0.92363	0.97460
0.927	13.80	0.0520	17.56	0.414	0.00883	0.105	192450.	0.2278	0.9316	0.9154	0.8528	1.00656	1.07041
0.976	13.14	0.0305	16.81	0.405	0.01125	0.111	118423.	0.2278	0.9316	0.8878	0.8271	1.08942	1.18010

Figure 9 Sample detailed output from QMIL

Once the geometry has been set by QMIL, the geometry data can be dumped into a text file which will act as the input file for QPROP.

### 3.2 QPROP:

QPROP is a solver which computes the aerodynamic performance of a propeller with known geometry (chord length distribution and pitch angles at each section). QPROP also provides information about the various propeller motor combinations possible and computes the motor efficiency for a particular propeller and its performance. Thus, QPROP requires two input files, one is the propeller input file containing the geometric data obtained from QMIL. The second file is the motor file which contains all the pertinent information about the motor being used for the propeller. A motor input file should provide the following information:

- 1). Motor type (1 for a brushless DC motor)
- 2). Motor internal resistance (R)
- 3). Motor no load current (Io): The motor no load current is the amount of current being used up by the motor when there is no mechanical load attached to the motor, in this case no propeller attached to the motor. The correct way of measuring the no load current is by attaching an ammeter between the SMPS (or the battery source being used) and the ESC (electronic speed

controller) which provides varying voltage to the BLDC motor in the form of analog signals which in turn controls the RPM of the motor. There should be no mechanical load of any kind attached to the motor and the circuit should be activated. The current registered by the ammeter for a particular power source voltage is the no load current of the motor for that particular voltage. It is important to note that while the no load current changes with the voltage of the power source, the change itself is quite low and thus motor manufacturers provide the no load current of the motor at 10 Volts assuming that using this value for all comparable voltages should be acceptable.

4). Kv rating of the motor (in case of a BLDC motor): Kv rating translates to the RPM/volt or the RPM at which motor rotates its output shaft for 1-volt power source. Suppose a 10-volt power source is being used and the Kv rating of a particular motor is X. Then, the maximum RPM achieved by the motor is going to be  $10X$  revolutions per minute.

The above parameters are used to calculate various important motor performance characteristics like:

$$\text{voltage} = V$$

$$\text{current} = I$$

$$\text{torque} = Q = (I - I_o)/Kv$$

$$\text{rot.speed} = w = (V - I * R) * Kv$$

$$\text{mech.power} = P = w * Q = (V - I * R) * (I - I_o)$$

$$\text{efficiency} = P / (I * V) = (1 - I * R / V) * (1 - I_o / I)$$

The motor being used for the project is the A2212 BLDC motor which has a 1400 Kv rating. The no load current for this motor at 10 Volts is 0.7 Amperes and it has an internal resistance of 0.065 ohms.

---

```
A2212 1400 Kv BLDC
1      ! motor type (brushless DC motor)
0.065    ! Rmotor (Ohms)
0.700    ! Io      (Amps)
1400.0   ! Kv      (rpm/Volt)
```

*Figure 10 Sample motor input file for QPROP*

QPROP is then run using a terminal/command prompt with the command:

```
qprop <qprop geometry file> <motor file> V1,V2,dV RPM
```

In the above command, V1 refers to the starting velocity, V2 is the ending velocity and dV is the velocity step size. Once this command is run, QPROP will provide the performance characteristics of the propeller geometry at each velocity starting from the starting velocity to the ending velocity.

#	1	2	3	4	5	6	7	8	9	10	11	12	13	14	15	16	17	18	19
#	V(m/s)	rpm	Dbeta	T(N)	Q(N-m)	Pshaft(W)	Volts	Amps	effmot	effprop	adv	CT	CP	DV(m/s)	eff	Pelec	Pprop	cl_avg	cd_avg
1.000	5000.	0.000	6.677	0.1155	66.45	4.717	17.6273	0.7270	0.1104	0.01367	0.3323E-01	0.4113E-02	12.714	0.0803	83.15	6.677	0.9837	0.1846E-01	
2.000	5000.	0.000	6.266	0.1125	58.91	4.689	17.1946	0.7306	0.2127	0.02734	0.3119E-01	0.4008E-02	11.0712	0.1554	86.63	12.53	0.8440	0.1674E-01	
3.000	5000.	0.000	5.826	0.1091	57.15	4.657	16.7068	0.7348	0.3059	0.04181	0.2900E-01	0.3888E-02	9.8119	0.2247	77.78	17.48	0.7805	0.1567E-01	
4.000	5000.	0.000	5.357	0.1052	55.08	4.619	16.1218	0.7396	0.3890	0.05468	0.2666E-01	0.3748E-02	8.5954	0.2877	74.47	21.43	0.7132	0.1525E-01	
5.000	5000.	0.000	4.866	0.1006	52.66	4.575	15.4462	0.7452	0.4614	0.06836	0.2419E-01	0.3583E-02	7.4261	0.3438	70.67	24.30	0.6429	0.1554E-01	
6.000	5000.	0.000	4.335	0.9521E-01	49.89	4.524	14.6585	0.7517	0.5218	0.08203	0.2158E-01	0.3392E-02	6.3061	0.3922	66.32	26.01	0.5697	0.1646E-01	
7.000	5000.	0.000	3.783	0.8897E-01	46.59	4.465	13.7443	0.7592	0.5684	0.09570	0.1883E-01	0.3170E-02	5.2363	0.4315	61.37	26.48	0.4938	0.1797E-01	
8.000	5000.	0.000	3.291	0.8179E-01	42.82	4.396	12.6908	0.7676	0.5980	0.10937	0.1593E-01	0.2914E-02	4.2167	0.4590	55.79	25.61	0.4151	0.2089E-01	
9.000	5000.	0.000	2.591	0.7358E-01	38.53	4.318	11.4871	0.7767	0.6053	0.12304	0.1289E-01	0.2621E-02	3.2477	0.4760	49.00	23.49	0.3340	0.2272E-01	
10.000	5000.	0.000	1.953	0.6427E-01	33.65	4.229	10.1231	0.7860	0.5803	0.13671	0.9728E-02	0.2299E-02	2.3291	0.4561	42.81	19.53	0.2510	0.2639E-01	
11.000	5000.	0.000	1.292	0.5402E-01	28.28	4.132	8.6193	0.7942	0.5024	0.15038	0.6430E-02	0.1924E-02	1.4660	0.3990	35.61	14.21	0.1673	0.3110E-01	
12.000	5000.	0.000	0.6319	0.4343E-01	22.74	4.031	7.0667	0.7983	0.3335	0.16495	0.3145E-02	0.1547E-02	0.6818	0.2662	28.48	7.583	0.0867	0.3738E-01	
13.000	5000.	0.000	-0.1160E-01	0.3284E-01	17.19	3.930	5.5140	0.7934	-0.0088	0.17772	-0.5773E-04	0.1170E-02	-0.0119	-0.0070	21.67	-0.1508	0.0110	0.4497E-01	
14.000	5000.	0.000	-0.6249	0.2295E-01	12.02	3.836	4.0653	0.7798	-0.7279	0.19140	-0.3110E-02	0.8178E-03	-0.6075	-0.5611	15.59	-8.749	-0.0580	0.5440E-01	
15.000	5000.	0.000	-1.191	0.1460E-01	7.645	3.756	2.8407	0.7165	-2.3361	0.20507	-0.5926E-02	0.5202E-03	-1.0978	-1.6739	10.67	-17.86	-0.1182	0.6587E-01	

Figure 11 Sample output from QPROP

Once QPROP has given its output, the data can be dumped into an excel file and performance curves can be plotted to understand the propeller performance.

### 3.3 PROPELLER DESIGN PROCESS

The propeller has been designed with the help of various design points and then comparing the design points with each other and APC 11x4.7 propeller, which is the reference propeller. Our aim is to develop a propeller which gives better efficiency and comparable thrust for lower advance ratios, the cruise range of slow flyer quad-copters being 2m/s to 6m/s. Each design point refers to the input cruise velocity, input rotational speed (RPM) and the input thrust for QMIL to generate the propeller geometry. All design points are at a Reynolds number of  $10^5$ . Since we will be testing out multiple airfoils, thus each design point will be applied for all the airfoils.

Before comparing the design points, it is important to have a computational model (QPROP) of the reference propeller, APC 11x4.7, ready. Its geometric data was taken from the University of Illinois, Urbana Champagne propeller data base and was dumped into a QPROP input geometry file. According to the manufacturers of the propeller, APC, a company based in the

United States, the propeller consists of Eppeler 63 airfoil for the majority of the blade length and has CLARK Y airfoil near the tip. Thus, in the propeller geometry, the first 15 sections, out of total 18 sections, are kept as Eppeler 63 and the last three sections are kept as CLARK Y.

```
APC 11x4.7

2           ! Nblades

0.4355  9.8901   ! CL0      CL_a
-0.1798  1.4681   ! CLmin    CLmax

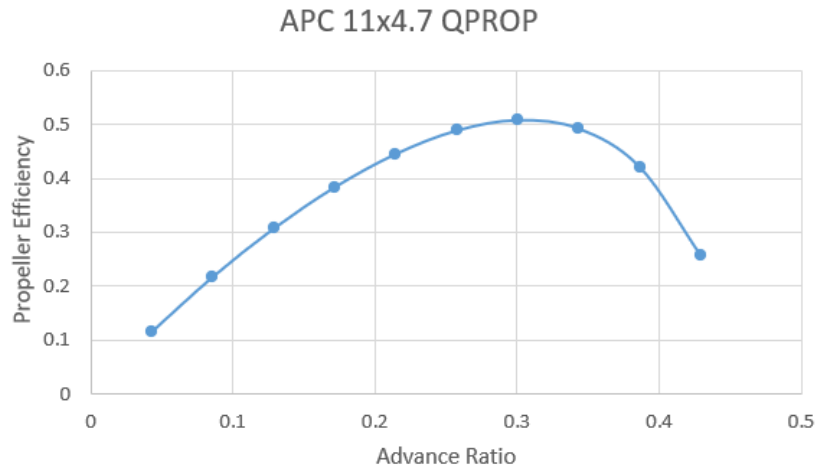
0.02115  0.0055882  0.064938  0.6028   ! CD0      CD2u     CD2l     CLCD0
100000   -0.5          ! REref    REexp

1.0      1.0      1.0   ! Rfac   Cfac   Bfac
0.0      0.0      0.0   ! Radd   Cadd   Badd

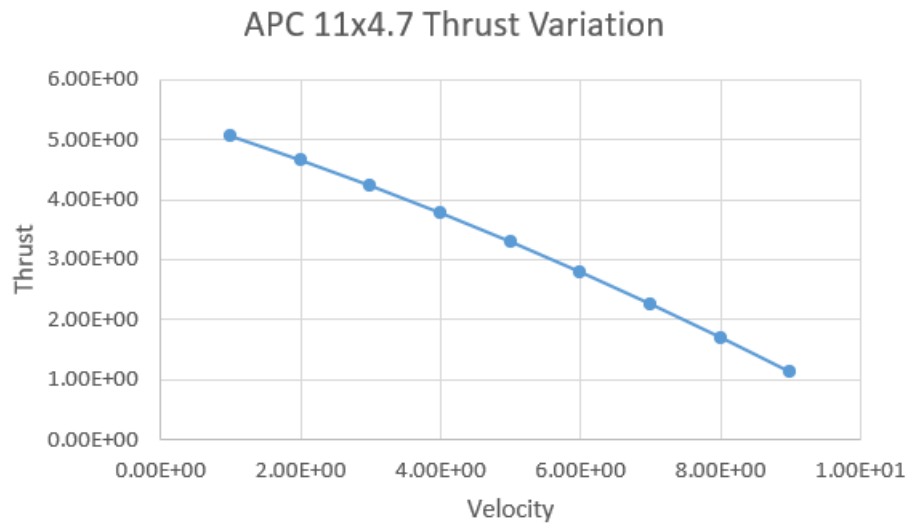
# r chord beta [ CL0  CL_a  CLmin CLmax  CD0   CD2u   CD2l   CLCD0  REref  REexp ]
0.020955 0.0156464 19.44
0.02794 0.0191389 21.61
0.034925 0.022352 22.25
0.04191 0.0252857 21.68
0.048895 0.0276606 20.53
0.05588 0.0294767 18.94
0.062865 0.0308737 17.1
0.06985 0.0317119 15.38
0.076835 0.032131 13.86
0.08382 0.0318516 12.51
0.090805 0.0310134 11.33
0.09779 0.0297561 10.27
0.104775 0.0278003 9.33
0.11176 0.0252857 8.43
0.118745 0.0220726 7.51
0.12573 0.0184404 4.61  0.3674 7.7928  -0.3727 1.3694  0.016907  0.0020025  0.021725  0.5797
0.132715 0.0117348 3.28  0.3674 7.7928  -0.3727 1.3694  0.016907  0.0020025  0.021725  0.5797
0.1397  0.0048895 1.93  0.3674 7.7928  -0.3727 1.3694  0.016907  0.0020025  0.021725  0.5797
```

*Figure 12 QPROP input file for APC 11x4.7*

The propeller is coupled with the A2212 BLDC motor and is run on QPROP with the rotational speed of the propeller being set as 5000 RPM. Once the data has been generated, it is dumped into an excel file and its performance curve plot is generated.



*Graph 3 Efficiency curve of APC 11x4.7*



*Graph 4 Thrust curve of APC 11x4.7*

As seen from the performance curves, APC 11x4.7 has a peak efficiency of 0.5084 at an advance ratio of 0.3 (7 m/s linear speed) and a maximum thrust of 5.15 N. In the cruise range of slow flyer quad-copters, the thrust produced by the propeller varies from 4.65 N to 2.8 N and the propeller efficiency varies from 0.2167 to 0.4891.

### **3.4 1<sup>st</sup> Design Point:**

The first design point was decided after a lot of experimentation and trial and error with the QMIL input file. For slow flyer propellers, the cruise speed is generally just before the peak efficiency and since the cruise range of slow flyer quad-copters is 2-6m/s, intuitively we should set the forward linear velocity somewhere in that range only. But since at those speeds, the thrust produced is quite high, the chord lengths of the propeller generated tend to be quite big.  
20

Since this is a quite small propeller, with a diameter of just 11 inches, or about 14 cm, chord lengths shouldn't exceed 4.5-5 cm. Keeping this in mind, the velocity and RPM for the QMIL input file were set as 10 m/s and 5000 RPM. The thrust was set as 3.5 N since according to the computational data provided by APC for 11x4.7 propeller, the thrust produced by it at 10 m/s and 5000 RPM is roughly equal to 3.5 N. The lift coefficient distribution along the blade length is kept as 0.6 at the root, 0.8 at the middle and 0.7 at the tip. This lift coefficient distribution is the industry standard for low speed propellers.

**NOTE:** Like almost all propeller related solvers, QMIL and QPROP don't work as efficiently and accurately for slow flying propellers compared to moderate to high speed propellers and this concern has been addressed in the 2<sup>nd</sup> and 3<sup>rd</sup> design points respectively.

### **3.5 2<sup>nd</sup> Design Point:**

Since the cruise speed in the 1<sup>st</sup> design point was set at 10 m/s, the peak efficiency was occurring at speeds in the range 11m/s-13m/s for various airfoils as expected. As will be shown in the later chapters, at the first design point, the efficiencies in the cruise range do not have a significant improvement over the efficiencies of the APC 11x4.7 and moreover the thrust generated by the propellers designed according to the first design point is quite low. Thus, to improve the performance of the propeller in lower speeds, in the 2<sup>nd</sup> design point, we needed to decrease the linear speed while simultaneously increase the RPM to account for the low thrust being generated by the 1<sup>st</sup> design point. As mentioned earlier, for lower speeds and higher RPMs, thrust to be generated is quite high which increases the chord length. Due to the minimum induced loss method of generating chord lengths, QMIL makes the big chord lengths at the root or very near to it, say at the next section to the root. With the maximum chord length at the root, which is already quite big for a propeller of 11-inch diameter, the chord length distribution decreases at a very fast rate meaning that chord lengths produced at the middle and the tip are quite small. It is important to understand that the relative velocity of the air is the least at the root, and increases till the tip, and since the elemental thrust produced for each section is proportional to the relative velocity of the wind at that section, for most propellers which have a maximum chord length near the centre or between the root and the centre of the blade length, the majority of the thrust is produced by the centre and the sections near the tip of the propeller blades. Blade roots hardly contribute to the overall thrust produced by the propeller blade and in some cases, root thrust can be negative too. This is primarily seen in large propeller blades as in those cases, the thrust and centrifugal loads on the propeller are quite high

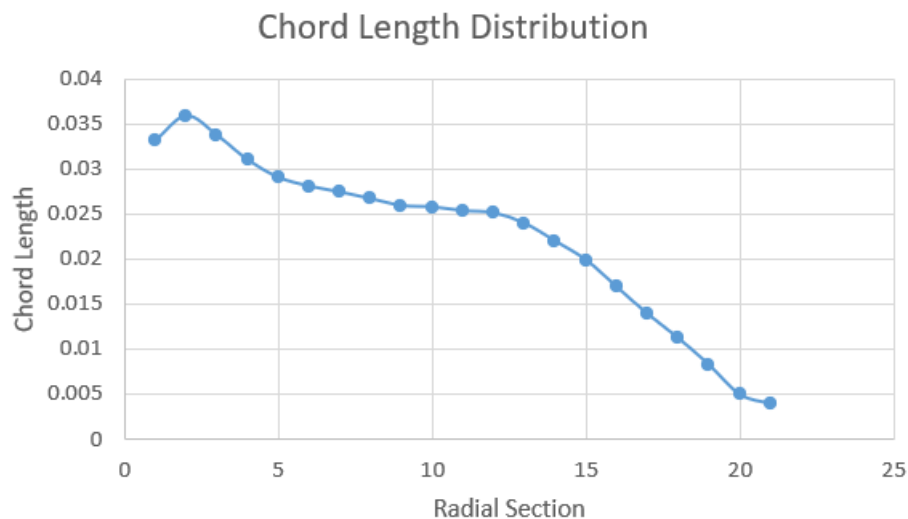
and the root has to provide structural rigidity to the blade and thus is not aerodynamically shaped. In our case, our propeller is small thus the overall load on the propeller is not so high thus the root, even though aerodynamically shaped, contributes too little to the overall thrust. Thus, having a very large chord length at the root and quite small chord lengths at the centre and the tip of the blade length provide very little thrust as a whole and since we wish for a higher thrust generation from our propeller, the chord lengths generated by QMIL are not used in the 2<sup>nd</sup> design iteration. Instead, a new chord distribution is generated by hit and trial method in order to generate adequate thrust. Since all our propellers designed in QMIL have 21 sections, the chord length distribution has been developed for 21 sections.

Radial Section	Chord Length (cm)
1	3.33155
2	3.5876
3	3.3728
4	3.0984
5	2.9055
6	2.8081
7	2.7433
8	2.6695
9	2.5933
10	2.578
11	2.5364
12	2.5126
13	2.3965
14	2.1975
15	1.9891

16	1.6891
17	1.3915
18	1.1235
19	0.8265
20	0.5
21	0.3975

*Table 1 Modified Chord length distribution for 2nd design point*

If observed carefully, it can be seen that the chord length, while is maximum near the root, does not decrease as rapidly till the tip. Moreover, the rate of decrease of chord lengths at the centre of the blade length (section 9 to 12) is quite insignificant and the chord length values are also quite high (~2.5 cm). This is to ensure that the thrust produced by this type of chord length distribution is adequate.



*Graph 5 Modified chord length distribution for 2nd design point*

The lift coefficient distribution has been kept as 0.3 at the root, 0.9 at the middle and 0.8 at the tip. This was done primarily to decrease the pitch and the pitch angles of the propeller in order to shift the efficiency plot to the left and thus have higher efficiency at lower speeds. Since the root of the blade doesn't contribute much to the thrust produced, decreasing the lift coefficient there won't have much effect on the thrust, considering thrust decreases with decreasing lift coefficient. Decreasing the lift coefficient leads to the pitch angles getting decreased. A rough

explanation for this would be to consider the lift polar of the particular airfoil section where the lift coefficient increases with increasing angle of attack till a maximum value. If the lift coefficient at the root is decreased from 0.6 to 0.3, this means that the angle of attack at that airfoil will be decreased. For a particular relative air velocity, the pitch angle will be lower for a lower angle of attack. Thus, the pitch angles obtained are lower across the blade length. Furthermore, since the coefficient of lift at the root has been decreased, and thus the angle of attack subsequently, the angle of attack at the root is further away from the optimal angle of attack thus decreasing the maximum efficiency achievable. Since our end goal is the efficiency in the lower advance ratios only, lowering maximum efficiency doesn't matter much. In summary, the 2<sup>nd</sup> design point is:

*Cruise velocity: 7 m/s*

*RPM = 7000*

*Thrust = 6 N*

*Propeller radius = 0.1397 m (11-inch propeller diameter)*

*Hub radius = 0.6 cm*

*Lift coefficient distribution:*

*Root: 0.3*

*Middle: 0.9*

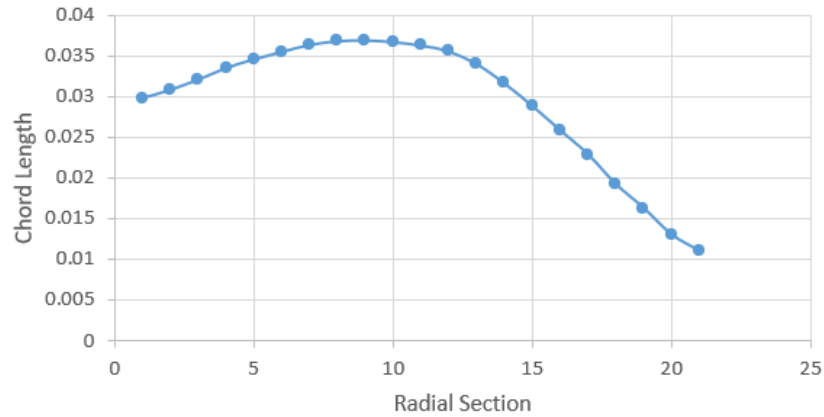
*Tip: 0.8*

### **3.6 3<sup>rd</sup> Design Point:**

The third design point was made solely to increase the thrust being produced by the propeller with the help of further chord length distribution manipulation. The chord lengths in this distribution have been increased (keeping the maximum chord length = 3.7 cm) and the maximum chord length position has been shifted to the centre of the blade, contrary to the previous design points, where the maximum chord lengths were near the root

Radial Section	Chord Length (cm)
1	2.9855
2	3.0876
3	3.2128
4	3.3584
5	3.4655
6	3.5581
7	3.6433
8	3.6895
9	3.7
10	3.678
11	3.6364
12	3.5626
13	3.4065
14	3.1675
15	2.8891
16	2.5891
17	2.2915
18	1.9235
19	1.6264
20	1.3
21	1.0975

*Table 2 Modified chord length distribution for 3rd design point*



*Graph 6 Modified chord length distribution for 3rd design point*

Other than the chord length distribution, all of the other parameters remain the same as the 2<sup>nd</sup> Design Point

## CHAPTER 4: Airfoils Used And Their Aerodynamic Analysis

A total of 10 airfoils have been used for this project. All of the selected airfoils are universally used for slow flyer propellers and are relatively thin. The airfoils selected are:

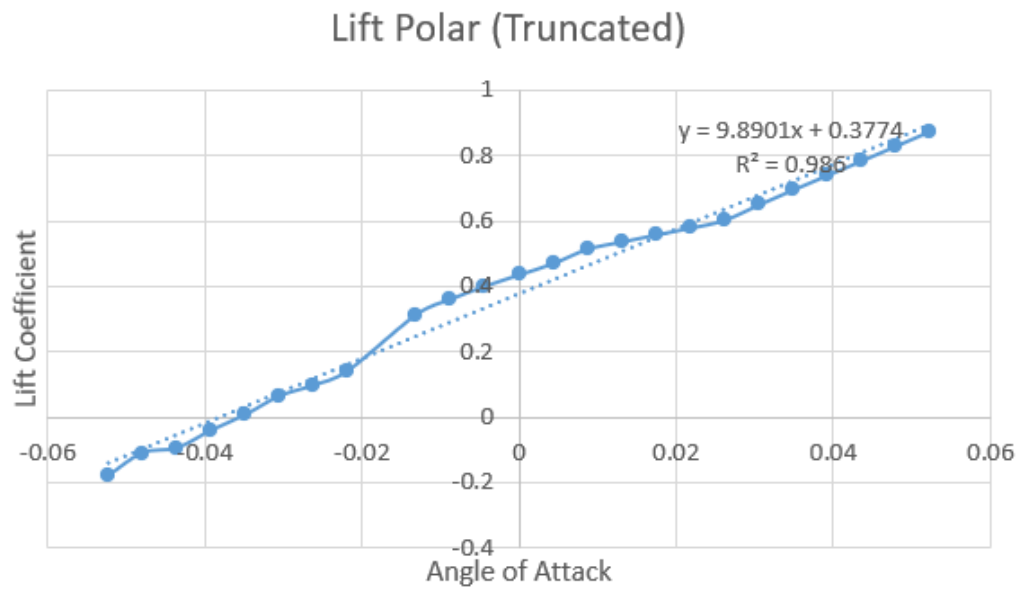
Airfoil	Thickness/Chord length = x% of chord length
Eppeler 63	4.25
Clark Y	11.7
ARAD 10	11.7
BE 50	7.3
MH22 7.2%	7.2
MH30 7.84%	7.84
MH32 8.7%	8.7
MH43 8.5%	8.5
MH64 8.59%	8.59
S7055	10.5

*Table 3 Selected airfoils and their thicknesses*

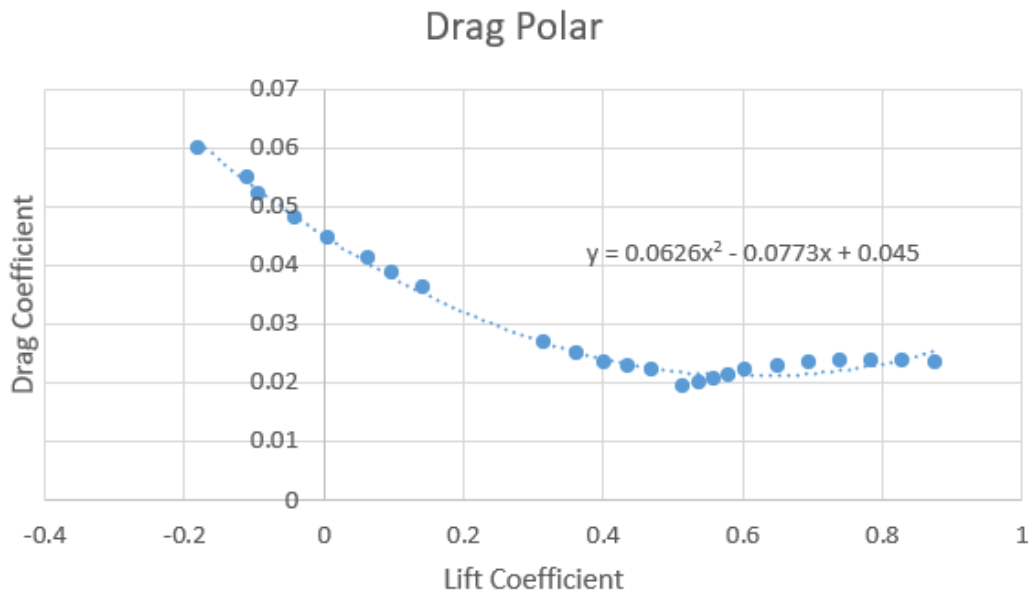
As mentioned in chapter 2, it is necessary to carry out an aerodynamic analysis of each airfoil to calculate various aerodynamic variables which are input into QMIL. Each airfoil is loaded into XFOIL and a polar analysis is carried out at Reynolds number of  $10^5$  for an angle of attack range of  $-40^\circ$  to  $40^\circ$ . Once the polar data is obtained, it is dumped into an excel file where the lift and drag curves are plotted and the lift curve is truncated obtain a good linear fit. Using a linear fit for the truncated lift curve and a parabolic fit for the drag curve, the aerodynamic variables are calculated.

**NOTE:** The aerodynamic variables, especially the ones related to drag, have been calculated from the parabolic fit curve on the drag polar and not the actual drag values obtained from XFOIL.

#### 4.1 Eppeler 63:



Graph 7 Eppeler 63 lift polar curve fitment

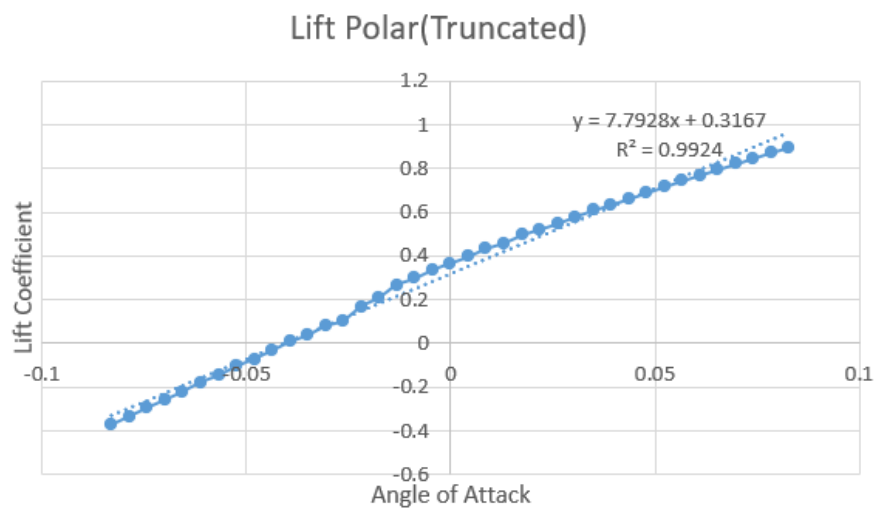


Graph 8 Eppeler 63 drag polar curve fitment

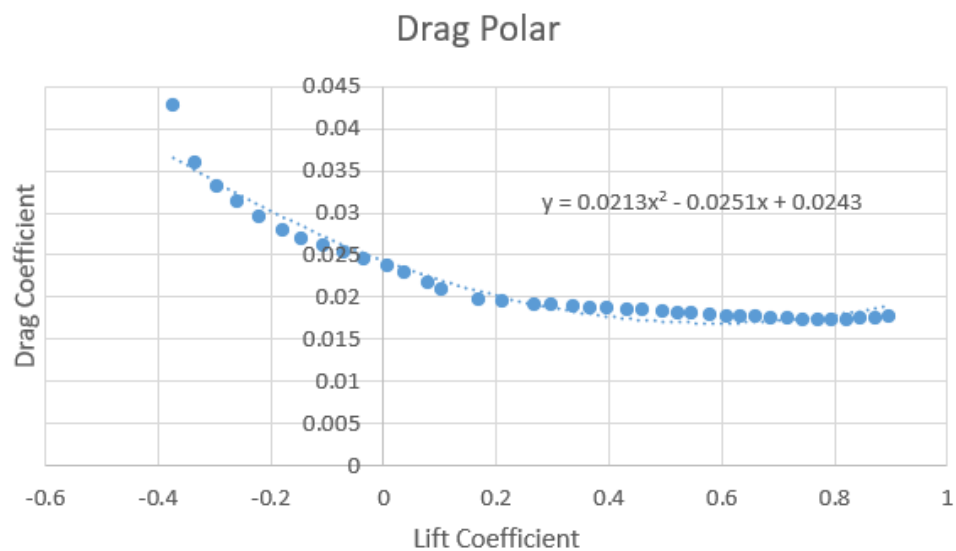
Aerodynamic Variable	Value
Cd0	0.01941
ClCd0	0.5143
Cd2l	0.084376
Cd2u	0.004342
Re <sub>ref</sub>	100000
Re <sub>exp</sub>	-0.5
Cl0	0.4355
ΔC <sub>Du</sub>	0.00395
ΔC <sub>Lu</sub>	0.9538
ΔC <sub>Ll</sub>	-0.6941
ΔC <sub>Dl</sub>	0.04065
Cl <sub>max</sub>	1.4681
Cl <sub>min</sub>	-0.1798
CdCl <sub>max</sub>	0.02336
CdCl <sub>min</sub>	0.06006
Cla	9.8901

Table 4 Aerodynamic variable values for Eppeler 63

## 4.2 Clark Y:



Graph 9 Clark Y lift polar curve fitment



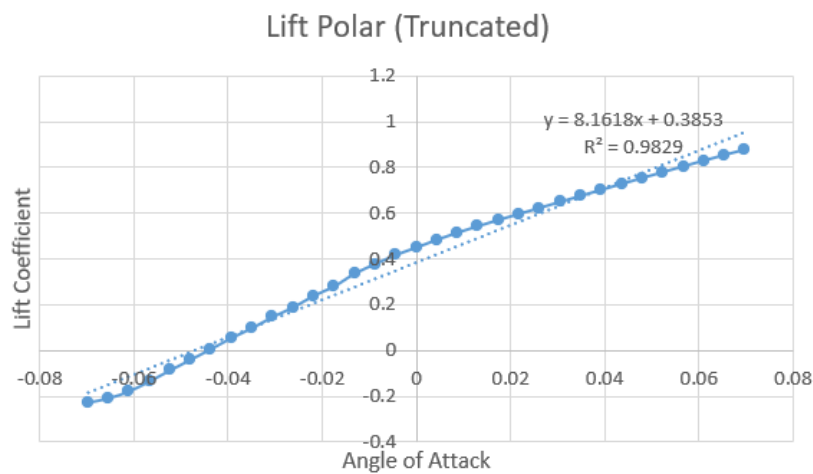
Graph 10 Clark Y drag polar curve fitment

Aerodynamic Variable	Value
Cd0	0.01727
ClCd0	0.7699
Cd2l	0.019456

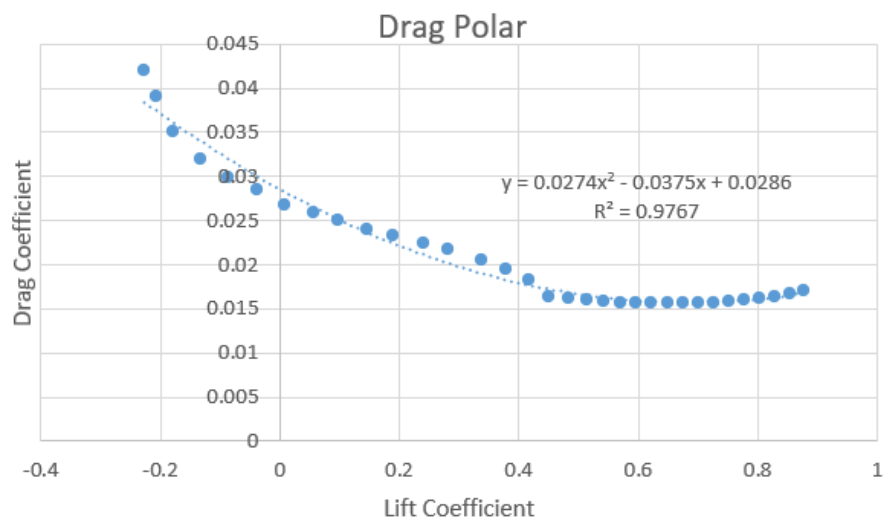
Cd2u	0.001224
Re <sub>ref</sub>	100000
Re <sub>exp</sub>	-0.5
Cl <sub>0</sub>	0.3674
ΔC <sub>Du</sub>	0.00044
ΔC <sub>Lu</sub>	0.5995
ΔC <sub>L1</sub>	-1.1426
ΔC <sub>D1</sub>	0.0254
Cl <sub>max</sub>	1.3694
Cl <sub>min</sub>	-0.3727
CdCl <sub>max</sub>	0.01771
CdCl <sub>min</sub>	0.04267
Cl <sub>a</sub>	7.7928

Table 5 Aerodynamic variable values for Clark Y

#### 4.3 ARAD-10:



Graph 11 ARAD-10 lift polar curve fitment



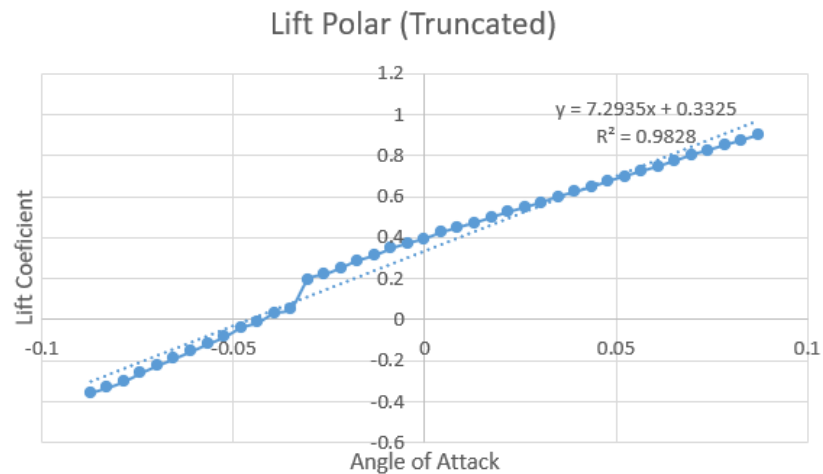
Graph 12 ARAD-10 drag polar curve fitment

Aerodynamic Variable	Value
$C_d 0$	0.01562
$C_l C_d 0$	0.6752
$C_d 2l$	0.032407
$C_d 2u$	0.001886
$Re_{ref}$	100000
$Re_{exp}$	-0.5
$C_l 0$	0.45
$\Delta C_{Du}$	0.00149
$\Delta C_{Lu}$	0.8889
$\Delta C_{Ll}$	-0.9012
$\Delta C_{Dl}$	0.02632
$C_l_{max}$	1.5641

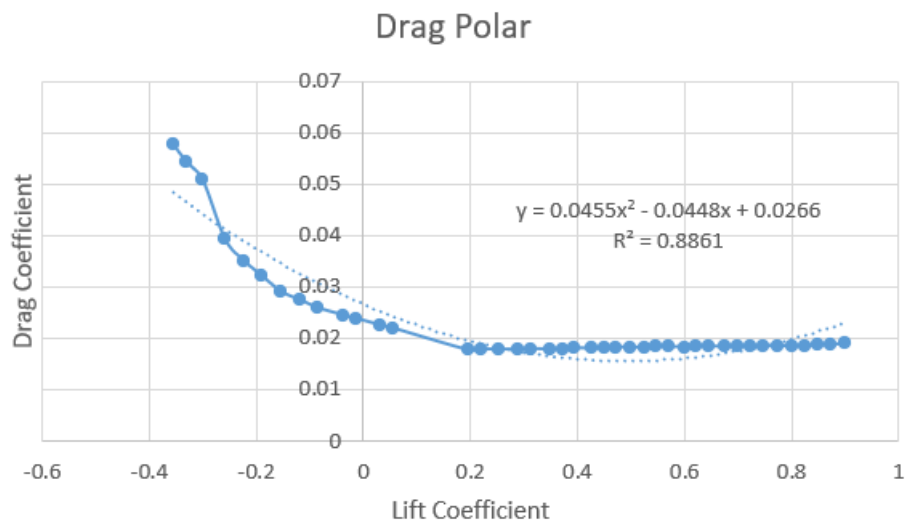
$C_{l\min}$	-0.226
$C_d C_{l\max}$	0.01771
$C_d C_{l\min}$	0.04194
$C_{la}$	8.1618

Table 6 Aerodynamic variable values for ARAD-10

#### 4.4 S7055



Graph 13 S7055 lift polar curve fitment

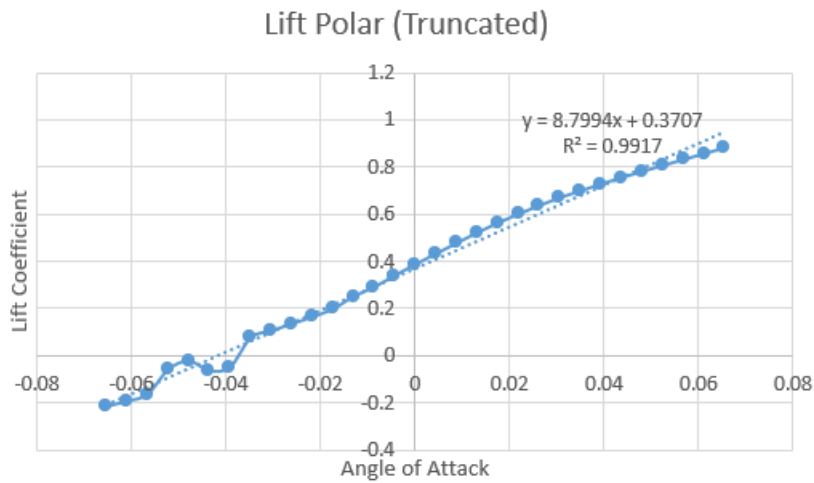


Graph 14 S7055 drag polar curve fitment

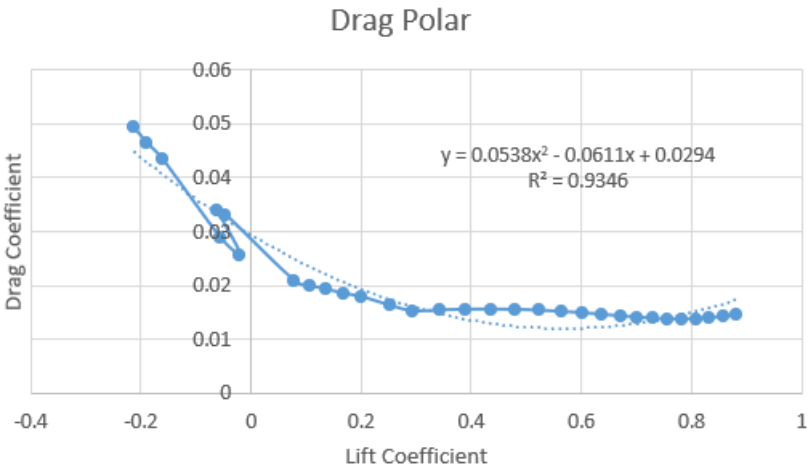
Aerodynamic Variable	Value
Cd0	0.01771
ClCd0	0.1947
Cd2l	0.131934
Cd2u	0.001054
Re <sub>ref</sub>	100000
Re <sub>exp</sub>	-0.5
Cl0	0.3952
ΔC <sub>Du</sub>	0.0012
ΔC <sub>Lu</sub>	1.0668
ΔC <sub>Ll</sub>	-0.55
ΔC <sub>Dl</sub>	0.03991
Cl <sub>max</sub>	1.2615
Cl <sub>min</sub>	-0.3553
CdCl <sub>max</sub>	0.01891
CdCl <sub>min</sub>	0.05762
Cla	7.2935

Table 7Aerodynamic variable values for S7055

#### 4.5. BE 50:



Graph 15 BE50 lift polar curve fitment



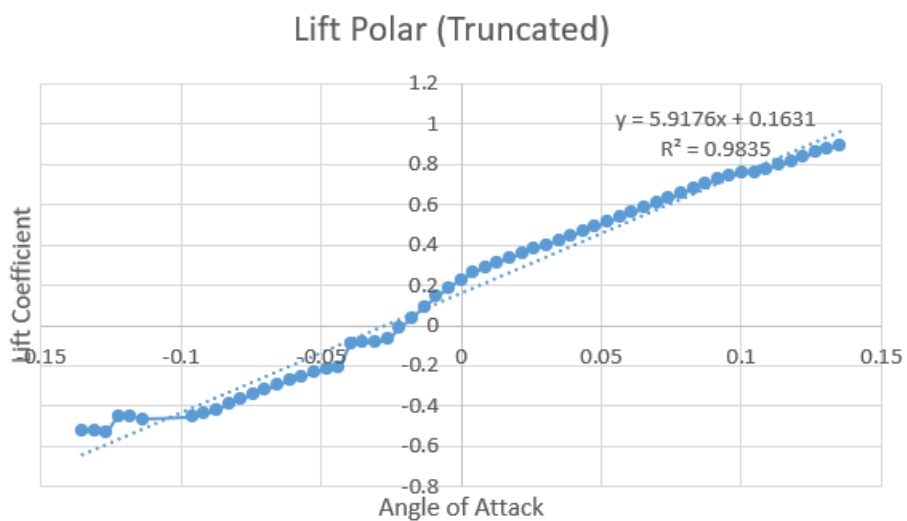
Graph 16 BE50 drag polar curve fitment

Aerodynamic Variable	Value
Cd0	0.0137
ClCd0	0.7829
Cd2l	0.03588
Cd2u	0.00222
Re <sub>ref</sub>	100000

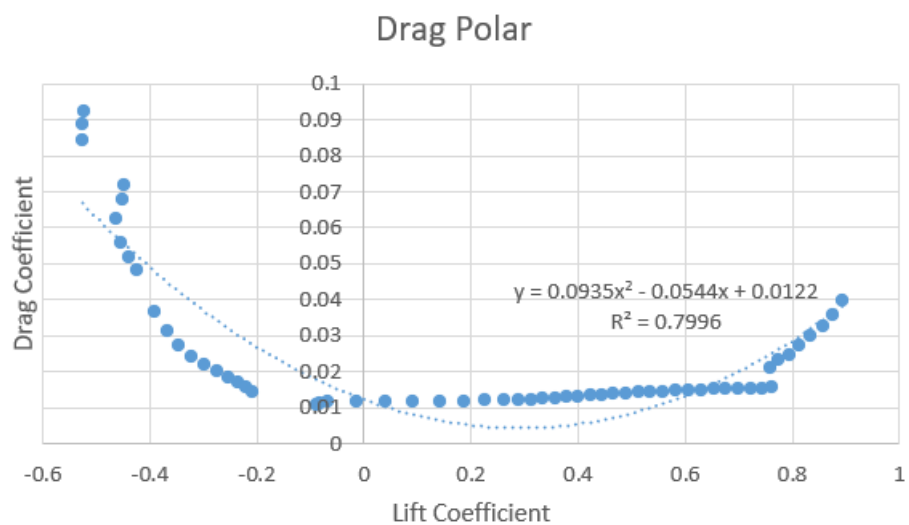
$Re_{exp}$	-0.5
$Cl_0$	0.3894
$\Delta C_{Du}$	0.00089
$\Delta C_{Lu}$	0.6326
$\Delta C_{Ll}$	-0.9953
$\Delta C_{Dl}$	0.03554
$Cl_{max}$	1.4155
$Cl_{min}$	-0.2124
$CdCl_{max}$	0.01459
$CdCl_{min}$	0.04924
$Cla$	8.7994

Table 8 Aerodynamic variable values for BE50

#### 4.6 MH22 (7.2%):



Graph 17 MH22 (7.2%) lift polar curve fitment



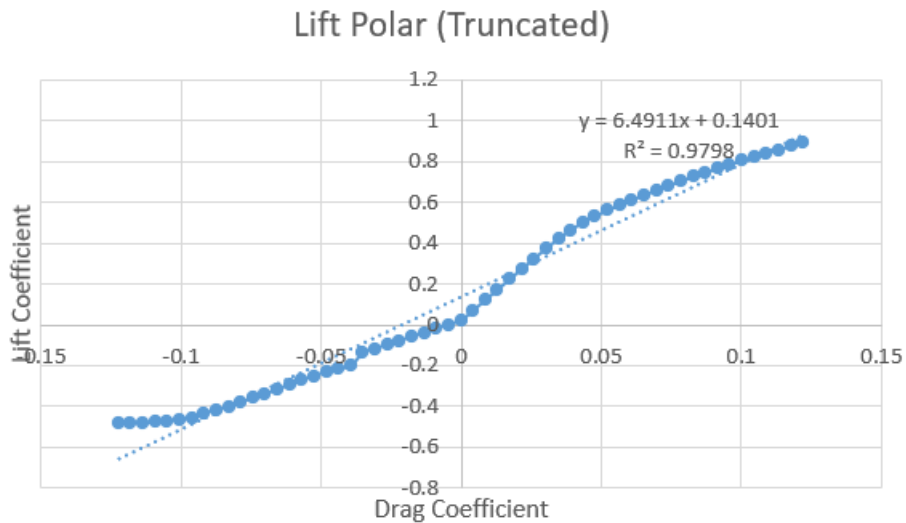
Graph 18 MH22 (7.2%) drag polar curve fitment

Aerodynamic Variable	Value
$C_d 0$	0.01066
$C_l C_d 0$	-0.0893
$C_d 2l$	0.385606
$C_d 2u$	0.027755
$Re_{ref}$	100000
$Re_{exp}$	-0.5
$C_l 0$	0.2273
$\Delta C_{Du}$	0.02882
$\Delta C_{Lu}$	1.019
$\Delta C_{L1}$	-0.4373
$\Delta C_{D1}$	0.07374
$C_l_{max}$	0.9297

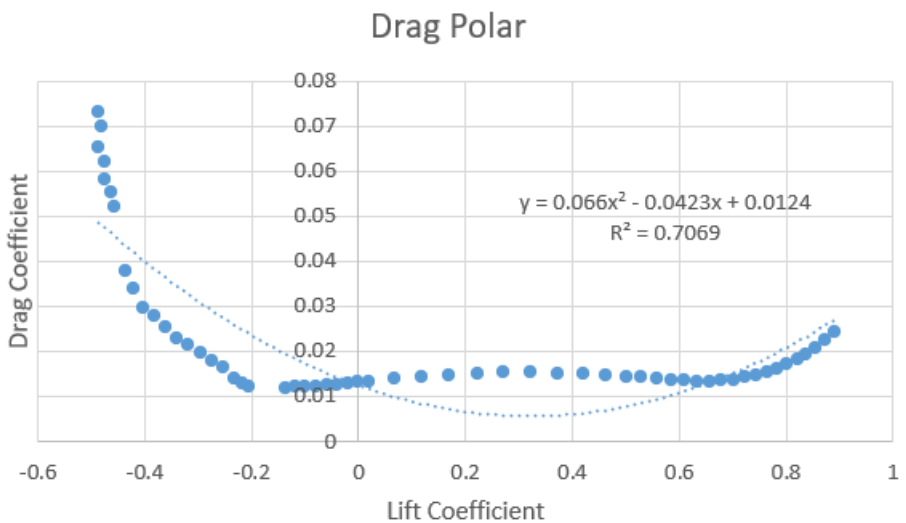
Cl <sub>min</sub>	-0.5266
CdCl <sub>max</sub>	0.03948
CdCl <sub>min</sub>	0.0844
Cl <sub>a</sub>	5.9176

Table 9 Aerodynamic variable values for MH22 (7.2%)

#### 4.7 MH30 (7.84%):



Graph 19 MH30 (7.84%) lift polar curve fitment

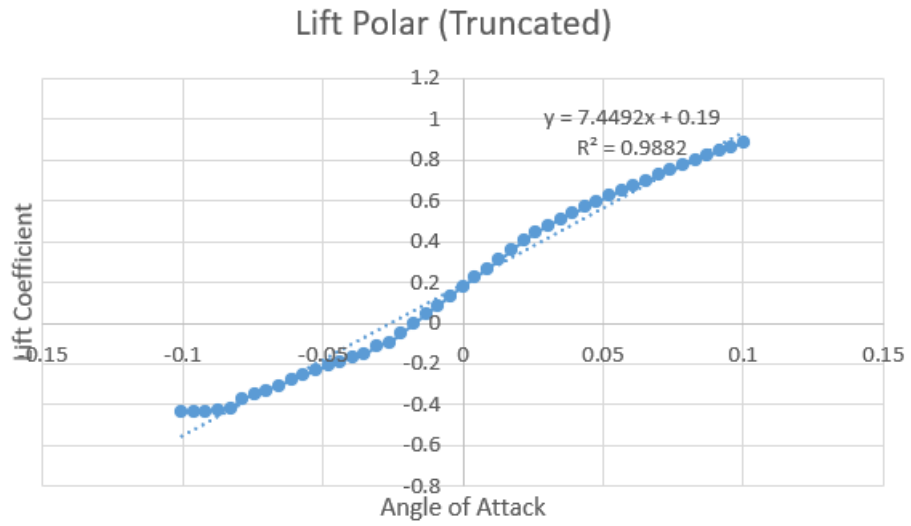


Graph 20 MH30 (7.84%) drag polar curve fitment

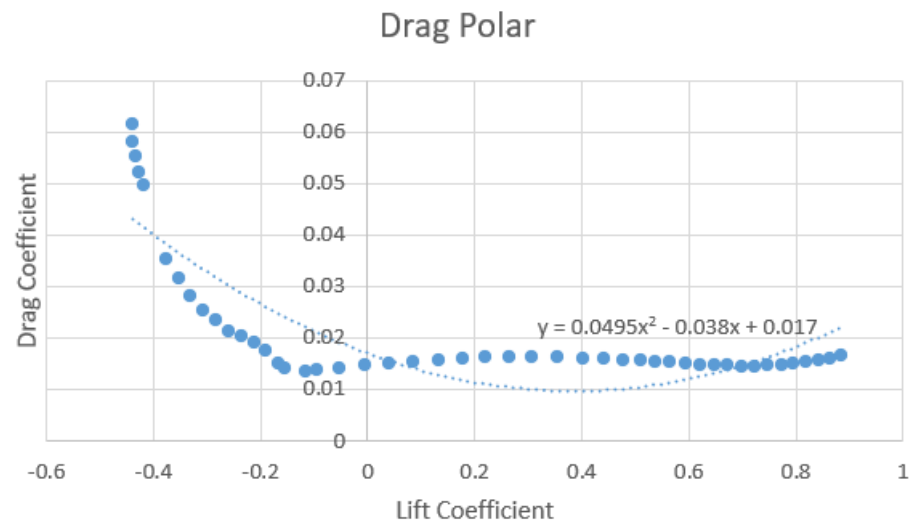
Aerodynamic Variable	Value
Cd0	0.01191
ClCd0	-0.1359
Cd2l	0.496708
Cd2u	0.009354
Re <sub>ref</sub>	100000
Re <sub>exp</sub>	-0.5
Cl0	0.0193
ΔC <sub>Du</sub>	0.01225
ΔC <sub>Lu</sub>	1.1444
ΔC <sub>Ll</sub>	-0.3509
ΔC <sub>Dl</sub>	0.06116
Cl <sub>max</sub>	1.0085
Cl <sub>min</sub>	-0.4868
CdCl <sub>max</sub>	0.02416
CdCl <sub>min</sub>	0.07307
Cla	6.4911

Table 10 Aerodynamic variable values for MH30 (7.84%)

#### 4.8 MH32 (8.7%):



Graph 21 MH32 (8.7%) lift polar curve fitment

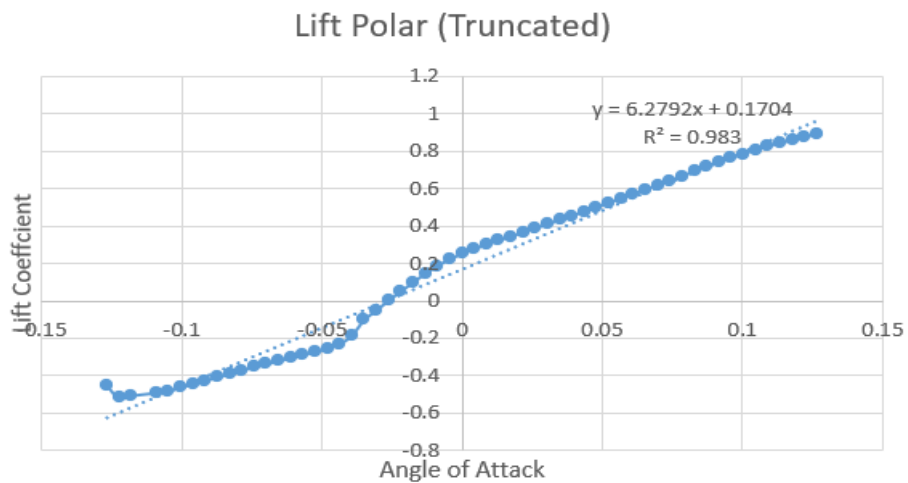


Graph 22 MH32 (8.7%) drag polar curve fitment

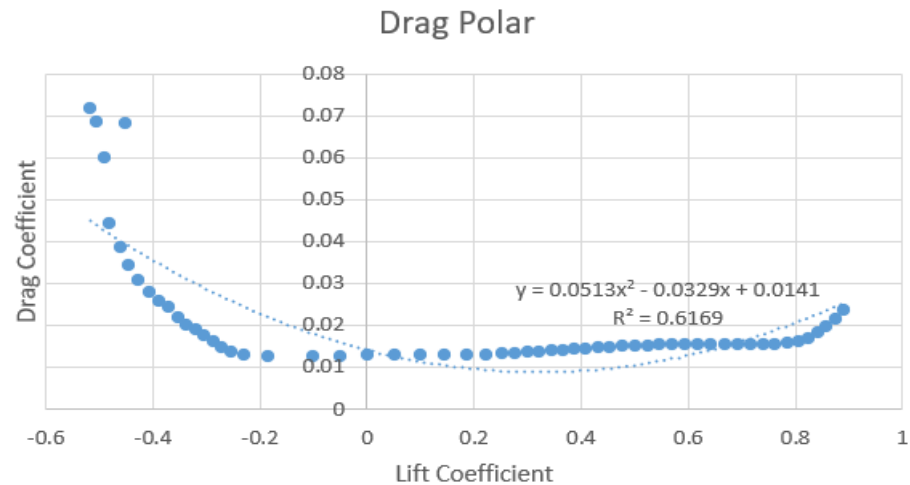
Aerodynamic Variable	Value
Cd0	0.01348
ClCd0	-0.1162
Cd2l	0.461513
Cd2u	0.001885
Re <sub>ref</sub>	100000
Re <sub>exp</sub>	-0.5
Cl0	0.1797
ΔC <sub>Du</sub>	0.00302
ΔC <sub>Lu</sub>	1.2659
ΔC <sub>Ll</sub>	-0.3226
ΔC <sub>Dl</sub>	0.04803
Cl <sub>max</sub>	1.1497
Cl <sub>min</sub>	-0.4388
CdCl <sub>max</sub>	0.0165
CdCl <sub>min</sub>	0.06151
Cla	7.4492

Table 11 Aerodynamic variable values for MH32 (8.7%)

#### 4.9 MH43 (8.5%):



Graph 23 MH43 (8.5%) lift polar curve fitment



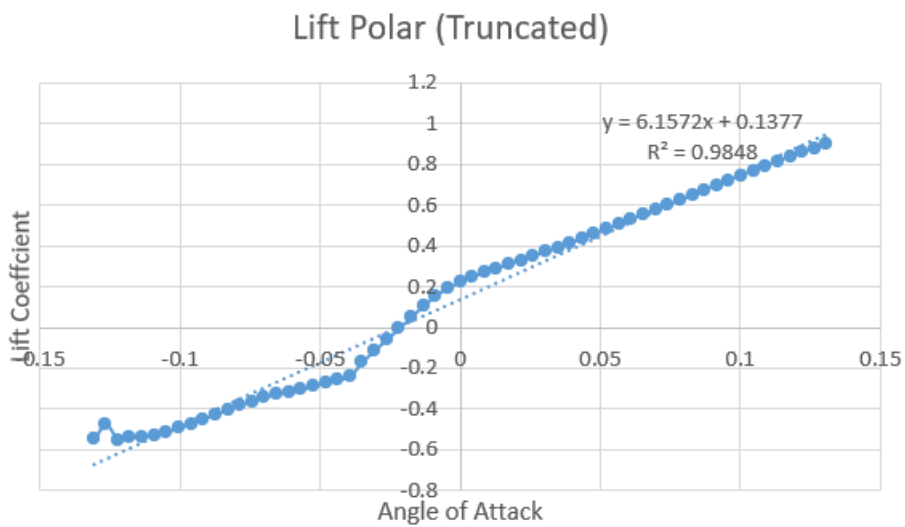
Graph 24 MH43 (8.5%) drag polar curve fitment

Aerodynamic Variable	Value
Cd0	0.01244
ClCd0	-0.1839
Cd2l	0.533645
Cd2u	0.007641
Re <sub>ref</sub>	100000

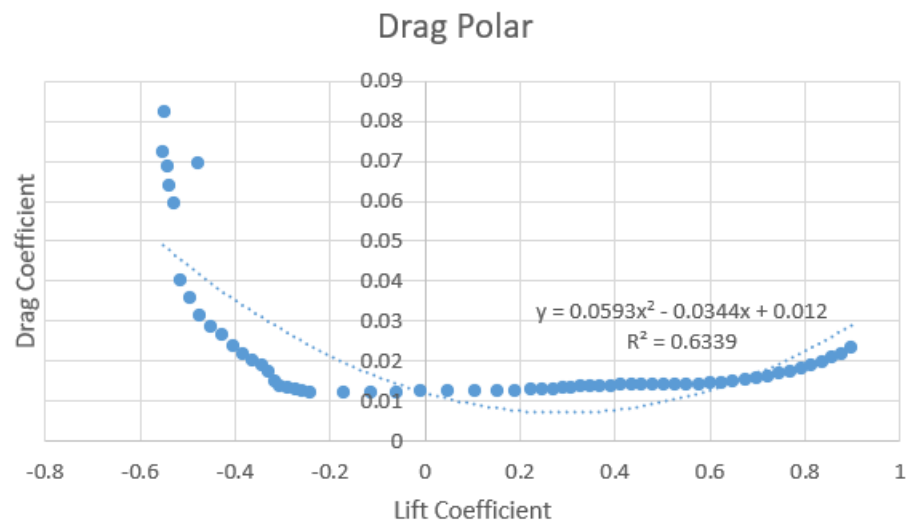
$Re_{exp}$	-0.5
$Cl_0$	0.2527
$\Delta C_{Du}$	0.01108
$\Delta C_{Lu}$	1.2042
$\Delta C_{Ll}$	-0.3338
$\Delta C_{Dl}$	0.05946
$Cl_{max}$	1.0203
$Cl_{min}$	-0.5177
$CdCl_{max}$	0.02352
$CdCl_{min}$	0.0719
$Cla$	6.2792

Table 12 Aerodynamic variable values for MH43 (8.5%)

#### 4.10 MH64 (8.59%):



Graph 25 MH64 (8.59%) lift polar curve fitment



Graph 26 MH64 (8.59%) drag polar curve fitment

Aerodynamic Variable	Value
Cd0	0.01188
ClCd0	-0.1713
Cd2l	0.420566
Cd2u	0.007853
Re <sub>ref</sub>	100000
Re <sub>exp</sub>	-0.5
Cl0	0.2223
ΔC <sub>Du</sub>	0.01124
ΔC <sub>Lu</sub>	1.1964
ΔC <sub>Ll</sub>	-0.3795
ΔC <sub>Dl</sub>	0.06057
Cl <sub>max</sub>	1.0251
Cl <sub>min</sub>	-0.5508

CdClmax	0.02312
CdClmin	0.07245
Cla	6.1572

Table 13 Aerodynamic variable values for MH64 (8.59%)

## Chapter 5: 1<sup>st</sup> Design Point

As mentioned in chapter 3, the 1<sup>st</sup> design point has the following QMIL input parameter:

Cruise linear speed (m/s)	10
Rotational Speed (RPM)	5000
Thrust (N)	3.5
Chord Length Distribution	QMIL
Lift coefficient Distribution	0.6,0.8,0.7
Blade Radius (m)	0.1397

Table 14 1st design point parameters

Since we have 10 airfoils, we will be generating a propeller for each airfoil using QMIL and using QPROP, we will be analysing their propeller performance which will be compared with APC 11x4.7 QPROP data in order to understand the validity of the design point and if some further changes need to be made. For a particular airfoil, its aerodynamic variables will be input into the QMIL file for generating the propeller geometry. The propeller performance of each propeller is calculated at a rotational speed of 5000 RPM.

### 5.1 Propeller with ARAD-10 airfoil:

```

Template prop

2          ! Nblades
0.4500   8.1618    ! CL0      CL_a
-0.2260   1.5641    ! CLmin   CLmax

0.01562   0.001886  0.032407  0.6752  ! CD0      CD2u     CD2l   CLCD0
100000.0 -0.5           ! REref   REexp

0.0  0.5  1.0  ! Xides   (r/R locations where design cl is specified)
0.6  0.8  0.7  ! CLdes   (specified cl)

0.006    ! hub radius(m)
0.1397   ! tip radius(m)
10.00    ! speed(m/s)
5000    ! rpm

3.5      ! Thrust(N)  ( 0 if power specified )
0.0      ! Power(W)   ( 0 if thrust specified )

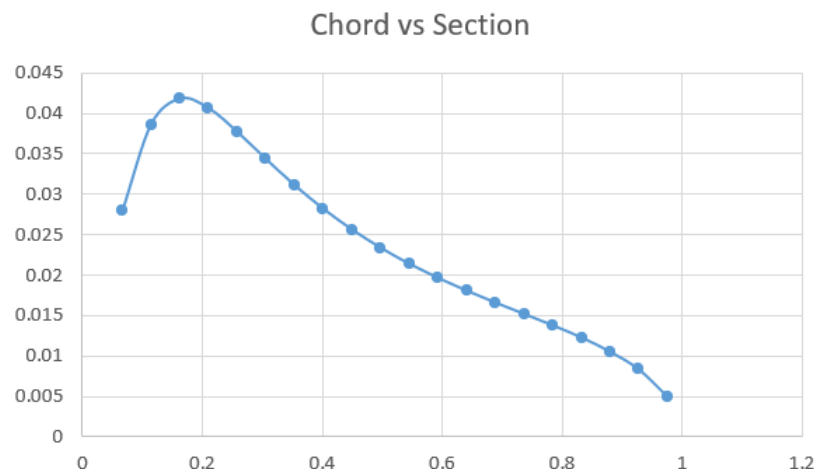
0  0.0  ! Ldes   [ KQdes ]
# 18    ! Nout    number of output stations (optional)

```

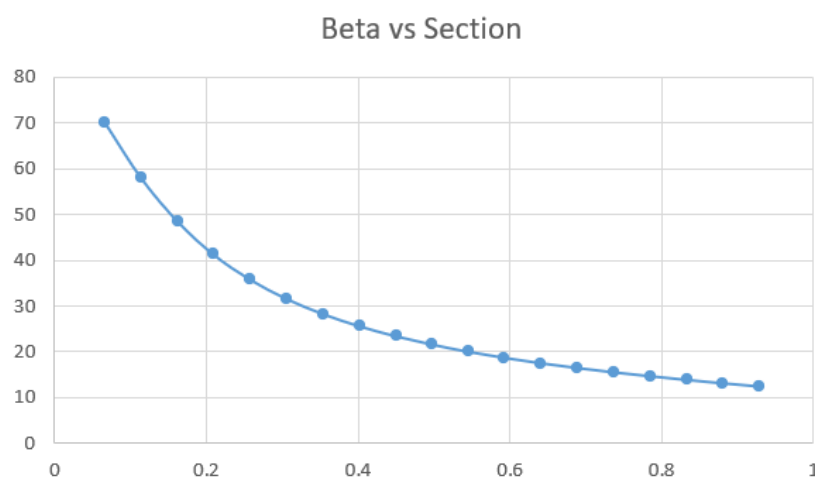
Figure 13 QMIL input file for ARAD-10

Radial Section (cm)	Chord Length (cm)	Pitch Angle (degree)
0.93599	2.7926	70.19
1.600655	3.8627	57.96
2.27711	4.1784	48.46
2.9337	4.0625	41.27
3.60426	3.7705	35.8
4.27482	3.4338	31.57
4.94538	3.1097	28.25
5.61594	2.8177	25.58
6.2865	2.5607	23.39
6.95706	2.3358	21.56
7.61365	2.1402	20.01
8.28421	1.9656	18.67
8.95477	1.8077	17.49
9.62533	1.661	16.45
10.29589	1.5199	15.5
10.96645	1.3788	14.65
11.63701	1.228	13.85
12.2936	1.0547	13.11
12.96416	0.8354	12.42
13.63472	0.4973	11.76

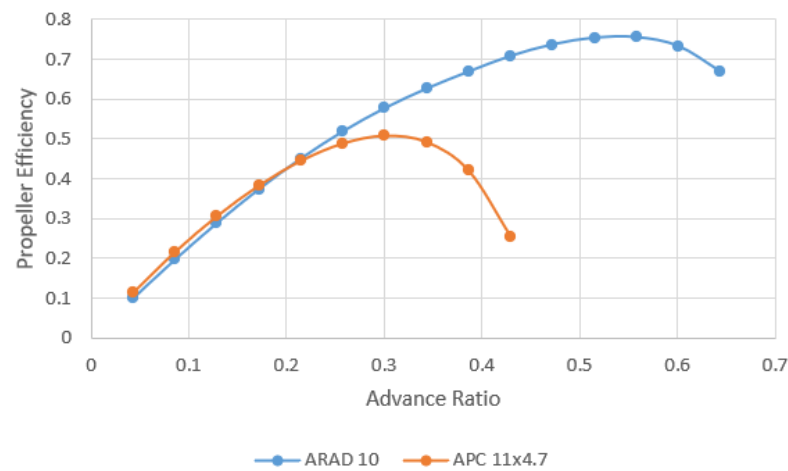
Table 15 QMIL generated propeller geometry for ARAD-10



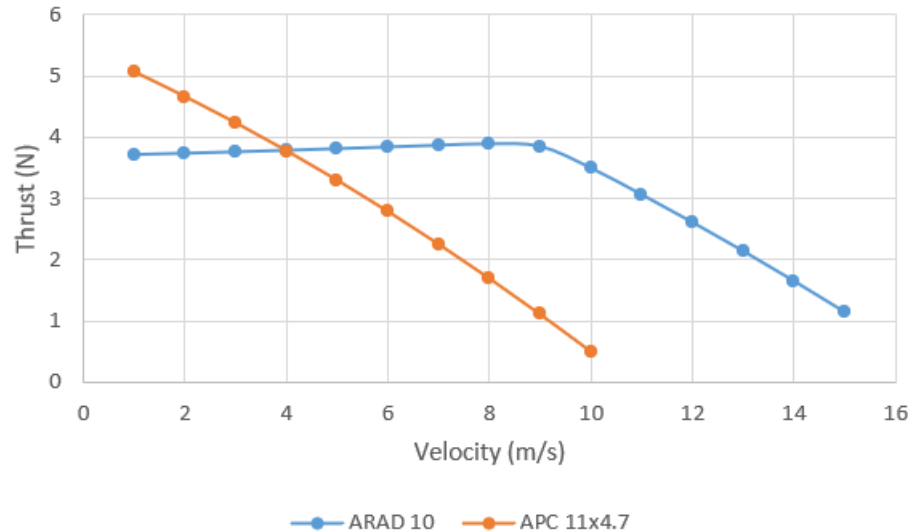
*Graph 27 QMIL generated chord distribution for ARAD-10*



*Graph 28 QMIL generated pitch angle distribution for ARAD-10*



*Graph 29 Propeller efficiency curve comparison between ARAD-10 and APC 11x4.7*



Graph 30 Thrust curve comparison between ARAD-10 and APC 11x4.7

## 5.2 Propeller with BE 50 airfoil

Template prop

```

2           ! Nblades

0.3894  8.7994    ! CL0      CL_a
-0.2124  1.4155    ! CLmin   CLmax

0.0137  0.00222  0.03588 0.7829  ! CD0      CD2u     CD2l   CLCD0
100000.0 -0.5          ! REref   REexp

0.0  0.5  1.0  ! XIdes   (r/R locations where design cl is specified)
0.6  0.8  0.7  ! CLdes   (specified cl)

0.006    ! hub radius(m)
0.1397   ! tip radius(m)
10.00    ! speed(m/s)
5000    ! rpm

3.5|    ! Thrust(N)  ( 0 if power specified )
0.0  ! Power(W)   ( 0 if thrust specified )

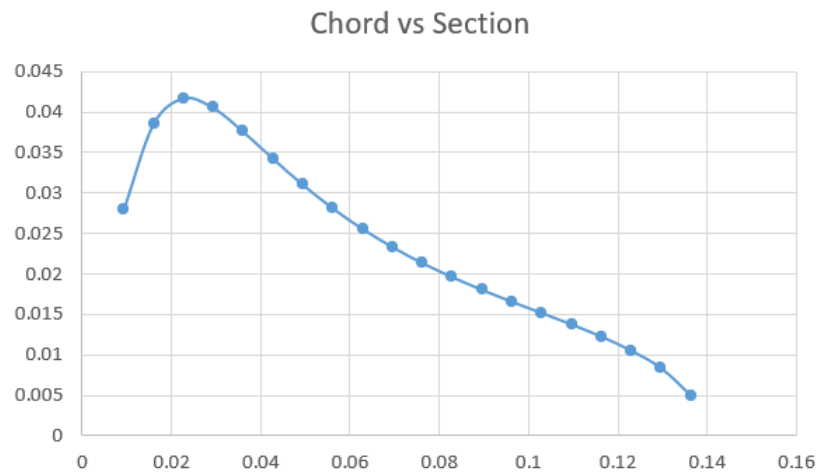
0   0.0  ! Ldes   [ KQdes ]
# 18    ! Nout    number of output stations (optional)

```

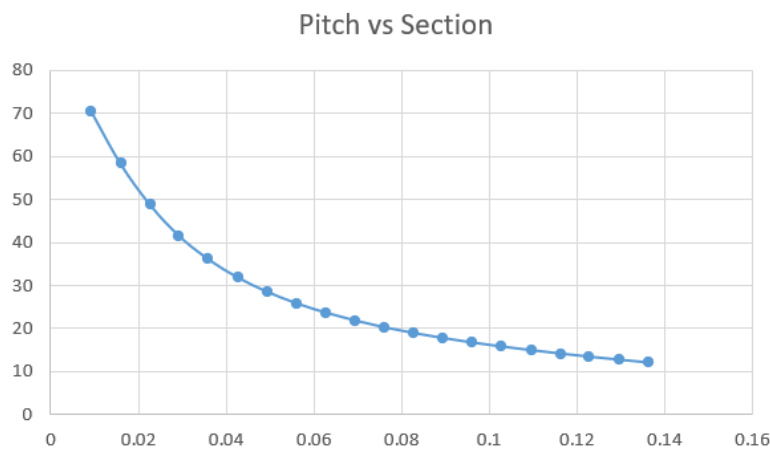
Figure 14 QMIL input file for BE 50

Radial Section (cm)	Chord Length (cm)	Pitch Angle (degree)
0.93599	2.789809	70.48
1.600655	3.858514	58.23
2.27711	4.174236	48.72
2.9337	4.058285	41.52
3.60426	3.764915	36.04
4.27482	3.428238	31.81
4.94538	3.105531	28.48
5.61594	2.813558	25.8
6.2865	2.55651	23.61
6.95706	2.33299	21.78
7.61365	2.13741	20.22
8.28421	1.962785	18.88
8.95477	1.804924	17.71
9.62533	1.658239	16.66
10.29589	1.518539	15.73
10.96645	1.376045	14.88
11.63701	1.225169	14.09
12.2936	1.053338	13.36
12.96416	0.835406	12.67
13.63472	0.495935	12.02

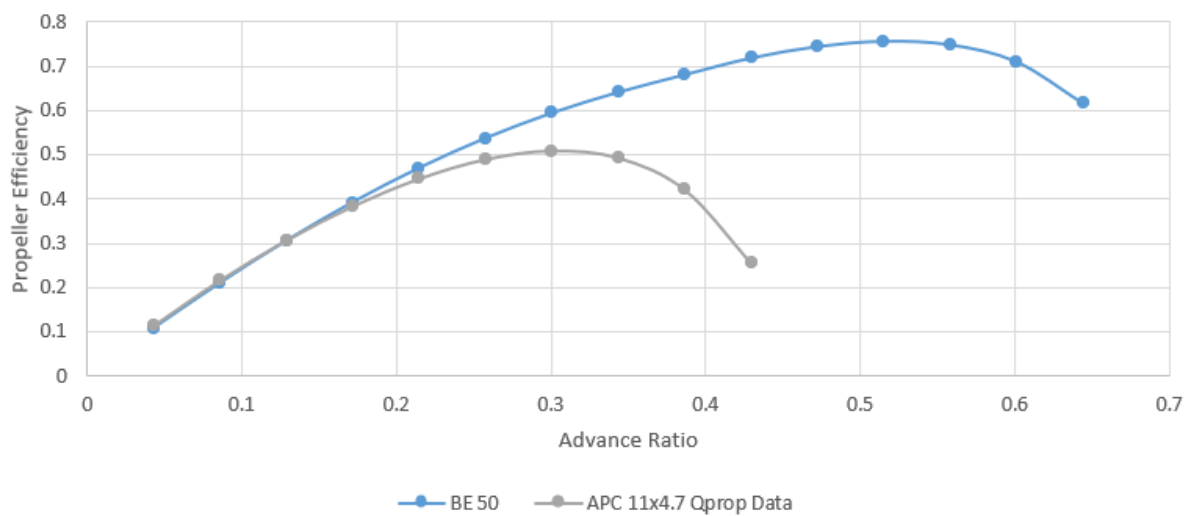
Table 16 QMIL generated propeller geometry for BE 50



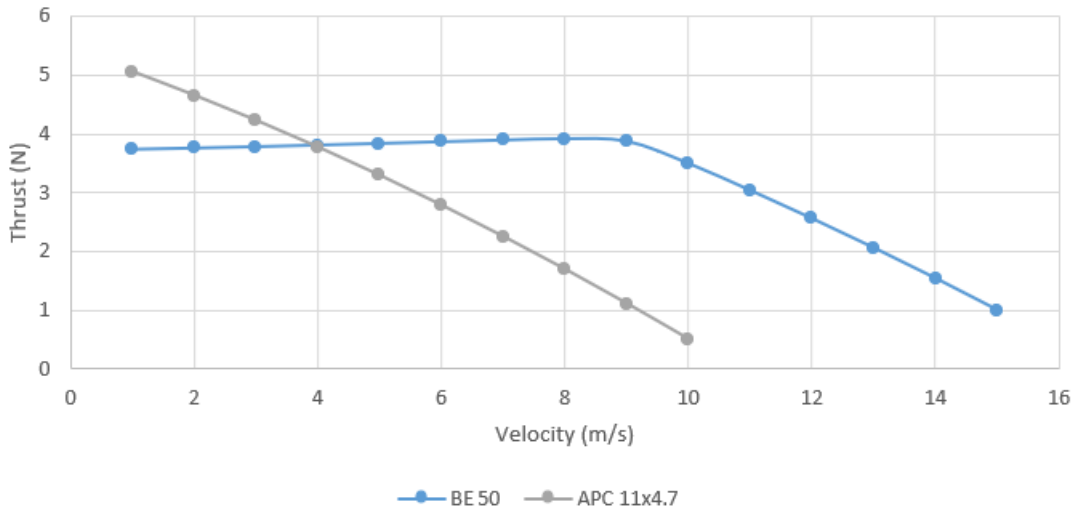
*Graph 31 QMIL generated chord length distribution for BE 50*



*Graph 32 QMIL generated pitch angle distribution for BE 50*



*Graph 33 Propeller efficiency curve comparison between BE 50 and APC 11x4.7*



Graph 34 Thrust curve comparison between BE 50 and APC 11x4.7

### 5.3 Propeller with Eppeler 63 Airfoil:

Template prop

```

2           ! Nblades

0.4355  9.8901      ! CL0      CL_a
-0.1798  1.4681      ! CLmin   CLmax

0.01941   0.004342   0.084376   0.5143   ! CD0      CD2u     CD2l     CLCD0
100000.0 -0.500          ! REref   REexp

0.0  0.5  1.0   ! XIdes   (r/R locations where design cl is specified)
0.6  0.8  0.7   ! CLdes   (specified cl)

0.006    ! hub radius(m)
0.1397   ! tip radius(m)
10.00    ! speed(m/s)
5000    ! rpm

3.5|    ! Thrust(N)   ( 0 if power specified )
0.0  ! Power(W)    ( 0 if thrust specified )

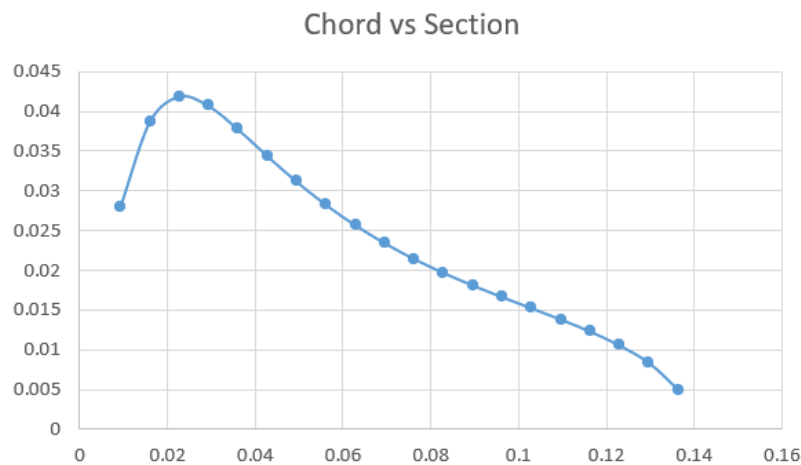
0   0.0  ! Ldes   [ KQdes ]
# 18    ! Nout    number of output stations (optional)

```

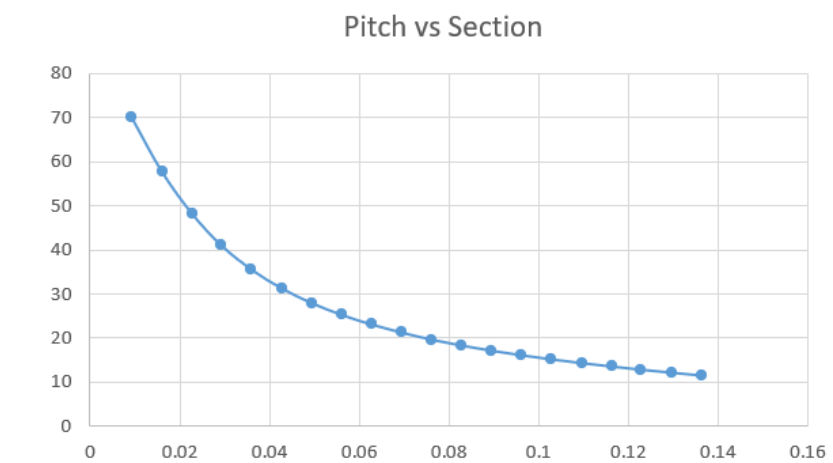
Figure 15 QMIL input file for Eppeler 63

Radial Section (cm)	Chord Length (cm)	Pitch Angle (degree)
0.93599	2.801	70.05
1.600655	3.8739	57.79
2.27711	4.191	48.26
2.9337	4.075	41.03
3.60426	3.7817	35.54
4.27482	3.4436	31.3
4.94538	3.1195	27.95
5.61594	2.8261	25.27
6.2865	2.5691	23.07
6.95706	2.3442	21.23
7.61365	2.1472	19.67
8.28421	1.9712	18.33
8.95477	1.8133	17.16
9.62533	1.6666	16.12
10.29589	1.5255	15.19
10.96645	1.383	14.35
11.63701	1.2308	13.57
12.2936	1.0575	12.85
12.96416	0.8382	12.18
13.63472	0.4987	11.54

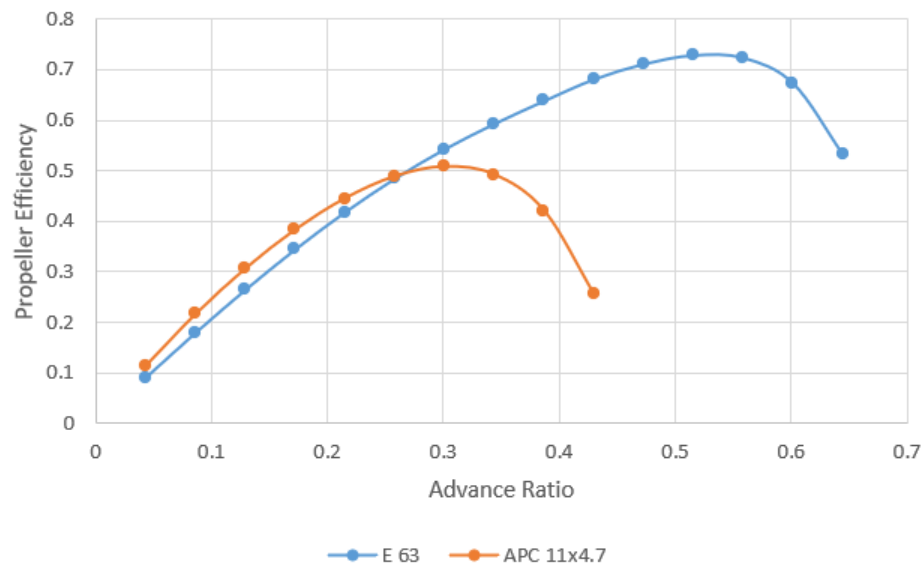
Table 17 QMIL generated propeller geometry for Eppeler 63



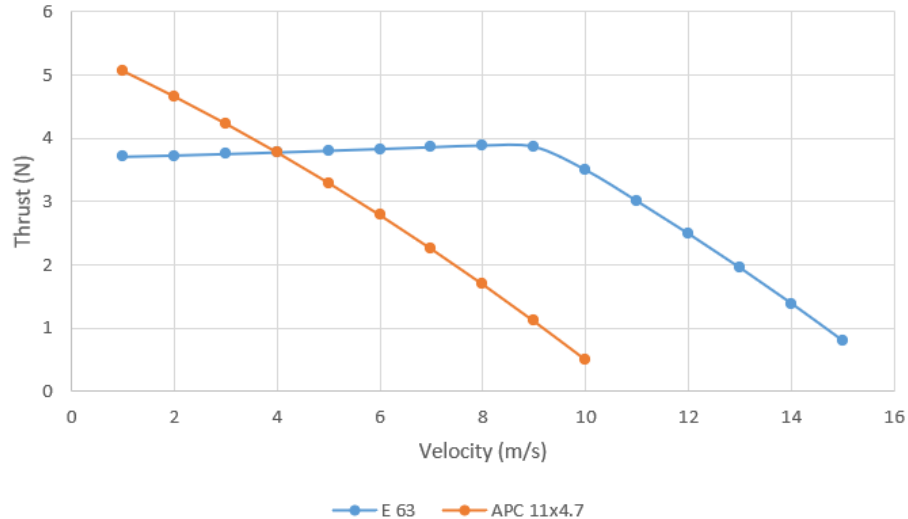
Graph 35 QMIL generated chord length distribution for Eppeler 63



Graph 36 QMIL generated pitch angle distribution for Eppeler 63



Graph 37 Efficiency curve comparison between Eppeler 63 and APC 11x4.7



Graph 38 Thrust curve comparison between Eppeler 63 and APC 11x4.7

#### 5.4 Propeller with CLARK Y Airfoil:

```

Template prop

2           ! Nblades

0.3674  7.7928      ! CL0      CL_a
-0.3727  1.3694      ! CLmin   CLmax

0.01727  0.001224  0.019456  0.7699  ! CD0      CD2u    CD2l    CLCD0
100000.0 -0.500       ! REref   REexp

0.0  0.5  1.0  ! XIdes  (r/R locations where design cl is specified)
0.6  0.8  0.7  ! CLdes  (specified cl)

0.006    ! hub radius(m)
0.1397   ! tip radius(m)
10.00    ! speed(m/s)
10000   ! rpm

3.5|     ! Thrust(N)  ( 0 if power specified )
0.0  ! Power(W)   ( 0 if thrust specified )

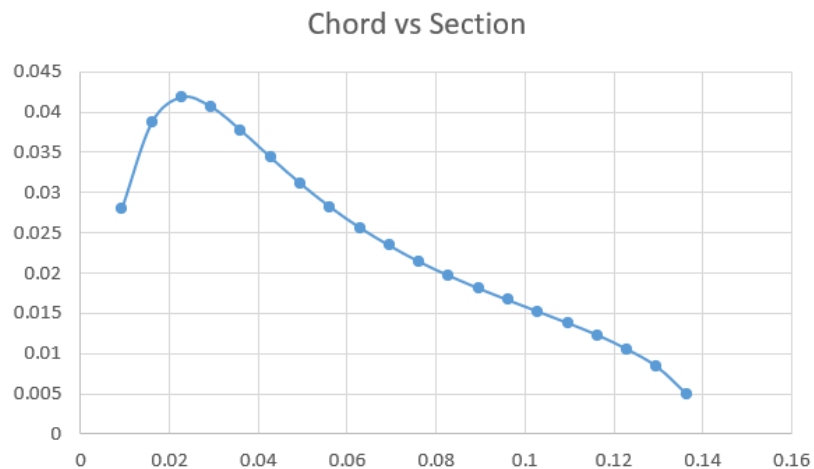
0  0.0  ! Ldes   [ KQdes ]
# 18    ! Nout    number of output stations (optional)

```

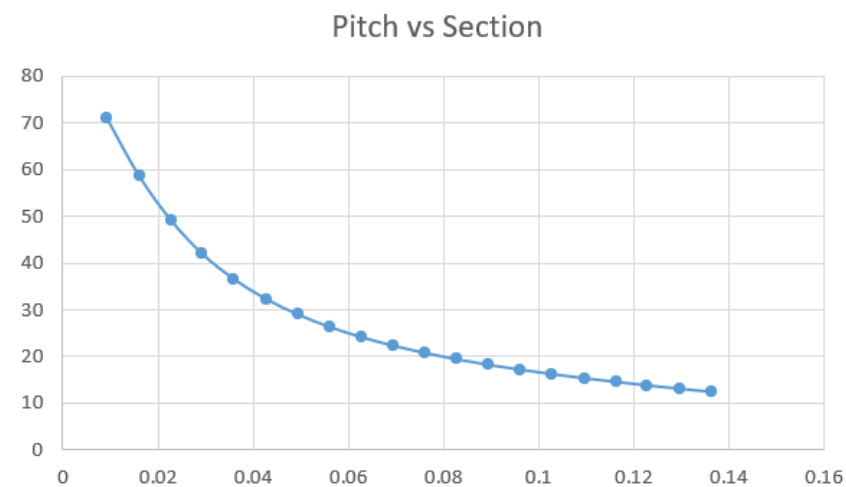
Figure 16 QMIL input file for CLARK Y

Radial Section (cm)	Chord Length (cm)	Pitch Angle (degree)
0.93599	2.7954	70.86
1.600655	3.8655	58.64
2.27711	4.1826	49.15
2.9337	4.0653	41.97
3.60426	3.7733	36.5
4.27482	3.4366	32.29
4.94538	3.1125	28.97
5.61594	2.8191	26.3
6.2865	2.5621	24.11
6.95706	2.3386	22.29
7.61365	2.1416	20.73
8.28421	1.967	19.39
8.95477	1.8091	18.21
9.62533	1.6624	17.17
10.29589	1.5213	16.22
10.96645	1.3788	15.36
11.63701	1.228	14.56
12.2936	1.0547	13.82
12.96416	0.8368	13.12
13.63472	0.4973	12.45

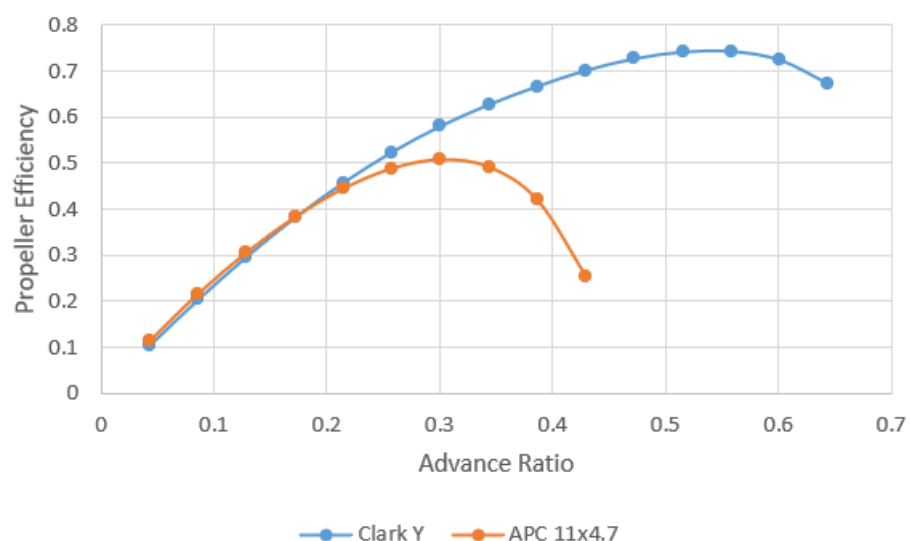
Table 18 QMIL generated propeller geometry for CLARK Y



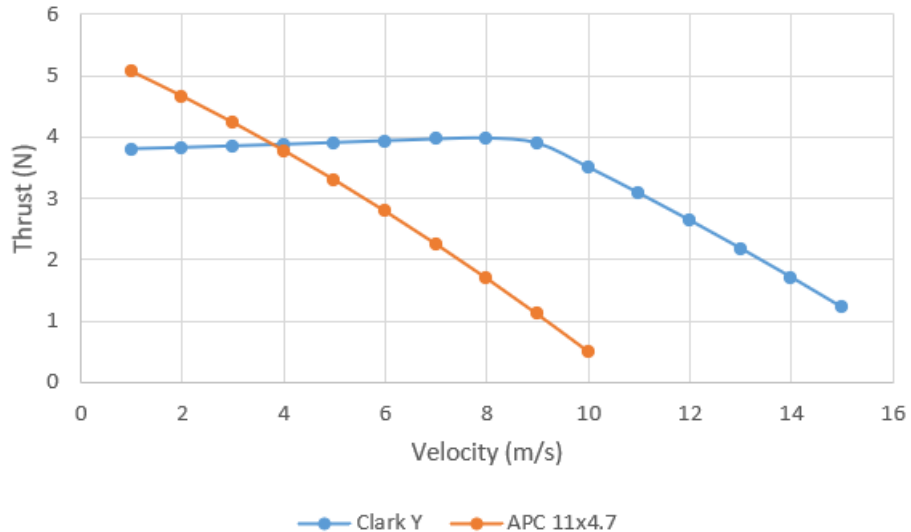
*Graph 39 QMIL generated chord length distribution for CLARK Y*



*Graph 40 QMIL generated pitch angle distribution for CLARK Y*



*Graph 41 Efficiency curve comparison between CLARK Y and APC 11x4.7*



Graph 42 Thrust curve comparison between CLARK Y and APC 11x4.7

### 5.5 Propeller with MH22 (7.2%) airfoil:

Template prop

```

2           ! Nblades

0.2273  5.9176      ! CL0      CL_a
-0.5266  0.9297      ! CLmin    CLmax

0.01066   0.027755   0.385606 -0.0893   ! CD0      CD2u     CD2l     CLCD0
100000.0 -0.500       ! REref    REexp

0.0  0.5  1.0      ! XIdes   (r/R locations where design cl is specified)
0.6  0.8  0.7      ! CLdes   (specified cl)

0.006    ! hub radius(m)
0.1397   ! tip radius(m)
10.00    ! speed(m/s)
5000    ! rpm

3.5|    ! Thrust(N)  ( 0 if power specified )
0.0  ! Power(W)   ( 0 if thrust specified )

0   0.0  ! Ldes   [ KQdes ]
# 18      ! Nout    number of output stations (optional)

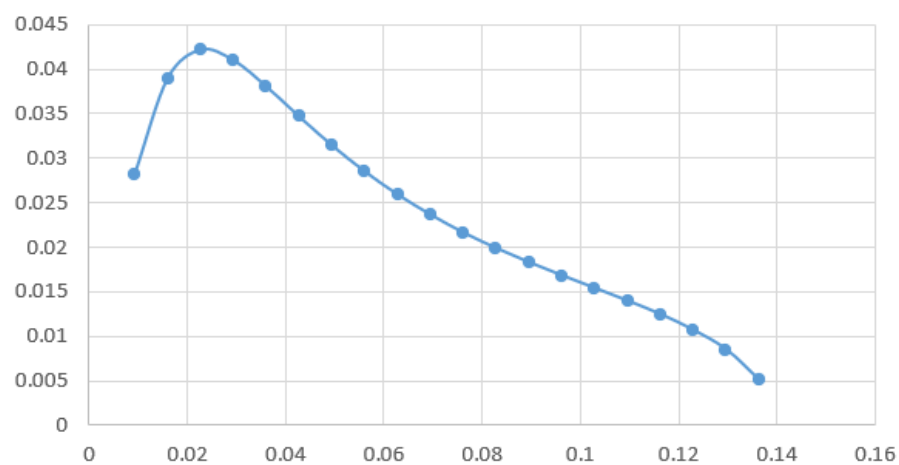
```

Figure 17 QMIL input file for MH22 (7.2%)

Radial Section (cm)	Chord Length (cm)	Pitch Angle (degree)
0.93599	2.8177	72.9
1.600655	3.8976	60.75
2.27711	4.2175	51.33
2.9337	4.1016	44.19
3.60426	3.8068	38.77
4.27482	3.4674	34.59
4.94538	3.1405	31.3
5.61594	2.8457	28.65
6.2865	2.5858	26.48
6.95706	2.3595	24.67
7.61365	2.1612	23.12
8.28421	1.9851	21.77
8.95477	1.8259	20.59
9.62533	1.6778	19.53
10.29589	1.5353	18.56
10.96645	1.3914	17.67
11.63701	1.2391	16.84
12.2936	1.0645	16.06
12.96416	0.8438	15.31
13.63472	0.5015	14.58

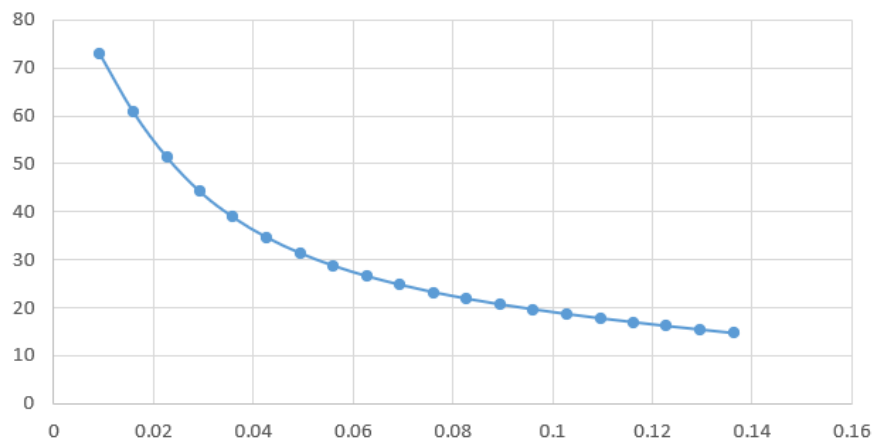
Table 19 QMIL generated propeller geometry for MH22 (7.2%)

Chord vs Section

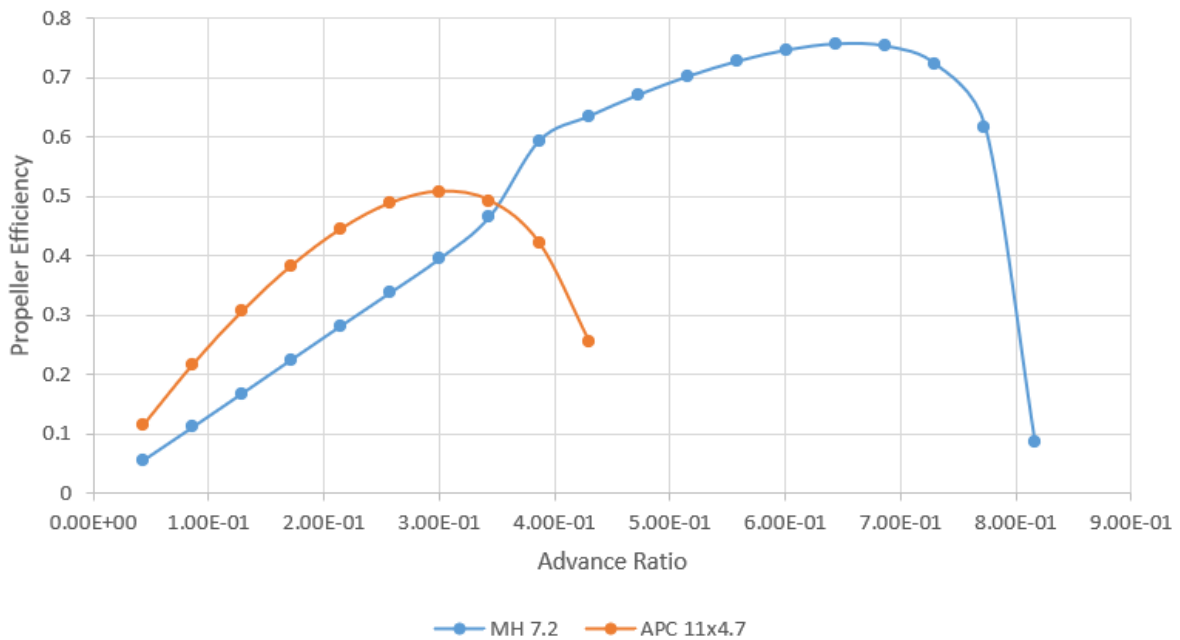


Graph 43 QMIL generated chord length distribution for MH22 (7.2%)

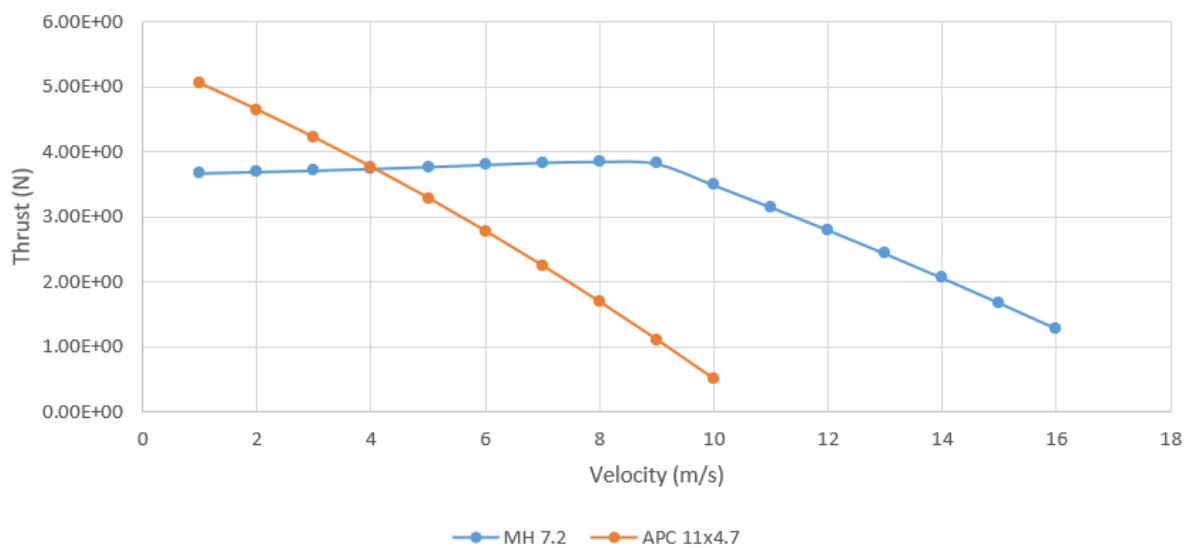
Pitch vs Section



Graph 44 QMIL generated pitch angle distribution for MH22 (7.2%)



Graph 45 Efficiency curve comparison between MH22 (7.2%) and APC 11x4.7



Graph 46 Thrust curve comparison between MH22 (7.2%) and APC 11x4.7

## 5.6 Propeller with MH30 (7.84%) airfoil:

Template prop

```

2           ! Nblades

0.0193  6.4911    ! CL0      CL_a
-0.4868  1.0085    ! CLmin   CLmax

0.01191  0.009354  0.496708 -0.1359  ! CD0      CD2u     CD2l     CLCD0
100000.0 -0.500          ! REref   REexp

0.0  0.5  1.0  ! XIdes   (r/R locations where design cl is specified)
0.6  0.8  0.7  ! CLdes   (specified cl)

0.006    ! hub radius(m)
0.1397   ! tip radius(m)
10.00    ! speed(m/s)
5000    ! rpm

3.5      ! Thrust(N)  ( 0 if power specified )
0.0  ! Power(W)    ( 0 if thrust specified )

0  0.0  ! Ldes   [ KQdes ]
# 18|  ! Nout    number of output stations (optional)

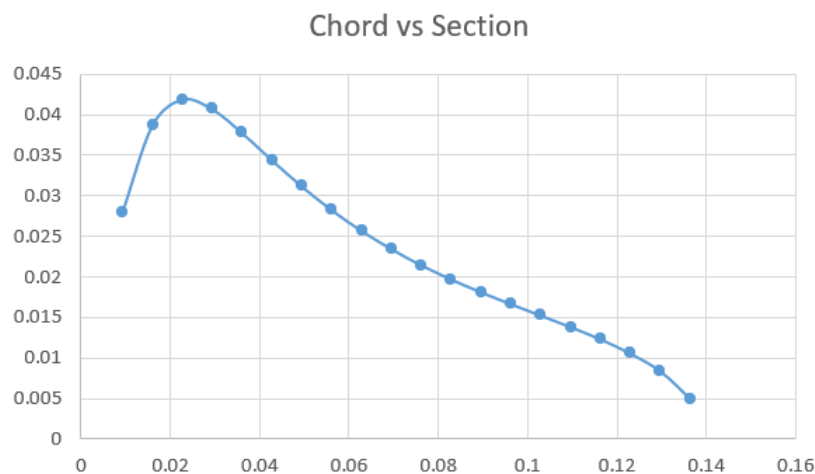
```

Figure 18 QMIL input file for MH30 (7.84%)

Radial Section (cm)	Chord Length (cm)	Pitch Angle (degree)
0.93599	2.801	74.35
1.600655	3.8739	62.18
2.27711	4.191	52.73
2.9337	4.075	45.57
3.60426	3.7817	40.14
4.27482	3.4436	35.94
4.94538	3.1195	32.64

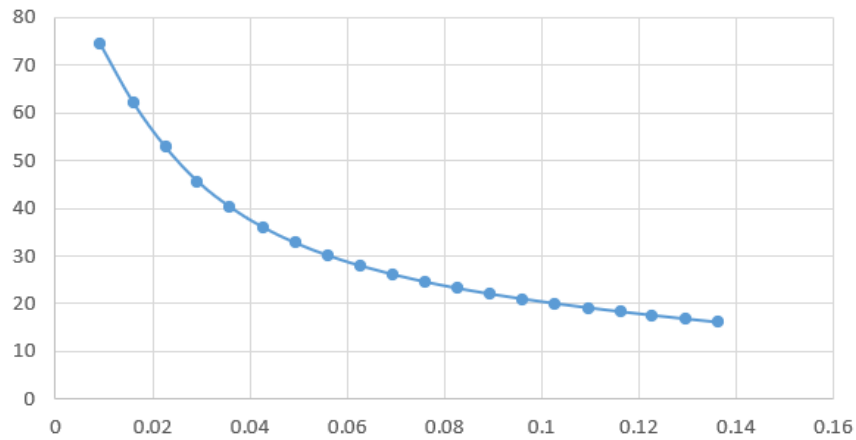
5.61594	2.8261	29.99
6.2865	2.5691	27.82
6.95706	2.3442	26
7.61365	2.1472	24.45
8.28421	1.9712	23.1
8.95477	1.8133	21.92
9.62533	1.6666	20.87
10.29589	1.5255	19.91
10.96645	1.383	19.03
11.63701	1.2308	18.21
12.2936	1.0575	17.44
12.96416	0.8382	16.71
13.63472	0.4987	16.01

Table 20 QMIL generated propeller geometry for MH30 (7.84%)

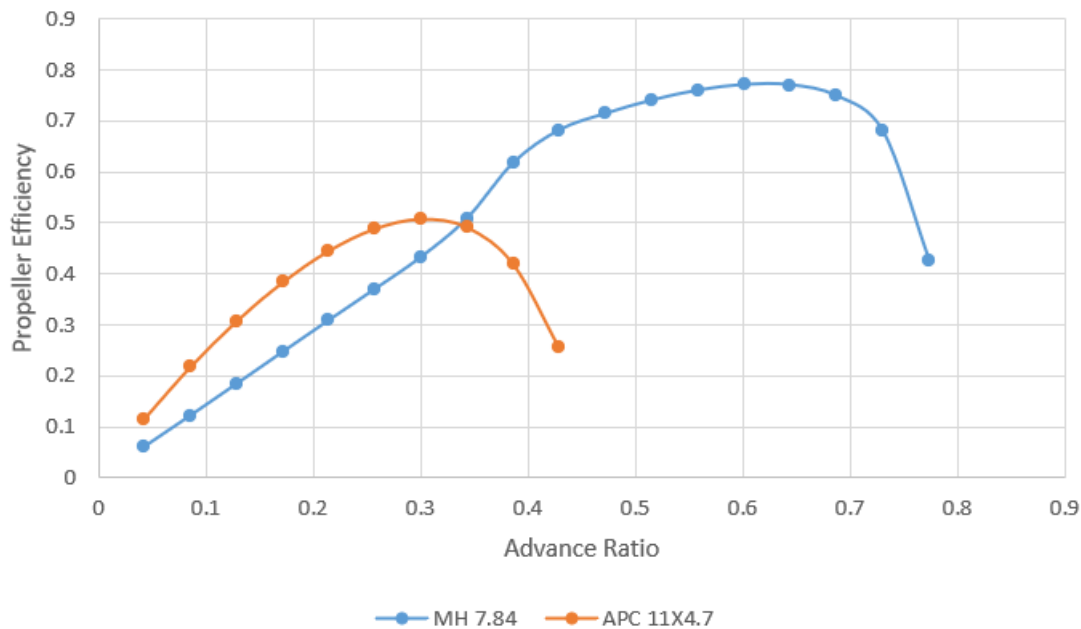


Graph 47 QMIL generated chord length distribution for MH30 (7.84%)

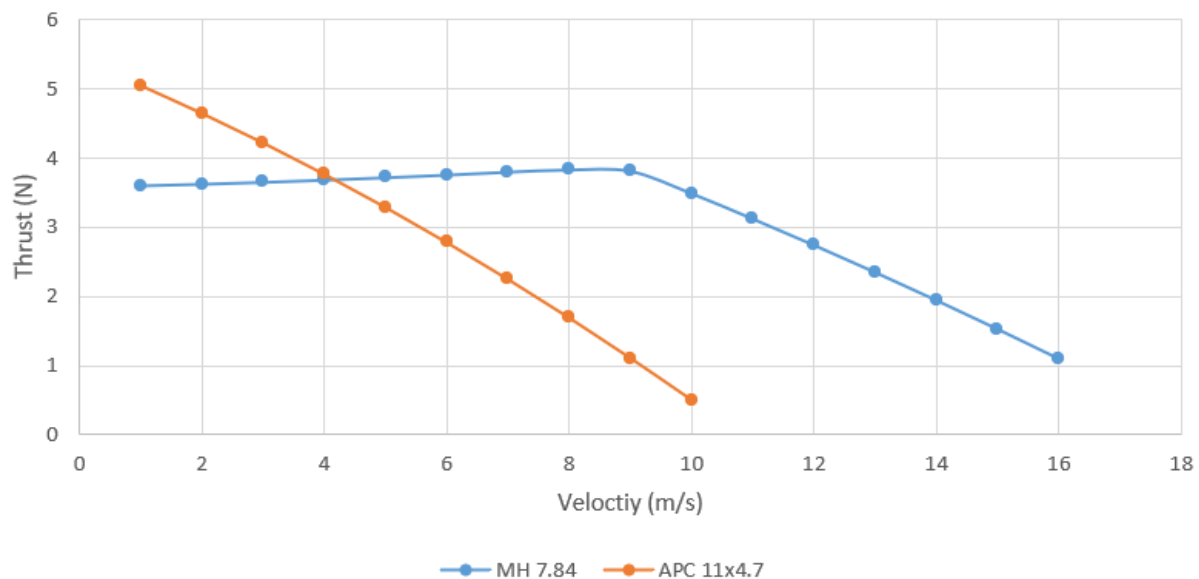
Pitch vs Section



Graph 48 QMIL generated pitch angle distribution for MH30 (7.84%)



Graph 49 Efficiency curve comparison between MH30 (7.84%) and APC 11x4.7



Graph 50 Thrust curve comparison between MH30 (7.84%) and APC 11x4.7

### 5.7 Propeller with MH32 (8.7%) airfoil:

Template prop

```

2           ! Nblades

0.2527  6.2792      ! CL0      CL_a
-0.5177  1.0203      ! CLmin   CLmax

0.01244   0.007641   0.533645 -0.1839  ! CD0      CD2u     CD2l   CLCD0
100000.0 -0.500        ! REref   REexp

0.0  0.5  1.0    ! XIdes   (r/R locations where design cl is specified)
0.6  0.8  0.7    ! CLdes   (specified cl)

0.006    ! hub radius(m)
0.1397   ! tip radius(m)
10.00    ! speed(m/s)
5000    ! rpm

3.5|    ! Thrust(N)  ( 0 if power specified )
0.0  ! Power(W)   ( 0 if thrust specified )

0   0.0  ! Ldes   [ KQdes ]
# 18       ! Nout    number of output stations (optional)

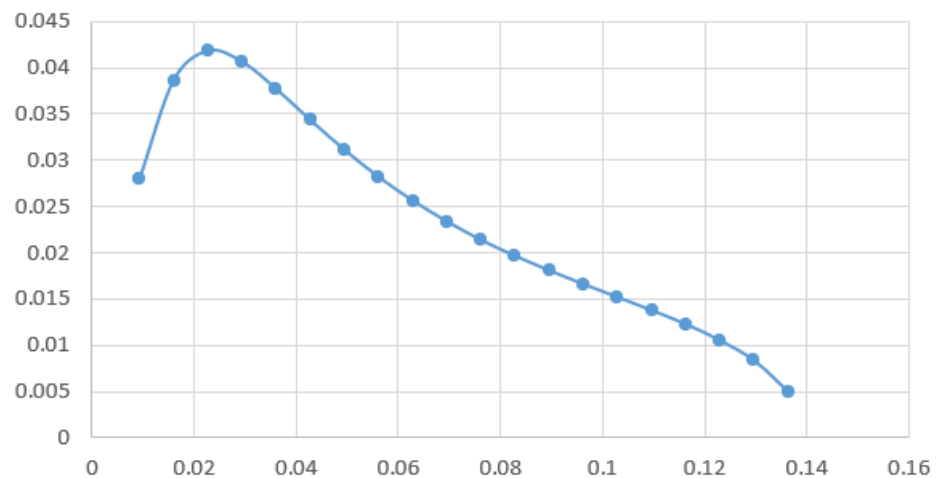
```

Figure 19 QMIL input file for MH32 (8.7%)

Radial Section (cm)	Chord Length (cm)	Pitch Angle (degree)
0.93599	2.7926	72.4
1.600655	3.8627	60.19
2.27711	4.1784	50.71
2.9337	4.0625	43.52
3.60426	3.7691	38.07
4.27482	3.4324	33.86
4.94538	3.1097	30.54
5.61594	2.8164	27.88
6.2865	2.5607	25.7
6.95706	2.3358	23.87
7.61365	2.1388	22.32
8.28421	1.9656	20.98
8.95477	1.8077	19.8
9.62533	1.661	18.75
10.29589	1.5199	17.8
10.96645	1.3774	16.94
11.63701	1.2266	16.14
12.2936	1.0547	15.39
12.96416	0.8354	14.68
13.63472	0.4973	14

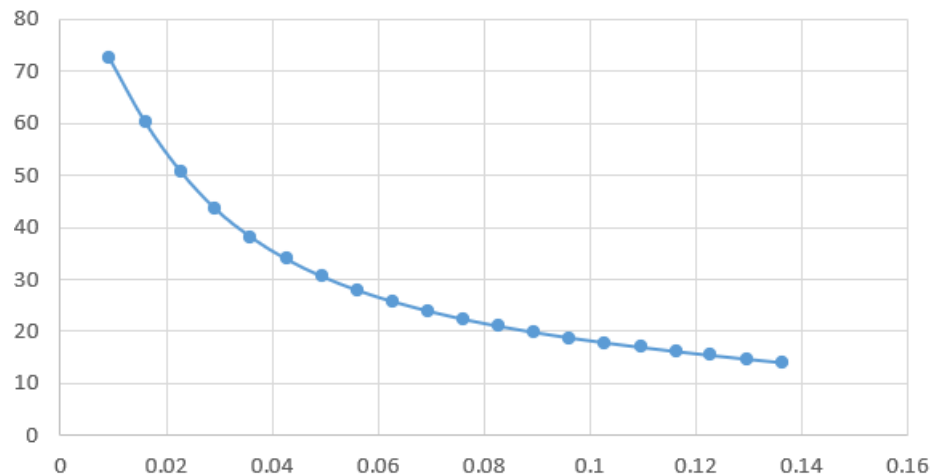
Table 21 QMIL generated propeller geometry for MH32 (8.7%)

Chord vs Section

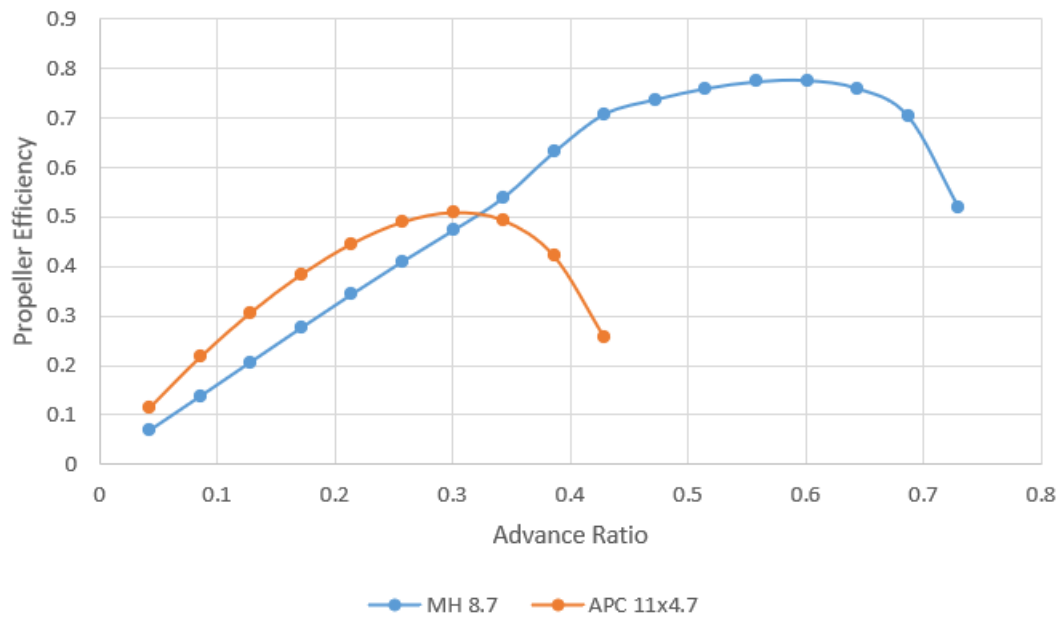


Graph 51 QMIL generated chord length distribution for MH32 (8.7%)

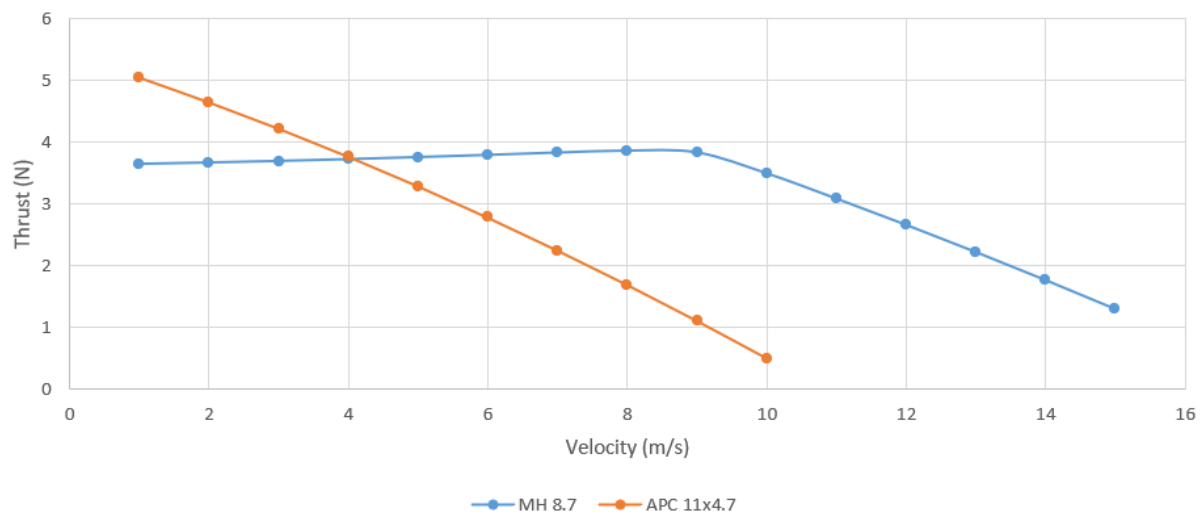
Pitch vs Section



Graph 52 QMIL generated pitch angle distribution for MH32 (8.7%)



Graph 53 Efficiency curve comparison between MH32 (8.7%) and APC 11x4.7



Graph 54 Thrust curve comparison between MH32 (8.7%) and APC 11x4.7

### 5.8 Propeller with MH43 (8.5%) airfoil:

Template prop

```

2           ! Nblades

0.2527  6.2792    ! CL0      CL_a
-0.5177  1.0203    ! CLmin   CLmax

0.01244  0.007641  0.533645 -0.1839  ! CD0      CD2u     CD2l     CLCD0
100000.0 -0.500          ! REref   REexp

0.0  0.5  1.0  ! Xides   (r/R locations where design cl is specified)
0.6  0.8  0.7  ! CLdes   (specified cl)

0.006    ! hub radius(m)
0.1397   ! tip radius(m)
10.00    ! speed(m/s)
5000    ! rpm

3.5|    ! Thrust(N)  ( 0 if power specified )
0.0  ! Power(W)   ( 0 if thrust specified )

0  0.0  ! Ldes   [ KQdes ]
# 18    ! Nout    number of output stations (optional)

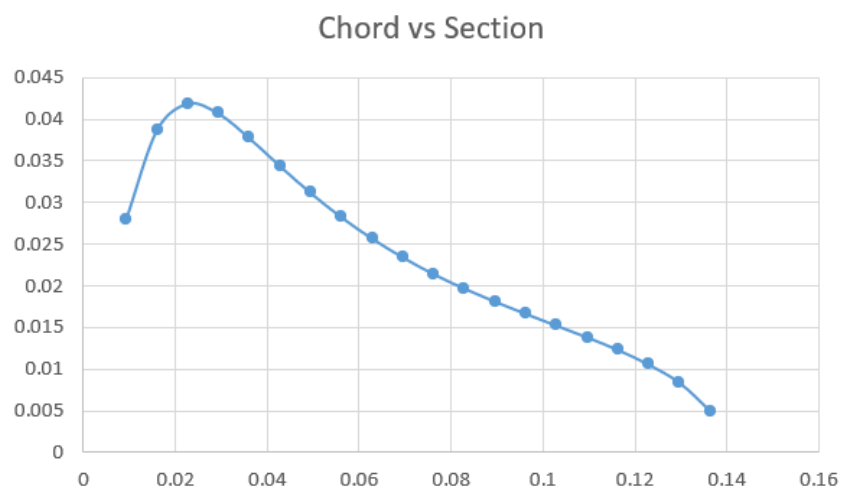
```

Figure 20 QMIL input file for MH43 (8.5%)

Radial Section (cm)	Chord Length (cm)	Pitch Angle (degree)
0.93599	2.801	72.41
1.600655	3.8739	60.24
2.27711	4.191	50.8
2.9337	4.075	43.65
3.60426	3.7817	38.22
4.27482	3.4436	34.03

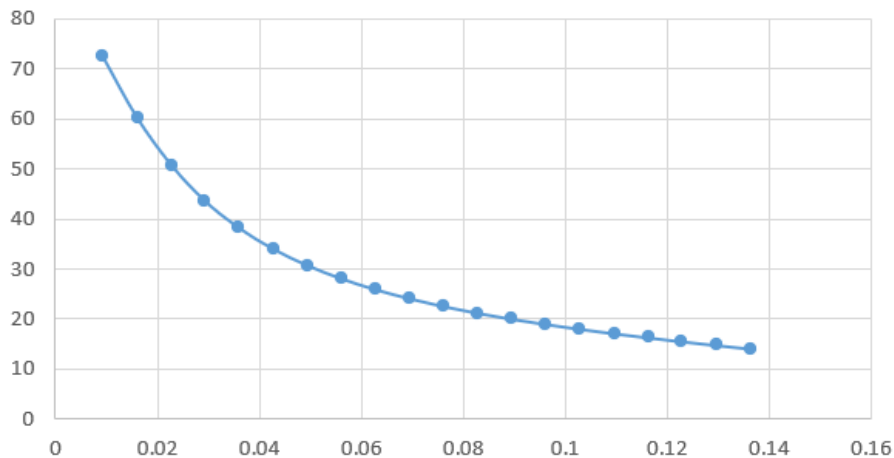
4.94538	3.1195	30.74
5.61594	2.8261	28.09
6.2865	2.5691	25.91
6.95706	2.3442	24.1
7.61365	2.1472	22.55
8.28421	1.9712	21.21
8.95477	1.8133	20.02
9.62533	1.6666	18.97
10.29589	1.5255	18.01
10.96645	1.383	17.12
11.63701	1.2308	16.3
12.2936	1.0575	15.53
12.96416	0.8382	14.79
13.63472	0.4987	14.08

Table 22 QMIL generated propeller geometry for MH43 (8.5%)

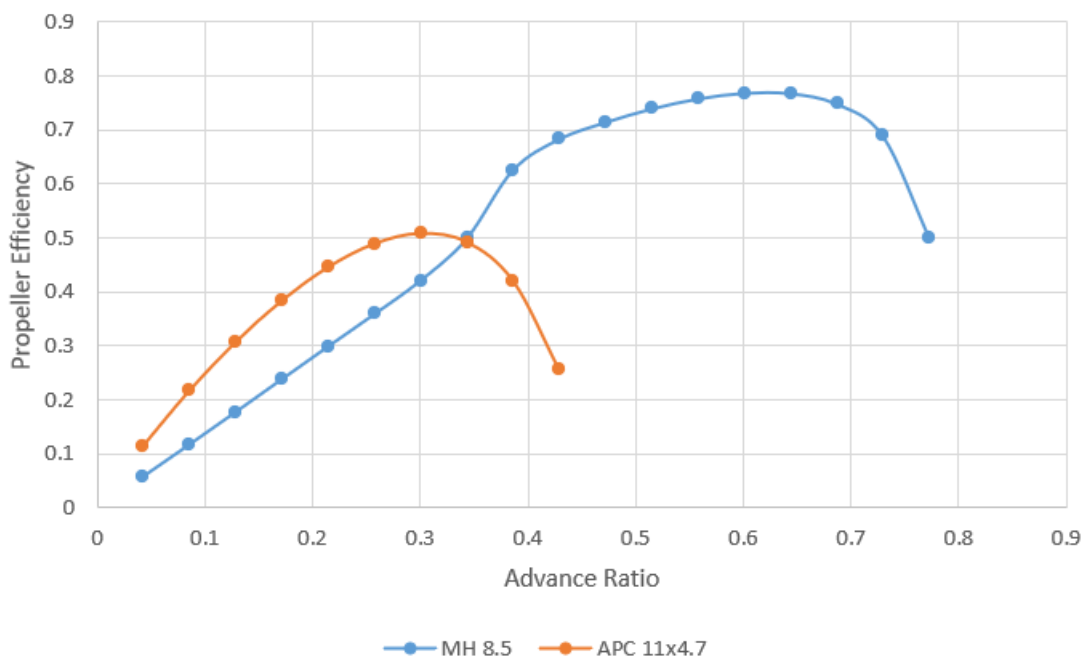


Graph 55 QMIL generated chord length distribution for MH43 (8.5%)

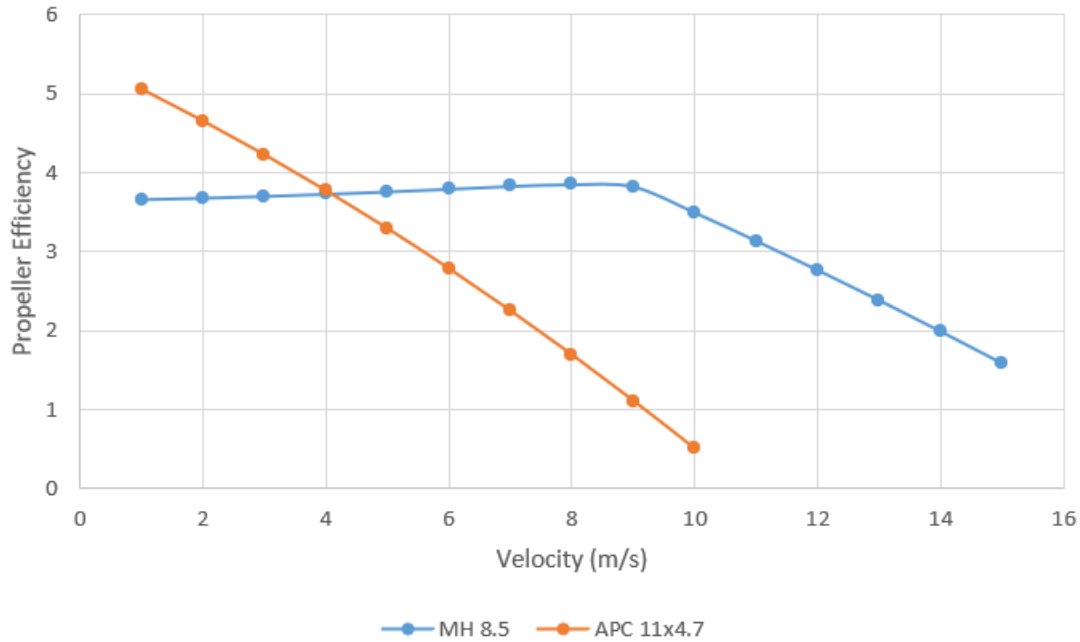
Pitch vs Section



Graph 56 QMIL generated pitch angle distribution for MH43 (8.5%)



Graph 57 Efficiency curve comparison between MH43 (8.5%) and APC 11x4.7



Graph 58 Thrust curve comparison between MH43 (8.5%) and APC 11x4.7

### 5.9 Propeller with MH64 (8.59%) airfoil:

```

Template prop

2          ! Nblades

0.2223  6.1572    ! CL0      CL_a
-0.5508  1.0251    ! CLmin   CLmax

0.01188  0.007853  0.420566 -0.1713  ! CD0      CD2u     CD2l     CLCD0
100000.0 -0.500        ! REref   REexp

0.0  0.5  1.0  ! XIdes  (r/R locations where design cl is specified)
0.6  0.8  0.7  ! CLdes  (specified cl)

0.006    ! hub radius(m)
0.1397   ! tip radius(m)
10.00    ! speed(m/s)
5000    ! rpm

3.5      ! Thrust(N)  ( 0 if power specified )
0.0  ! Power(W)    ( 0 if thrust specified )
|
0  0.0  ! Ldes   [ KQdes ]
# 18    ! Nout    number of output stations (optional)

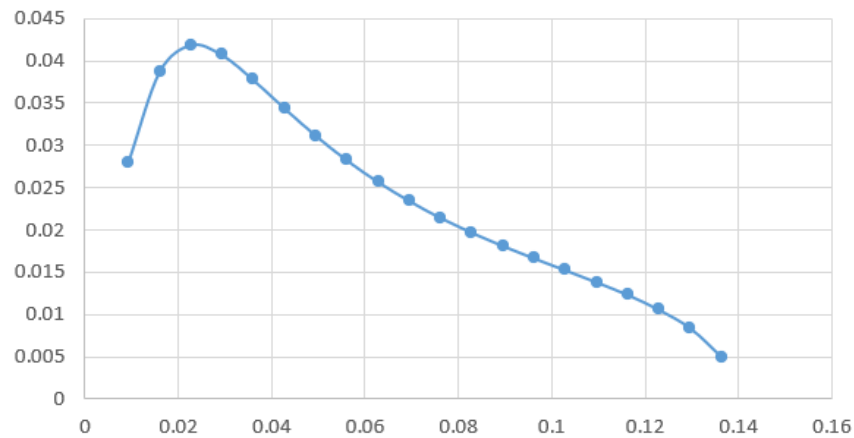
```

Figure 21 QMIL input file for MH64 (8.59%)

Radial Section (cm)	Chord Length (cm)	Pitch Angle (degree)
0.93599	2.7996	72.76
1.600655	3.8725	60.6
2.27711	4.1896	51.16
2.9337	4.0737	44.01
3.60426	3.7803	38.59
4.27482	3.4422	34.4
4.94538	3.1181	31.11
5.61594	2.8247	28.46
6.2865	2.5677	26.29
6.95706	2.3428	24.48
7.61365	2.1458	22.93
8.28421	1.9698	21.59
8.95477	1.8119	20.4
9.62533	1.6652	19.34
10.29589	1.5241	18.38
10.96645	1.3816	17.5
11.63701	1.2308	16.67
12.2936	1.0575	15.9
12.96416	0.8382	15.15
13.63472	0.4987	14.44

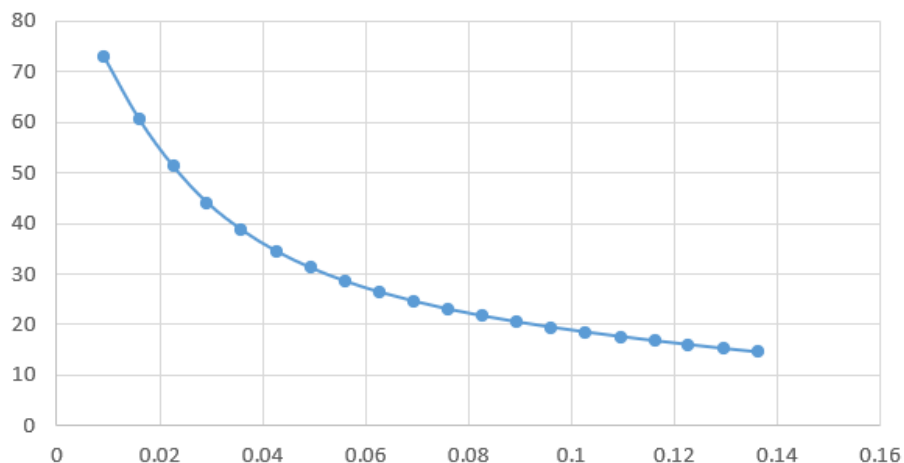
Table 23 QMIL generated propeller geometry for MH64 (8.59%)

Chord vs Section

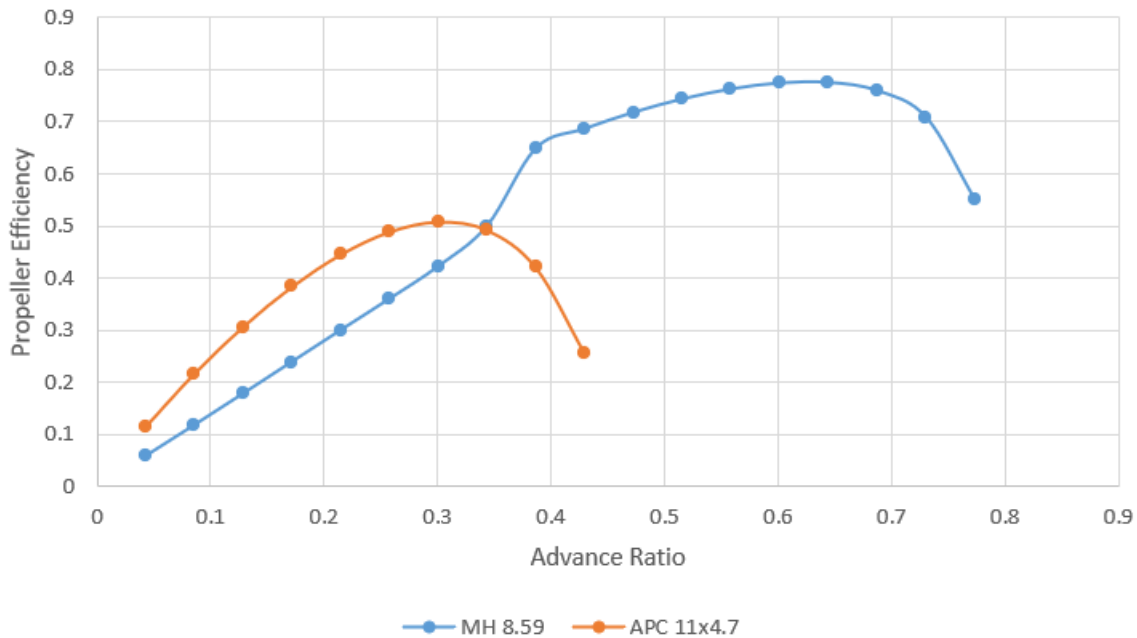


Graph 59 QMIL generated chord length distribution for MH64 (8.59%)

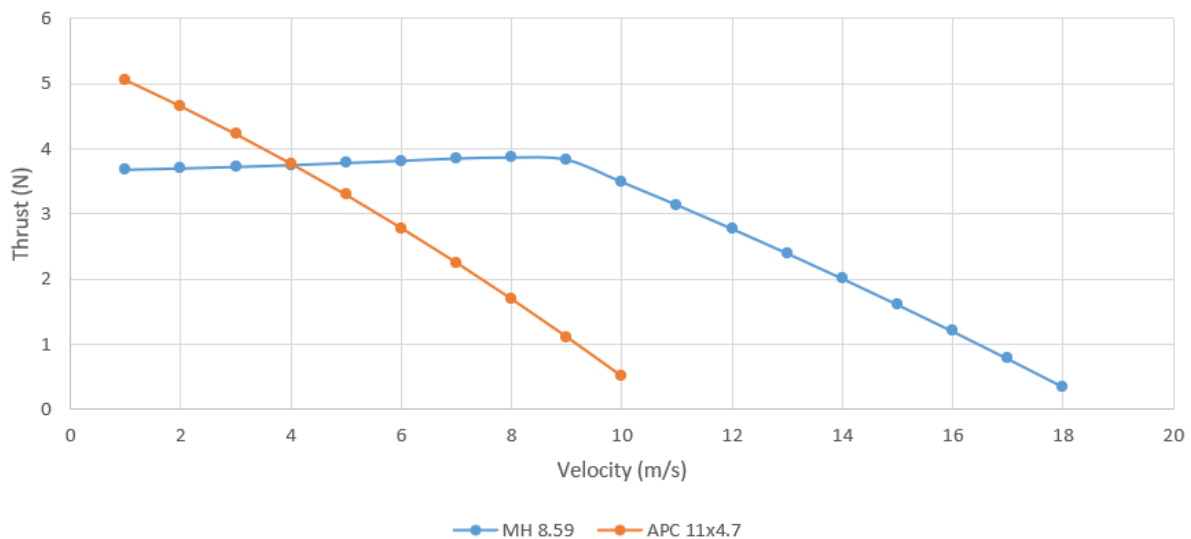
Pitch vs Section



Graph 60 QMIL generated pitch angle distribution for MH64 (8.59%)



Graph 61 Efficiency curve comparison between MH64 (8.59%) and APC 11x4.7



Graph 62 Thrust curve comparison between MH64 (8.59%) and APC 11x4.7

### 5.10 Propeller with S7055 airfoil:

```

Template prop

2          ! Nblades

0.3952  7.2935    ! CL0      CL_a
-0.3553  1.2615    ! CLmin    CLmax

0.01771   0.001054  0.131934  0.1947  ! CD0      CD2u     CD2l     CLCD0
100000.0 -0.500           ! REref    REexp

0.0  0.5  1.0  ! XIdes  (r/R locations where design cl is specified)
0.6  0.8  0.7  ! CLdes   (specified cl)

0.006    ! hub radius(m)
0.1397   ! tip radius(m)
10.00    ! speed(m/s)
5000    ! rpm

3.5      ! Thrust(N)  ( 0 if power specified )
0.0  ! Power(W)   ( 0 if thrust specified )

0  0.0  ! Ldes   [ KQdes ]
# 18    ! Nout    number of output stations (optional)

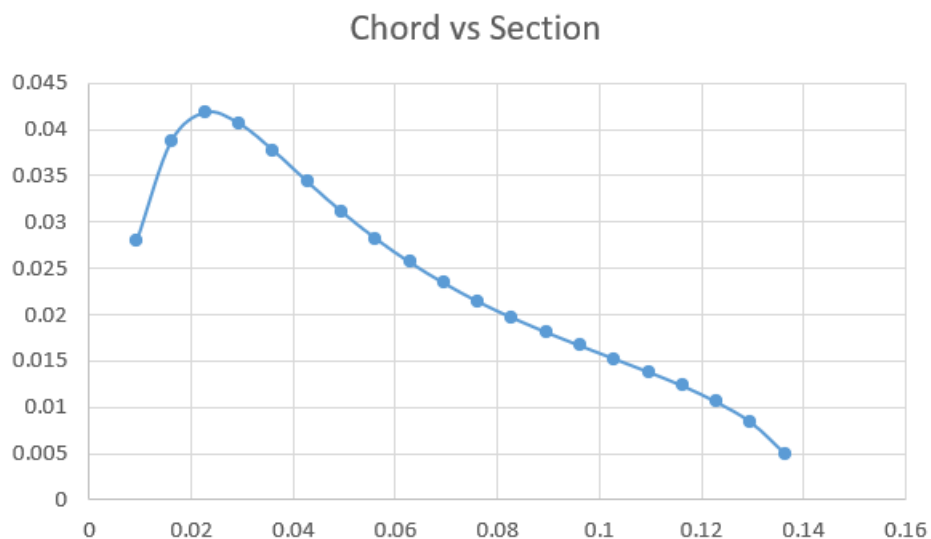
```

Figure 22 QMIL input file for S7055

Radial Section (cm)	Chord Length (cm)	Pitch Angle (degree)
0.93599	2.7968	70.79
1.600655	3.8683	58.58
2.27711	4.1854	49.11
2.9337	4.0681	41.93
3.60426	3.7761	36.48
4.27482	3.438	32.27
4.94538	3.1139	28.95
5.61594	2.8219	26.29

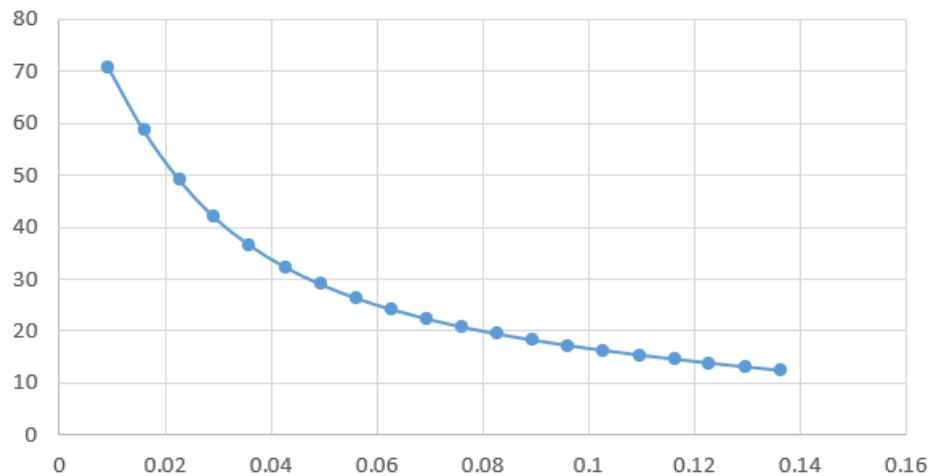
6.2865	2.5649	24.11
6.95706	2.34	22.28
7.61365	2.143	20.73
8.28421	1.9684	19.39
8.95477	1.8105	18.21
9.62533	1.6638	17.16
10.29589	1.5227	16.21
10.96645	1.3802	15.35
11.63701	1.2294	14.54
12.2936	1.0561	13.79
12.96416	0.8368	13.07
13.63472	0.4973	12.39

Table 24 QMIL generated propeller geometry for S7055

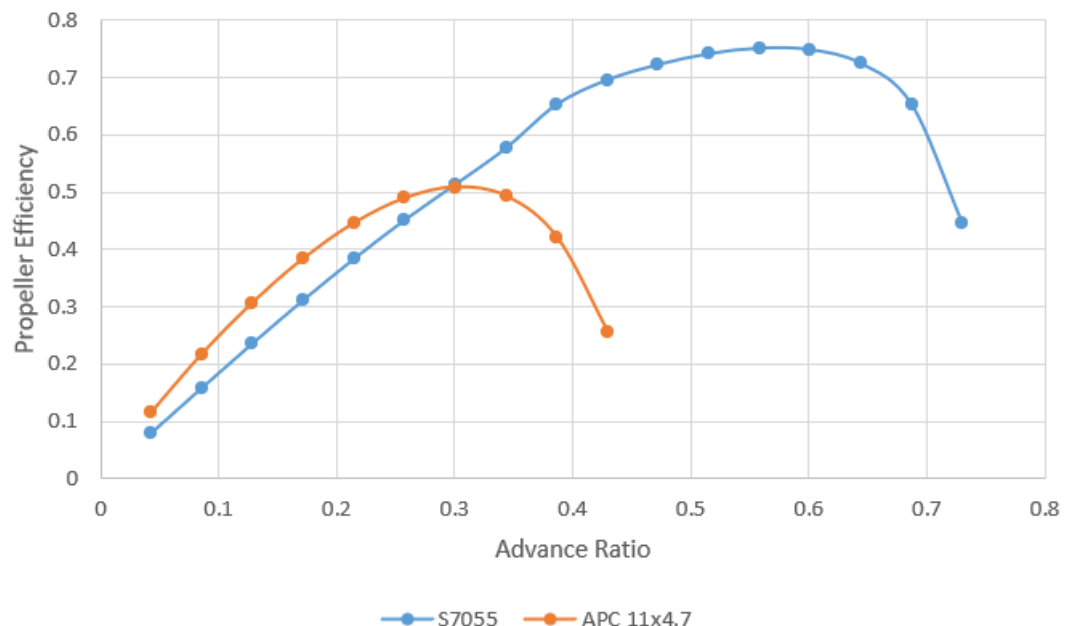


Graph 63 QMIL generated chord length distribution for S7055

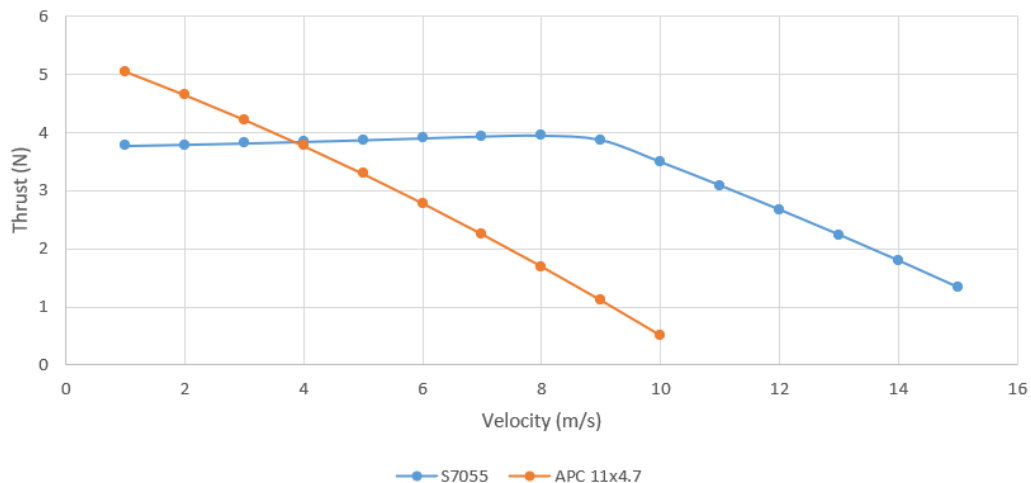
Pitch vs Section



Graph 64 QMIL generated pitch angle distribution for S7055



Graph 65 Efficiency curve comparison between S7055 and APC 11x4.7



Graph 66 Thrust curve comparison between S7055 and APC 11x4.7

### 5.11 General Observations Regarding First Design Point:

Airfoil used in Propeller	Peak Propeller efficiency	Advance ratio	Maximum Thrust Produced (N)
BE 50	0.7562	0.515	3.894
ARAD 10	0.7545	0.558	3.894
CLARK Y	0.7425	0.558	3.973
Eppeler 63	0.729	0.515	3.884
MH22 (7.2%)	0.7568	0.644	3.854
MH30 (7.84%)	0.771	0.6013	3.837
MH32 (8.7%)	0.7762	0.6013	3.858
MH43 (8.5%)	0.7686	0.6013	3.852
MH64 (8.59%)	0.7747	0.644	3.871
S7055	0.7508	0.558	3.95

Table 25 Summary of aerodynamic performance characteristics at 1st design point

Velocity	ARAD10		BE50		CLARKY		E63		MH7.2	
	D <sub>eff</sub>	d <sub>T</sub>								
2	-1.91	-0.915	-0.69	-0.896	-1.27	-0.833	-3.66	-0.929	-10.52	-0.957
3	-1.76	-0.465	-0.15	-0.445	-0.98	-0.381	-4.16	-0.479	-13.84	-0.508
4	-0.97	0.0140	0.870	0.0360	-0.18	0.099	-3.85	0	-15.81	-0.0208
5	0.5	0.521	2.44	0.544	1.22	0.608	-2.67	0.507	-16.31	0.481
6	2.92	1.06	4.81	1.08	3.48	1.15	-0.39	1.04	-15.07	1.02

Table 26 Comparison of thrust and propeller efficiency between the 1st design point and APC

11x4.7

In the above tables, for a particular velocity:

$$D_{eff} (\%) = 100 * (\text{Efficiency of QMIL generated propeller} - \text{Efficiency of APC } 11x4.7)$$

$$d_T (N) = \text{Thrust produced by QMIL generated propeller} - \text{Thrust produced by APC } 11x4.$$

Velocity	MH7.84		MH8.7		MH8.5		MH8.59		S7055	
	D <sub>eff</sub>	d <sub>T</sub>								
2	-9.54	-1.02	-7.98	-0.987	-9.92	-0.974	-9.89	-0.952	-5.87	-0.862
3	-12.32	-0.57	-10.04	-0.535	-12.9	-0.524	-12.85	-0.502	-7.11	-0.412
4	-13.74	-0.084	-10.81	-0.052	-14.51	-0.043	-14.45	-0.02	-7.26	0.069
5	-13.7	0.431	-10.2	0.461	-14.63	0.467	-14.56	0.492	-6.25	0.578
6	-11.93	0.977	-7.97	1	-13	1.01	-12.92	1.03	-3.84	1.12

Table 27 Comparison of thrust and propeller efficiency between the 1st design point and APC

11x4.7

With regards to propeller efficiency, it can be observed that for airfoils like ARAD 10, CLARK Y and BE 50, the QMIL generated propeller has a very insignificant increase compared to the propeller efficiency of APC 11x4.7 in the cruise range of 2m/s to 6m/s (advance ratio = 0.086 to 0.258). All the Martin Heppler (MH) airfoils, S7055 and Eppeler 63 give much lower efficiencies in the cruise range.

With regards to the thrust produced, a very non-intuitive trend is observed for all the propellers generated by QMIL. In all the cases, the thrust increases till a certain velocity after which it decreases. Ideally, the thrust decreases with increasing speed as the speed and quantity of impinging air particles on the blade increases for high velocities. But in this, the thrust increases, which may be explained by the value of the angle of attack at each section of the blade. As the forward linear speed is increased, the flow angle increases due to which angle of attack decreases. In cases where the angle of attack for the initial velocities is significantly higher than the optimal angle of attack (common in cases of high pitch angles, like the first design point), as the angle of attack decreases, and thus comes closer to the optimal angle of attack, for increasing forward velocities, the thrust also increases a little till a maximum after which thrust again decreases. In cases where the thrust decreases constantly, the angle of attacks for initial velocities is quite close to the optimal angle of attack (in cases of low pitch angles). For all the QMIL generated propellers, the thrust is lower than the thrust produced by APC 11x4.7 for velocities 2 m/s to 4 m/s while for 4 m/s to 6 m/s, the thrust produced by these propellers are greater than the thrust produced by APC 11x4.7.

### ***5.12 Main Take Aways From The First Design Point***

Since we are hardly getting any significant propeller efficiency improvements in the cruise range, this design point will have to be further modified to obtain higher efficiencies for lower speeds (2m/s to 6m/s). As discussed in chapter 3, one way of achieving higher propeller efficiencies for lower advance ratios (i.e. shifting the efficiency curve towards left) is by decreasing the pitch. Additionally, we would also desire a higher thrust generation, targeting significantly higher values of thrust for all the velocities in the cruise range.

## CHAPTER 6: 2<sup>nd</sup> Design Point

The parameters of the 2<sup>nd</sup> design point are as follows:

Cruise linear speed (m/s)	7
Rotational Speed (RPM)	7000
Thrust (N)	6
Chord Length Distribution	Modified for greater thrust
Lift coefficient Distribution	0.3,0.9,0.8
Blade Radius (m)	0.1397

*Table 28 2nd design point parameters*

### 6.1 Explanation of the parameter modifications

As mentioned in chapter 5, the primary aim of the 2<sup>nd</sup> design point is to decrease the pitch angles of the propeller so that we can achieve significantly higher propeller efficiencies than APC 11x4.7 for lower advance ratios. After repeated experimentation in QMIL, it was found that decreasing the pitch angles led to decrease in the overall pitch and pitch angles of the propeller. In order to account for the decreased thrust due to lower lift coefficient at the root, the lift coefficient values at the middle and tip of the blade are increased by 0.1 each. The chord length distribution has been modified in order to generate more propeller thrust. The chord length distribution generated from Qmil is problematic because the maximum chord length occurs at the root and exponentially decreases till the tip. Since the relative velocity of air at the root is very small, the contribution to the overall thrust from the root is negligible. Moreover, with this distribution the middle of the blade length has quite small chord length and since, the middle section contributes more to the thrust, the overall thrust generated by the propeller comes out to be quite low. Thus the propeller chord length distribution has been modified such that the values of the chord lengths at the middle sections is reasonably high. For detailed chord length distribution refer to chapter 3.

## 1). Propeller with ARAD-10 airfoil:

```
Template prop

2          ! Nblades

0.4500  8.1618    ! CL0      CL_a
-0.2260  1.5641    ! CLmin   CLmax

0.01562  0.001886  0.032407 0.6752 ! CD0      CD2u     CD2l     CLCD0
100000.0 -0.5           ! REref   REexp

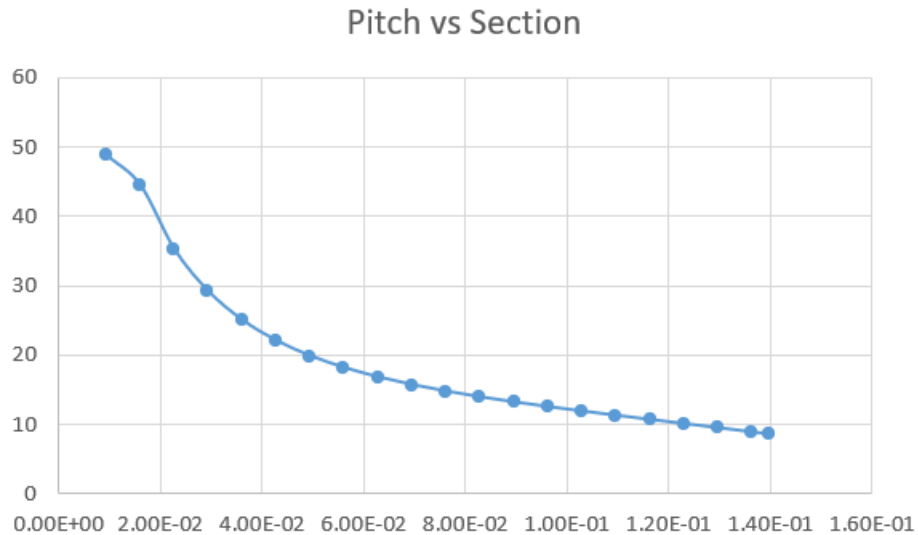
0.0  0.5  1.0  ! XIdes   (r/R locations where design cl is specified)
0.3  0.9  0.8  ! CLdes   (specified cl)

0.006    ! hub radius(m)
0.1397   ! tip radius(m)
7.00     ! speed(m/s)
7000    ! rpm

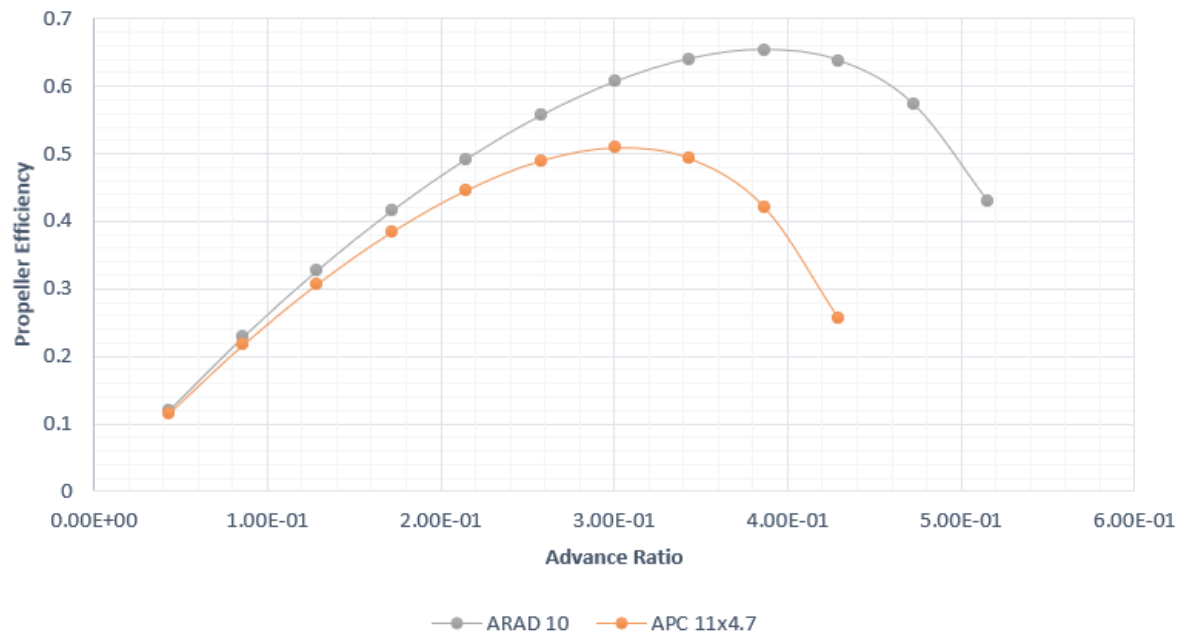
6.0      ! Thrust(N)  ( 0 if power  specified )
0.0 ! Power(W)    ( 0 if thrust specified )

0  0.0  ! Ldes   [ KQdes ]
# 18    ! Nout    number of output stations (optional)
```

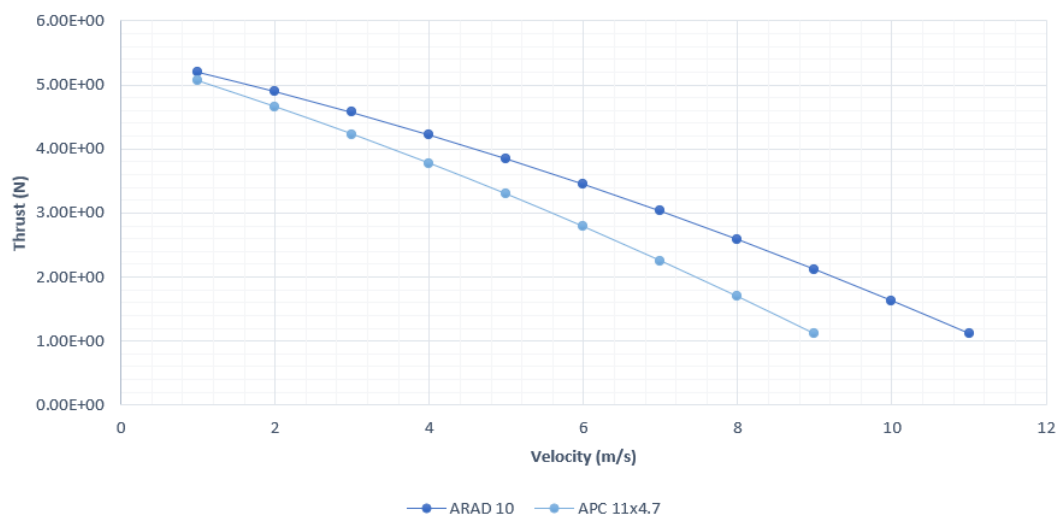
Figure 23 QMIL input file for ARAD-10



Graph 67 QMIL generated pitch angle distribution for ARAD-10



Graph 68 Efficiency curve comparison between ARAD-10 and APC 11x4.7



Graph 69 Thrust curve comparison between ARAD-10 and APC 11x4.7

## 2). Propeller with BE 50 airfoil:

```

Template prop

2           ! Nblades

0.3894  8.7994      ! CL0      CL_a
-0.2124  1.4155      ! CLmin    CLmax

0.0137   0.00222   0.03588  0.7829  ! CD0      CD2u     CD2l     CLCD0
100000.0 -0.5          ! REref    REexp

0.0  0.5  1.0      ! XIdes   (r/R locations where design cl is specified)
0.3  0.9  0.8      ! CLdes   (specified cl)

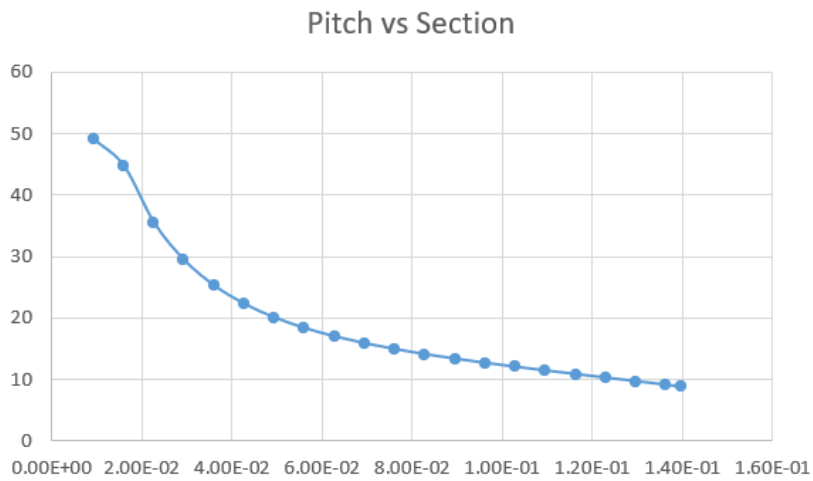
0.006      ! hub radius(m)
0.1397     ! tip radius(m)
7.00       ! speed(m/s)
7000       ! rpm

6.0        ! Thrust(N)  ( 0 if power specified )
0.0        ! Power(W)    ( 0 if thrust specified )

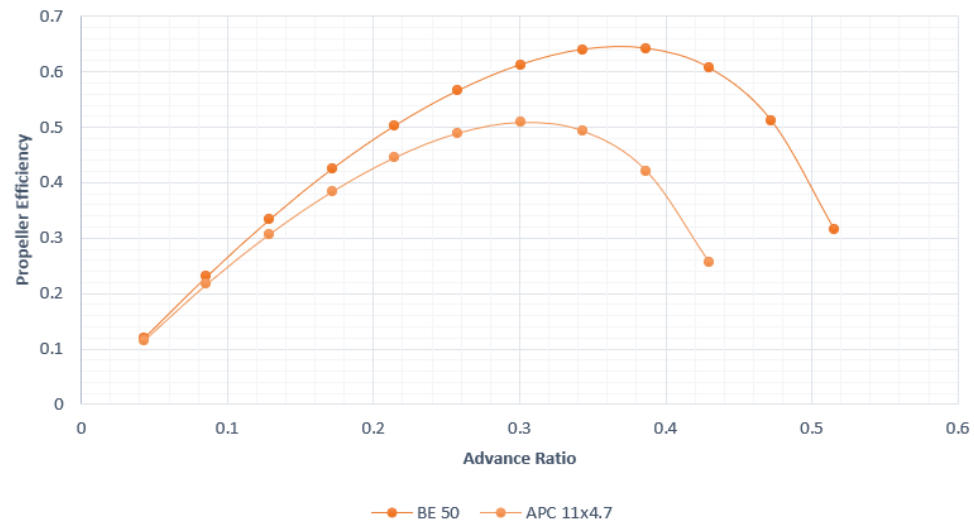
0  0.0      ! Ldes    [ KQdes ]
# 18        ! Nout    number of output stations (optional)

```

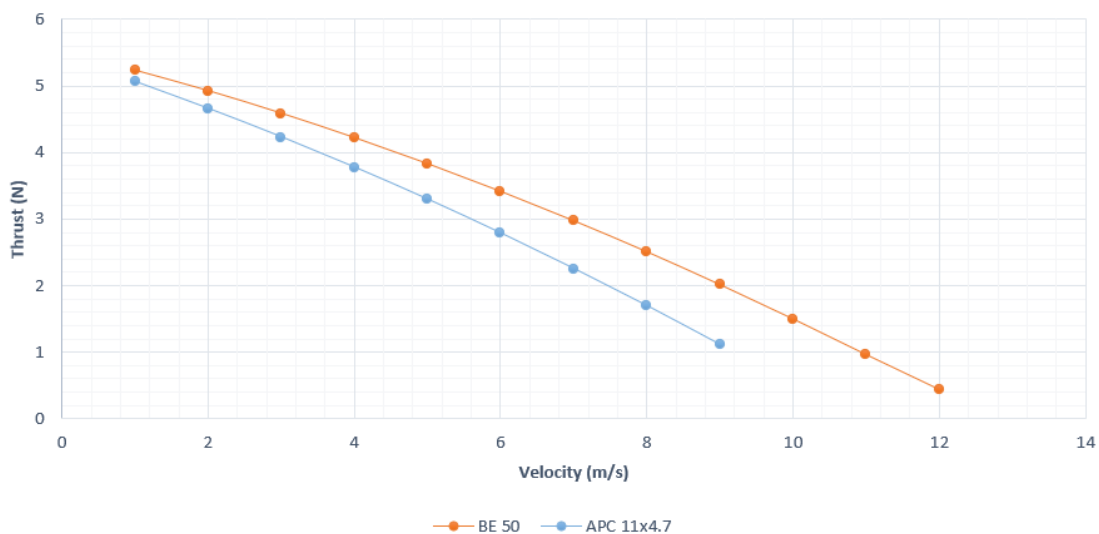
Figure 24 QMIL input file for BE50



Graph 70 QMIL generated pitch angle distribution for BE50



Graph 71 Efficiency curve comparison between BE50 and APC 11x4.7



Graph 72 Thrust curve comparison between BE50 and APC 11x4.7

### 3). Propeller with Eppeler 63 airfoil:

```

Template prop

2           ! Nblades

0.4355  9.8901    ! CL0      CL_a
-0.1798  1.4681    ! CLmin   CLmax

0.01941   0.004342  0.084376  0.5143  ! CD0      CD2u     CD2l   CLCD0
100000.0 -0.500          ! REref   REexp

0.0  0.5  1.0    ! XIdes   (r/R locations where design cl is specified)
0.3  0.9  0.8|  ! CLdes   (specified cl)

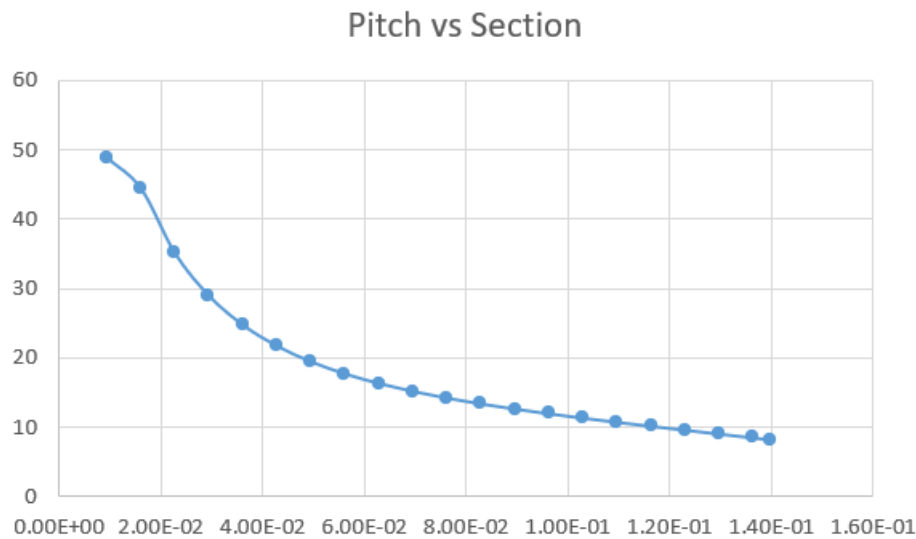
0.006    ! hub radius(m)
0.1397   ! tip radius(m)
7.00     ! speed(m/s)
7000    ! rpm

6.0      ! Thrust(N)  ( 0 if power specified )
0.0 ! Power(W)    ( 0 if thrust specified )

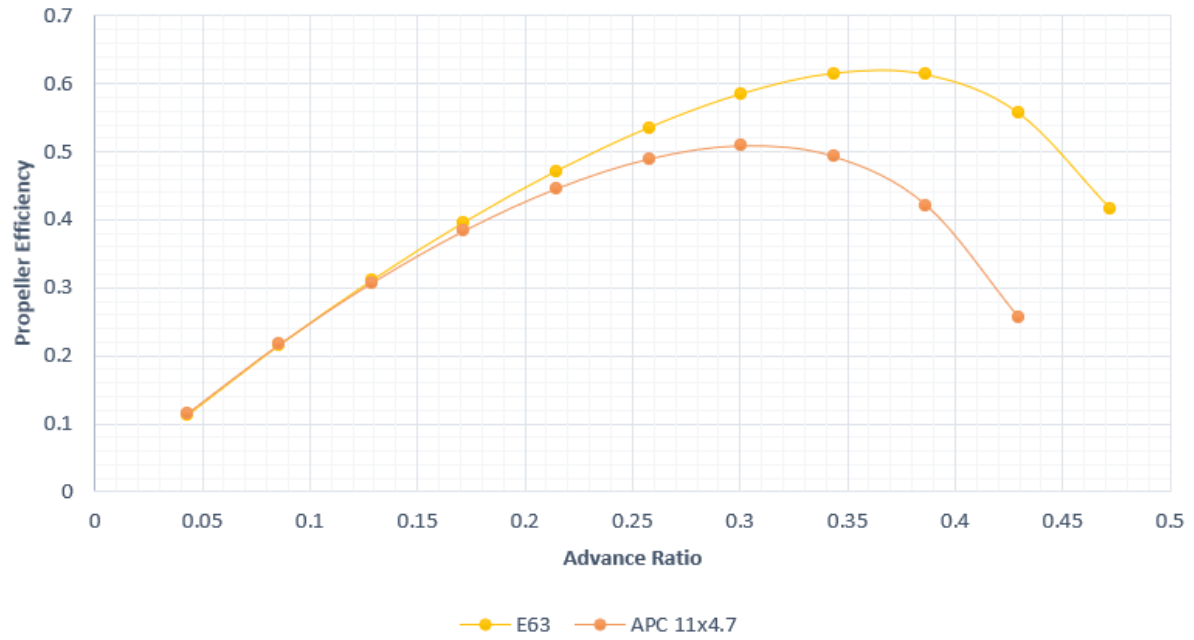
0  0.0  ! Ldes   [ KQdes ]
# 18       ! Nout    number of output stations (optional)

```

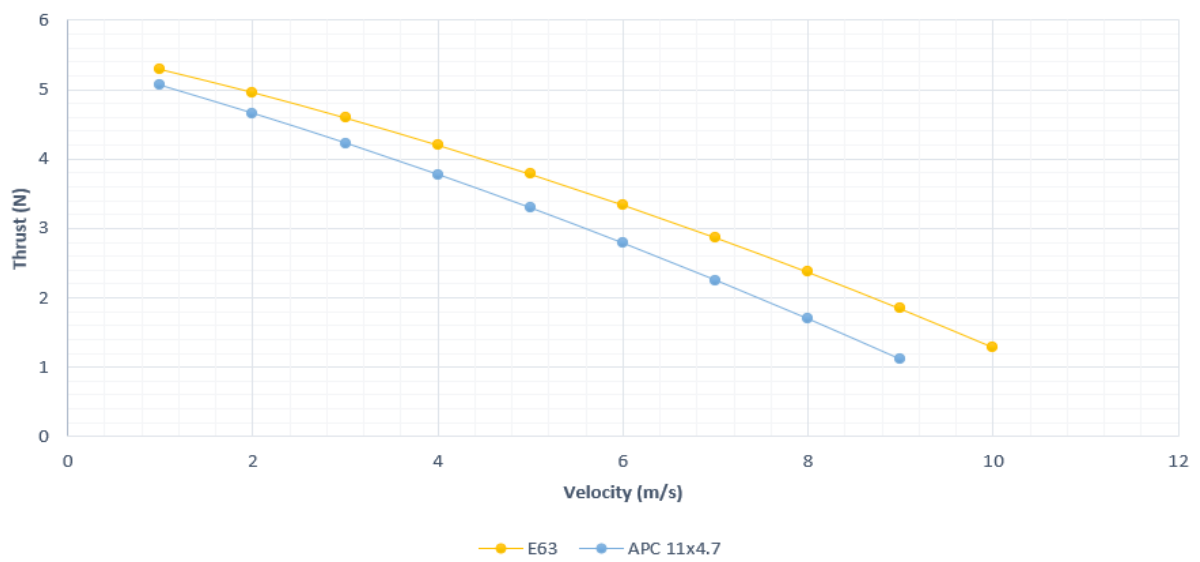
Figure 25 QMIL input file for Eppeler 63



Graph 73 QMIL generated pitch angle distribution for Eppeler 63



Graph 74 Efficiency curve comparison between Eppeler 63 and APC 11x4.7



Graph 75 Thrust curve comparison between Eppeler 63 and APC 11x4.7

#### 4). Propeller with CLARK Y airfoil:

Template prop

```

2           ! Nblades

0.3674  7.7928      ! CL0      CL_a
-0.3727  1.3694      ! CLmin   CLmax

0.01727   0.001224  0.019456  0.7699  ! CD0      CD2u     CD2l    CLCD0
1000000.0 -0.500          ! REref   REexp

0.0  0.5  1.0  ! XIdes  (r/R locations where design cl is specified)
0.3  0.9  0.8| ! CLdes  (specified cl)

0.006      ! hub radius(m)
0.1397     ! tip radius(m)
7.00       ! speed(m/s)
7000       ! rpm

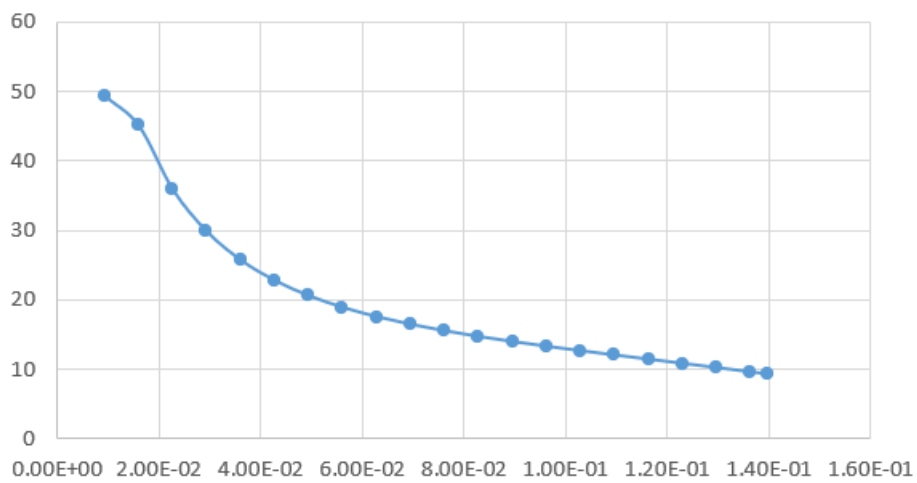
6.0        ! Thrust(N)  ( 0 if power specified )
0.0  ! Power(W)    ( 0 if thrust specified )

0  0.0  ! Ldes  [ KQdes ]
# 18    ! Nout    number of output stations (optional)

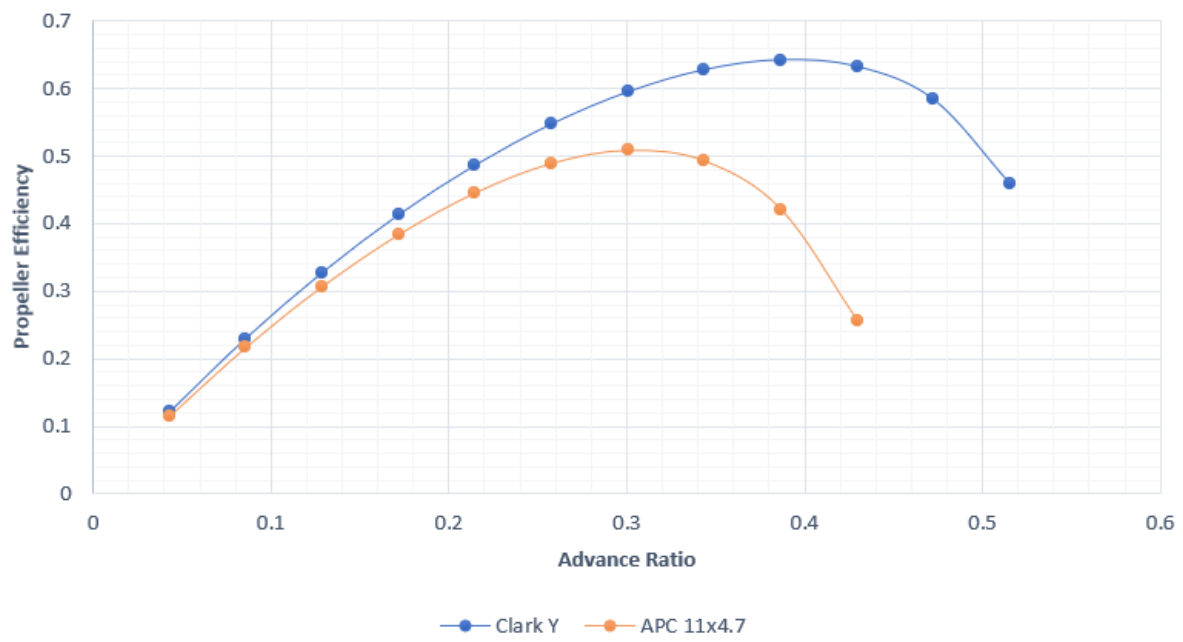
```

Figure 26 QMIL input file for CLARK Y

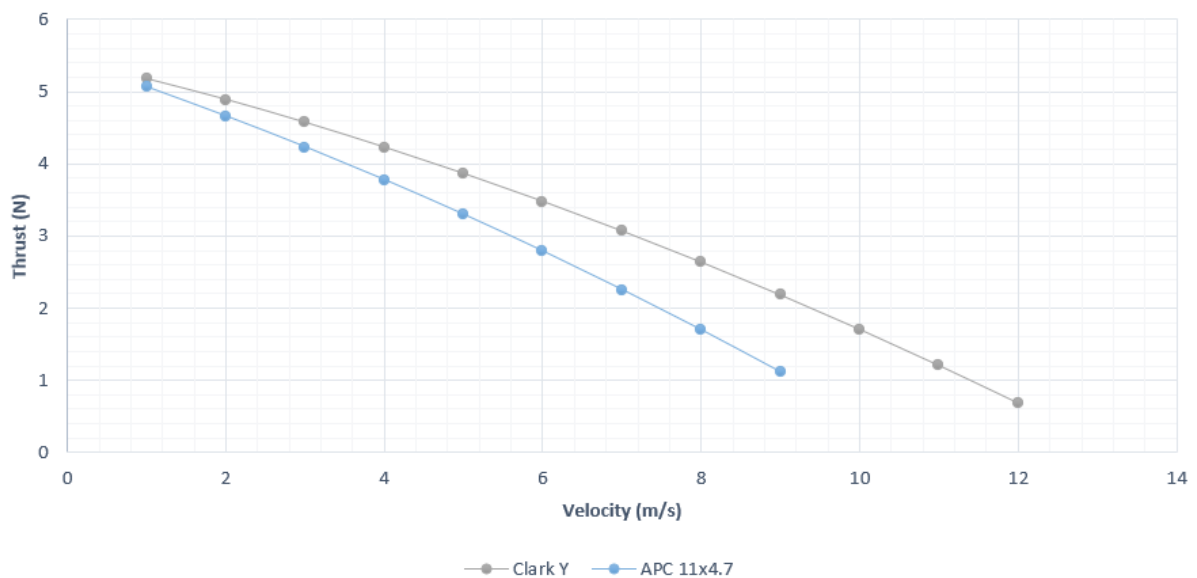
Pitch vs Section



Graph 76 QMIL generated pitch angle distribution for CLARK Y



Graph 77 Efficiency curve comparison between CLARK Y and APC 11x4.7



Graph 78 Thrust curve comparison between CLARK Y and APC 11x4.7

### 5). Propeller with MH22 (7.2%) airfoil:

```

Template prop

2           ! Nblades

0.2273  5.9176    ! CL0      CL_a
-0.5266  0.9297    ! CLmin   CLmax

0.01066   0.027755  0.385606 -0.0893  ! CD0      CD2u     CD2l     CLCD0
100000.0 -0.500          ! REref   REexp

0.0  0.5  1.0    ! XIdes   (r/R locations where design cl is specified)
0.3  0.9  0.8|  ! CLdes   (specified cl)

0.006    ! hub radius(m)
0.1397   ! tip radius(m)
7.00     ! speed(m/s)
7000    ! rpm

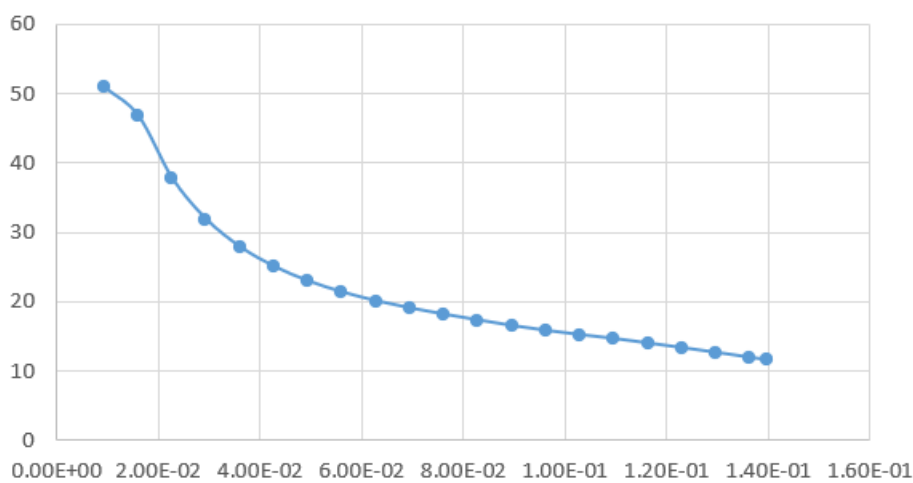
6.0      ! Thrust(N)  ( 0 if power specified )
0.0  ! Power(W)    ( 0 if thrust specified )

0  0.0  ! Ldes   [ KQdes ]
# 18       ! Nout    number of output stations (optional)

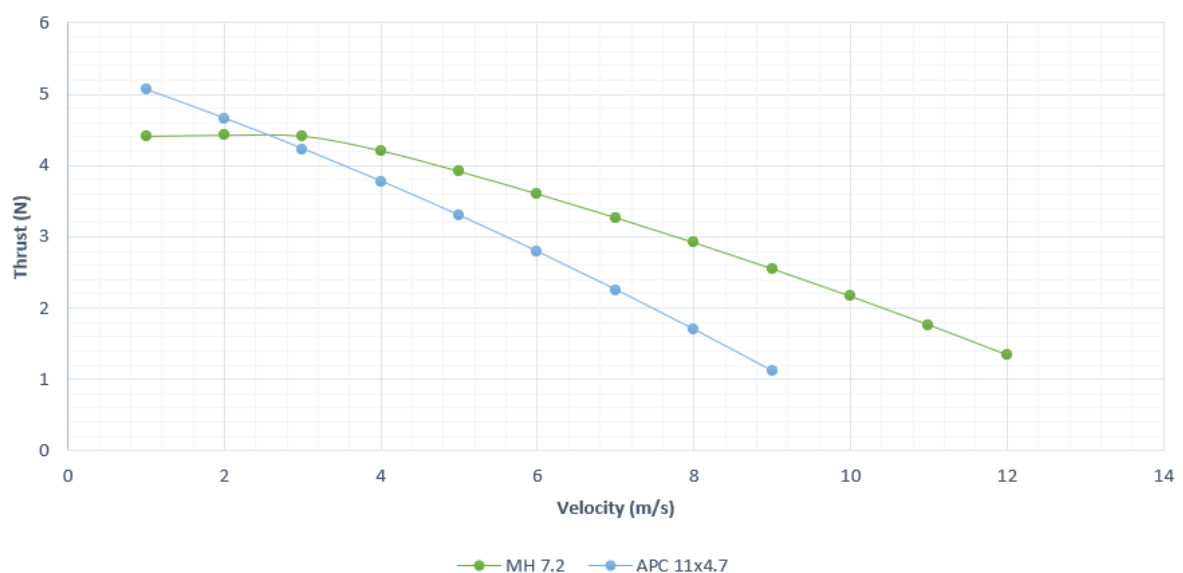
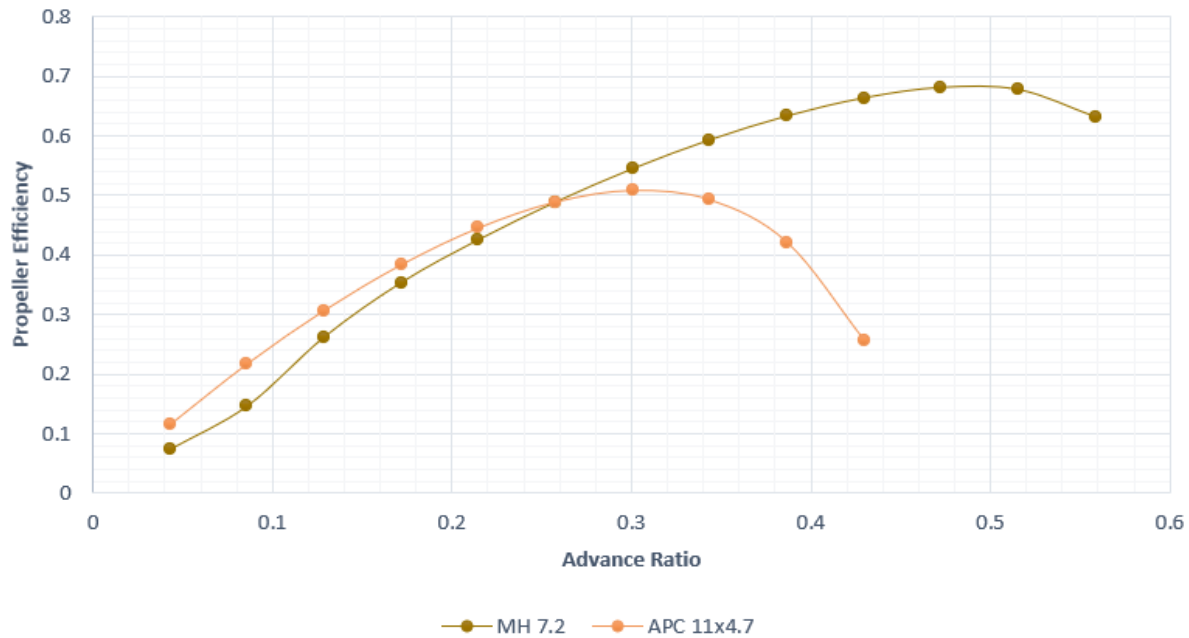
```

Figure 27 QMIL input file for MH22 (7.2%)

Pitch vs Section



Graph 79 QMIL generated pitch angle distribution for MH22 (7.2%)



## 6). Propeller with MH30 (7.84%) airfoil:

```

Template prop

2           ! Nblades

0.0193  6.4911    ! CL0      CL_a
-0.4868  1.0085    ! CLmin    CLmax

0.01191   0.009354  0.496708 -0.1359  ! CD0      CD2u     CD2l     CLCD0
100000.0 -0.500          ! REref    REexp

0.0  0.5  1.0    ! XIdes   (r/R locations where design cl is specified)
0.3  0.9  0.8    ! CLdes   (specified cl)

0.006    ! hub radius(m)
0.1397   ! tip radius(m)
7.00     ! speed(m/s)
7000    ! rpm

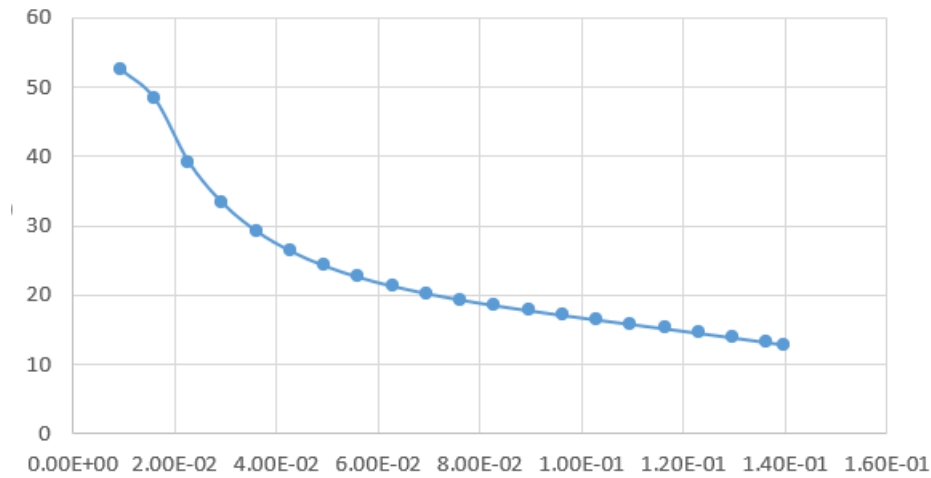
6.0      ! Thrust(N)  ( 0 if power specified )
0.0      ! Power(W)   ( 0 if thrust specified )

0  0.0    ! Ldes   [ KQdes ]
# 18       ! Nout    number of output stations (optional)

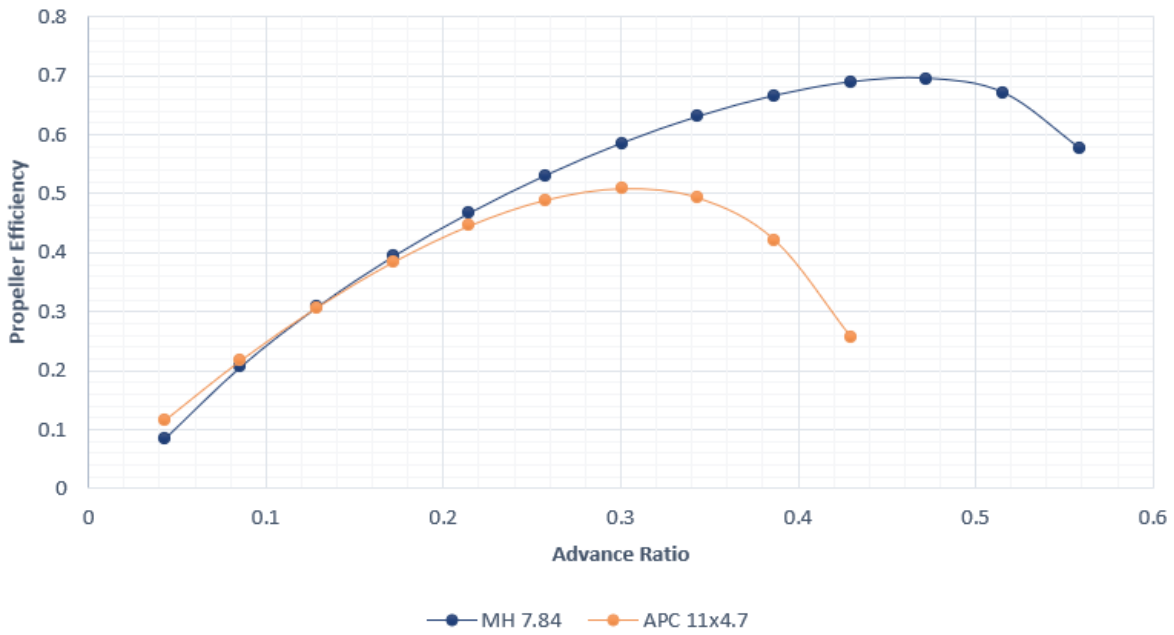
```

Figure 28 QMIL input file for MH30 (7.84%)

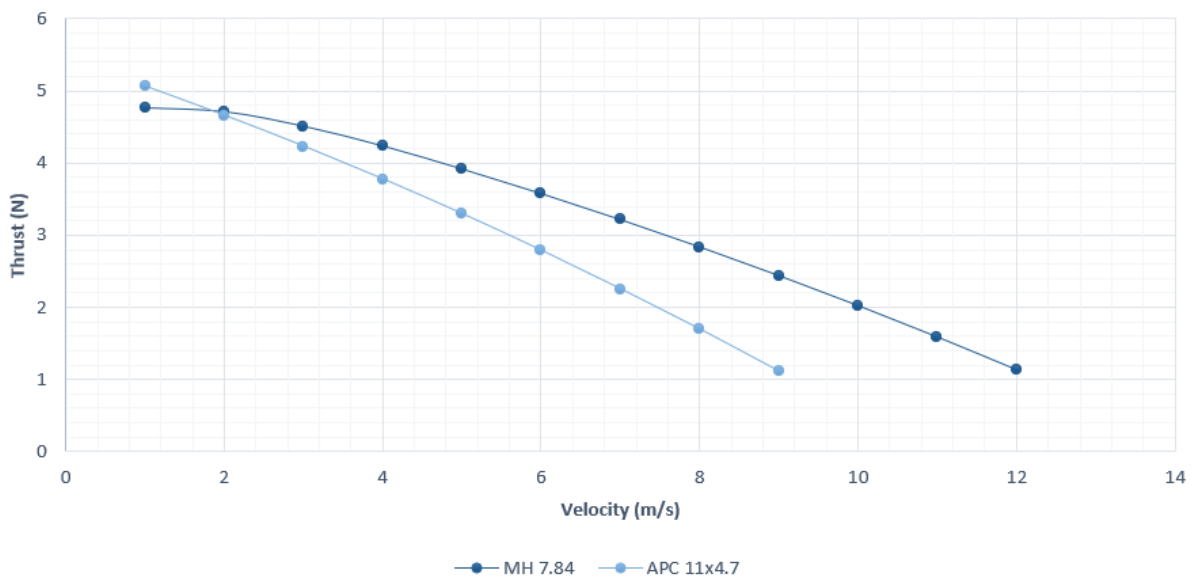
Pitch vs Section



Graph 82 QMIL generated pitch angle distribution for MH30 (7.84%)



Graph 83 Efficiency curve comparison between MH30 (7.84%) and APC 11x4.7



Graph 84 Thrust curve comparison between MH30 (7.84%) and APC 11x4.7

## 7). Propeller with MH32 (8.7%) airfoil:

```

Template prop

2           ! Nblades

0.1797  7.4492    ! CL0      CL_a
-0.4388  1.1497    ! CLmin   CLmax

0.01348   0.001885  0.0461513 -0.1162  ! CD0      CD2u     CD2l   CLCD0
100000.0 -0.500          ! REref   REexp

0.0  0.5  1.0    ! XIdes   (r/R locations where design cl is specified)
0.3  0.9  0.8    ! CLdes   (specified cl)

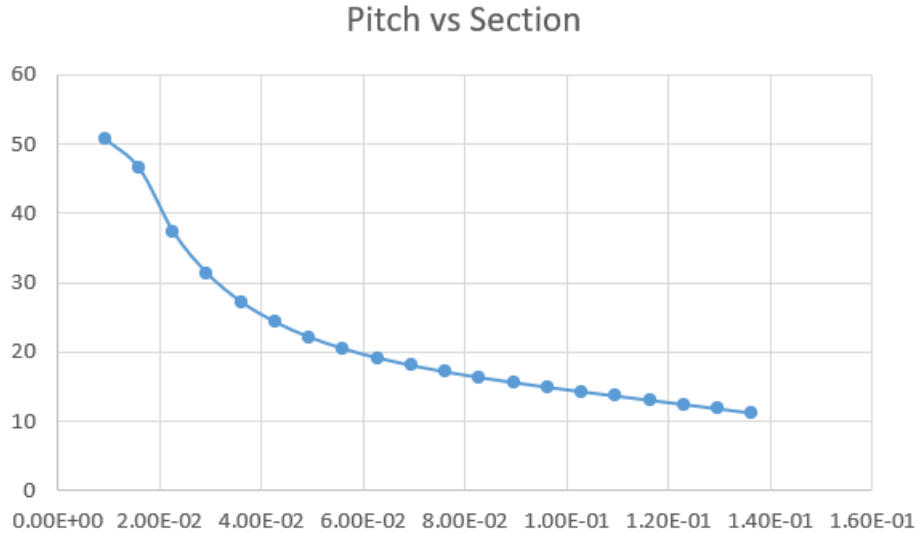
| 0.006    ! hub radius(m)
0.1397    ! tip radius(m)
7.00       ! speed(m/s)
7000       ! rpm

6.0        ! Thrust(N)  ( 0 if power specified )
0.0 ! Power(W)    ( 0 if thrust specified )

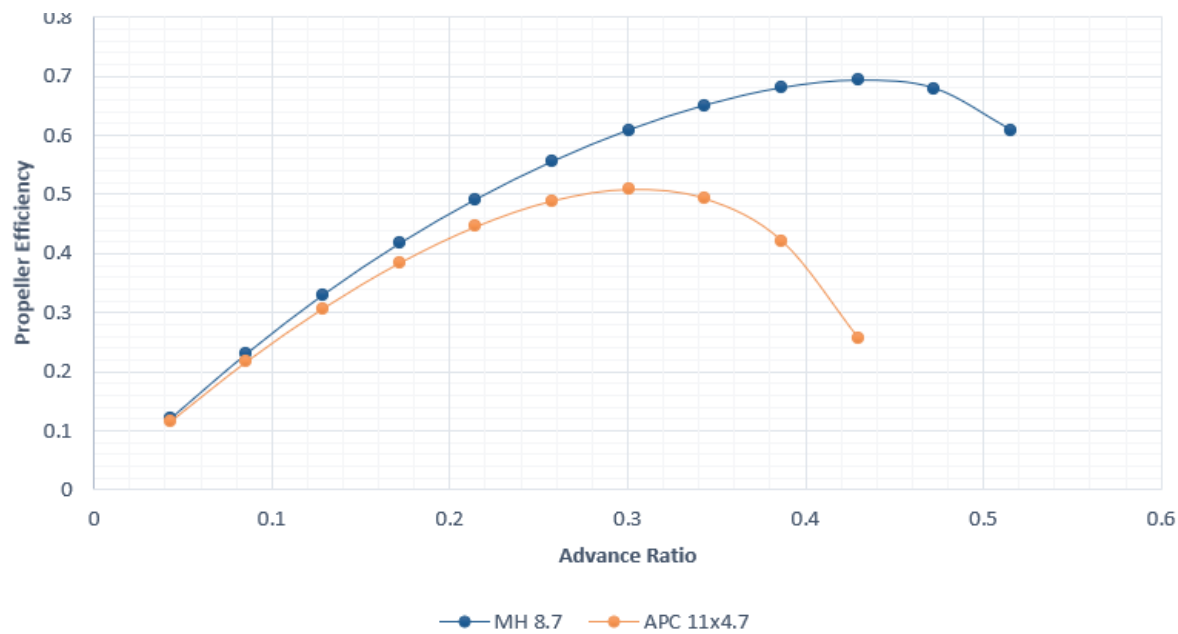
0  0.0    ! Ldes   [ KQdes ]
# 18       ! Nout    number of output stations (optional)

```

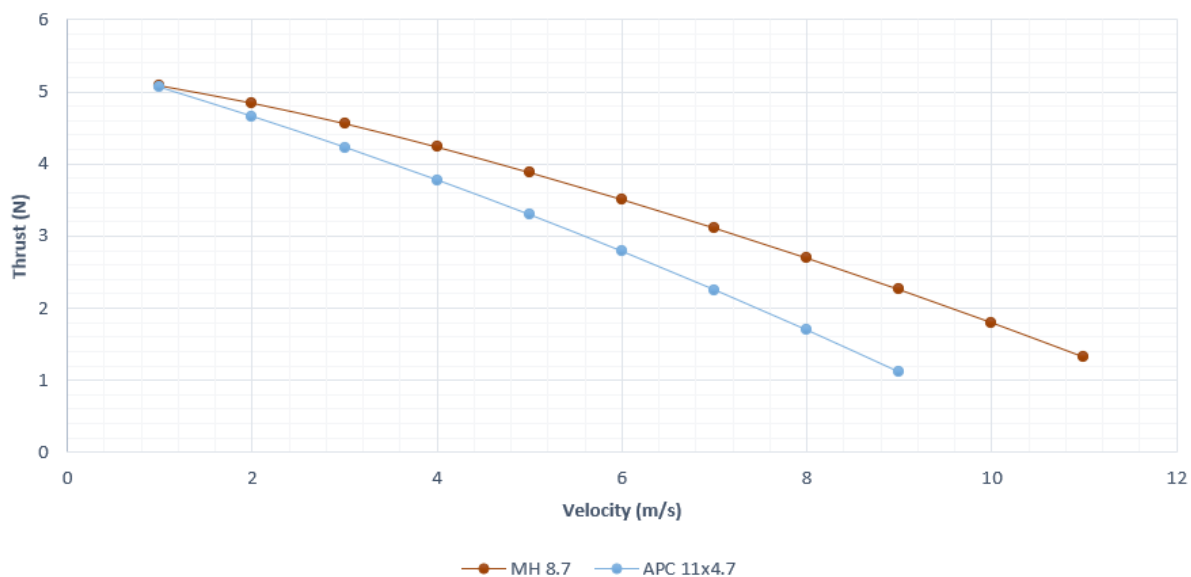
Figure 29 QMIL input file for MH32 (8.7%)



Graph 85 QMIL generated pitch angle distribution for MH32 (8.7%)



Graph 86 Efficiency curve comparison between MH32 (8.7%) and APC 11x4.7



Graph 87 Thrust curve comparison between MH32 (8.7%) and APC 11x4.7

### 8). Propeller with MH43 (8.5%) airfoil:

Template prop

```

2           ! Nblades

0.2527  6.2792    ! CL0      CL_a
-0.5177  1.0203    ! CLmin   CLmax

0.01244   0.007641  0.533645 -0.1839  ! CD0      CD2u     CD2l     CLCD0
100000.0 -0.500          ! REref   REexp

0.0  0.5  1.0  ! XIdes  (r/R locations where design cl is specified)
0.3  0.9  0.8  ! CLdes  (specified cl)

0.006    ! hub radius(m)
0.1397   ! tip radius(m)
7.00     ! speed(m/s)
7000    ! rpm

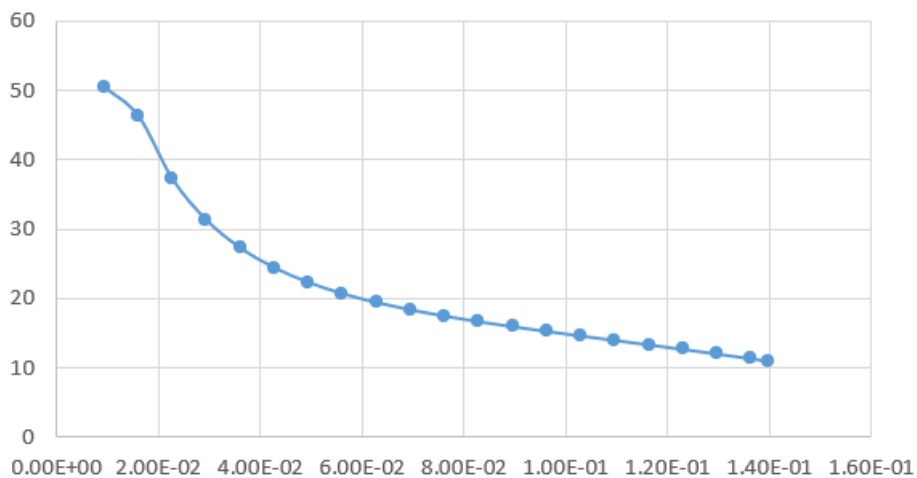
6.0|     ! Thrust(N)  ( 0 if power specified )
0.0  ! Power(W)    ( 0 if thrust specified )

0  0.0  ! Ldes   [ KQdes ]
# 18    ! Nout    number of output stations (optional)

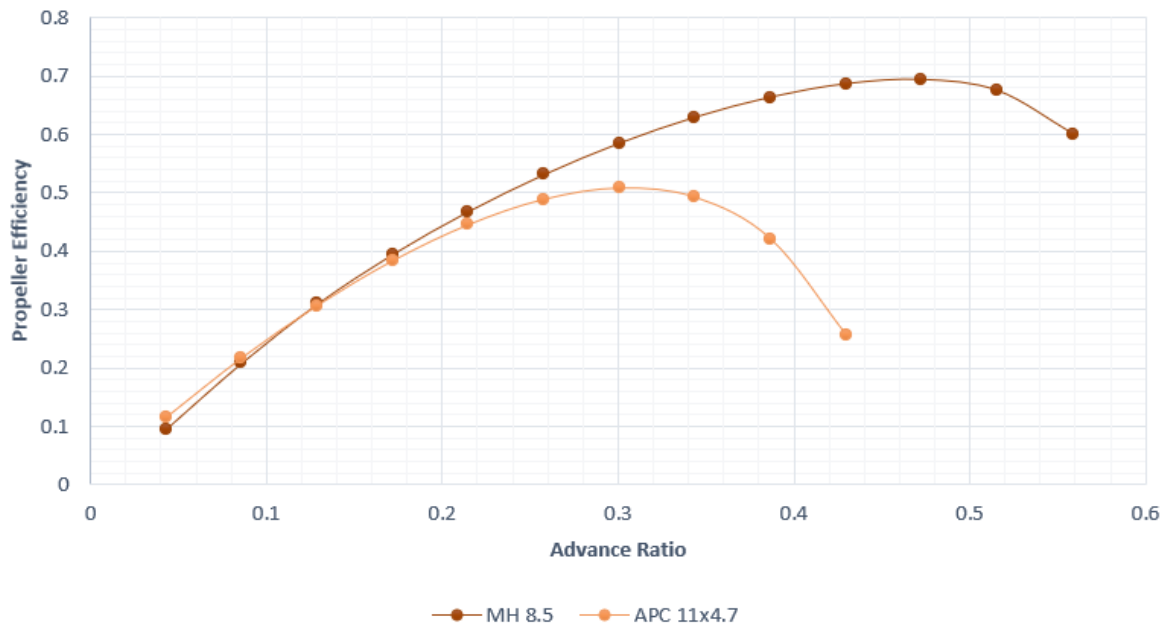
```

Figure 30 QMIL input file for MH43 (8.5%)

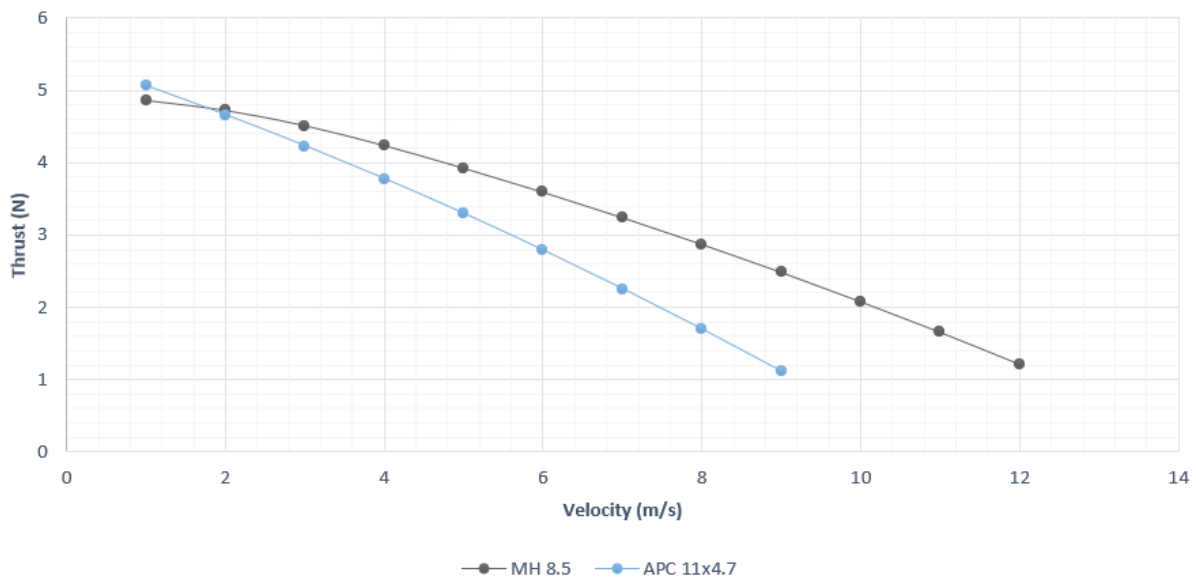
Pitch vs Section



Graph 88 QMIL generated pitch angle distribution for MH43 (8.5%)



Graph 89 Efficiency curve comparison between MH43 (8.59%) and APC 11x4.7



Graph 90 Thrust curve comparison between MH43 (8.5%) and APC 11x4.7

## 9). Propeller with MH64 (8.59%) airfoil:

```

Template prop

2           ! Nblades

0.2223  6.1572    ! CL0      CL_a
-0.5508  1.0251    ! CLmin   CLmax

0.01188   0.007853  0.420566 -0.1713  ! CD0      CD2u     CD2l   CLCD0
100000.0 -0.500          ! REref   REexp

0.0  0.5  1.0  ! XIdes  (r/R locations where design cl is specified)
0.3  0.9  0.8  ! CLdes  (specified cl)

0.006    ! hub radius(m)
0.1397   ! tip radius(m)
7.00     ! speed(m/s)
7000    ! rpm

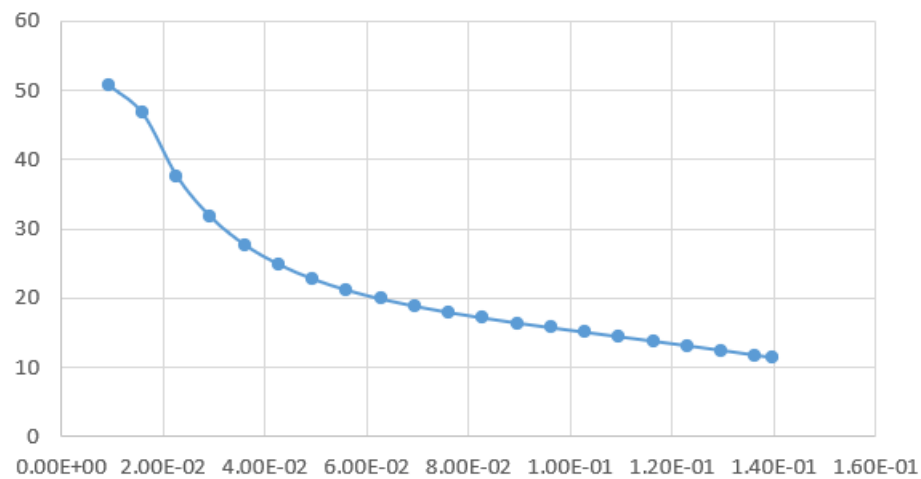
6.0|    ! Thrust(N)  ( 0 if power specified )
0.0 ! Power(W)    ( 0 if thrust specified )

0  0.0  ! Ldes  [ KQdes ]
# 18       ! Nout    number of output stations (optional)

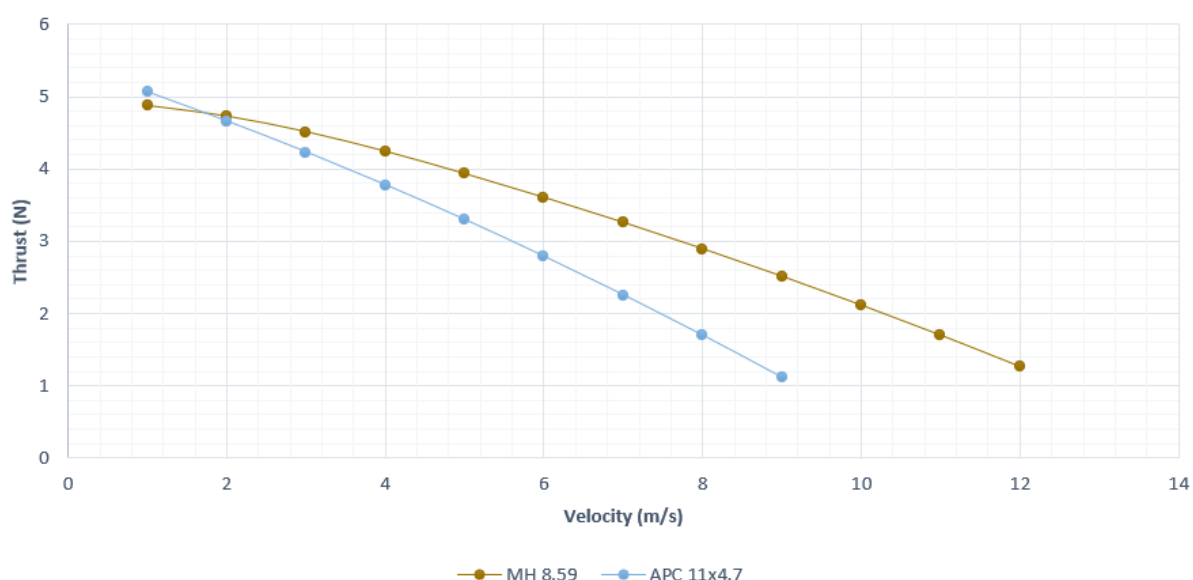
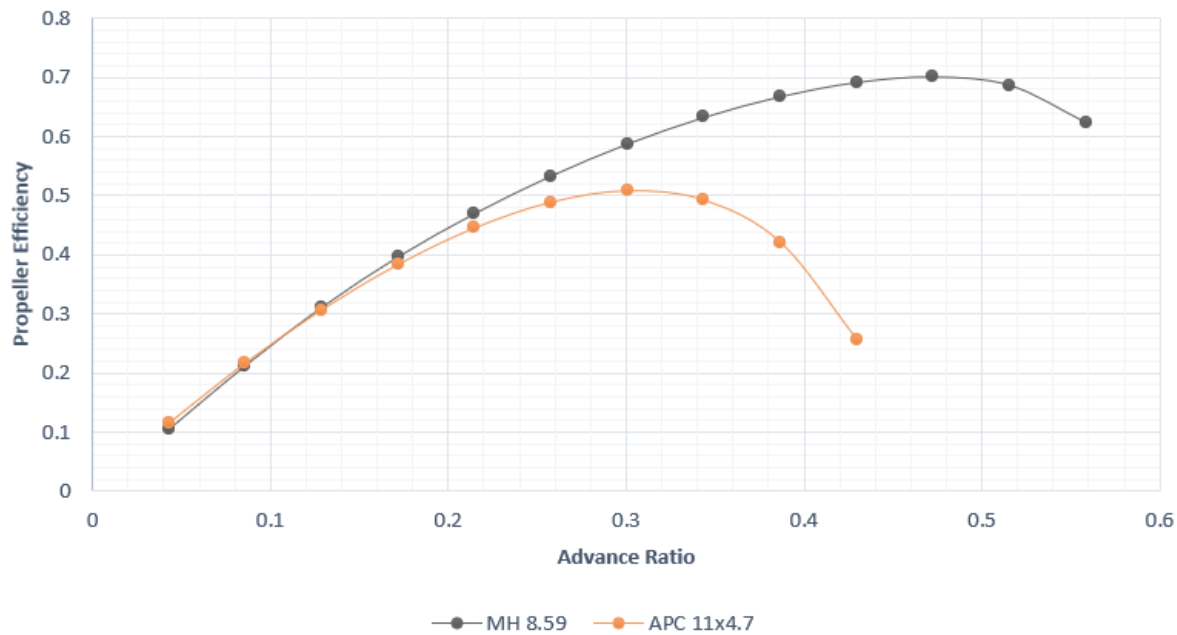
```

Figure 31 QMIL input file for MH64 (8.59%)

Pitch vs Section



Graph 91 QMIL generated pitch angle distribution for MH64 (8.59%)

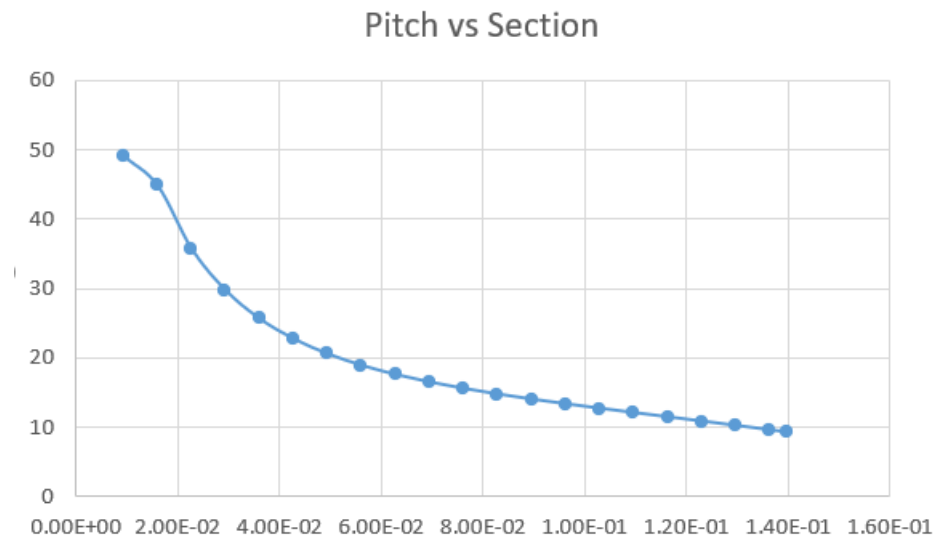


## 10). Propeller with S7055 airfoil:

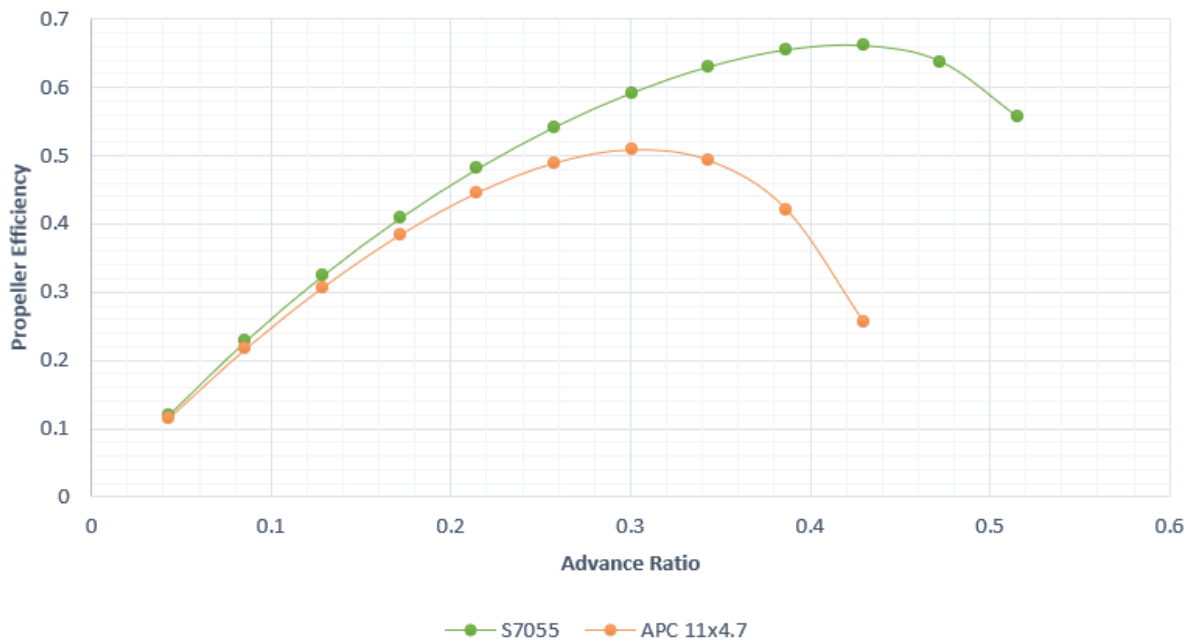
Template prop

```
2           ! Nblades  
  
| 0.3952  7.2935    ! CL0      CL_a  
| -0.3553  1.2615    ! CLmin   CLmax  
  
| 0.01771  0.001054  0.131934  0.1947  ! CD0      CD2u     CD2l     CLCD0  
| 100000.0 -0.500          ! REref   REexp  
  
0.0  0.5  1.0  ! XIdes  (r/R locations where design cl is specified)  
0.3  0.9  0.8  ! CLdes   (specified cl)  
  
0.006    ! hub radius(m)  
0.1397   ! tip radius(m)  
7.00     ! speed(m/s)  
7000    ! rpm  
  
6.0      ! Thrust(N)  ( 0 if power specified )  
0.0      ! Power(W)   ( 0 if thrust specified )  
  
0  0.0  ! Ldes   [ KQdes ]  
# 18      ! Nout    number of output stations (optional)
```

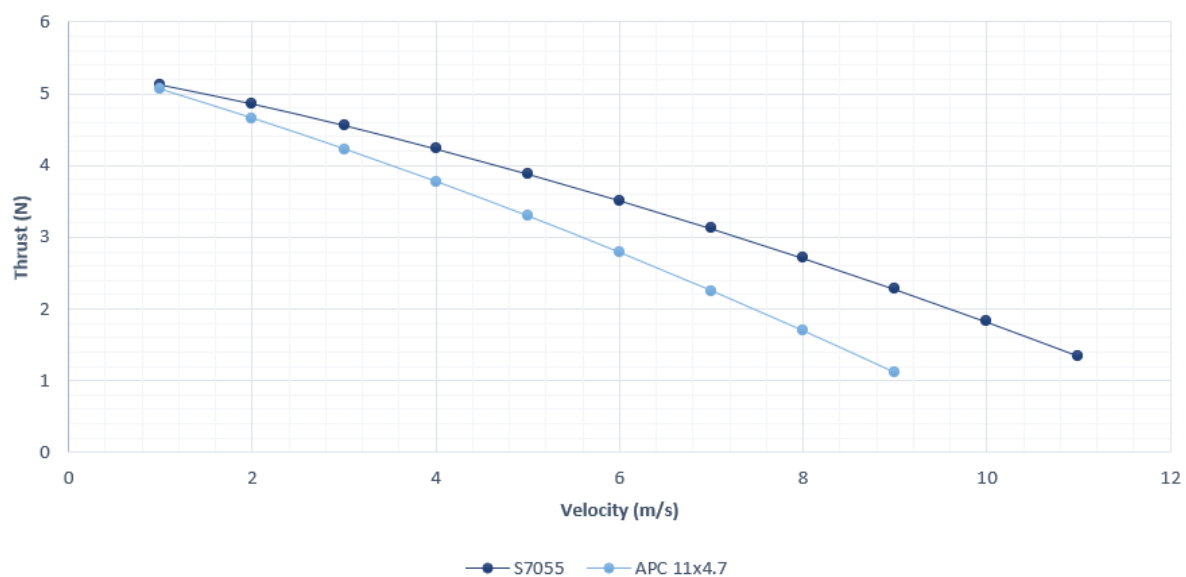
Figure 32 QMIL input file for S7055



Graph 94 QMIL generated pitch angle distribution for S7055



Graph 95 Efficiency curve comparison between S7055 and APC 11x4.7



Graph 96 Thrust curve comparison between S7055 and APC 11x4.7

## 6.2 General Observations From 2<sup>nd</sup> Design Point:

Airfoil used in Propeller	Peak Propeller efficiency	Advance ratio	Maximum Thrust Produced (N)
BE 50	0.6417	0.3865	5.21
ARAD 10	0.6535	0.3865	5.231
CLARK Y	0.6424	0.3865	5.171
Eppeler 63	0.6149	0.3436	5.293
MH22 (7.2%)	0.6809	0.4724	4.424
MH30 (7.84%)	0.6953	0.4724	4.76
MH32 (8.7%)	0.693	0.429	5.081
MH43 (8.5%)	0.694	0.4724	4.86
MH64 (8.59%)	0.7015	0.4724	4.872
S7055	0.6611	0.429	5.12

Table 29 Summary of aerodynamic performance characteristics at 2nd Design Point

Velocity	ARAD10		BE50		CLARKY		E63		MH7.2	
	D <sub>eff</sub>	d <sub>T</sub>								
2	1.17	0.248	1.35	0.270	1.33	0.231	-0.12	0.307	-7.1	-0.230
3	2.06	0.347	2.62	0.358	2.07	0.341	0.38	0.368	-4.48	0.184
4	3.17	0.450	4.09	0.446	2.94	0.453	1.25	0.429	-3.02	0.432
5	4.64	0.557	5.7	0.535	4.09	0.570	2.59	0.491	-2.02	0.621

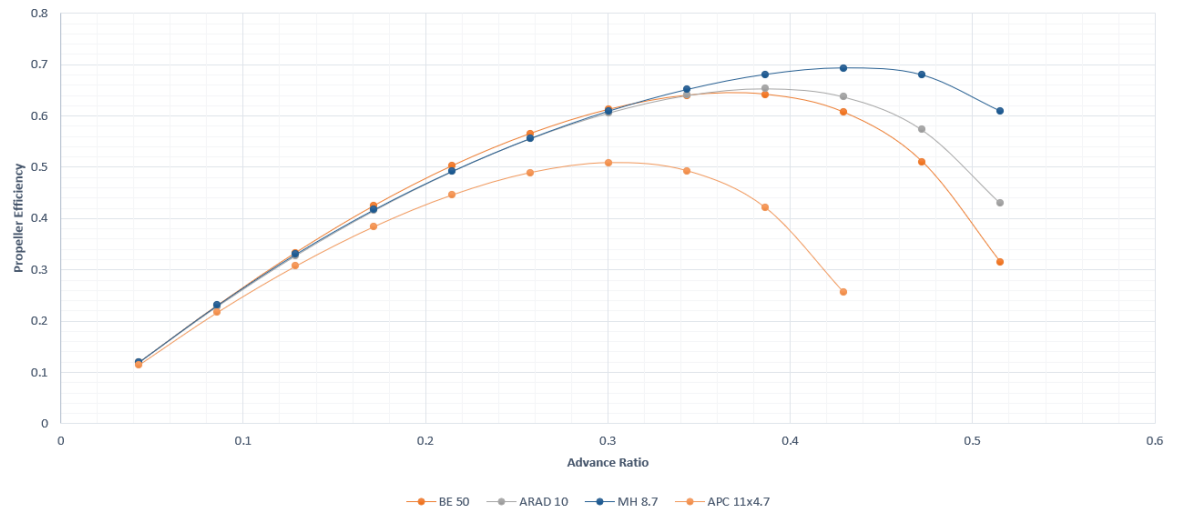
6	6.7	0.668	7.63	0.627	5.82	0.692	4.6	0.555	-0.05	0.813
---	-----	-------	------	-------	------	-------	-----	-------	-------	-------

*Table 30 1). Comparison of propeller efficiency and thrust between 2nd Design point and APC 11x4.7*

Velocity	MH7.84		MH8.7		MH8.5		MH8.59		S7055	
	D <sub>eff</sub>	d <sub>T</sub>								
2	-1.02	0.0520	1.39	0.185	-0.75	0.0670	-0.45	0.0710	1.22	0.202
3	0.05	0.278	2.33	0.329	0.31	0.283	0.44	0.282	1.81	0.330
4	0.98	0.459	3.32	0.458	1.14	0.462	1.32	0.465	2.5	0.457
5	2.15	0.620	4.62	0.585	2.26	0.629	2.45	0.636	3.53	0.588
6	4.19	0.788	6.66	0.719	4.22	0.805	4.45	0.816	5.28	0.727

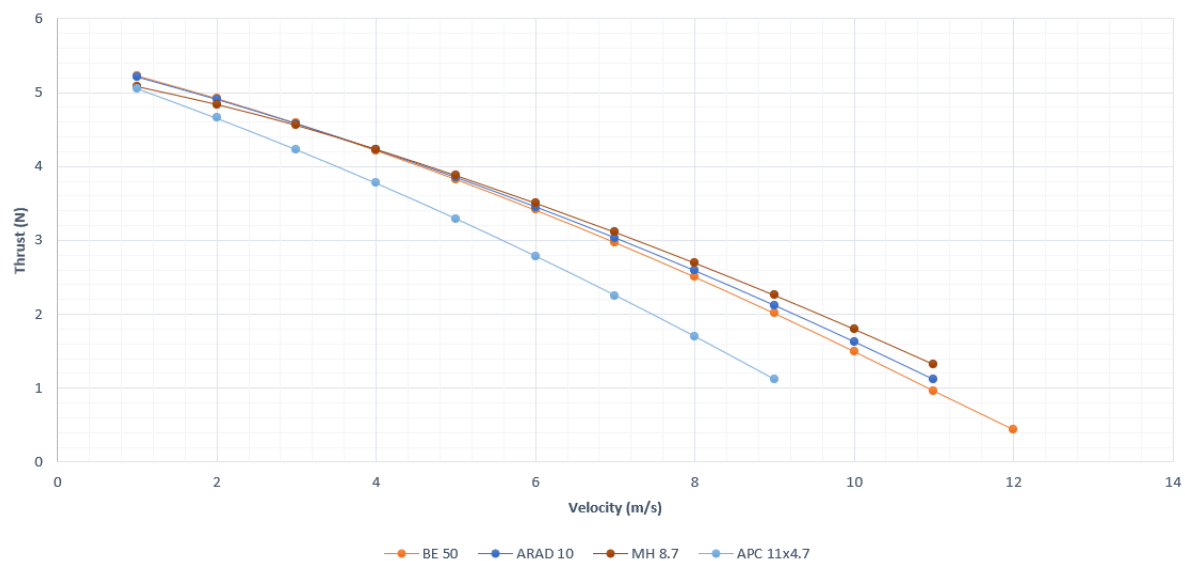
*Table 31 2). Comparison of propeller efficiency and thrust between 2nd Design point and APC 11x4.7*

As expected, for the 2<sup>nd</sup> design point, the peak efficiency, albeit a little less, is occurring at lower advance ratios compared to the 1<sup>st</sup> design point for all the propellers and thus, for most of the propellers, the propeller efficiency in the cruise range is significantly higher than the propeller efficiency of APC 11x4.7. Since the chord length was also modified, the thrust produced by the propellers also has increased and for the most cases, is more than the propeller thrust of APC 11x4.7 in the cruise range. Among the 10 propellers generated, the propeller with BE 50 as its airfoil shows the most significant increase in efficiency as compared to APC 11x4.7 in the cruise range followed closely by the propellers made by ARAD-10 and MH32 (8.7%). All the other propellers give lesser efficiencies than these three propellers.



Graph 97 Efficiency curve comparison for BE50, ARAD-10, MH32 (8.7%) and APC 11x4.7

Since, we want to keep a balance between the efficiency of the propeller and the thrust produced by this, the thrust provided by these 3 propellers are also compared.



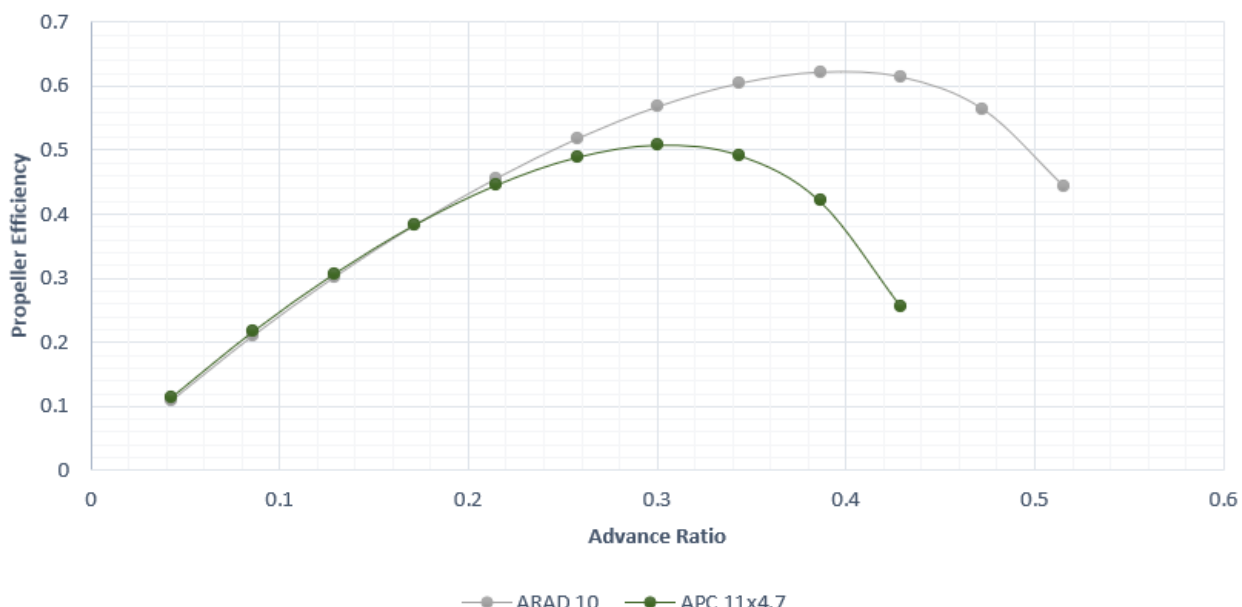
Graph 98 Thrust curve comparison for BE50, ARAD-10, MH32 (8.7%) and APC 11x4.7

If we observe the thrust curves in the cruise range 2m/s to 6m/s, there is not much difference in thrusts, but from 2m/s to 4m/s, the thrust produced by MH32 (8.7%) is slightly lower than the almost equal thrusts of ARAD-10 and BE 50. After 4m/s however, we observe that the thrust produced by MH32 (8.7%) is more than both ARAD-10 and BE50. Since all these propellers show almost equally good performance compared to APC 11x4.7, if the 2<sup>nd</sup> design point is chosen as the final design point, all these three propellers will be studied upon further.

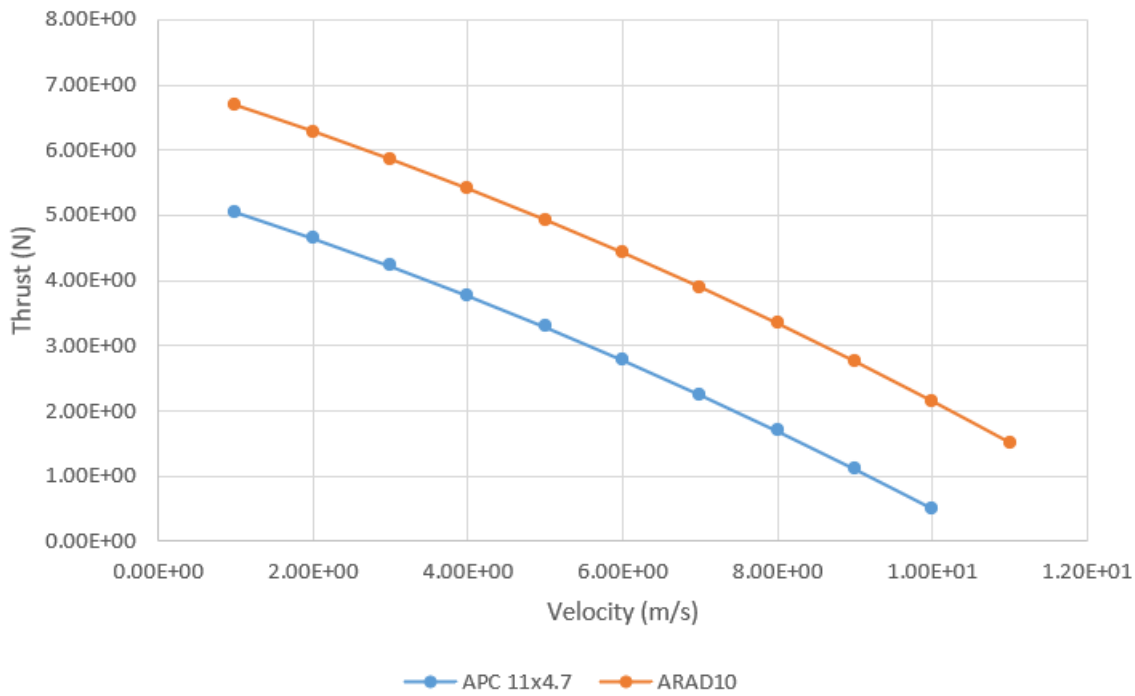
## CHAPTER 7: 3<sup>rd</sup> Design Point

In the 2<sup>nd</sup> design point, we saw significant improvement in lower velocity efficiencies but the difference between the thrust of the propellers on 2<sup>nd</sup> design point and APC 11x4.7 was not too high, although the 2<sup>nd</sup> design point propellers were giving higher thrusts. Thus, the purpose of this design point is to simply further modify the chord lengths of the propeller in order to create higher thrusts. Rest of the design point parameters like forward linear velocity, rotational speed and lift coefficient distribution remains the same. Since increasing the thrust may lead to a drop in efficiencies, this design point will be chosen only if the propeller efficiencies are significantly higher than the efficiencies of APC 11x4.7 in the cruise range. For the chord length distribution, refer to chapter 3.

### 1). Propeller with ARAD-10 airfoil:

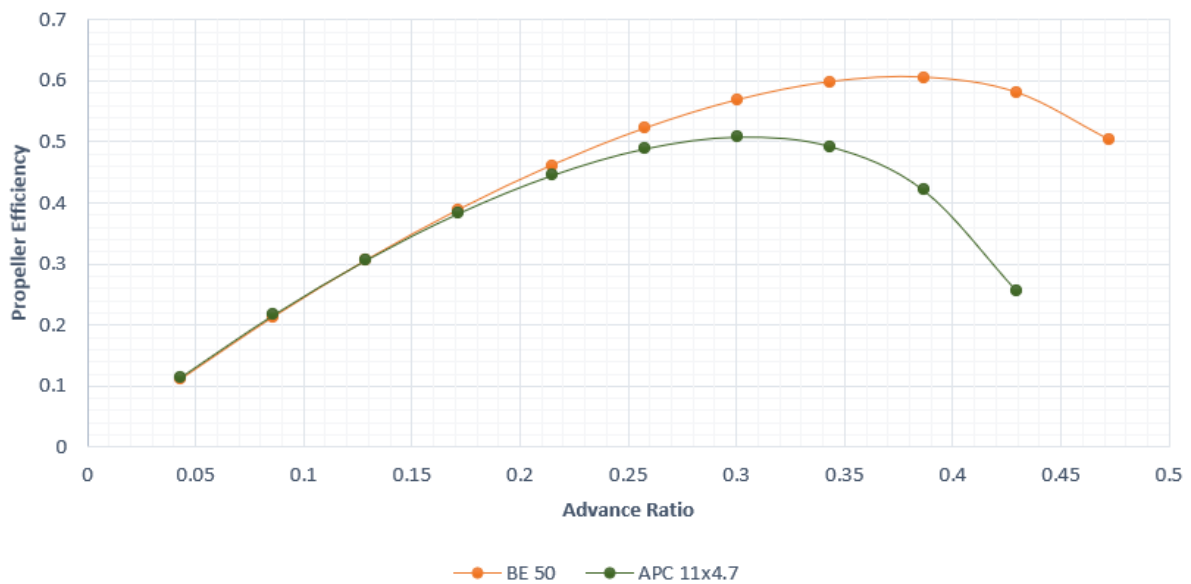


Graph 99 Efficiency curve comparison between ARAD-10 and APC 11x4.7

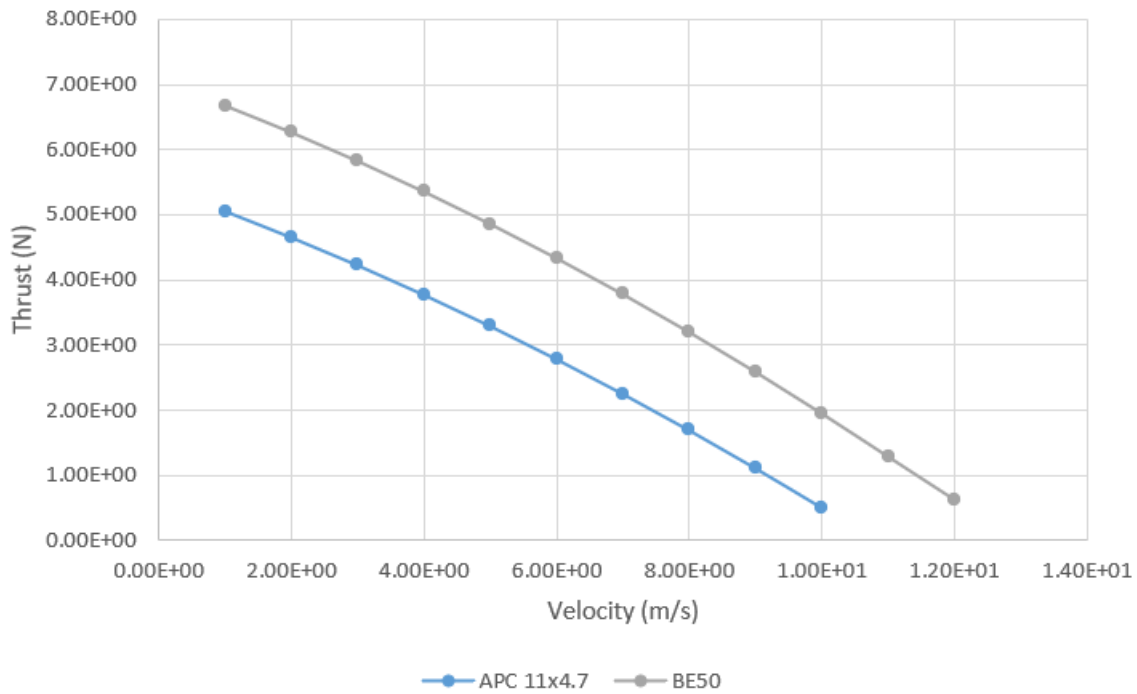


Graph 100 Thrust curve comparison between ARAD-10 and APC 11x4.7

## 2). Propeller with BE50 airfoil:

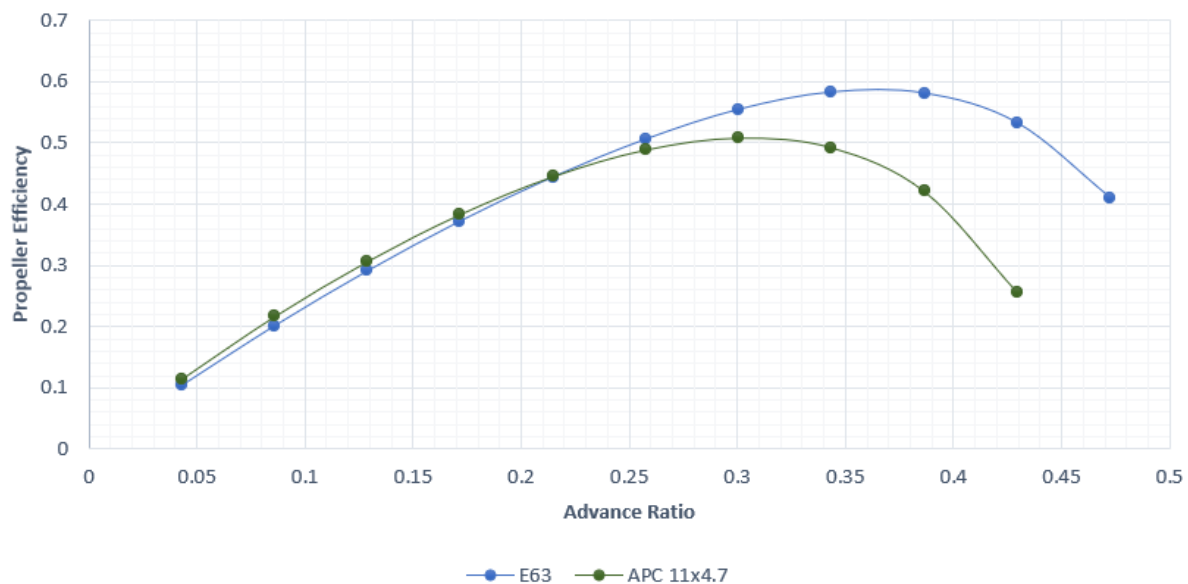


Graph 101 Efficiency curve comparison between BE50 and APC 11x4.7

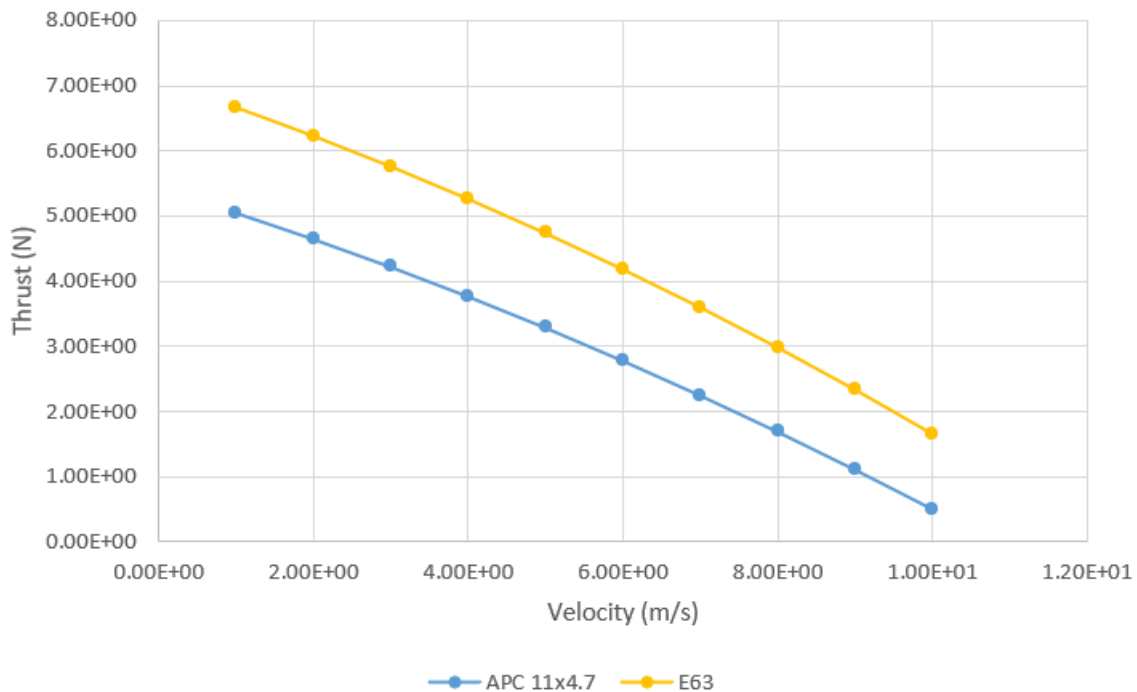


Graph 102 Thrust curve comparison between BE50 and APC 11x4.7

### 3). Propeller with Eppeler 63 airfoil:

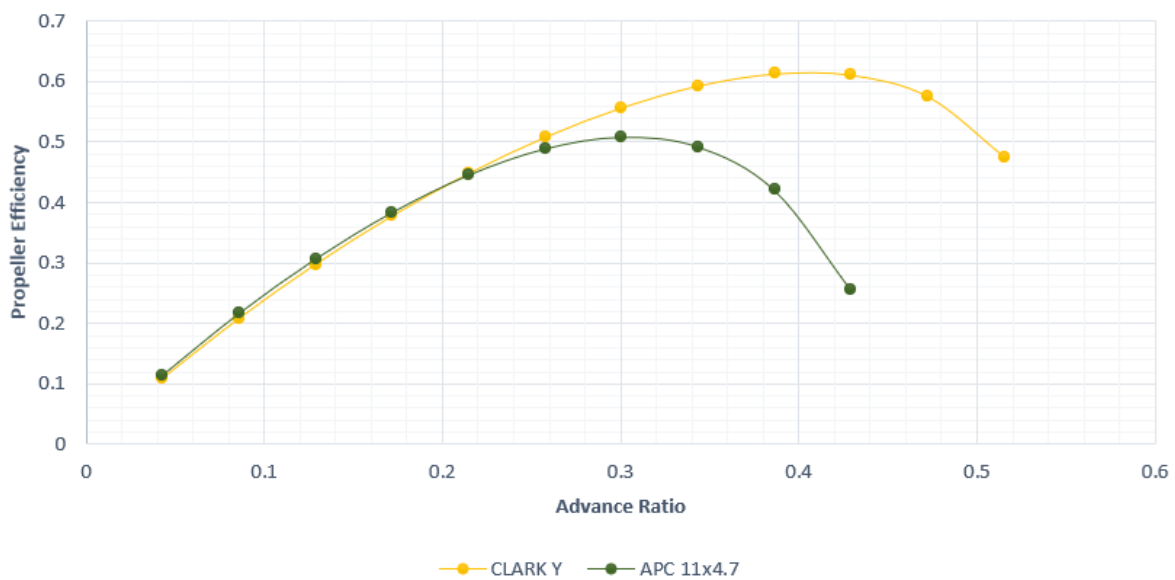


Graph 103 Efficiency curve comparison between Eppeler 63 and APC 11x4.7

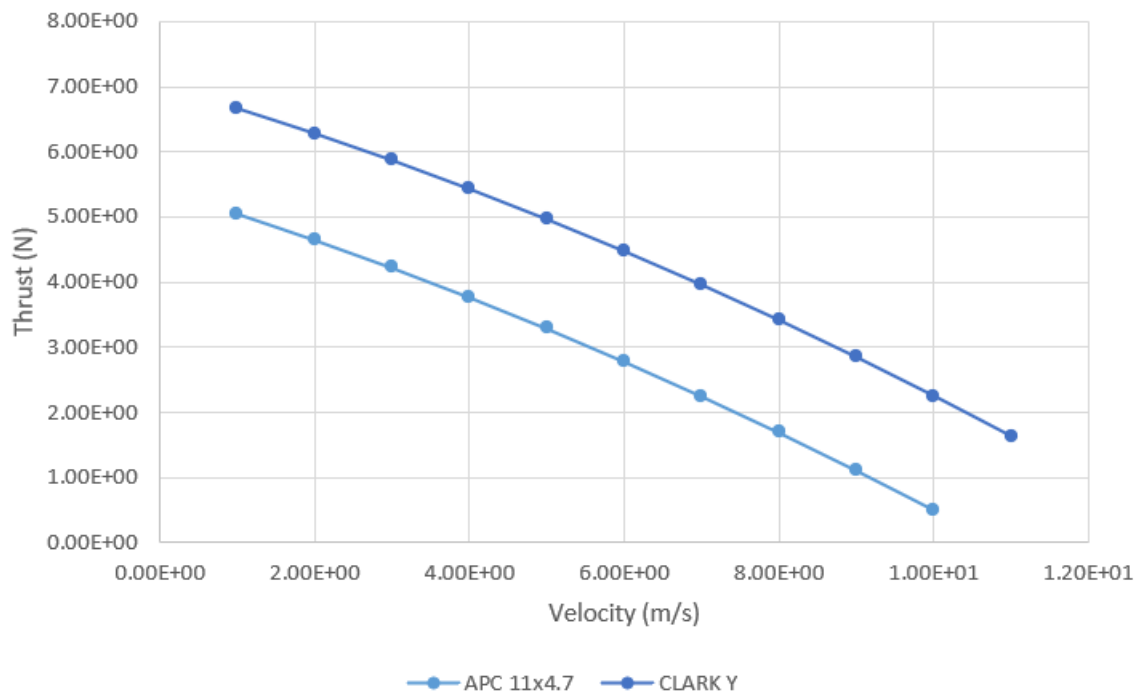


Graph 104 Thrust curve comparison between Eppeler 63 and APC 11x4.7

#### 4). Propeller with CLARK Y airfoil:

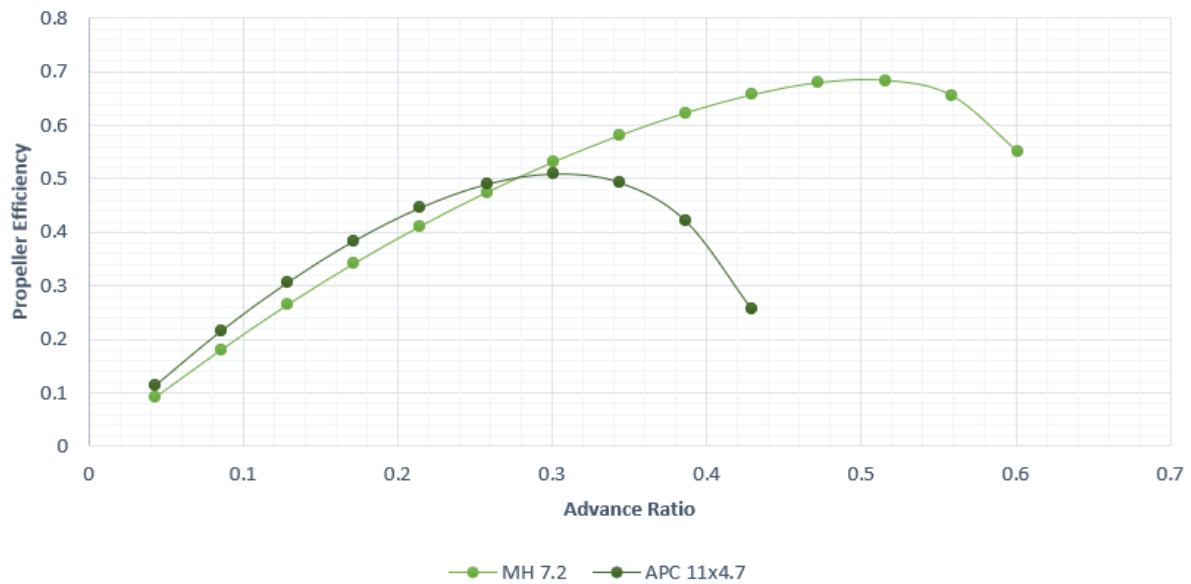


Graph 105 Efficiency curve comparison between CLARK Y and APC 11x4.7

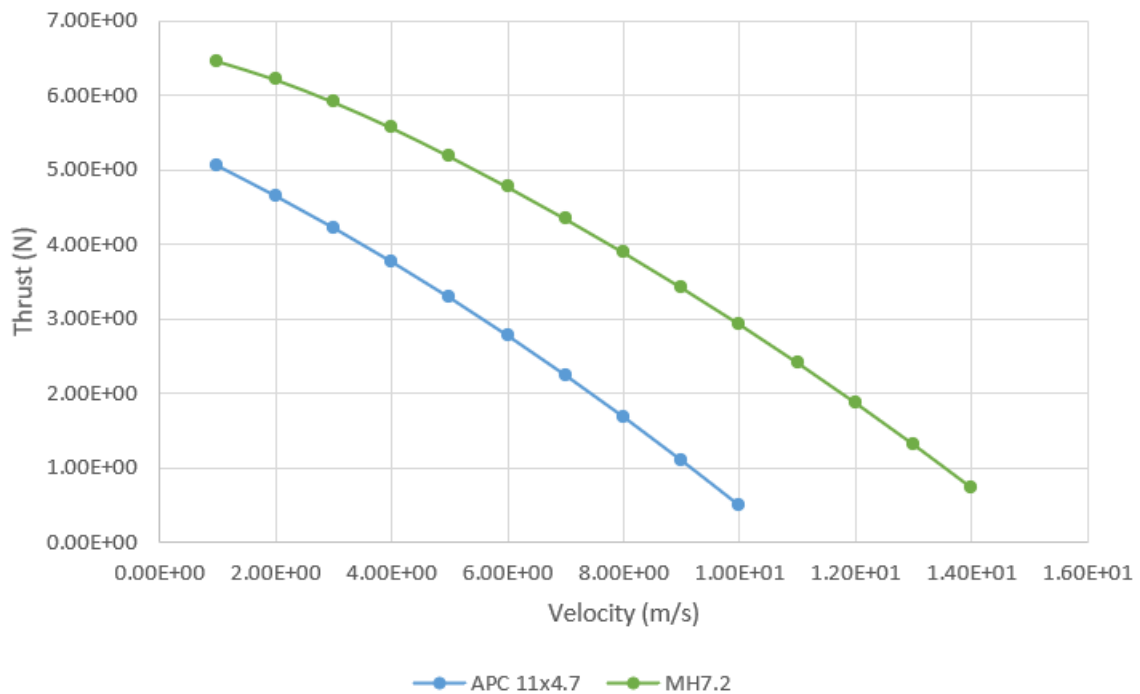


Graph 106 Thrust curve comparison between CLARK Y and APC 11x4.7

### 5). Propeller with MH22 (7.2%) airfoil:

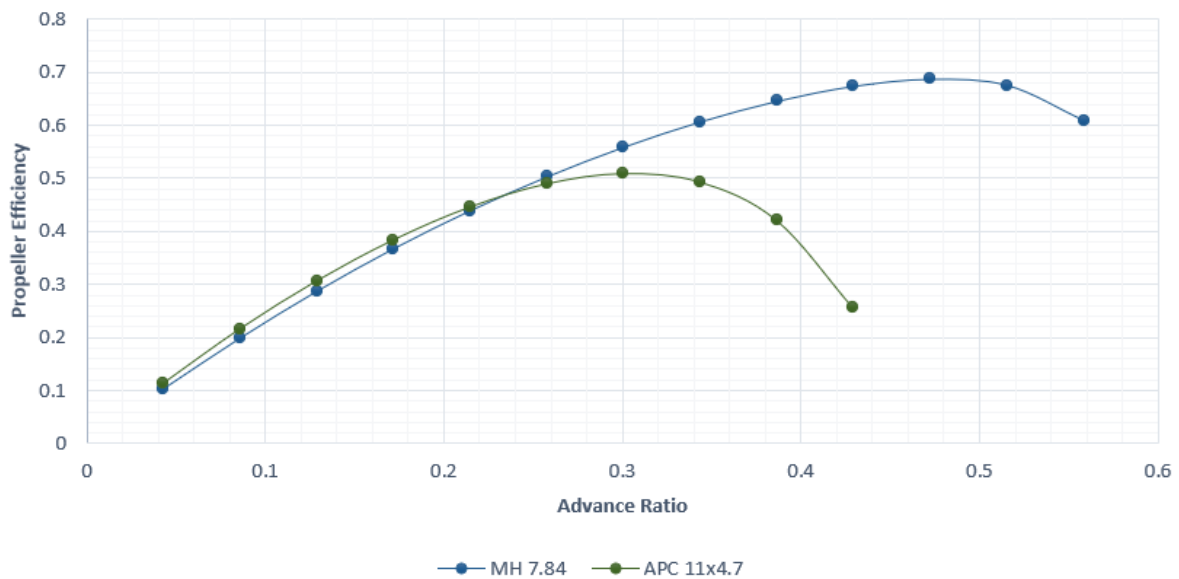


Graph 107 Efficiency curve comparison between MH22 (7.2%) and APC 11x4.7

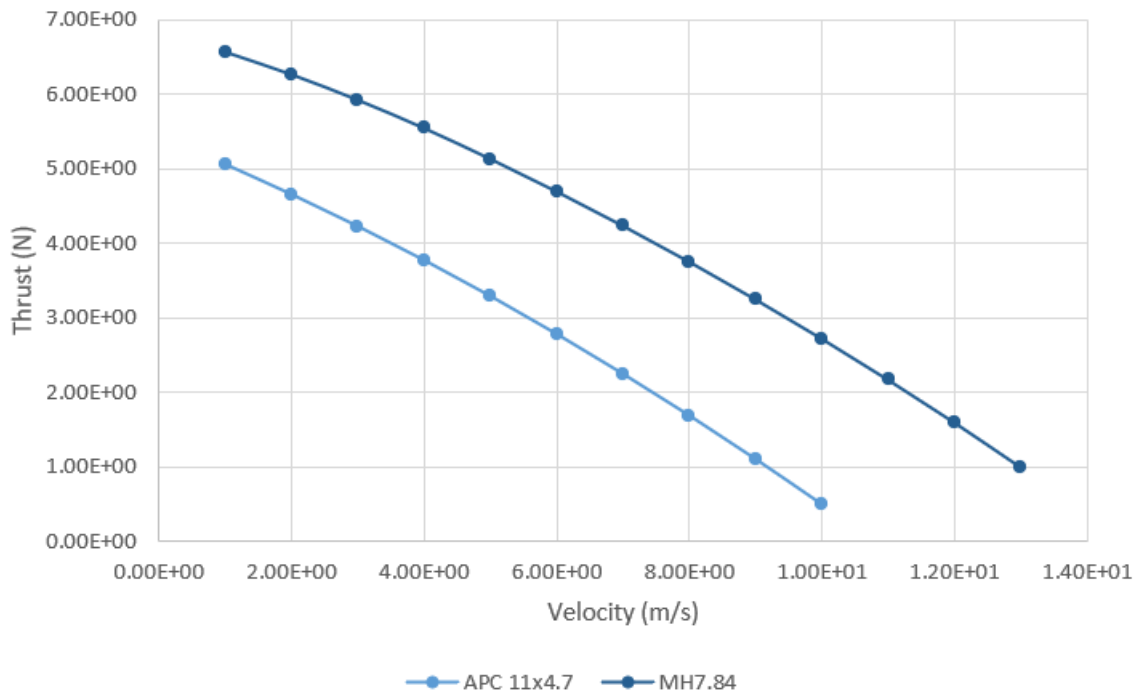


Graph 108 Thrust curve comparison between MH22 (7.2%) and APC 11x4.7

#### 6). Propeller with MH30 (7.84%) airfoil:

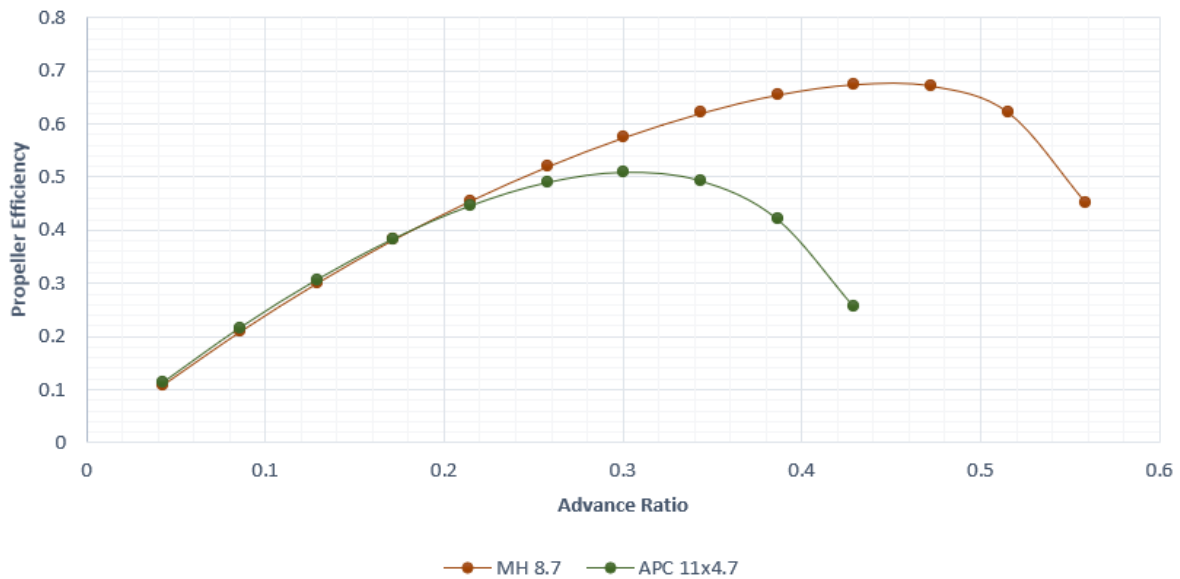


Graph 109 Efficiency curve comparison between MH30 (7.84%) and APC 11x4.7

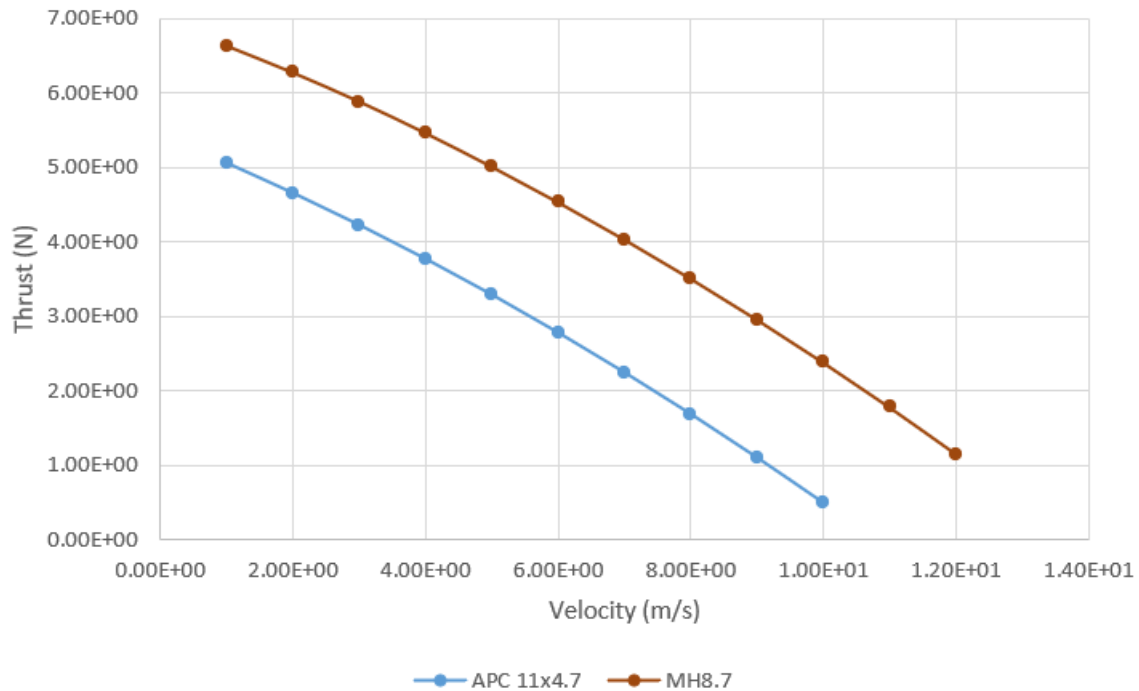


Graph 110 Thrust curve comparison between MH30 (7.84%) and APC 11x4.7

### 7). Propeller with MH32 (8.7%) airfoil:

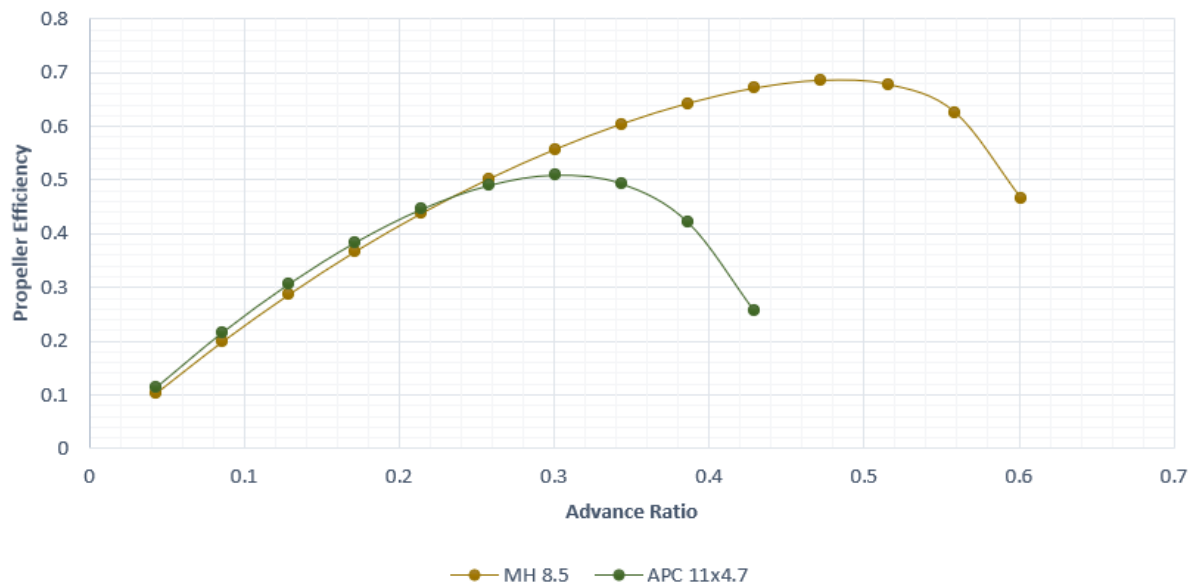


Graph 111 Efficiency curve comparison between MH32 (8.7%) and APC 11x4.7

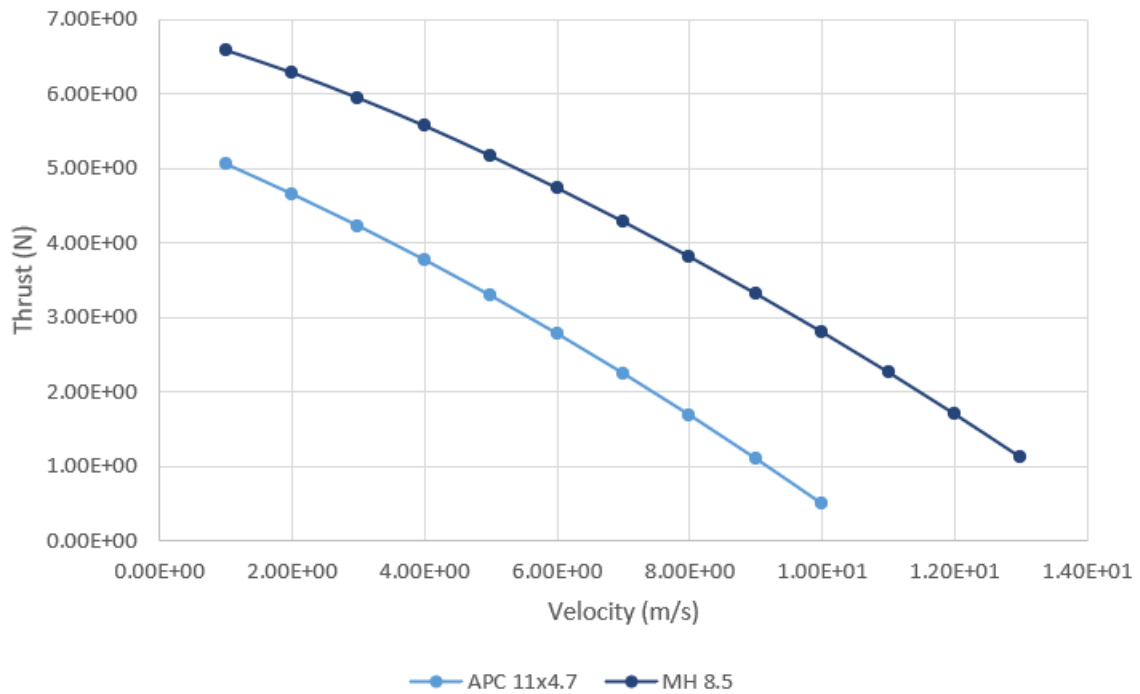


Graph 112 Thrust curve comparison between MH32 (8.7%) and APC 11x4.7

#### 8). Propeller with MH43 (8.5%) airfoil:

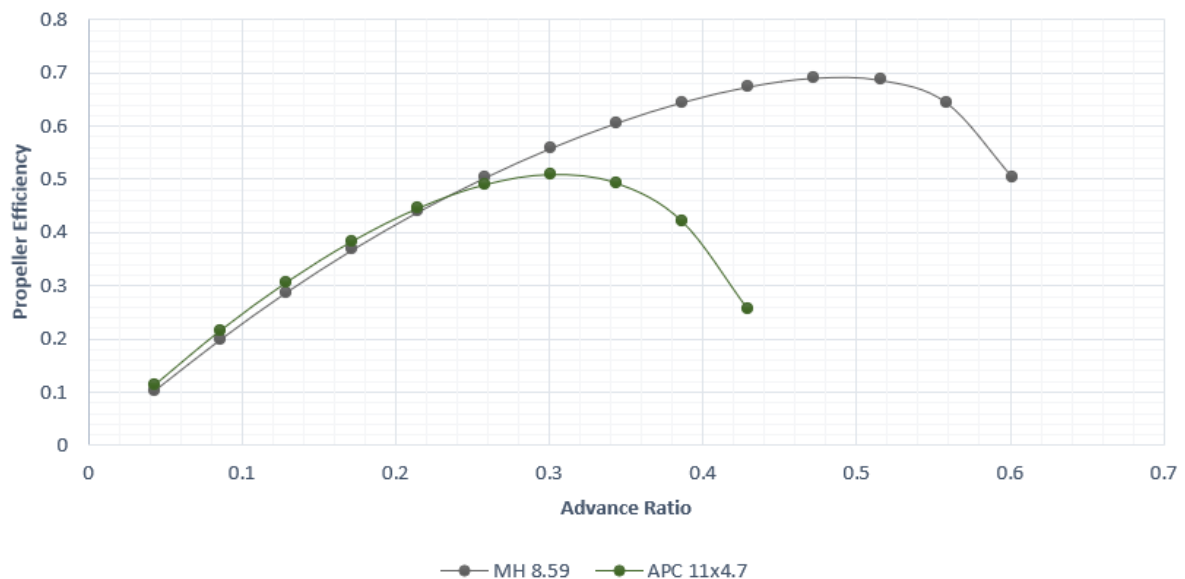


Graph 113 Efficiency curve comparison between MH43 (8.5%) and APC 11x4.7

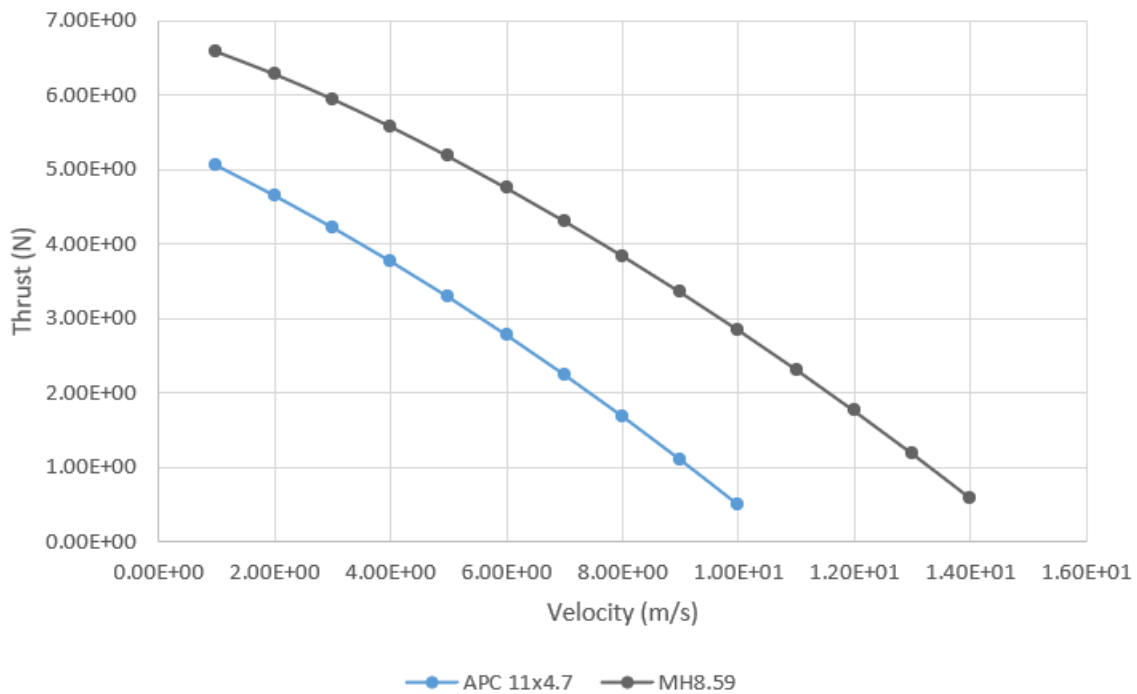


Graph 114 Thrust curve comparison between MH43 (8.5%) and APC 11x4.7

#### 9). Propeller with MH64 (8.59%) airfoil:

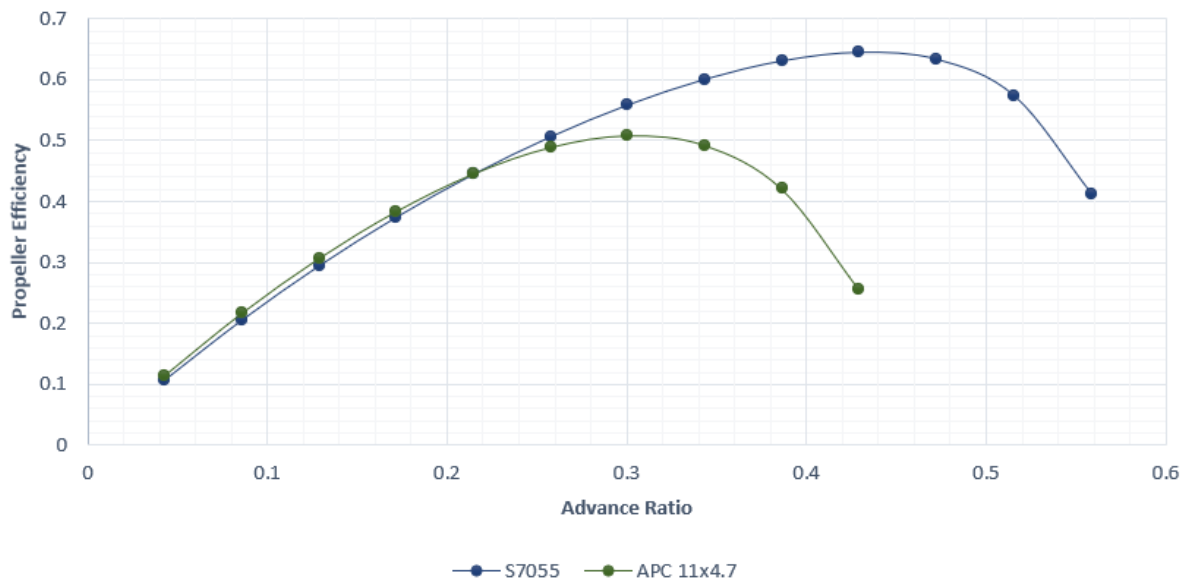


Graph 115 Efficiency curve comparison between MH64 (8.59%) and APC 11x4.7

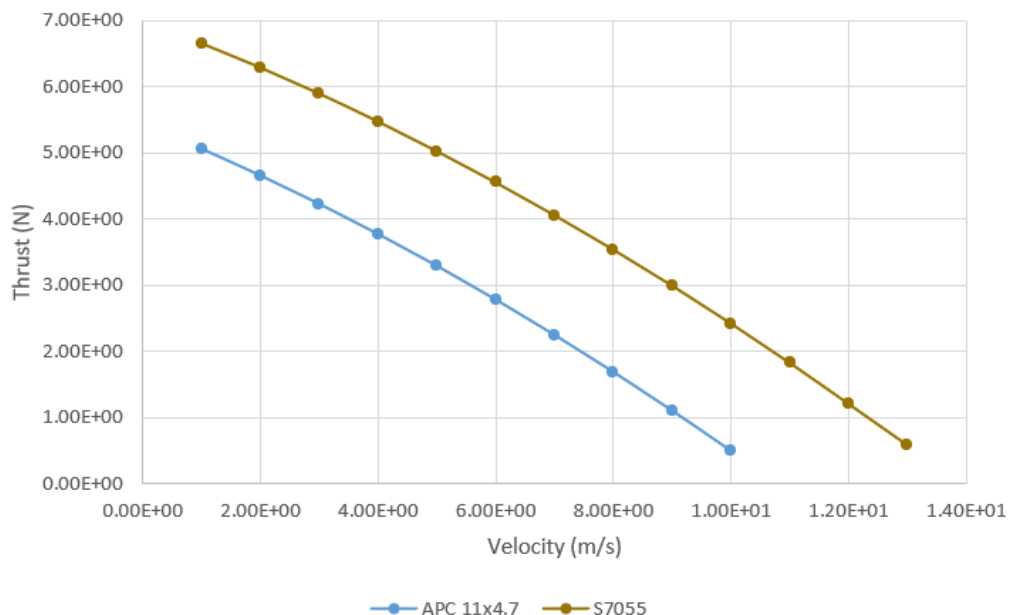


Graph 116 Thrust curve comparison between MH64 (8.59%) and APC 11x4.7

#### 10). Propeller with S7055 airfoil:



Graph 117 Efficiency curve comparison between S7055 and APC 11x4.7



Graph 118 Thrust curve comparison between S7055 and APC 11x4.7

### 7.1 General Observations From 3<sup>rd</sup> Design Point

Airfoil used in Propeller	Peak Propeller efficiency	Advance ratio	Maximum Thrust Produced (N)
BE 50	0.6199	0.3150	6.687
ARAD 10	0.6320	0.3543	6.677
CLARK Y	0.6222	0.3543	6.672
Eppeler 63	0.5944	0.3150	6.676
MH22 (7.2%)	0.6676	0.4330	6.467
MH30 (7.84%)	0.6787	0.4330	6.567
MH32 (8.7%)	0.6764	0.3937	6.636
MH43 (8.5%)	0.6785	0.4330	6.583
MH64 (8.59%)	0.6869	0.4330	6.586
S7055	0.6418	0.3937	6.657

Table 32 Summary of aerodynamic characteristics for 3rd Design point

Velocity	ARAD10		BE50		CLARKY		E63	MH7.2		
	D <sub>eff</sub>	d <sub>T</sub>								
2	-0.59	1.63	-0.4	1.61	-0.88	1.63	-1.51	1.58	-3.65	1.57
3	-0.49	1.63	-0.08	1.60	-0.90	1.65	-1.57	1.54	-4.24	1.69
4	-0.01	1.63	0.54	1.58	-0.57	1.66	-1.13	1.50	-4.23	1.80
5	1.03	1.64	1.59	1.57	0.28	1.68	-0.11	1.45	-3.44	1.89
6	2.87	1.64	3.27	1.55	1.93	1.69	1.68	1.41	-1.49	1.99

Table 33 1). Thrust and propeller efficiency comparison between 3rd design point and APC 11x4.7

Velocity	MH7.84		MH8.7		MH8.5		MH8.59		S7055	
	D <sub>eff</sub>	d <sub>T</sub>								
2	-1.87	1.61	-0.77	1.62	-1.77	1.63	-1.71	1.63	-1.09	1.64
3	-2.02	1.70	-0.64	1.66	-1.99	1.71	-1.85	1.72	-1.19	1.67
4	-1.67	1.77	-0.1	1.69	-1.66	1.80	-1.54	1.81	-0.91	1.70
5	-0.66	1.84	1.01	1.72	-0.72	1.87	-0.58	1.89	-0.05	1.74
6	1.37	1.91	3.08	1.75	1.24	1.95	1.41	1.97	1.74	1.77

Table 34 2). Thrust and propeller efficiency comparison between 3rd design point and APC 11x4.7

In this design point, while thrust increases quite significantly, the propeller efficiencies in the cruise range (2m/s to 4m/s) have decreased compared to 2<sup>nd</sup> Design Point. In all the propellers, the propeller efficiency is not greater than the efficiency of APC 11x4.7 for all the velocities in the cruise range and the magnitude of increase in efficiency is also quite less. Irrespective of the impressive amounts of thrust being generated in this case, propeller efficiency is lost for lower advance ratios and thus this design point will be rejected since the primary aim of our design is to have significantly greater efficiencies and comparable (preferably higher) thrusts compared to APC 11x4.7 propeller for lower advance ratios.

## **CHAPTER 8: Chosen Design Point and Further Modification of Design**

The final design point chosen was the 2<sup>nd</sup> design point on the basis of the balance it provided between higher propeller efficiencies within the cruise range and decent amount of thrust. As mentioned in chapter 6, the propellers having the airfoils MH32 (8.7%), ARAD-10 and BE50 show the best performance for the 2<sup>nd</sup> design point. Now the next step will be to look for ways to further improve the design in terms of either increasing efficiencies in the cruise range (i.e. further shifting the efficiency plot towards left) or increasing the thrust being produced.

### ***8.1 Thin tip propellers***

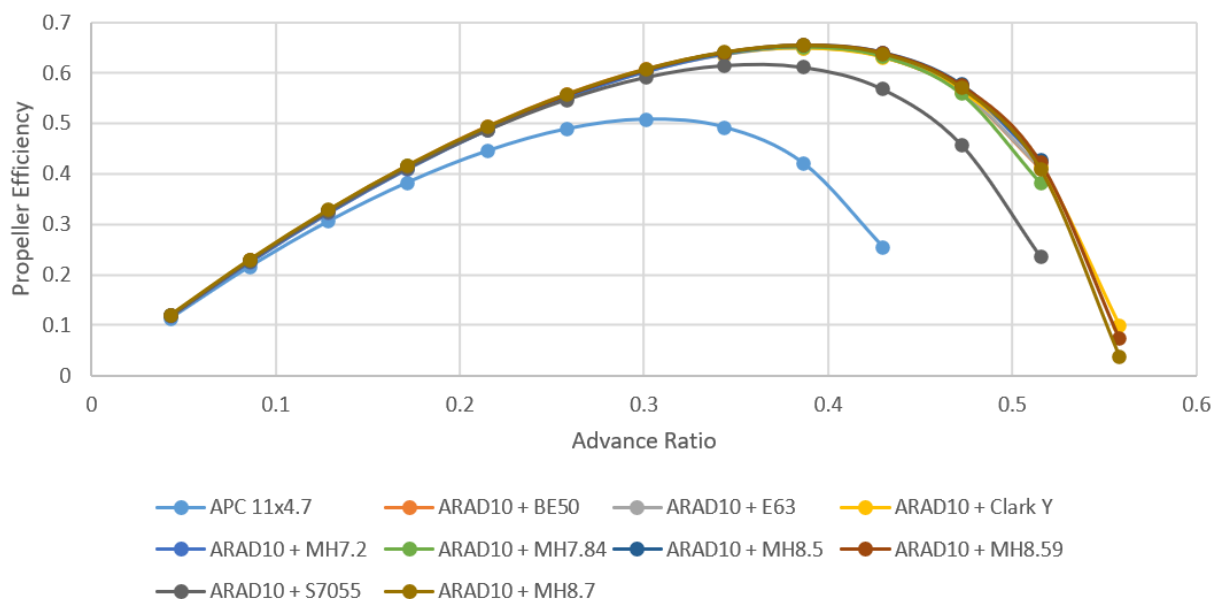
As discussed in chapter 3, a second way of shifting the efficiency curve towards the left is by changing the airfoils in the propeller. Most of the commercially available propellers with multiple airfoils usually have thinner airfoils at the tip and thicker airfoils near the root. A similar kind of airfoil variation will be followed for the three selected propellers where only the last three sections leading up to the tip of the blade will be replaced by a thinner airfoil. Rest of the 18 sections in the propeller will be of the original airfoil. The geometry, specifically the pitch angle distribution of the propeller will be the same as that of the propeller which is purely made of ARAD-10 airfoil. Changing airfoils usually have a very minuscule effect on the advance ratio of the peak efficiency but using thinner airfoils at the tip does help in decreasing the drag at those sections which help in increasing the contribution of those sections to the total thrust thus increasing the overall thrust.

#### ***1). ARAD-10 Propeller:***

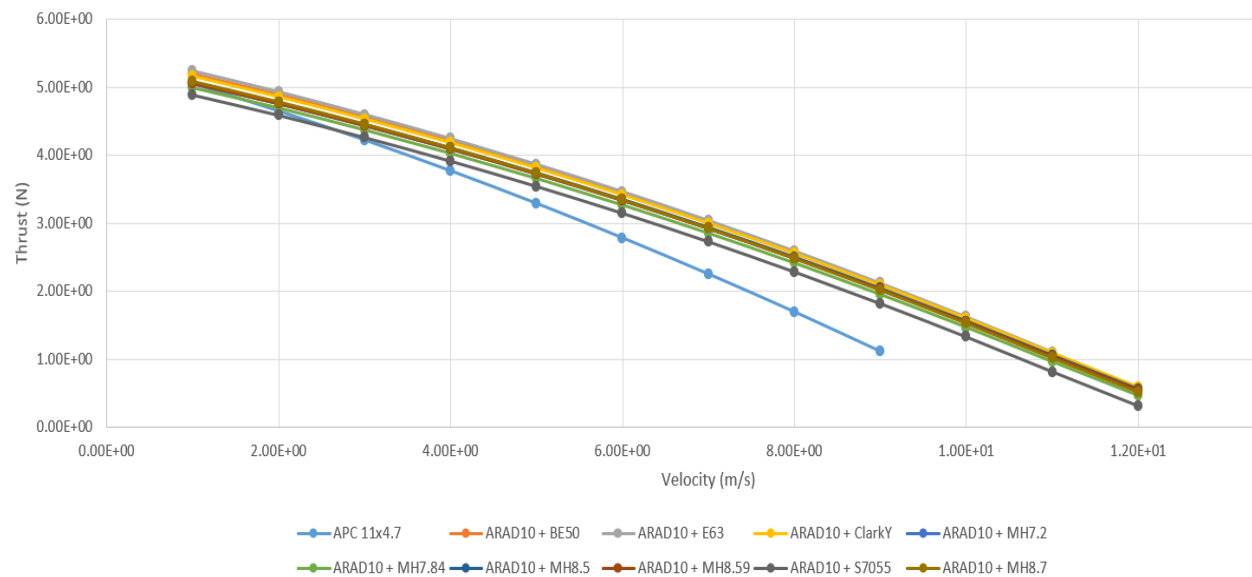
For this propeller, the first 18 sections will be ARAD10 airfoil while the last three sections will be an airfoil which is thinner than ARAD10. Since the thickness by chord length ratio of ARAD-10 airfoil is 10% of the chord length, all airfoils having thickness by chord length ratio less than 10% will be eligible to be used as the tip airfoils. Such airfoils are:

Airfoil	Thickness/chord length = X% of chord length
BE 50	7.3
Eppeler 63	4.25
MH22 (7.2%)	7.2
MH30 (7.84%)	7.84
MH32 (8.7%)	8.7
MH43 (8.5%)	8.5
MH64 (8.59%)	8.59

Table 35 Airfoils eligible to be used as thin tip airfoils for the propeller made of ARAD-10



Graph 119 Efficiency curve comparison between all the possible thin tip propellers made of ARAD-10



Graph 120 Thrust curve comparison between all the possible thin tip propellers made of ARAD-10

Velocity	E63 as tip		BE50 as tip		CLARKY as tip		MH 7.2 as tip		MH 7.84 as tip	
	d <sub>eff</sub> (%)	d <sub>T</sub> (N)								
2	-0.32	0.031	0.09	-0.008	0.07	-0.039	-0.29	-0.143	0.07	-0.204
3	-0.43	0.026	0.15	-0.009	0.05	-0.038	-0.39	-0.137	0.08	-0.199
4	-0.49	0.022	0.2	-0.011	0.01	-0.037	-0.44	-0.130	0.07	-0.194
5	-0.52	0.017	0.21	-0.013	-0.06	-0.036	-0.46	-0.123	0.05	-0.190
6	-0.52	0.013	0.17	-0.014	-0.15	-0.035	-0.44	-0.115	0.01	-0.185

Table 36 1). Thrust and Propeller efficiency comparison between all possible thin tip ARAD-10 propellers and the pure ARAD-10 propeller

Velocity	MH 8.5 as tip		MH 8.59 as tip		S7055 as tip		MH 8.7 as tip	
	d <sub>eff</sub> (%)	d <sub>T</sub> (N)						
2	-0.01	-0.122	0.03	-0.137	-0.02	-0.313	0.15	-0.117

3	-0.04	-0.117	0.01	-0.132	-0.12	-0.311	0.17	-0.115
4	-0.07	-0.111	0	-0.125	-0.27	-0.308	0.17	-0.113
5	-0.1	-0.106	-0.02	-0.120	-0.49	-0.307	0.15	-0.110
6	-0.12	-0.099	-0.03	-0.113	-0.86	-0.305	0.12	-0.109

*Table 37 2). Thrust and Propeller efficiency comparison between all possible thin tip ARAD-10 propellers and the pure ARAD-10 propeller*

In the above table,  $d_{eff}$  refers to the percentage change in propeller efficiency between the thin tip propeller and the original propeller and  $d_T$  refers to the change in thrust produced by the thin tip propeller and the original one. For ARAD-10 airfoil propeller, only in the case of Eppeler 63 as the tip airfoil, the thrust produced is increased but by a very small margin while its propeller efficiency in the cruise range takes a dip by small but significant percentages. The maximum increase in efficiency is seen when MH32 (8.7%) is kept as the tip airfoil but in that case, the thrust decreases by a significant margin. A good balance is maintained in the case of BE50 as tip airfoil in which although the thrust decreases, the magnitude is insignificant while there is a slight increase in the efficiency. Thus, for the case of ARAD-10 as the main airfoil of the propeller, the tip airfoil is chosen as BE50.

**NOTE:** In the case where S7055 is the tip airfoil, the advance ratio for the peak propeller efficiency decreases by one step size (or the velocity for peak efficiency decreases by 1m/s) i.e. the efficiency curve slightly shifts to the left, but as observed, it does not lead to the propeller efficiency increasing in the cruise range and thus is not chosen.

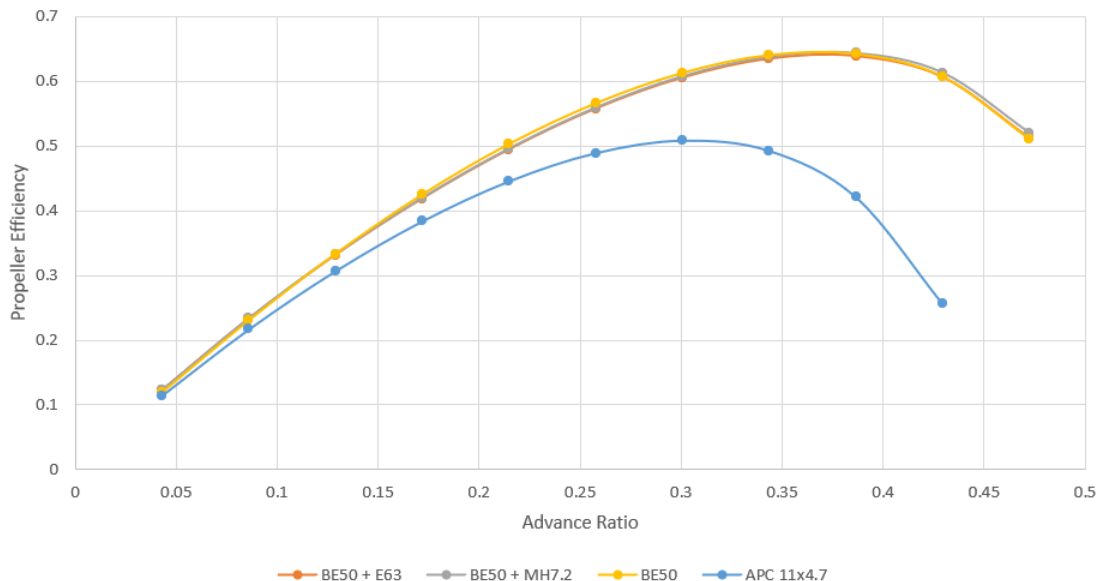
## **2). BE50 Propeller:**

BE 50 airfoil has a thickness to chord length ratio of 7.3% of chord length so airfoils having a thickness to chord length ratio of less than 7.3% will be used at the tip of the propeller. Similar to the above case, the first 18 sections will belong to BE 50 with the last 3 sections up to the tip belonging to the thinner airfoils. The geometry of the propeller will be the same as that of the propeller made purely of the BE 50 airfoil.

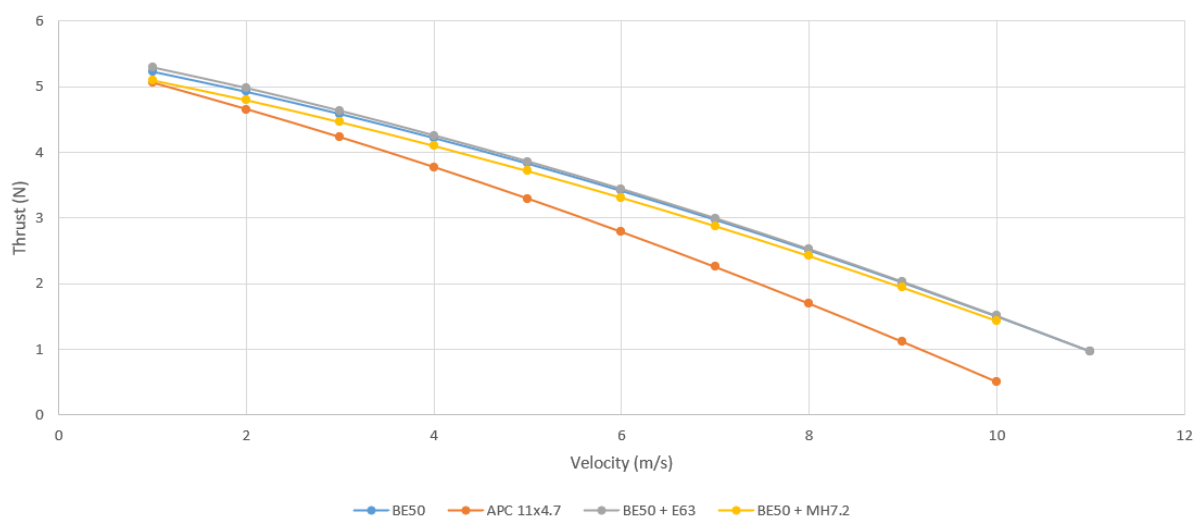
The airfoils which qualify as thin tip airfoils for this propeller are:

Airfoil	Thickness/chord length = X% of chord length
Eppeler 63	4.25
MH22 (7.2%)	7.2

Table 38 Airfoils eligible to be used as thin tip airfoils for the propeller made of BE50



Graph 121 Efficiency curve comparison between all the possible thin tip propellers made of BE50



Graph 122 Thrust curve comparison between all the possible thin tip propellers made of BE50

Velocity	Eppeler 63 as thin tip		MH22 (7.2%) as thin tip	
	$d_{eff}$ (%)	$d_T$ (N)	$d_{eff}$ (%)	$d_T$ (N)
2	0.26	0.048	0.35	-0.129
3	-0.14	0.041	-0.04	-0.125
4	-0.58	0.035	-0.47	-0.12
5	-0.79	0.031	-0.67	-0.113
6	-0.77	0.028	-0.63	-0.114

Table 39 Thrust and propeller efficiency comparision between Eppeler 63 and MH22 (7.2%) thin

As observed, in the case of Eppeler 63 as a thin tip airfoil, there is a very small increase in the thrust produced along with a small but significant decrease in the propeller efficiency in the cruise range. On the other hand, using MH22 (7.2%) as a thin tip propeller is not at all preferable as there is significant decrease in both the thrust and the propeller efficiency. Considering that there is hardly any gain by using thin tip propellers, for the propeller having BE 50 as the main airfoil, there will be no additional thin tip airfoils.

### 3) MH32 (8.7%) propeller:

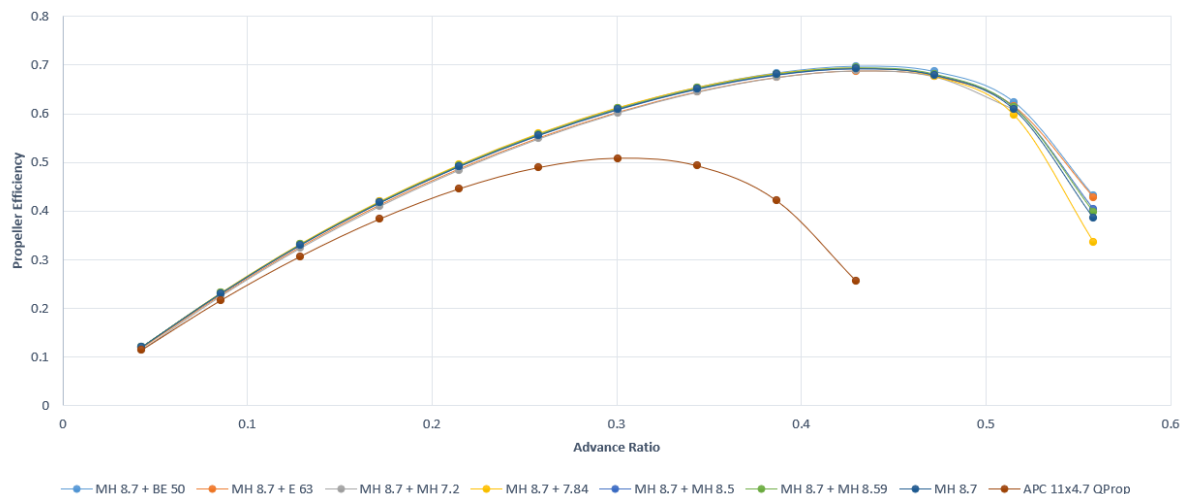
The Martin Heppler series airfoil MH32 (8.7%) has a thickness to chord length ratio of 8.7% of the chord length thus the airfoils which can be used as thin tip airfoils need to have a thickness to chord length ratio of less than 8.7%. Similarly, in this case, the propeller will have the same geometry as that of the propeller made of purely MH32 (8.7%).

The airfoils which qualify to be used as thin tip airfoils are:

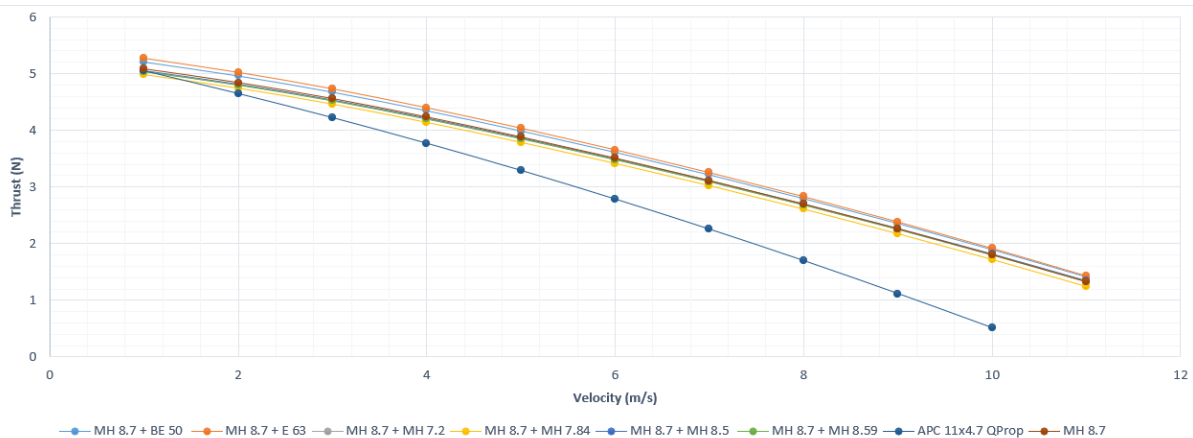
Airfoil	Thickness/Chord length = X% of the chord length
BE 50	7.3
Eppeler 63	4.25

MH22 (7.2%)	7.2
MH30 (7.84%)	7.84
MH43 (8.5%)	8.5
MH64 (8.59%)	8.59

Table 40 Airfoils eligible to be used as thin tip airfoils for the propeller made of MH32 (8.7%)



Graph 123 Efficiency curve comparison between all the possible thin tip propellers for MH32 (8.7%)



Graph 124 Thrust curve comparison between all the possible thin tip propellers for MH32 (8.7%)

Velocity	BE50 as Thin Tip		Eppeler 63 as Thin Tip		MH22 (7.2%) as Thin Tip	
	$d_{eff}$ (%)	$d_T$ (N)	$d_{eff}$ (%)	$d_T$ (N)	$d_{eff}$ (%)	$d_T$ (N)
2	0.14	0.127	-0.23	0.177	-0.46	-0.044
3	0.17	0.171	-0.33	0.171	-0.59	-0.039
4	0.20	0.163	-0.41	0.163	-0.68	-0.035
5	0.21	0.157	-0.48	0.157	-0.72	-0.030
6	0.22	0.111	-0.53	0.150	-0.73	-0.025

Table 41 1). Thrust and Propeller efficiency comparison between the thin tip propellers for MH32 (8.7%) and the propeller made purely of MH32 (8.7%)

Velocity	MH30 (7.84%) as Thin Tip		MH43 (8.5%) as Thin Tip		MH64 (8.59%) as Thin Tip	
	$d_{eff}$ (%)	$d_T$ (N)	$d_{eff}$ (%)	$d_T$ (N)	$d_{eff}$ (%)	$d_T$ (N)
2	0.17	-0.099	0.04	-0.018	0.09	-0.034
3	0.24	-0.096	0.05	-0.014	0.13	-0.030
4	0.28	-0.093	0.05	-0.011	0.14	-0.027
5	0.29	-0.091	0.04	-0.007	0.14	-0.023
6	0.30	-0.088	0.03	-0.003	0.14	-0.019

Table 42 2). Thrust and Propeller efficiency comparison between the thin tip propellers for MH32 (8.7%) and the propeller made purely of MH32 (8.7%)

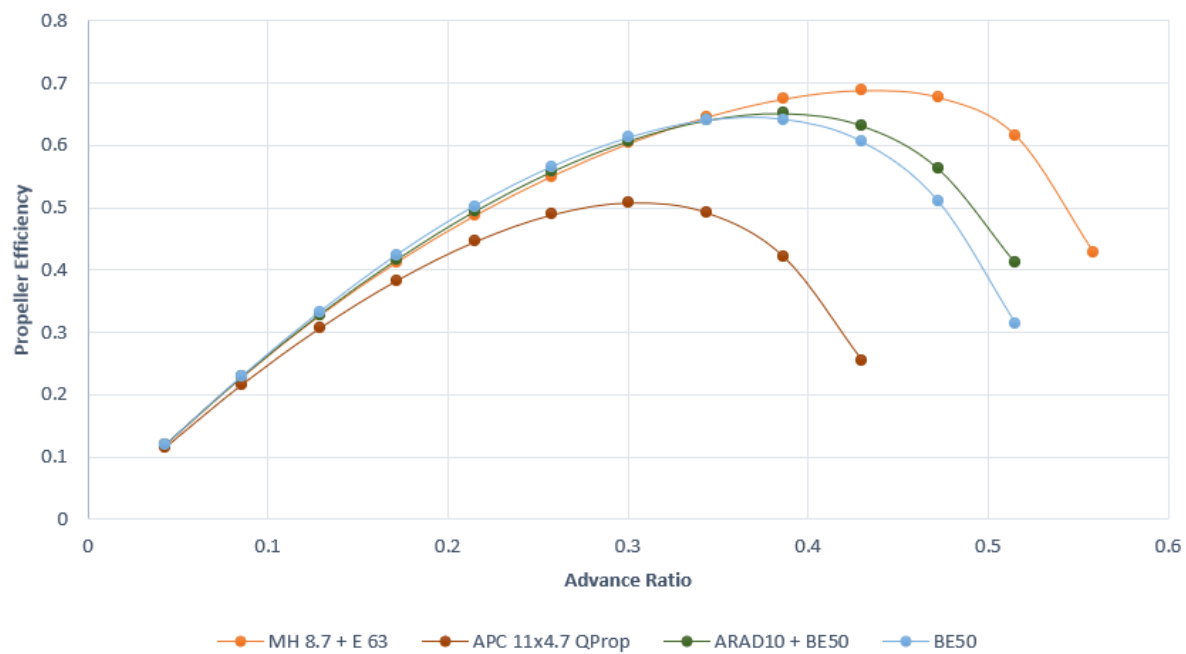
As observed for this propeller, the airfoils Eppeler 63 and BE50 as thin tip airfoils provide significant improvement in the total thrust being generated with Eppeler 63 providing the maximum increase. Rest of the airfoils lead to a decrease in the total thrust and thus will not be considered. BE 50 airfoil also increases the propeller efficiency in the cruise range slightly

while Eppeler 63 decreases. For BE 50 airfoil, there is a slight increase in the propeller efficiency but the thrust is not as high as provided by Eppeler 63. Considering the major improvement in thrust which Eppeler 63 provides, it is safe to say that the efficiency decrease is negligible and thus for the case of the propeller made out of MH32 (8.7%), Eppeler 63 will be used as the thin tip airfoil.

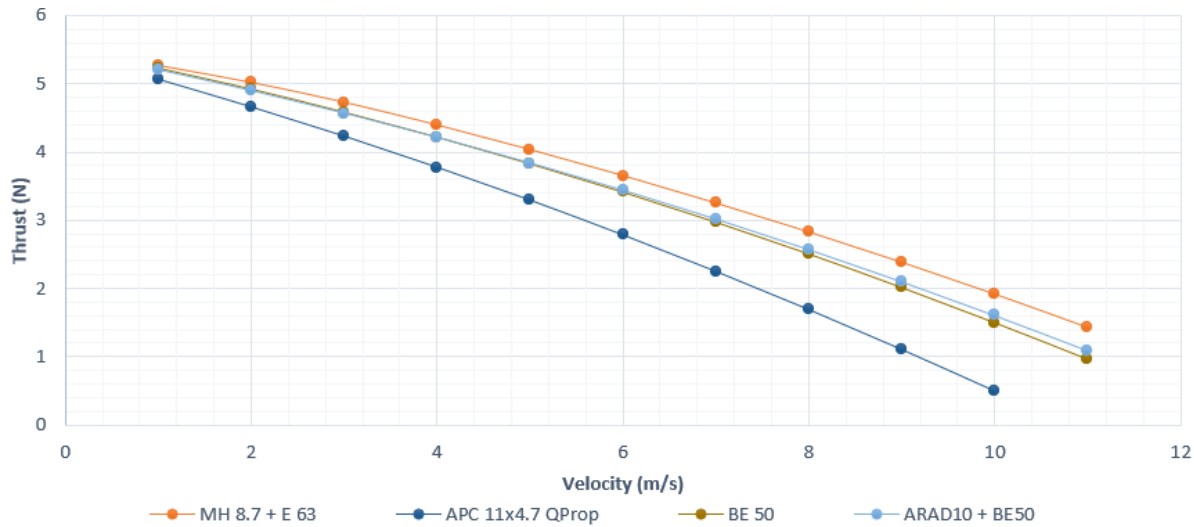
## **8.2 Comparison of thin tip propellers:**

As discussed above, the final thin tip propellers which have been chosen are:

- 1). ARAD-10 propeller with BE50 airfoil at its tip
- 2). BE50 propeller with no additional airfoil at its tip
- 3). MH32 (8.7%) propeller with Eppeler 63 airfoil at its tip.



*Graph 125 Efficiency curve comparison between the three selected thin tip propellers and APC 11x4.7*



Graph 126 Thrust curve comparison between the three selected thin tip propellers and APC 11x4.7

Velocity	ARAD10 + BE50		BE50		MH32 (8.7%) + E63	
	d <sub>eff</sub> (%)	d <sub>T</sub> (N)	d <sub>eff</sub> (%)	d <sub>T</sub> (N)	d <sub>eff</sub> (%)	d <sub>T</sub> (N)
2	1.26	0.240	1.35	0.270	1.16	0.362
3	2.21	0.338	2.62	0.358	2.00	0.500
4	3.37	0.439	4.09	0.446	1.91	0.621
5	4.85	0.544	5.7	0.535	4.41	0.742
6	6.87	0.654	7.63	0.627	6.13	0.869

Table 43 Thrust and propeller efficiency comparison between ARAD10 + BE50 BE50 MH32 (8.7%) + E63

In the above table:

$d_{eff}$  = % increase in propeller efficiency compared to APC 11x4.7

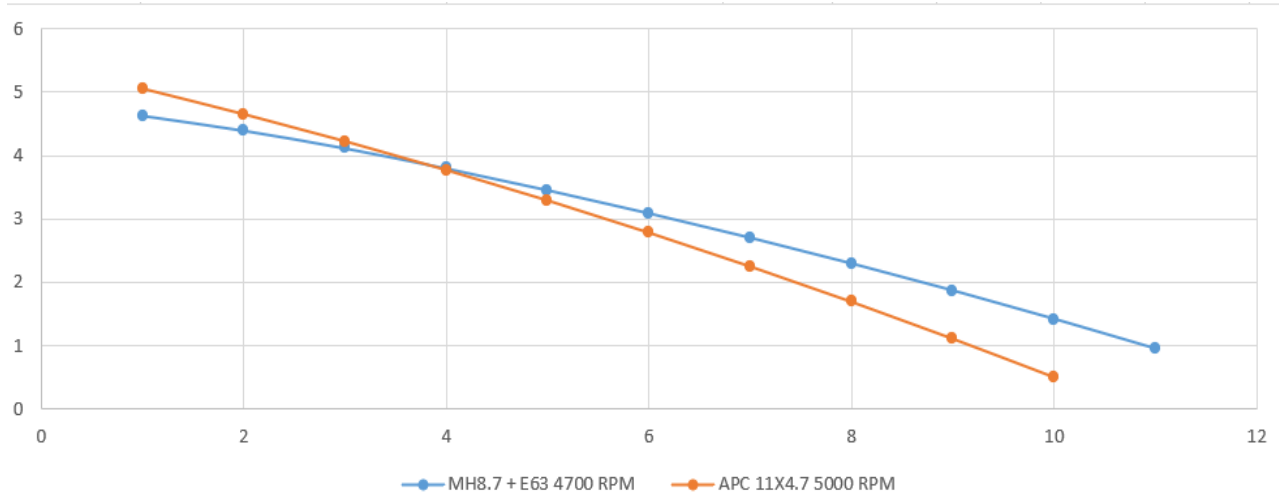
$d_T$  = increase in total thrust produced compared to APC 11x4.7

As observed in the above table, BE50 propeller shows the highest increase in the propeller efficiency whereas the MH32 (8.7%) propeller with Eppeler 63 as tip airfoil shows the least increase in propeller efficiency, although the difference between the efficiencies is quite low. In terms of thrust, MH32 (8.7%) propeller with Eppeler 63 as tip airfoil shows the largest

improvement in thrust, the increase in thrust compared to APC 11x4.7 at 6m/s reaching close to 1 N. In fact, the improvement in thrust in MH32 (8.7%) and Eppeler 63 propeller is significantly higher compared to the other two propellers. Considering the drop in propeller efficiency is not that significant, due to improvement in the total thrust being produced in the cruise range, the final propeller selected is the one with MH32 (8.7%) and Eppeler 63.

### ***8.3 Further Advantage of the final propeller design:***

As observed, we get more thrust and propeller efficiency for the cruise range of 2m/s to 6m/s compared to APC 11x4.7 but thrust and propeller efficiency aren't the only parameters which are getting improved with the design. The final propeller gives a higher thrust than APC 11x4.7 at 5000 RPM which means that the propeller will give almost equal thrusts for lower rotational speeds. If QPROP is run on the propeller for a rotational speed of 4700 RPM, then we get slightly lower thrusts than the APC 11x4.7 for 2m/s to 4m/s and slightly higher thrusts than APC 11x4.7 for 4m/s to 6m/s.



*Graph 127 Thrust comparison between the selected propeller at 4700 RPM and APC 11x4.7 at 5000 RPM*

Since, our propeller is rotating at a lower RPM, this means the power output on the motor shaft will be lower and thus the electrical power provided to the motor will be lower which means battery power is saved.

Velocity (m/s)	APC 11x4.7 (5000 RPM) (W)	MH32 (8.7%) + E63 (4700RPM) (W)	Electrical Power saved (W)
2	55.98	47.53	8.45
3	53.64	46.86	6.78
4	50.77	45.75	5.02
5	47.38	44.14	3.24
6	43.51	41.93	1.58

*Table 44 Electrical power consumption comparison between the final selected propeller and APC 11x4.7*

Rough calculations can be made to find out the flight time extensions when our propeller is used instead of APC 11x4.7 on a quadcopter. Suppose the battery being used in the quadcopter has 6 cells, a 25 C rating and a 10000 mAh capacity. Since there will be 4 propellers in a quadcopter, in an hour, each propeller will receive 2500 mA of current. QPROP provides us with the current load data for a particular velocity, thus we can calculate the discharge times of the battery at each velocity.

Velocity (m/s)	APC 11x4.7 Propeller		MH32 8.7% + E63 Propeller		Flight Time Extension (%)
	Current Load (A)	Discharge Time (mins)	Current Load (A)	Discharge Time (mins)	
2	12.7269	11.7860	11.5674	12.9675	10.02386
3	12.2770	12.2179	11.4287	13.1248	7.722541
4	11.7179	12.8009	11.1999	13.3930	4.625041
5	11.0460	13.5796	10.8622	13.8093	1.692107
6	10.2657	14.6120	10.3965	14.4280	-1.25812

*Table 45 Quadcopter flight time comparison between the final selected propeller and APC 11x4.7*

Thus, we observe for a particular battery, in the velocity range of 2m/s to 5m/s, the quadcopter has a higher flight time when it is using our propeller compared to when it is using APC 11x4.7.

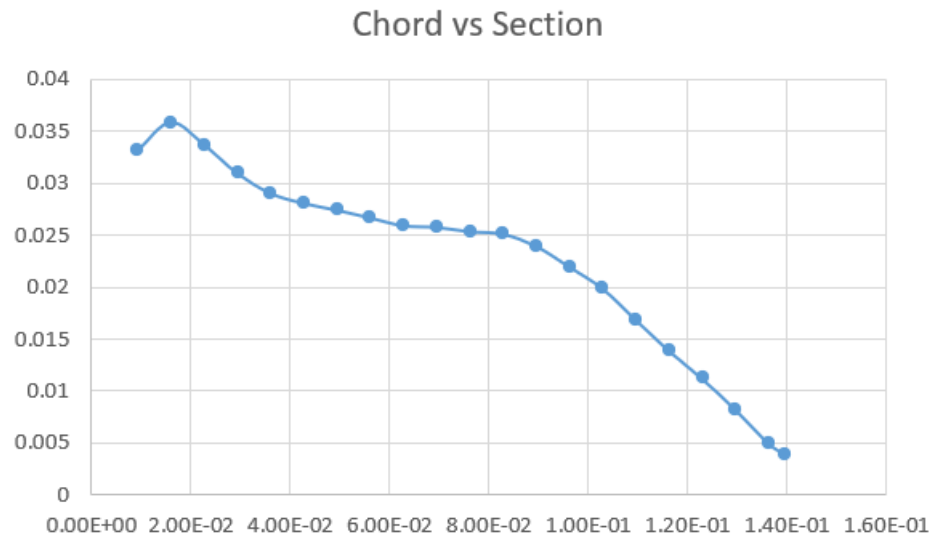
# CHAPTER 9: Final Propeller Design

## 9.1 Geometry

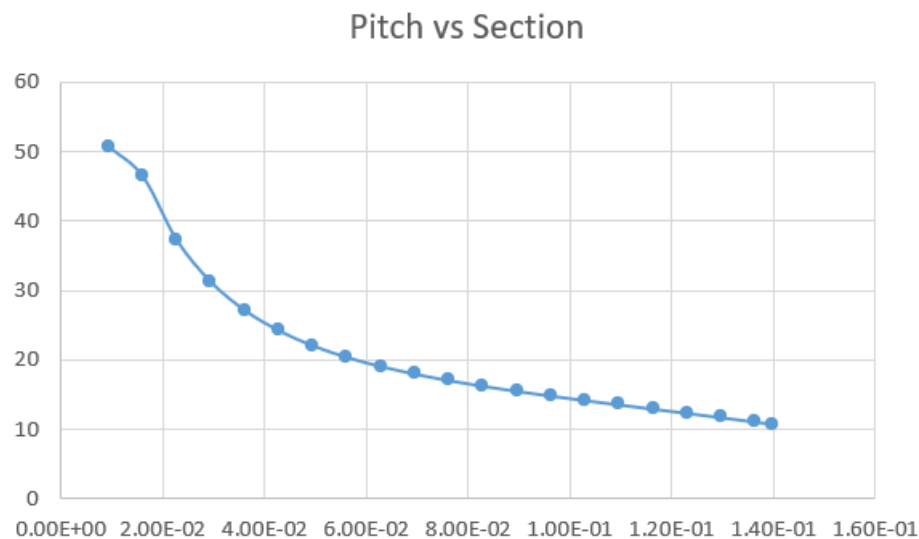
Radial Section (cm)	Chord Length (cm)	Pitch Angle (°)	Airfoil
0.934	3.3155	50.8040	MH32 (8.7%)
1.600	3.5876	46.5326	MH32 (8.7%)
2.270	3.3728	37.3536	MH32 (8.7%)
2.940	3.0984	31.3418	MH32 (8.7%)
3.610	2.9055	27.2360	MH32 (8.7%)
4.280	2.8081	24.3081	MH32 (8.7%)
4.950	2.7433	22.1354	MH32 (8.7%)
5.610	2.6695	20.4634	MH32 (8.7%)
6.280	2.5933	19.1322	MH32 (8.7%)
6.950	2.5780	18.0373	MH32 (8.7%)
7.620	2.5364	17.1077	MH32 (8.7%)
8.290	2.5126	16.2941	MH32 (8.7%)
8.960	2.3965	15.5610	MH32 (8.7%)
9.620	2.1975	14.8825	MH32 (8.7%)
10.293	1.9891	14.2393	MH32 (8.7%)
10.962	1.6891	13.6167	MH32 (8.7%)
11.630	1.3915	13.0036	MH32 (8.7%)
12.299	1.1235	12.3913	MH32 (8.7%)
12.967	0.8265	11.7729	Eppeler 63
13.636	0.5000	11.1434	Eppeler 63

13.970	0.3975	10.8244	Eppeler 63
--------	--------	---------	------------

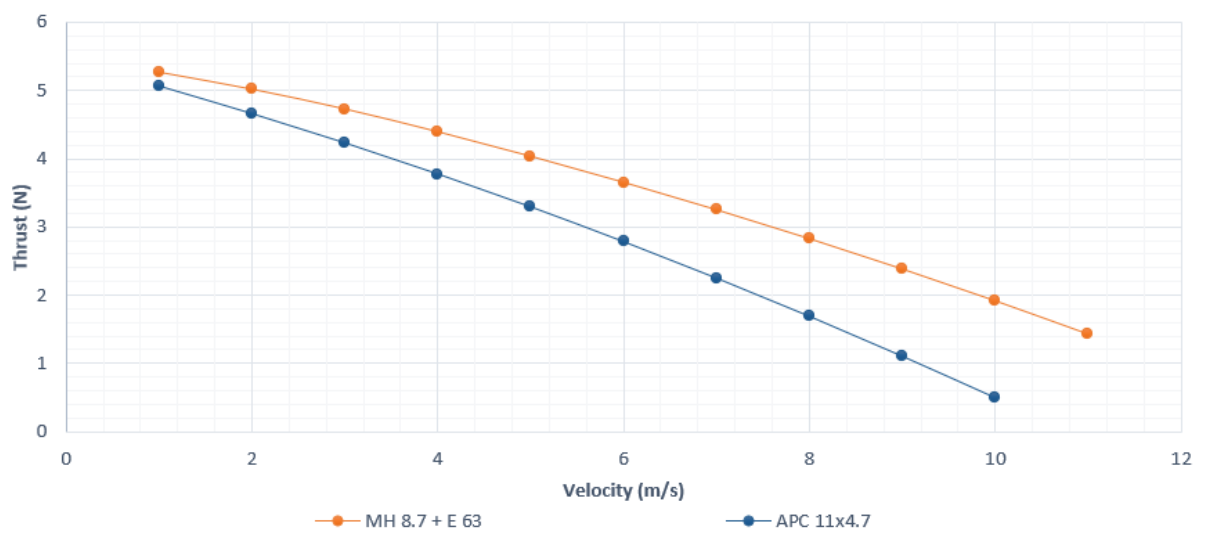
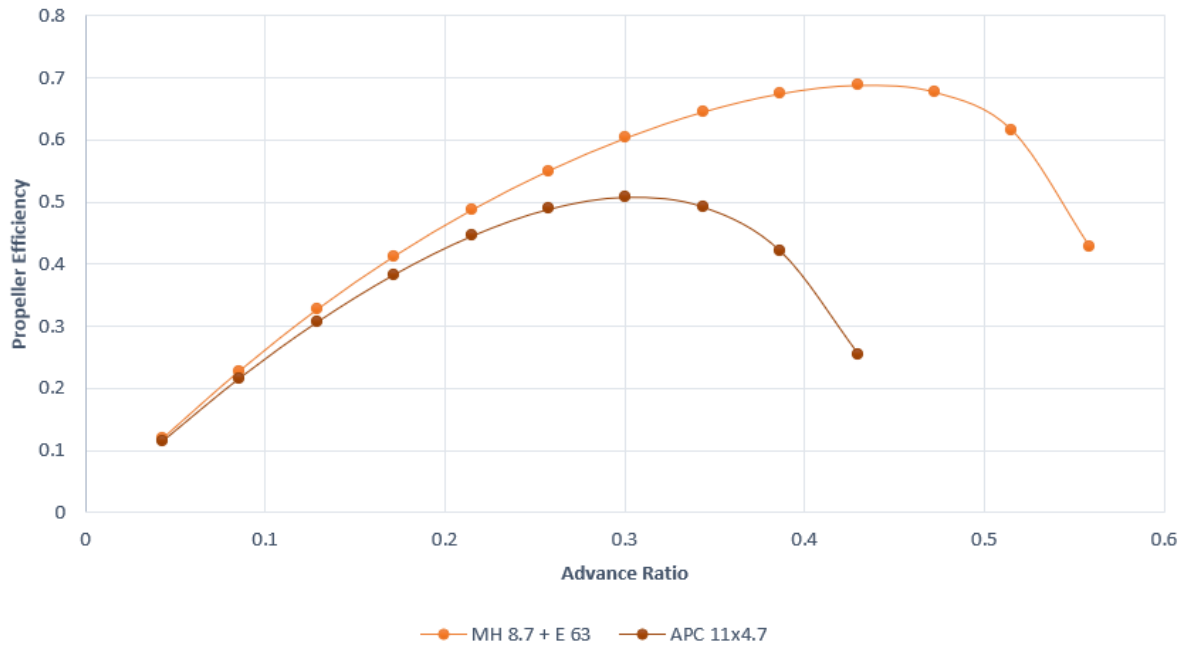
Table 46 Propeller geometry of the final selected propeller



Graph 128 Chord length distribution of the final selected propeller



Graph 129 Pitch angle distribution of the final selected propeller



## **9.2 CAD of the propeller:**

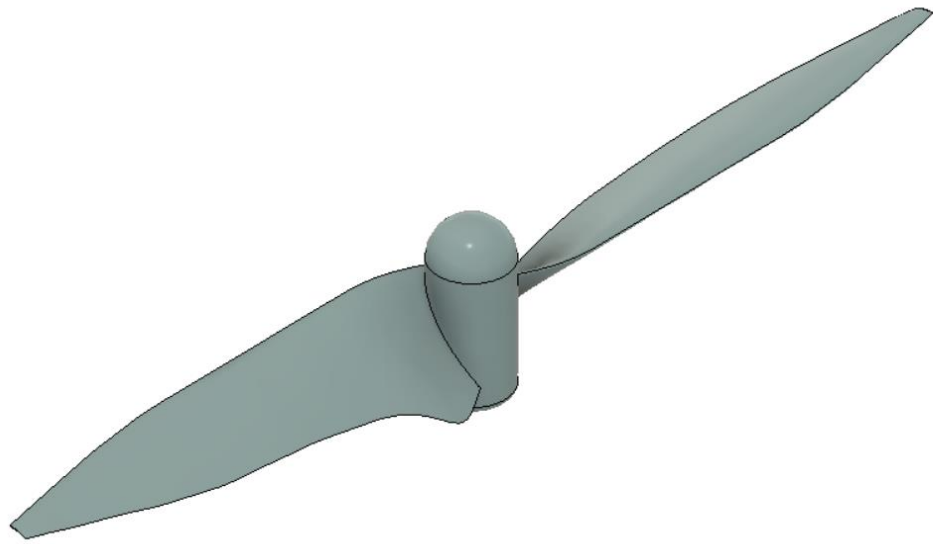


*Figure 33 Orthogonal view of the propeller CAD*

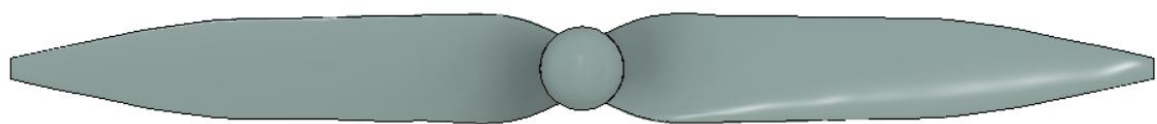


*Figure 34 Top view of the propeller CAD*

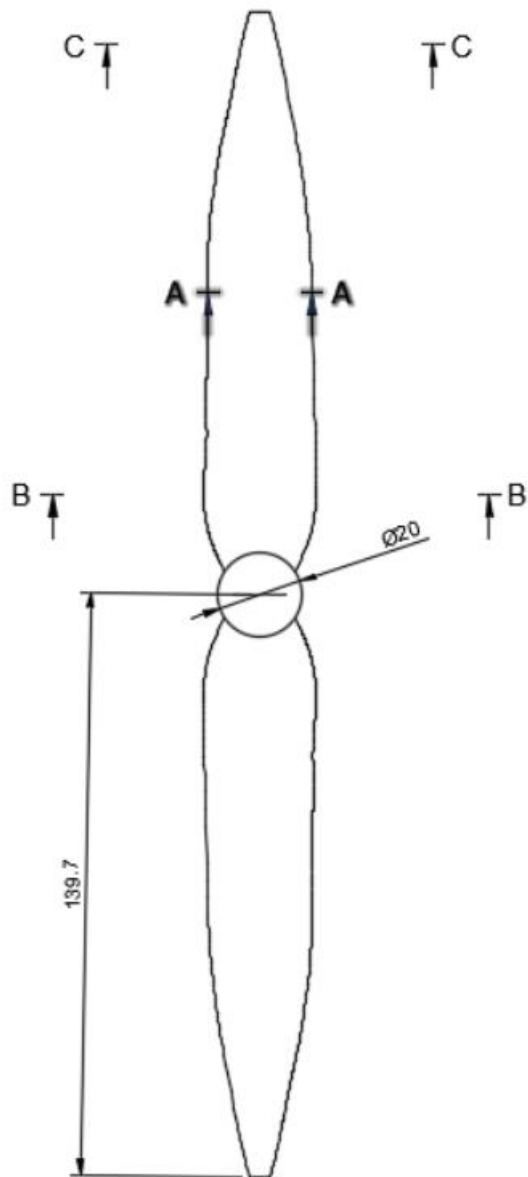
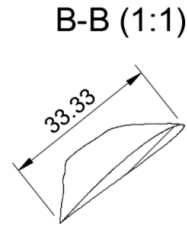


Figure 35 Top view of the propeller and propeller dimensions

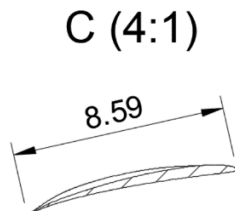
**A-A (1:1)**



Figure 36 Section AA (at the middle of the propeller blade)



*Figure 37 Section BB (at the root of the propeller blade)*



*Figure 38 Section CC (at the tip of the propeller blade)*

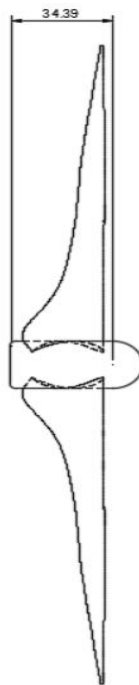


*Figure 39 Side profile of the propeller*

In the CAD of the propeller, the hub diameter has been slightly increased from 1.2 cm to 2 cm which covers up the first radial station designed. The reason for doing this is to facilitate ease of modelling because when the hub diameter is kept as 1.2 cm, a section of surface needs to be designed connecting the first section and the hub which often leads to some CAD irregularities. Since CFD of the propeller needs to be carried out to get formal aerodynamic results, CAD irregularities are unwanted. Since the first section is covered up, there will be little decrease in

the overall thrust, although the magnitude will be minuscule since the root section contributes very little to the aerodynamic performance.

### ***9.3 Pitch of the propeller:***

As mentioned in chapter 1, the pitch of a propeller is given by:

$$P_D = 2\pi r_r \tan \beta_r$$

Taking the ~74<sup>th</sup> section as the representative section,

$$\beta_r = 14.2393^\circ$$

$$r_r = 0.10293 \text{ meters}$$

From the above data, we get the propeller pitch as **6.46 inches**.

# CHAPTER 10: Obtaining Formal Aerodynamic Performance Of The Propeller Using Computational Fluid Dynamics

## 10.1 Introduction

Computational Fluid Dynamics is a tool for mimicking wind tunnel testing using computer simulations which can save a lot of resources in terms of finances as well as efforts. It has been established as an essential part of the design process of almost all the products which involve fluid flows like microfluidics in biomedical engineering, internal flows in turbomachinery, external flows in aerodynamics, refrigeration and air-conditioning etc.

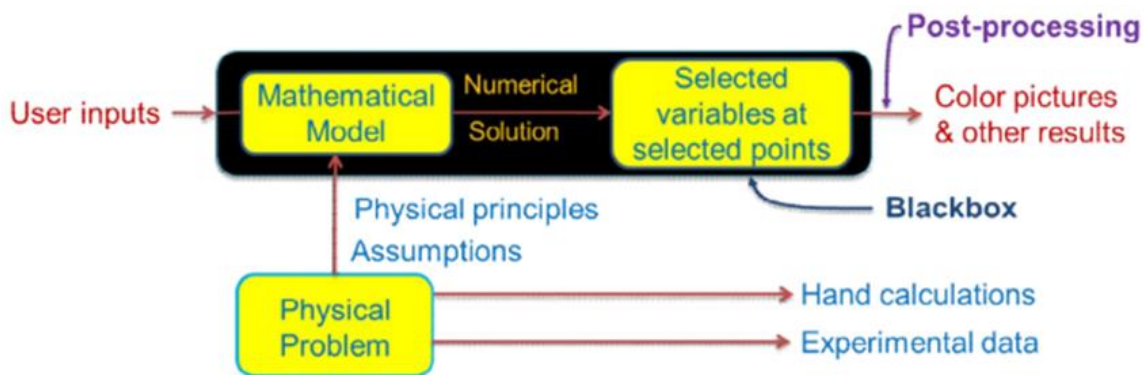


Figure 40 General procedure for any computer simulation

The general procedure for CFD analysis can be summarised as follows:

1. Creation of geometry and fluid domain.
2. Meshing or discretization of domain into smaller elements.
3. Setup of Physics in terms of solver settings, turbulence models and boundary conditions.
4. Post Processing of results

Detailed explanation of the above-mentioned steps has been provided in the following sections

## 10.2 Governing Equations

- General transport equation

$$\left\{ \begin{array}{l} \text{rate of} \\ \text{accumulation} \end{array} \right\} + \left\{ \begin{array}{l} \text{transport by} \\ \text{convection} \end{array} \right\} = \left\{ \begin{array}{l} \text{transport by} \\ \text{diffusion} \end{array} \right\} + \left\{ \begin{array}{l} \text{source} \\ \text{terms} \end{array} \right\}$$

- Conservation of mass (continuity equation)

$$\frac{\partial \rho}{\partial t} + \vec{\nabla} \cdot (\rho \vec{v}) = 0$$

- Conservation of momentum

$$\rho \frac{\partial \vec{v}}{\partial t} + \rho(\vec{v} \cdot \vec{\nabla})\vec{v} = -\vec{\nabla}p + \mu \Delta \vec{v} + \rho \vec{f}_e$$

### **10.3 Meshing and its requirements**

When dealing with systems comprising fluid flows, most of the mathematical models used comprise the governing equations in the form of complicated Partial Differential Equations (PDEs). Many times, analytical closed form solutions to these equations are either impossible or very tedious.

Therefore, Numerical Methods of solving equations are gaining popularity which work on the following principle:

Any system of Algebraic equations can be converted to a system of linear algebraic equations with variables at nodes or cell centre values.

For implementation of numerical methods, the fundamental requirement is the discretization of the entire fluid domain. The required variables are subsequently calculated at the certain points (nodes or cell centres).

#### **10.3.1 Choosing the Correct Mesh**

The ease of the solution (in terms of rate of convergence and desired accuracy) is influenced greatly by the mesh used in the system.

Intuitively one is inclined to think that finer the mesh, more the accuracy but that is not ideally the case as explained below. There are mainly two kinds of errors associated with numerical solutions of PDEs:

**Discretization error-** It is generated from the fact that all fluid properties inside a cell or element are assumed constant throughout the cell.

**Linearization error-** The generated equations as a result of numerical methods are evaluated about certain guess values and approximate linear equations are obtained.

### 10.3.2 Consequences of over-refined mesh

- The finer the mesh, less is the discretization error.
- The finer the mesh, the harder it becomes for the linearization error to converge below desired residual value.

Therefore, it is important to choose the correct fineness of the mesh in accordance with the geometry properties and the desired accuracy with computational ease.

A solution in CFD is considered valid only if it remains unchanged even after changing the mesh as the fluid flow properties are governed by proven mathematical models whereas discretization is influenced by the choice of the engineer. This is the reason why meshing is considered to be the most critical and governing step for a successful CFD simulation and needs to be studied and analysed carefully.

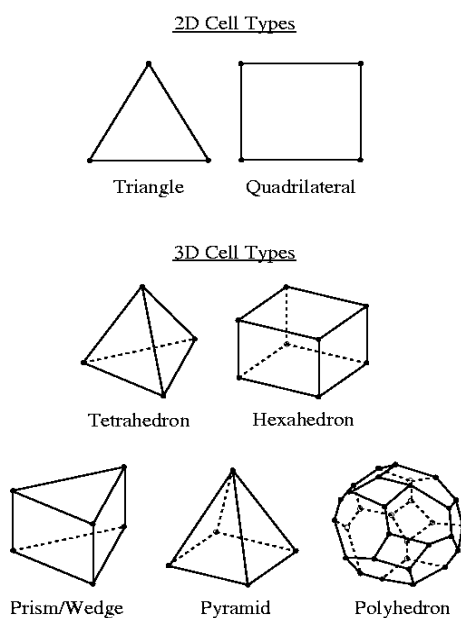


Figure 41 Types of cells used in mesh.

### **10.3.3 Comparison of Cell Types**

<b>Hexahedral Elements</b>	<b>Tetrahedral Elements</b>	<b>Polyhedral Elements</b>
They are generally used in structured mesh.	They are generally used in unstructured mesh.	They are used in unstructured mesh.
They should be constricted to simpler geometries.	They are ideal for complex geometries.	They can be used for complex geometries especially in recirculating flows.
The entire domain is covered using less elements.	More elements are required to cover the geometry compared to hexahedral.	Less elements are required compared to tetrahedral.
Less elements lead to less variables and therefore less processing time.	More elements proportionally increase the processing time.	These provide highly accurate results with least computing time due to less no. of cells along with large no. of neighbours
Aligning the elements normal to the direction of flow can result in less numerical errors.	Tendency of over-refinement can cause problems with convergence or stability of the solution.	Large no. of faces as well as neighbours makes them ideal for calculations of gradients and flows near the walls.

*Table 47 Comparison of Cell Types*

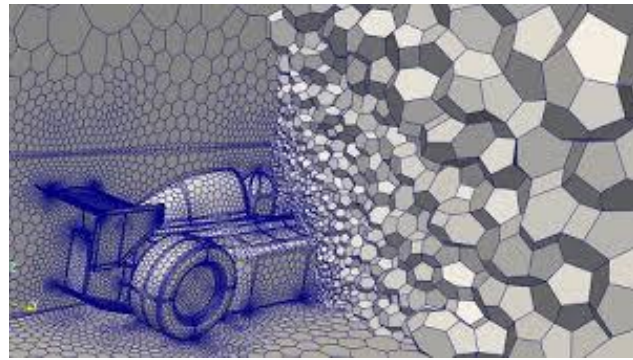


Figure 42 Polyhedral Mesh

## 10.4 Mesh Quality

The accuracy of the solution is greatly influenced by the mesh quality which is governed mainly by two parameters:

1. Geometrical properties of individual cells.
2. Orientation of these cells with respect to fluid flow.

The above-mentioned parameters are qualitatively and quantitatively measured from the following parameters:

1. Skewness
2. Smoothness
3. Aspect Ratio

### Skewness

It measures the deviation of geometrical properties of a cell from an ideal geometry. For example; the skewness of a 2D triangular cell is compared with equilateral triangle. Two methods which are generally implemented to evaluate skewness are:

#### 10.4.1 Volume Based Approach

$$\text{Skewness} = (\text{vol of ideal cell} - \text{vol of cell}) / (\text{vol of ideal cell})$$

This method is applicable only to triangles and tetrahedra and not to squares and hexa-hedra.

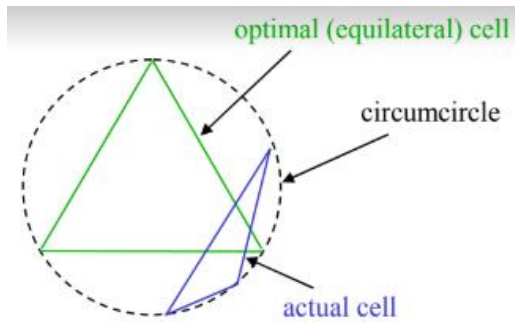


Figure 43 Volume based approach

#### 10.4.2. Angle Based approach

It measures the deviation of angles of the desired cell from those of an ideal cell (usually a regular polygon).

$$\text{Skewness} = \max [(\max - 90)/90, (\mathbf{90} - \min)/90]$$

This approach is advantageous as it applies to all geometries which cannot be evaluated using volume based approach.



Figure 44 Angle based approach

#### 10.4.3 Equiangle Skewness

This defines the general formula for angle based approach for skewness for any arbitrary geometry

$$\text{Skewness} = \max[(\max - e)/(180 - e), (e - \min)/e]$$

e is the angle for the regular polygon used for comparison.

**Range of Skewness** lies from [0 1) and it should be as low as possible.

## Smoothness

It governs the change in size as we move from one cell to another. The change in size should be gradual as in saying that the transition should be smooth.

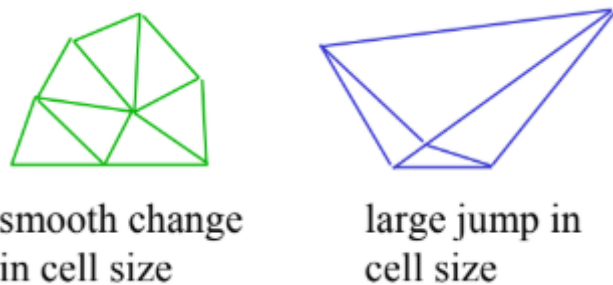


Figure 45 Smoothness

## Aspect Ratio

It measures the ratio of longest dimension to the shortest dimension of a cell. The aspect ratio should be maintained nearly 1.

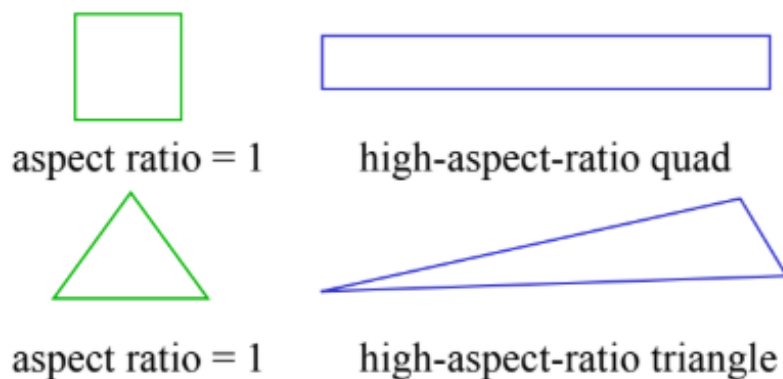


Figure 46 Aspect ratio

## ***10.5 General Guidelines in Quality***

- The aspect ratio should be nearly 1 where flow is multidimensional.
- Quad or Hex cells can be elongated in fully developed 1D flow along the direction of flow. e.g. the rectangular cells can be elongated towards the flow inside a boundary layer.
- The size ratio for adjacent cells should not exceed 1.2.
- The cell counts should be minimized without a very generous compromise with accuracy.
- Strategies to decrease the cell count:
  - Use non-uniform meshing such that localised clustering is possible.
  - Use the adaptive mesh.
- The chart for empirical values of skewness has been given below.

<b>Value of Skewness</b>	0-0.25	0.25-0.50	0.50-0.80	0.80-0.95	0.95-0.99	0.99-1.00
<b>Cell Quality</b>	excellent	good	acceptable	poor	sliver	degenerate

*Table 48 5 General Guidelines in Quality*

- The generated mesh should always be checked for the above mentioned characteristics
- In case of violations of any of the above mentioned guidelines, preferably redesign the mesh.

### ***10.5.1 Objectives of a perfect mesh***

- No. of elements should be as low as possible to reduce the no. of variables and proportionally the computation time without the loss of accuracy.
- The critical regions of the flow (boundary layers, high velocity gradients, multi-dimensional flows) should be compensated with finer mesh to get accurate results.

- The transition from regions of fine mesh to coarse mesh should be smooth as governed by recommended values of quality parameters mentioned above.
- The solution obtained is valid only if doesn't change with changing the mesh. This is a very important step in verification of the simulation.

### ***10.5.2 Sizing***

There are four ways of defining sizing in local mesh control namely:

1. Element sizing: it specifies average element edge length on edges, faces or bodies.
2. No. of Divisions: it specifies the no. of elements on the edge.
3. Body of Influence: it specifies average element size in a body.
4. Sphere of Influence: governs the average element size in the sphere.

### ***10.5.3 Biasing***

1. Bias Type: it defines a pattern in which elements should be arranged and can be selected from the drop down menu in sizing definition.
2. Bias Option
  - Bias Factor: it can be checked below the bias option and is defined as the ratio of the largest to smallest element.
  - Smooth Transition: it is defined by growth rate which considers the sizes of neighbouring elements.

$$\text{Growth rate} = \text{Bias Factor}^{1/(n-1)}$$

n gives the no. of divisions

### ***10.5.4 Behaviour***

Two options are provided for this:

1. Soft: sizing may deviate from specified values in consideration with proximity and curvatures in geometry.
2. Hard: sizing will strictly adhere to the specified value.

### **10.5.6 Sphere of Influence**

It is defined around a vertex or a body in which we do not want the element sizes to vary. This can be accessed with or without the advanced size function.

### **10.5.7 Body of influence**

Certain bodies/surfaces/lines can be created with the sole purpose of refining the mesh. This feature is available only when advanced sizing function is ON.

### **10.5.8 Mapped Face Meshing**

This feature can be used to create structured mesh on mappable surfaces. This feature is employed to generate a roughly uniform structural mesh on nearly rectangular surfaces to avoid complexities.

## **10.6 Turbulence Modelling**

### **10.6.1 Introduction**

Turbulent Flow is characterised by randomness in fluid flow characteristics, majorly velocity and pressure. It is modeled as a process in which energy is absorbed by large eddies, transmitted to smaller eddies and dissipated by eddies of  $Re \sim 1$ , that is when viscous forces are balanced by inertia forces. This type of Flow is modeled by time averaging of fluid properties over a characteristic time scale which gives rise to Reynold's Averaged Navier Stokes equations (RANS), further giving rise to a new stress tensor called Reynold's Stress. This stress tensor contains 6 variables which when modeled by Eddy Viscosity Turbulence Model reduce to one variable called turbulent viscosity. The aim of any Turbulence Model is to provide equations to find this turbulent viscosity.

$$\mathbf{u} = \bar{\mathbf{u}} + \mathbf{u}'$$

(instantaneous parameter = averaged parameter + deviation parameter)

$$\rho \frac{\partial u}{\partial t} + \rho \left( u \frac{\partial u}{\partial x} + v \frac{\partial u}{\partial y} \right) = - \frac{\partial p}{\partial x} + \mu \nabla^2 u$$

$$\rho \frac{\partial \bar{u}}{\partial t} + \rho \left( \bar{u} \frac{\partial \bar{u}}{\partial x} + \bar{v} \frac{\partial \bar{v}}{\partial y} \right) = - \frac{\partial \bar{p}}{\partial x} + \mu \nabla^2 \bar{u} - \rho \left( \overline{u' \frac{\partial u'}{\partial x}} + \overline{v' \frac{\partial u'}{\partial y}} \right)$$

$$\begin{aligned} \rho \frac{\partial \bar{u}}{\partial t} + \rho \left( \bar{u} \frac{\partial \bar{u}}{\partial x} + \bar{v} \frac{\partial \bar{v}}{\partial y} \right) &= - \frac{\partial \bar{p}}{\partial x} + \mu \nabla^2 \bar{u} \\ &+ \left( \frac{\partial}{\partial x} (-\rho \overline{u' u'}) + \frac{\partial}{\partial y} (-\rho \overline{u' v'}) \right) \end{aligned}$$

$$\rho \left( \bar{u} \frac{\partial \bar{u}}{\partial x} + \bar{v} \frac{\partial \bar{v}}{\partial y} \right) = - \frac{\partial \bar{p}}{\partial x} + \mu \nabla^2 \bar{u} + \bar{f}_{turb,x}$$

The additional variable added to the system, i.e the Reynold's Stress is given by:

$$-\rho \overline{u'_i u'_j}$$

### 10.6.2 Boussinesq Approach

It is a method of modelling the Reynold's Stress tensor as a function of the corresponding velocity gradients, thereby reducing the number of unknowns to a single variable called turbulent viscosity or eddy viscosity( $t$ ). It is based on the assumption that the eddy viscosity is an isotropic scalar( direction and point independent). The equation is given by:

$$-\rho \overline{u'_i u'_j} = \mu_t \left( \frac{\partial u_i}{\partial x_j} + \frac{\partial u_j}{\partial x_i} \right) - \frac{2}{3} \left( \rho k + \mu_t \frac{\partial u_k}{\partial x_k} \right) \delta_{ij}$$

Where  $t$  is the turbulent or eddy viscosity, the only variable to be determined, which is a function of the length scale and time scale of the turbulent eddies.

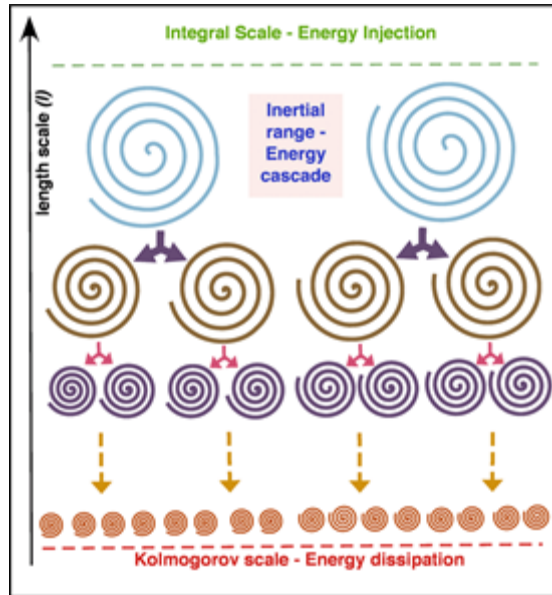
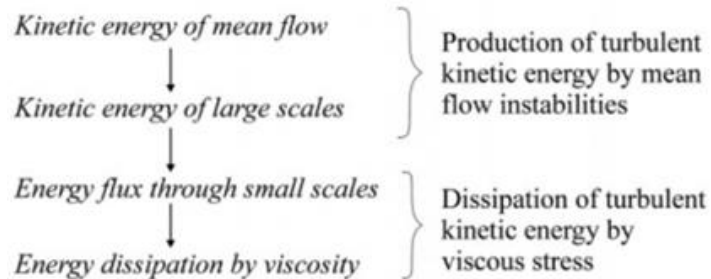


Figure 47 Mechanism of turbulence



## 10.7 Spalart Allmaras Model

- It is a one equation model that solves for the time scale. The length scale has to be inferred from geometry parameters.
- It has been designed as a high Re model and in Fluent it has been integrated to use wall functions.
- This model has been designed for applications related to external aerodynamics at high Reynolds number, as it fails to model boundary layer separation.
- The equations are modelled for turbulent kinematic viscosity from where turbulent viscosity can be determined.

### 10.7.1 Transport equation:

$$\frac{\partial}{\partial t}(\rho \tilde{v}) + \frac{\partial}{\partial x_i}(\rho \tilde{v} u_i) = G_v + \frac{1}{\sigma_{\tilde{v}}} \left[ \frac{\partial}{\partial x_j} \left\{ (\mu + \rho \tilde{v}) \frac{\partial \tilde{v}}{\partial x_j} \right\} + C_b 2\rho \left( \frac{\partial \tilde{v}}{\partial x_j} \right)^2 \right] - Y_v + S_{\tilde{v}}$$

$G_v$  is called the production term which quantifies the production of turbulence viscosity

$Y_v$  is called the dissipation term which quantifies the dissipation of energy from the smallest eddies.

$S_v$  is formally called the source the source term which can be user defined.

All these terms are complex functions of the turbulent viscosity directly or indirectly. Hence this model is able to quantify the turbulent viscosity using a simple equation.

$$\mu_t = \rho \tilde{v} f_{v1}$$

Where,

$$f_{v1} = \frac{\chi^3}{\chi^3 + C_{v1}^3} \quad \chi \equiv \frac{\tilde{v}}{v}$$

Assumptions:

- Only the first term in the RHS of Boussinesq approximation is used. i.e.:

$$-\rho \overline{u'_i u'_j} = \mu_t \left( \frac{\partial u_i}{\partial x_j} + \frac{\partial u_j}{\partial x_i} \right)$$

Limitations:

- Isotropy of turbulent viscosity may be invalid in some fluid flows.

- This model can produce arbitrary results with unsteady flows.
- It is suited mostly for high Reynold no. flows.

### Best Practices

- This model should be employed for high Re no. flows.
- This model is generally used for applications in wall bounded flows and boundary layers with adverse pressure gradients.
- This model finds most of its applications in the aerospace industry, majorly in simulations involving external flow aerodynamics.

### **10.8 K-Epsilon Model**

- Two equations are used for evaluation based on turbulent kinetic energy (lengthscale) and dissipation of this energy (time scale).
- Foundation of this model is also based on the complete Boussinesq approximation.
- It can take buoyancy and temperature gradient effects into consideration.
- Further developments have divided this model into 3 sub categories as follows:
  1. Standard k-
  2. RNG k-
  3. Realizable k-
- The two equations after evaluation give the k and terms which are modeled to give the turbulent viscosity as follows:

$$\mu_t = \rho C_\mu \frac{k^2}{\varepsilon}$$

where  $C_\mu$  is a constant

Transport Equations:

$$\frac{\partial}{\partial t}(\rho k) + \frac{\partial}{\partial x_i}(\rho k u_i) = \frac{\partial}{\partial x_j} \left[ \left( \mu + \frac{\mu_t}{\sigma_k} \right) \frac{\partial k}{\partial x_j} \right] + G_k + G_b - \rho \varepsilon - Y_M + S_k$$

and

$$\frac{\partial}{\partial t}(\rho \varepsilon) + \frac{\partial}{\partial x_i}(\rho \varepsilon u_i) = \frac{\partial}{\partial x_j} \left[ \left( \mu + \frac{\mu_t}{\sigma_\varepsilon} \right) \frac{\partial \varepsilon}{\partial x_j} \right] + C_{1\varepsilon} \frac{\varepsilon}{k} (G_k + C_{3\varepsilon} G_b) - C_{2\varepsilon} \rho \frac{\varepsilon^2}{k} + S_\varepsilon$$

$G_k$  is the term giving generation of turbulent kinetic due to velocity gradients

$G_b$  is the term giving turbulence generation due to buoyancy effects.

$Y_m$  involves the compressibility effects.

$S_k, S_\varepsilon$  are the source terms.

#### Limitations

- It cannot be used for transitional flows and is valid only for fully turbulent flows.
- This model is recommended for high Reynold's no. flows.
- Limitations posed by Boussinesq approximation.

#### Best Practices

- Due to limitations, it is best advised to not use the standard version of this model. Therefore, two refinements of this model namely RNG and Realizable have been accommodated in Fluent.

#### RNG K-Epsilon

- It involves an additional term in the dissipation equation that models swirling flows with enhanced accuracy.
- It offers better accuracy for rapidly strained flows.
- This model calculates the Prandtl no. itself analytically rather than taking input from the user.

- It can accommodate low Re no. flows to some extent if care is taken regarding the near wall treatment.
- The default setting is with high Re Value.
- It also offers higher accuracy for streamline curvature flows.

### Realizable K-Epsilon

- The term Realizable implies that the model satisfies the mathematical constraints on Reynold's stress tensor consistent with the physics of turbulent flows, as it does not allow the normal stress components to fall to negative values.
- This model is considered superior to its predecessors.
- This model gives more accurate results for flows like spreading of planar and round jets.
- It can model boundary layer flows with high accuracy along with separating flows.

### **10.9 K-Omega Model**

- This is quite similar to k-e model as the dissipation has been replaced by specific dissipation (/k). Omega is modelled as an inverse time scale associated with turbulence.
- It can be used for low Re no. values by using suitable correction factors.
- This model is best used for free shear flows.

Transport equations:

$$\frac{\partial}{\partial t}(\rho k) + \frac{\partial}{\partial x_i}(\rho k u_i) = \frac{\partial}{\partial x_j} \left( \Gamma_k \frac{\partial k}{\partial x_j} \right) + G_k - Y_k + S_k$$

and

$$\frac{\partial}{\partial t}(\rho \omega) + \frac{\partial}{\partial x_i}(\rho \omega u_i) = \frac{\partial}{\partial x_j} \left( \Gamma_\omega \frac{\partial \omega}{\partial x_j} \right) + G_\omega - Y_\omega + S_\omega$$

G terms stand for production terms.

Y terms stand for dissipation terms.

S terms stand for source terms.

terms stand for effective diffusivities which are modelled as below.

$$\Gamma_k = \mu + \frac{\mu_t}{\sigma_k}$$

$$\Gamma_\omega = \mu + \frac{\mu_t}{\sigma_\omega}$$

Where terms denote the respective Prandtl Nos.

#### Limitations

- It requires finer grid such that  $y+=1$  is ensured in the near wall region

#### Best Practices

- This model should be applied for measuring wakes, mixing layers, jet flows.
- It can also be used for wall bounded and free shear flows.

### **10.10 K-Kl-Omega Model**

- This is a three equation model.
- It models kinetic energy separately for laminar and turbulent flows along with an inverse turbulent time scale
- This model is best suited for transition flows which can be clearly interpreted from the governing equations.

#### Transport Equations:

$$\frac{Dk_T}{Dt} = P_{K_T} + R + R_{NAT} - \omega k_T - D_T + \frac{\partial}{\partial x_j} \left[ \left( v + \frac{\alpha_T}{\alpha_k} \right) \frac{\partial k_T}{\partial x_j} \right]$$

$$\frac{Dk_L}{Dt} = P_{K_L} - R - R_{NAT} - D_L + \frac{\partial}{\partial x_j} \left[ v \frac{\partial k_L}{\partial x_j} \right]$$

$$\frac{D\omega}{Dt} = C_{\omega 1} \frac{\omega}{k_T} P_{k_T} + \left( \frac{C_{\omega R}}{f_W} - 1 \right) \frac{\omega}{k_T} (R + R_{NAT}) - C_{\omega 2} \omega^2$$

$$+ C_{\omega 3} f_{\omega} \alpha_T f_W^2 \frac{\sqrt{k_T}}{d^3} + \frac{\partial}{\partial x_j} \left[ \left( v + \frac{\alpha_T}{\alpha_{\omega}} \right) \frac{\partial \omega}{\partial x_j} \right]$$

Limitation:

- This model is valid only where isotropy assumption is reasonable.
- Solution of three equations can increase the computational costs.

Best Practices

- This model should be used where laminar or turbulent nature of the flow is not certain.

### **10.11 Transition SST Model**

- Standard SST model works by applying k-omega model at the wall and k-epsilon model in the bulk, with a blending function to ensure smooth transition between the two.
- This is a Four equation model that couples the two equations from SST-K-Omega model with one intermittency equation and second momentum thickness equation which studies the onset criteria of transition.

Transport equation:

$$\frac{\partial}{\partial t} (\rho k) + \frac{\partial}{\partial x_i} (\rho k u_i) = \frac{\partial}{\partial x_j} \left( \Gamma_k \frac{\partial k}{\partial x_j} \right) + G_k - Y_k + S_k$$

and

$$\frac{\partial}{\partial t} (\rho \omega) + \frac{\partial}{\partial x_j} (\rho \omega u_j) = \frac{\partial}{\partial x_j} \left( \Gamma_{\omega} \frac{\partial \omega}{\partial x_j} \right) + G_{\omega} - Y_{\omega} + D_{\omega} + S_{\omega}$$

(SST-k-omega)

$$\frac{\partial(\rho\gamma)}{\partial t} + \frac{\partial(\rho U_j \gamma)}{\partial x_j} = P_{\gamma 1} - E_{\gamma 1} + P_{\gamma 2} - E_{\gamma 2} + \frac{\partial}{\partial x_j} \left[ \left( \mu + \frac{\mu_t}{\sigma_\gamma} \right) \frac{\partial \gamma}{\partial x_j} \right]$$

(Intermittency)

$$\frac{\partial(\rho R \tilde{e}_{\theta t})}{\partial t} + \frac{\partial(\rho U_j R \tilde{e}_{\theta t})}{\partial x_j} = P_{\theta t} + \frac{\partial}{\partial x_j} \left[ \sigma_{\theta t} \left( \mu + \mu_t \right) \frac{\partial R \tilde{e}_{\theta t}}{\partial x_j} \right]$$

(Momentum Thickness equation)

Limitations

- Higher computational costs due to increased no. of equations.

Best Practices

- This model should be used where transition flows are expected.
- This model is considered the most robust and is recommended to beginners for CFD simulations.

## **10.12 CFD Best Practices**

### **10.12.1 Domain Selection**

The geometrical parameters of the domain selected for CFD analysis of any geometry influence the stability as well as the accuracy of the solution by preventing fluid backflow, wall effects, etc.

The domain size is determined by the following guidelines:

1. Flow velocity (V)
2. Characteristic Length (L)
3. Upstream Length (X)

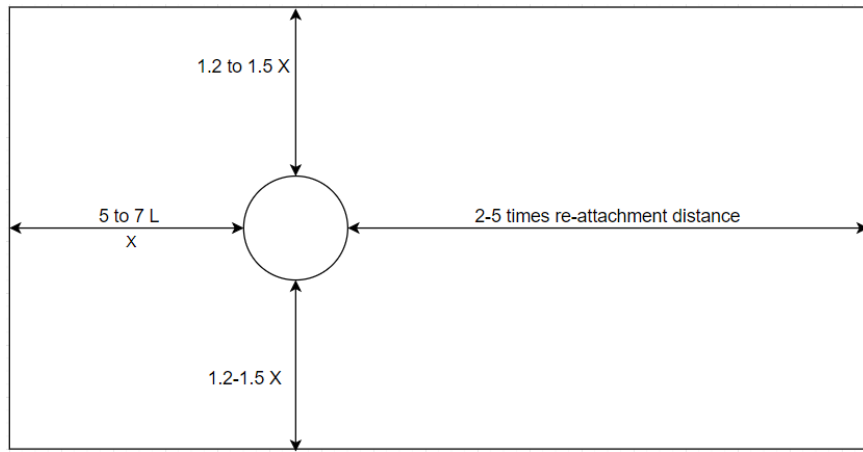


*Figure 48 Guidelines for domain sizing*

### Residual Limits

The default values for residual limits which should be attained for convergence in ANSYS Fluent are set to 1e-3. Although for CFD analysis for aerospace applications, it is recommended to use the residual limits of the order of 1e-6. For very accurate analysis, residual limits as low as 1e-9 should be used. The residuals for solving a heat transfer problem or when utilizing the energy equations in fluent, the minimum order of convergence is 1e-6.

The lower the residual limits, higher is the accuracy as well as the computational time. Therefore, optimization for a better solution is dependent on the engineer.

### Boundary-Layer Capturing

Dimensionless parameter  $y+$  is used for mesh refinement for improving the accuracy of capturing boundary layer flows and the resultant forces due to them. The recommended  $y+$  value which should be used depends on the combination of the turbulence model and wall function being used.

1. K-Epsilon with Enhanced wall treatment:  $30 < y+ < 300$
2. Low-Re models (K-Omega, TSST, K-Kl-Omega):  $y+ < 5$

Also, the aspect ratio of elements being used for capturing boundary layer flows should not exceed 40.

## Meshing

- While giving inflation to the body either of the two methods must be followed,
- The first layer thickness must be computed analytically in order to achieve a required  $y+$  value.
- The total layer thickness has to be computed by numerically calculating the thickness of the boundary layer.
- Utilization of the multi-zone mesh method for complicated geometry is suggested.
- A structures mesh should satisfy the following conditions,  
 $1 < AR(\text{Aspect ratio}) < 40$
- Element quality  $> 0.85$  for at least 25% of overall cells.
- Utilize mosaic meshing feature in ANSYS 2019 R1 for reducing the number of cells without compromising on the accuracy of the results.

## Best practices for Obtaining Convergence

The standard procedure for obtaining a faster solution convergence is as following,

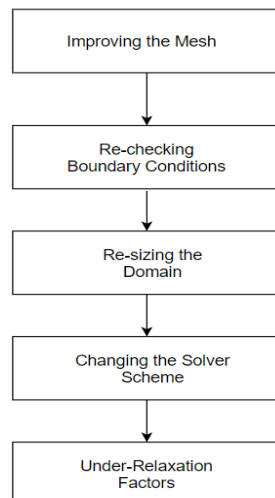


Figure 49 Factors to be considered for convergence in decreasing order of priority

- The following method is generally utilized for obtaining problem and solution convergence, Reducing the respective Under relaxation factors and proceeding with the simulation until the flow develops and then gradually increase the URF values

incrementally maintaining the solution stability. This should be performed until the solution and problem convergence is attained.

### Turbulence Models

1. **Spalart Allmaras:** one equation model, to be used only when a change in kinetic energy is to be determined. This model is Ideal for external aerodynamic flows.
2. **K-Epsilon Realizable:** Very robust and highly recommended for most of the subsonic incompressible flows with a combination of enhanced wall treatment, Coupled scheme and pseudo-transient approach.
3. **K-Omega SST:** Recommended for internal flows and can be used for high speed, compressible flows. Though it is highly popular for low Reynolds number 2D flows also.
4. **TSST:** It should be used for determination of transition point is the main aim of the analysis.

Turbulence Model	Subsonic Incompressible	Subsonic Compressible	Transonic	Supersonic	Internal Flow	External Flow	Reynold's No.	Transition
Spalart Allmaras	NO	Depends on Re	YES	NO	NO	YES	High	NO
K-Epsilon Realizable	YES	NO (exceptions, IC engine Combustion)	NO	NO	YES	YES	High	NO
K-Omega SST	YES	YES	YES	YES	YES	YES	Low	YES
TSST	YES	YES	YES	YES	YES	YES	Low	YES

Table 49 Reference Chart for Turbulence Models (Validated by ANSYS Expert)

## **10.13 Turbulence Definition**

Various parameters are available for defining turbulence in ANSYS Fluent boundary conditions:

1. **Intensity and Characteristic Length:** This approach should be used for external flows.
2. **Intensity and Hydraulic Diameter:** This approach should be used for internal flows.
3. **Intensity and Viscosity Ratio:** This approach should be used for multi-phase flows.
4. **K and Epsilon:** For other cases.

## **10.14 Solver Settings**

The following solver settings would be the most optimum settings for obtaining faster solution convergence,

Gradient	Least Square Cell-Based
Pressure	Second Order
Momentum	Second Order Upwind
Turbulent Kinetic Energy	Second Order Upwind
Turbulent Dissipation	Second Order Upwind

*Table 50 Solver settings of the CFD model*

### **10.14.1 Initialization**

1. FMG Initialization – This is the most accurate type of initialization but the procedure for implementation is quite complicated therefore it is not very prevalent.
2. Hybrid Initialization – It initializes the setup after performing 10 iterations. This approach is highly recommended.
3. Standard Initialization – This computes the values from a specified boundary condition. It should be used for simple 2D flows.

### **10.14.2 External Flows**

The setup utilized for Alpha full body CFD analysis was analysed by the ANSYS Expert and the following suggestions were provided,

1. **Geometry:** The domain size has to be increased by a great extent. The new sizing nomenclature has to be utilized. Additionally, the geometry should be scaled down to 1:3 or 1:2 model in order to reduce the overall domain size and ultimately the computing power and time.
2. **Mesh:** The execution of the meshing is in order and the maximum number of elements cannot be reduced drastically using ANSYS Meshing. Utilizing the ANSYS fluent 2019 R1 mosaic meshing would accelerate the result by effectively reducing the total number of elements by one-third.
3. **Setup:** Usage of second order solver schemes will provide faster convergence of the solution. Additionally, hybrid initialization has to be employed for a better kick-start to the solution convergence.

### **10.14.3 Internal rotary flows**

The setup being used for Alpha's propeller analysis was analysed by the ANSYS Expert after which two modifications were made,

1. **Meshing:** use of patch conformal method in mesh methodology was suggested to ensure better connectivity of nodes between rotor and stator.
2. **Setup:** Enabling of a laminar zone in rotor domain was suggested due to the presence of viscous sublayer in the boundary layer formed over the alpha propeller.

## **10.15 CFD Analysis for 8x3.8 APC Propeller**

### **10.15.1 Introduction**

Analysis of Rotating machinery using CFD is a distinguished field in itself and is very different from simulations falling under steady-state or other categories. CFD analysis of propeller was required to be conducted using ANSYS Fluent for the propeller to be used in the UAV. Therefore, a pre-analysis study had to be conducted in order to establish the most accurate and

trustworthy system of CFD setup in terms of the mesh fineness, domain geometries and turbulence model to be used. Therefore, an additional CFD analysis was performed on APC 8x3.8 propeller whose experimental data was available for Thrust, Power and Torque coefficients along-with an accurate 3D scan from KTH Sweden. The analysis was performed using the Moving Reference Frame (MRF) method at steady state.

### 10.15.3 Geometry

The geometry used for the simulation has been illustrated in fig :

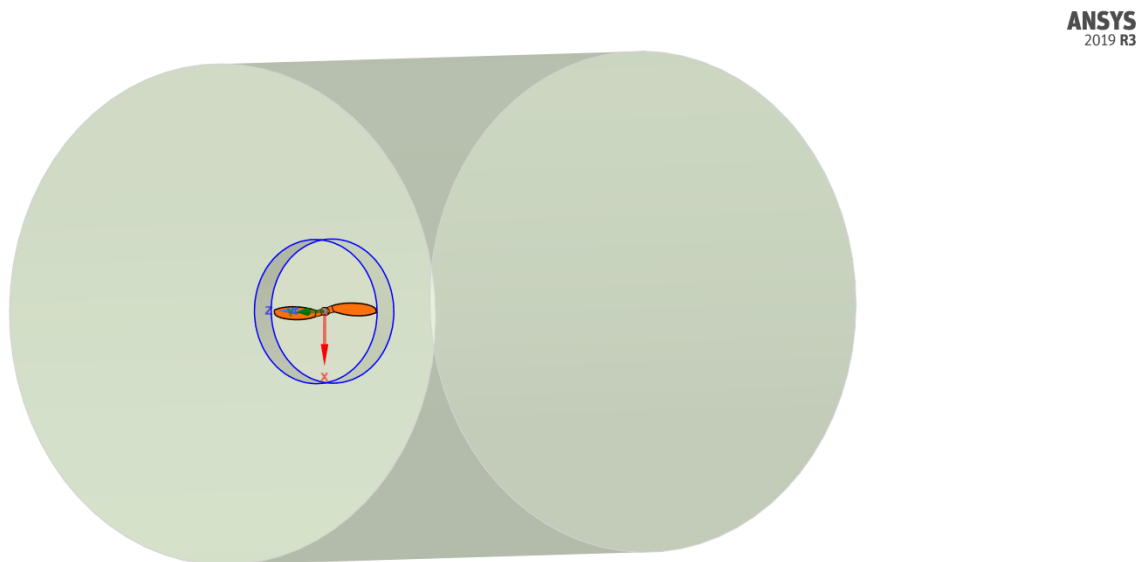


Figure 50 Geometry used for MRF

It can be seen from fig 53 that the domain has been divided into two solid segments enclosing the propeller:

1. **Rotor:** this is the inner cylindrical domain which encloses the rotor directly and has been provided to serve as a rotating reference frame with the propeller wall that has been subtracted as Boolean from the system.
2. **Stator:** This is the outer cylindrical domain enclosing the rotor which would serve as a stationary fluid domain for the analysis.

#### 10.15.4 Mesh

The mesh used for this analysis was a combination of structured and unstructured mesh called mosaic mesh which is one of the latest features included in ANSYS Fluent meshing 2019 R1 version which included a body of influence and an inflation layer near the propeller for assuring the appropriate fineness near the propeller. Polyhedral elements were used which have the ability,

Mesh Parameters:

1. Minimum Element Size: 50 microns (near the leading and trailing edges)
2. Maximum Element Size: 30 mm
3. Inflation Layer: Smooth transition with 5 layers
4. Curvature Normal Angle – 10

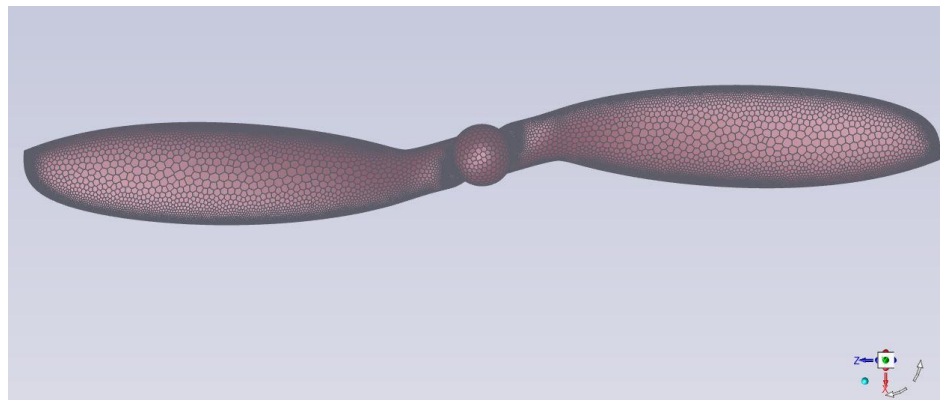


Figure 51 Propeller Mesh

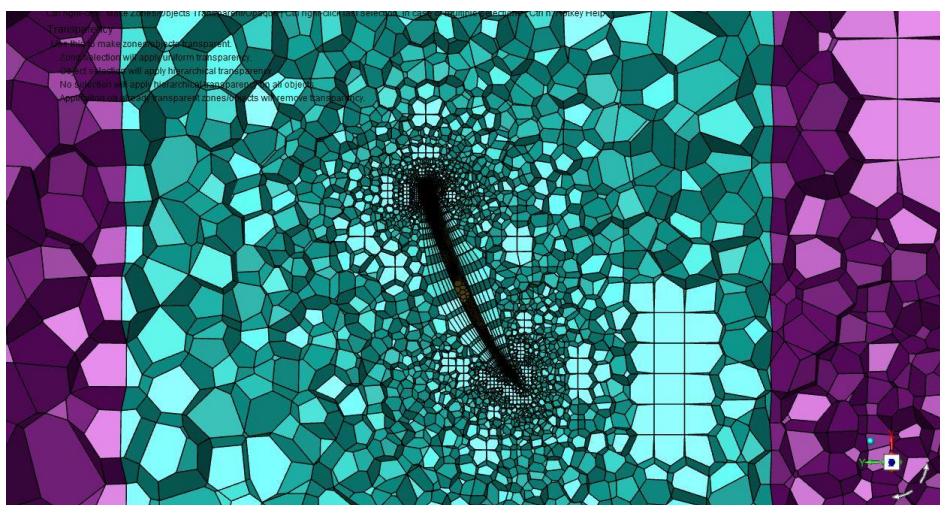


Figure 52 Boundary Layer Mesh for Propeller Section



Figure 53 Sectional View of Complete Mesh

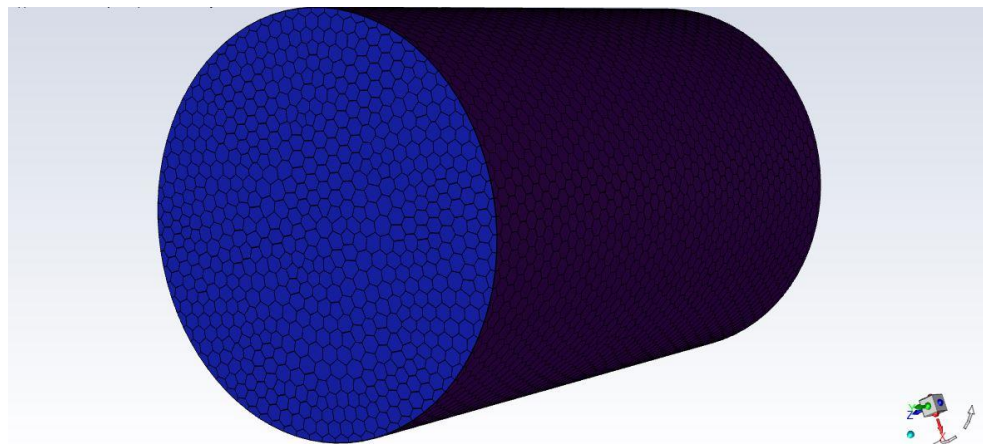


Figure 54 Complete Mesh Orthogonal View

### 10.16 Moving Reference Frame (MRF) Approach

This adds a rotary acceleration term as a source term to the momentum equations for solving rotary flow problems using a steady state approach in CFD. An option for pseudo transient is also available for enhancing the accuracy using automated time-steps in the solver.

## Validation for multiple advance ratios

The validation case for APC 8X3.8 SF propeller was extended to multiple advance ratios for 5012 RPM using the same mesh as mentioned above with k-omega SST turbulence model. Y

The various contours, streamlines and velocity vectors have been illustrated in the following sections:

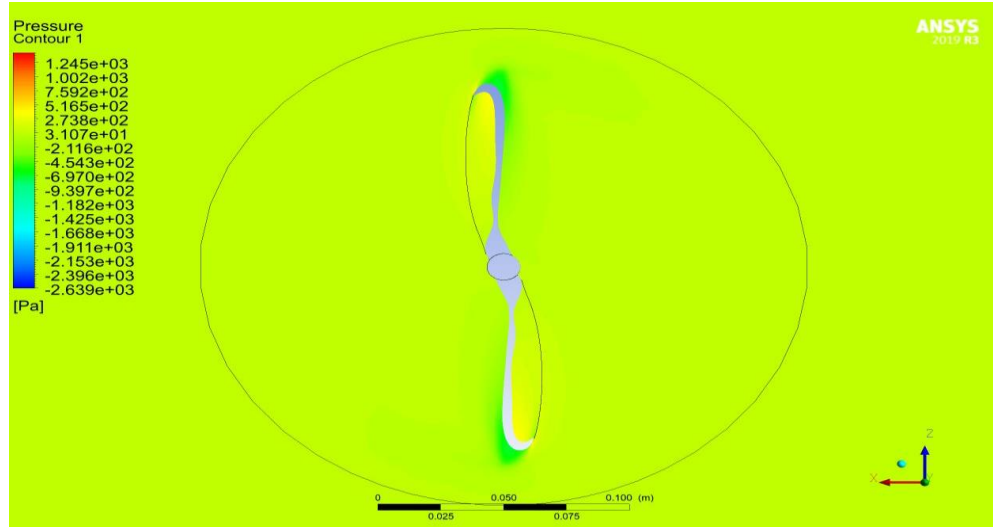


Figure 55 Pressure contours

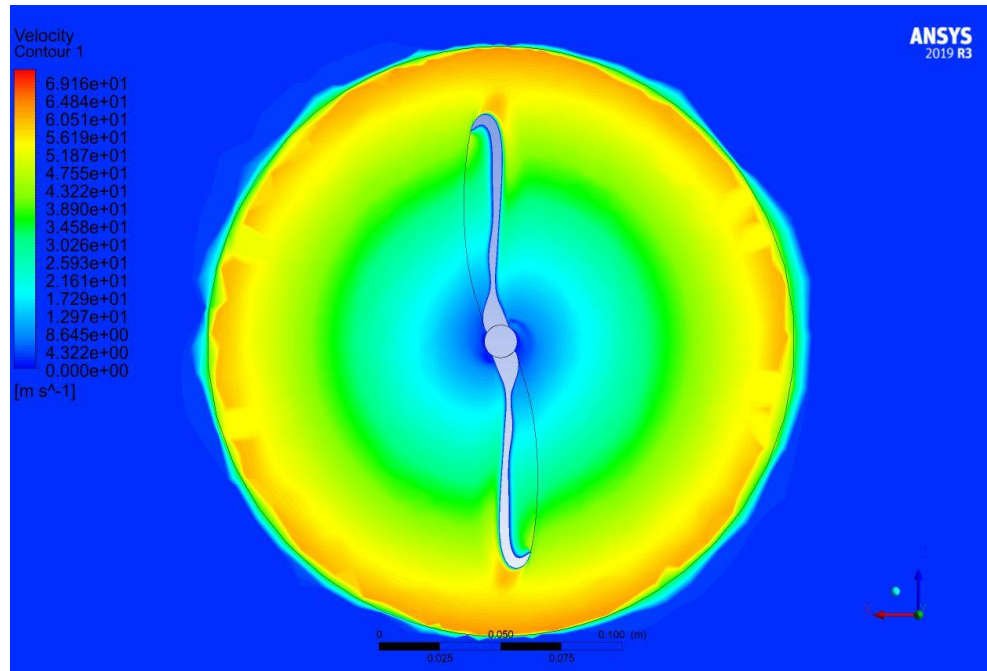


Figure 56 Velocity contours front view

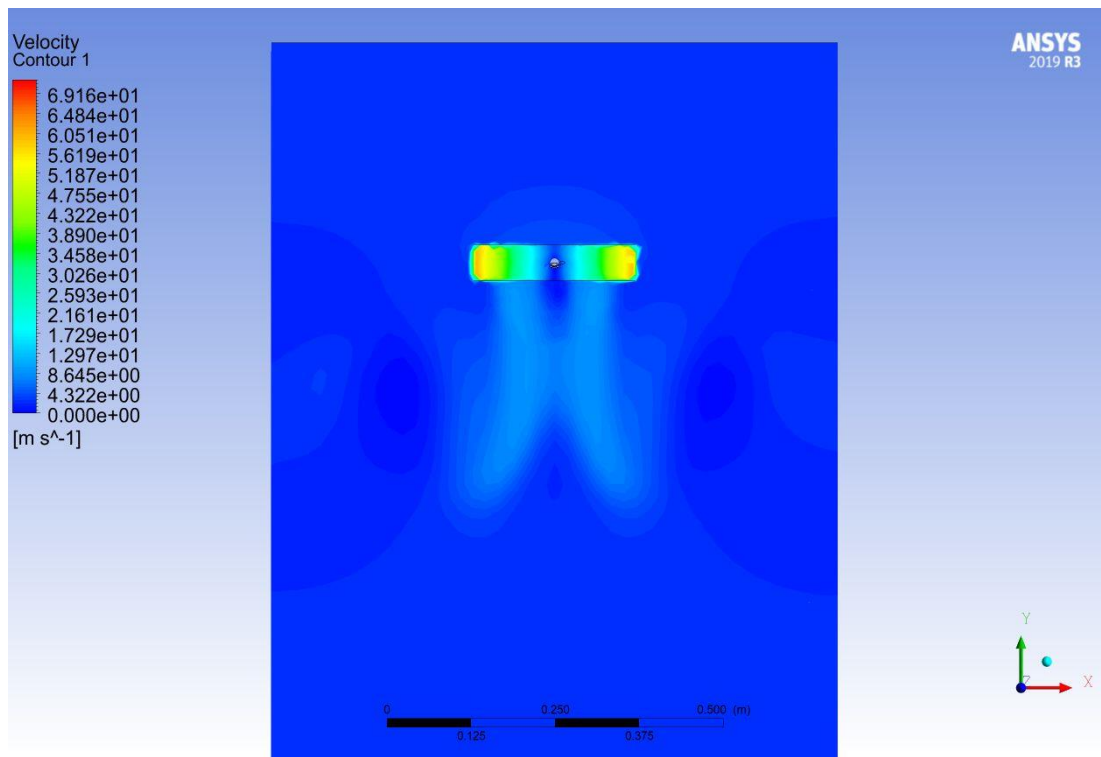


Figure 57 Velocity contours side view

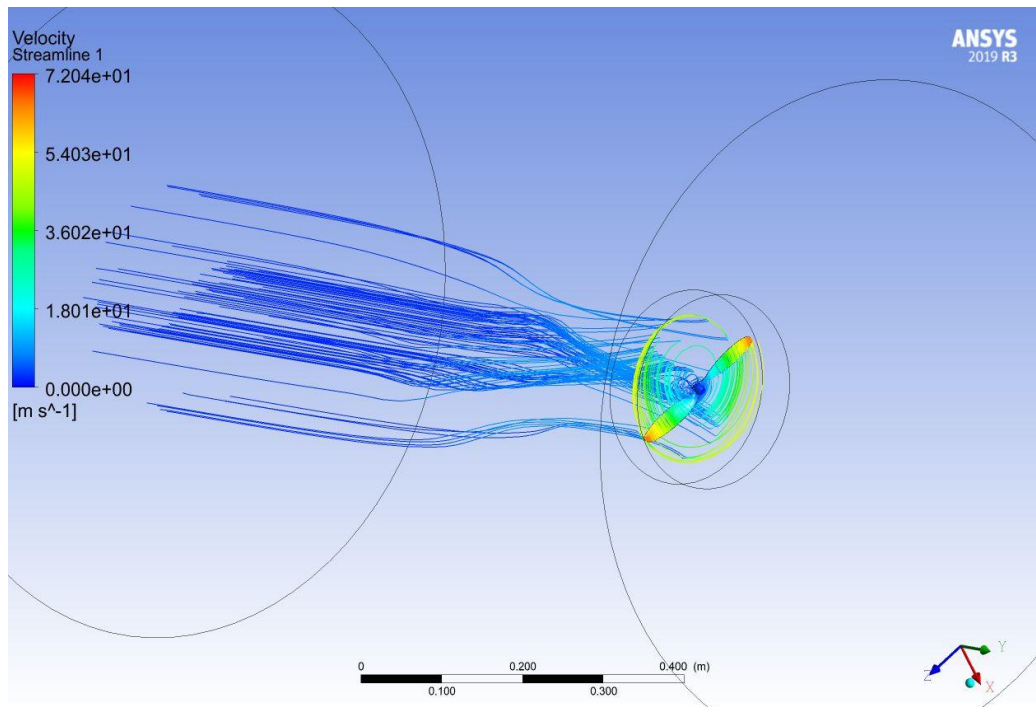


Figure 58 Streamlines Result

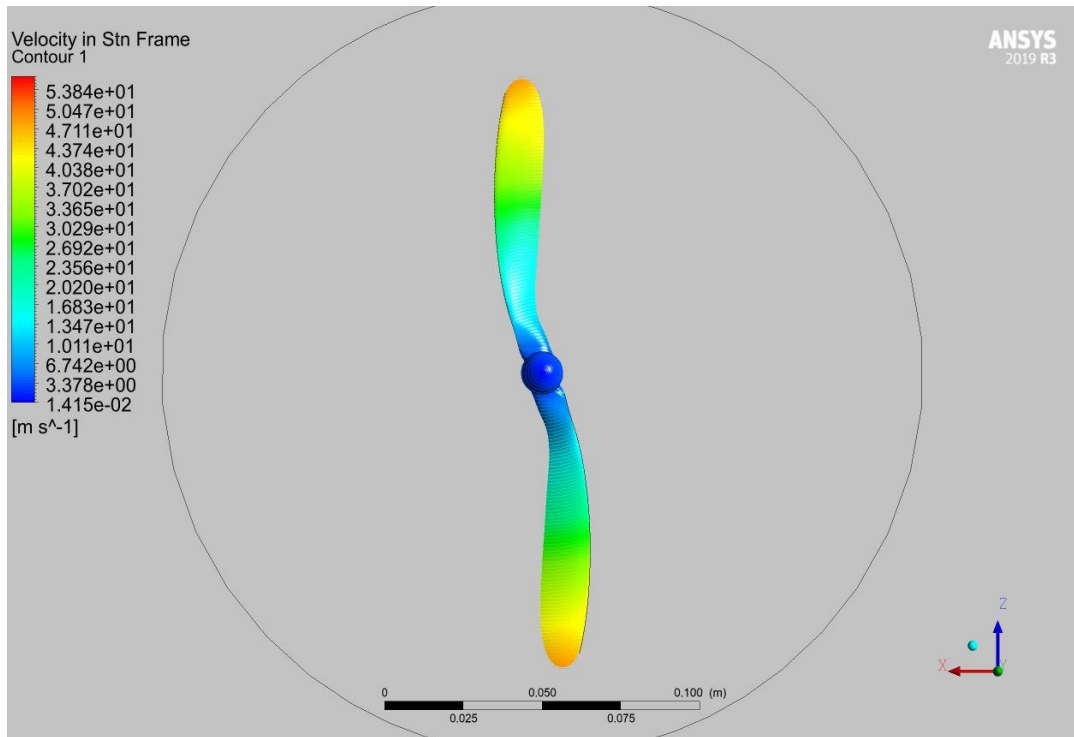


Figure 59 Propeller rotation

## Results

Experimental			CFD		Error%	
Velocity (m/s)	Thrust (N)	Torque(Nm)	Thrust (N)	Torque(Nm)	Thrust	Torque
2.34240832	1.3057455	0.0201715	1.34	0.02176	0.026234	0.0787499
2.987419307	1.2372522	0.01988872	1.295	0.02153	0.046674	0.0825232
3.547560427	1.174588	0.01960594	1.225	0.02119	0.042919	0.0807948
4.158623467	1.0973508	0.01913464	1.137	0.0207	0.036132	0.0818074

Table 51 Comparison of thrust and torque values between the CFD data and the wind tunnel data of APC 8x3.8

## Inferences And Conclusions

- The error percentage is significantly low with this setup.
- Use of capturing Proximity and Curvature settings for the meshing generates a smoother and stable mesh compared to default settings.

- Mesh defeathering should be set to off when performing results involving airfoil sections in order to prevent the distortion of trailing edges.
- Gravity has been ignored in this setup.

#### CFD Analysis for MH32 (8.7%) + Eppeler 63 Propeller and APC 11x4.7

After the CFD validation was achieved for experimental data, a comparative study was implemented between the designed UAV propeller and the commercial APC 11x4.7 SF propeller in order to supplement the results generated by Qmil and Qprop.

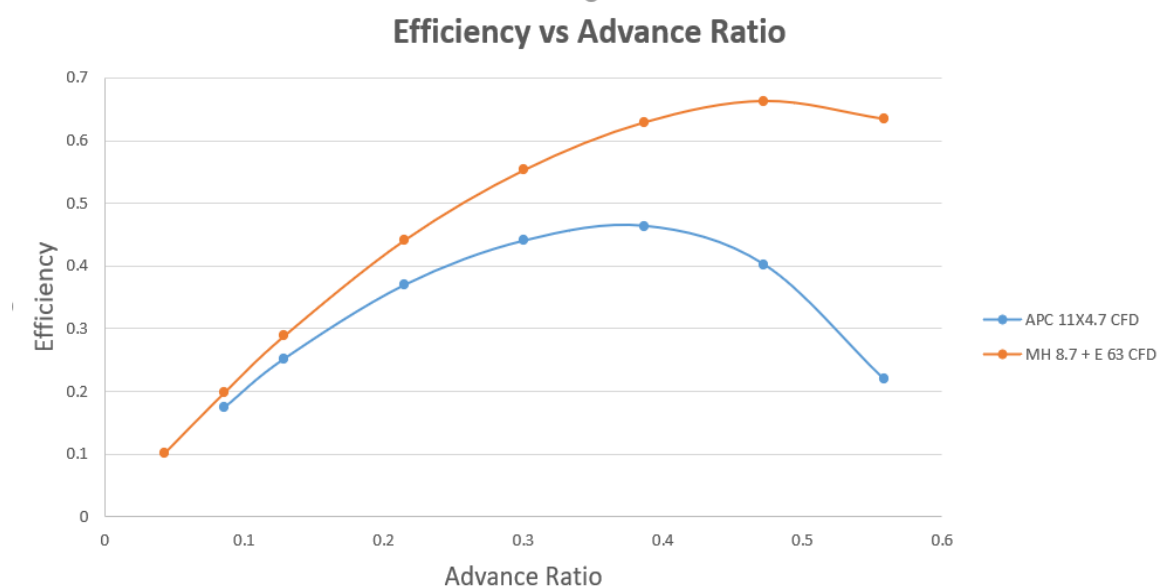
The Turbulence model used was K-Omega SST with same setup parameters used in the validation case for CFD with 11x3.8.

APC 11x4.7 SF				
5000 RPM				
V (m/s)	Thrust (N)	Torque (N-m)	Prop Efficiency	Adv Ratio
2	3.387	0.074	0.174829554	0.085898
3	3.287	0.0746	0.252454728	0.128848
5	2.91	0.0752	0.369527301	0.214746
7	2.3746	0.0721	0.440306013	0.300644
9	1.74	0.0645	0.463696076	0.386543
11	1.087	0.0568	0.402045561	0.472441
13	0.4361	0.0494	0.219181486	0.558339

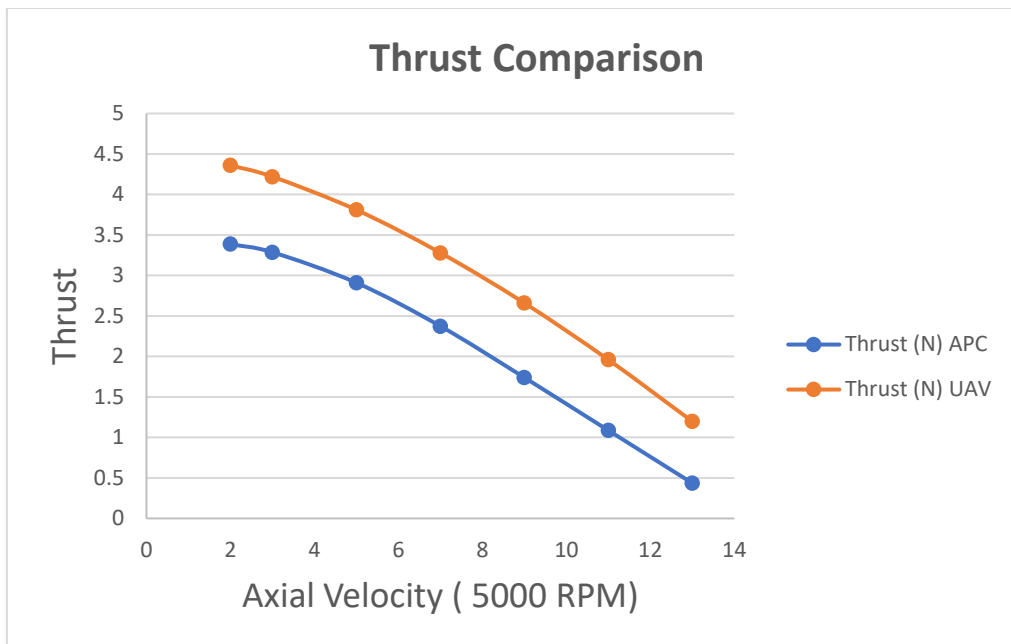
Table 52 CFD aerodynamic data for APC 11x4.7

MH 8.7 + E63 Propeller				
5000 RPM				
V (m/s)	Thrust (N)	Torque (N-m)	Prop Efficiency	Adv Ratio
1	4.41	0.0836	0.100747363	0.042949
2	4.36	0.0843	0.197556029	0.085898
3	4.22	0.0839	0.288186162	0.128848
5	3.81	0.0826	0.440469976	0.214746
7	3.28	0.0793	0.552968095	0.300644
9	2.66	0.0727	0.628913783	0.386543
11	1.96	0.0621	0.66306871	0.472441
13	1.198	0.0469	0.634203604	0.558339

Table 53 CFD aerodynamic data for the final selected propeller



Graph 132: Comparison of the efficiency data extracted from CFD for the final selected propeller and APC 11x4.7



*Graph 133: Comparison of the thrust data extracted from CFD for the final selected propeller and APC 11X4.7*

### ***Conclusions and Inferences***

- The best suited turbulence model for rotary flows is k - omega SST with  $y+ = 1$ .
- CFD underpredicts the thrust and torque values compared to solvers like Qmil and Qprop but overpredicts the same compared to experimental data.
- The momentum data at high rpms deviates from the general trend which might be due to ignorance of compressibility effects.

## CHAPTER 11: Strength Of The Propeller

Now that the design of the propeller has been validated using CFD, it is important to check whether it is strong enough to bear the aerodynamic loads. There will be two kinds of stresses applied on the propeller: bending stress due to the thrust generation and the centrifugal stress due to rotation of the propeller. Assuming that the propeller is not rotated at a rotational speed more than 10,000 RPM, which already is a high enough value for a slow flyer propeller, the worst-case design point for the propeller will be when it is rotating at a speed of 10000 RPM and is static, i.e. there is no linear forward speed. The strength is calculated using finite element analysis in ANSYS. The material used for the propeller is ABS Plastic, a composite polymer used extensively in 3D printing applications. Since ABS plastic is a composite, it has varying material properties in different planes and directions but its isotropic approximation is taken for the analysis in ANSYS.

Young's Modulus	2200 MPa
Poisson's Ratio	0.39
Bulk Modulus	3333.3 MPa
Shear Modulus	791.37 MPa
Tensile Strength at Fracture	43 MPa
Tensile Strength at Yield	48 MPa

*Table 54 Material mechanical properties for ABS Plastic*

The model is meshed using standard size tetrahedral 3D mesh elements, a kind of mesh suitable for strength calculations.

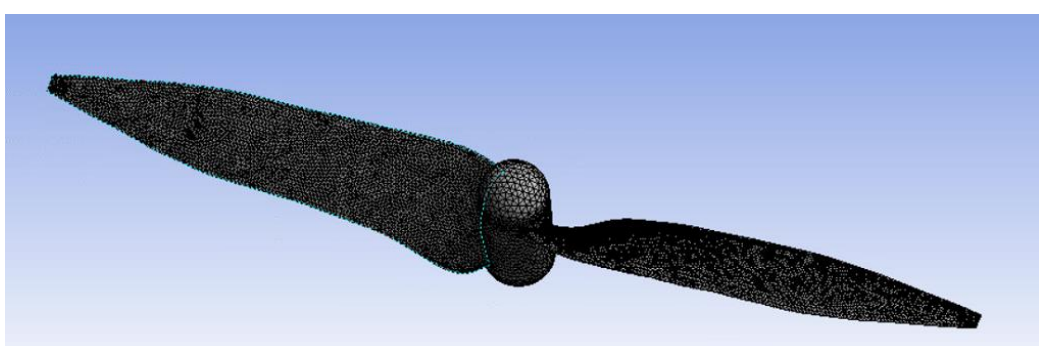


*Figure 60 Meshed model of the propeller*

The propeller is provided a fixed support at its hub with a rotational speed of 10000 RPM (1047.2 rad/s) being provided to the support.

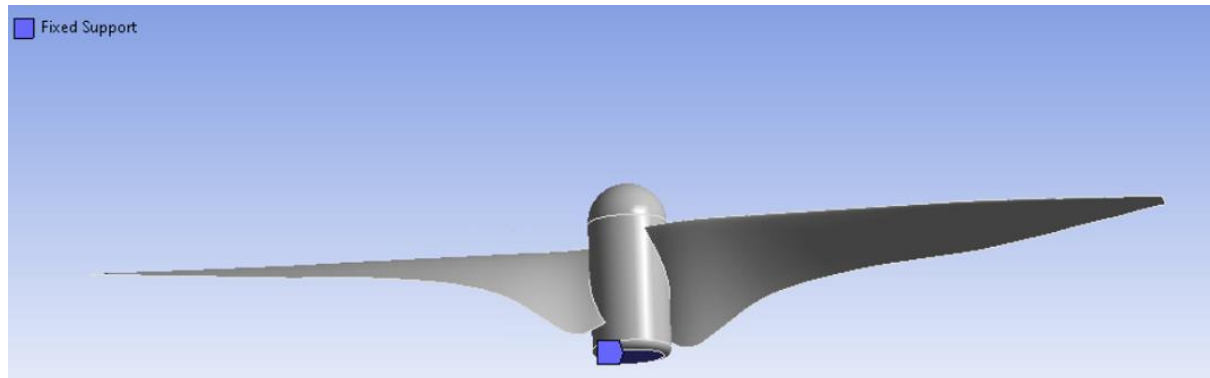


*Figure 61 Model setup for the propeller in static structural workbench in ANSYS*

The thrust load generated in ANSYS Fluent is imported into the Static Structural workbench to act as a pressure load on the propeller mesh surface.

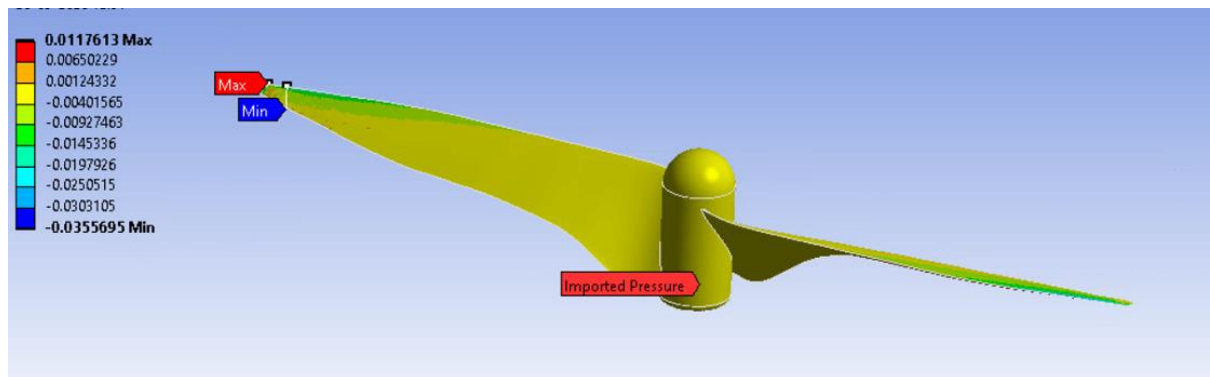


*Figure 62 Imported CFD thrust load on the propeller*

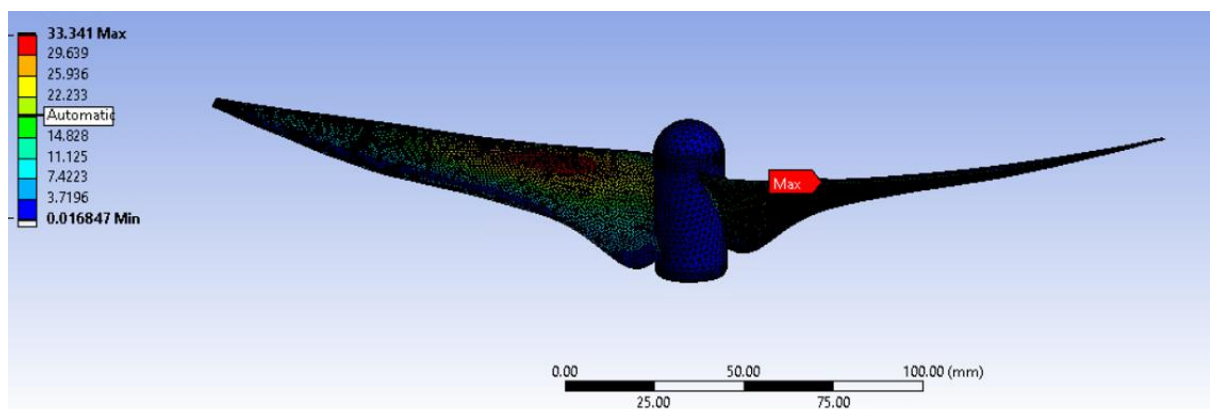


*Figure 63 Von-Mises stress distribution in the propeller*

The stress is given in the form of Von-Mises stress, which is basically the total strain distortion energy in the propeller geometry, or the equivalent stress combining the bending stress and the centrifugal stress. The maximum stress developed in the propeller is 33.341 MPa. Since the ultimate tensile strength of ABS Plastic is 43 MPa, that leaves us with safety factor of 1.289, which in aerospace applications is a perfectly acceptable value.

**NOTE:** In aerospace applications, factor of safety standard is quite low as the robustness of structures is quite limited due to aerodynamic shape requirements.

## REFERENCES

- [1] Prathapanayaka R1, Vinod Kumar N2, Krishnamurthy S J3, CSIR-National Aerospace Laboratories, Bangalore, ‘Design, analysis, fabrication and testing of mini propeller for MAVS’
- [2] Ian P. Tracy, ‘Propeller Design and Analysis for a Small, Autonomous UAV’
- [3] Song Xiang, Yuan-qiang Liu, Gang Tong, Wei-ping Zhao, Sheng-xi Tong, ‘An improved propeller design method for the electric aircraft’
- [4] Alexandru Dumitache, Mihai Victor Pricop, Mihai Niculescu, Marius Gabriel Cojocaru, ‘Design and Analysis methods for UAV rotor blades’
- [5] William R Liller, ‘Design of small propellers operating at low Reynolds numbers and associated experimental evaluation’
- [6] Gregory A. Williamson, ‘Experimental wind tunnel study of airfoils with large flap deflections at low Reynolds numbers’
- [7] Michael S. Selig, James J. Guglielmo, Andy P. Broeren, Philippe Giguere, ‘Summary of low speed airfoil data’.
- [8] Michael Brown, Antonio Sanchez-Caja, Phillip Duerr, Ilkka Saisto, ‘Improving propeller efficiency through tip loading’
- [9] E. Eugene Larabee, ‘Practical design of minimum induced loss propellers’
- [10] Gabriel Raducanu, Radu-Mihai Dinca, ‘Airplane propellers aerodynamic design and performances analysis’
- [11] David Lee Wall, ‘Optimum Propeller design for electric UAVs’
- [12] Brain David Rutkay, ‘A process for the design and manufacture of propellers for small UAVs’
- [13] Snorri Gudmundson, ‘General aviation aircraft design: Applied methods and procedures’
- [14] Introduction to aircraft Propulsion, Prof. Bhaskar Roy, IIT Bombay, NPTEL lecture series
- [15] Mark Drela, ‘QPROP formulation’
- [16] Andre Bakker, ‘Applied Computational Fluid dynamics’

- [17] Ozen Engineering Inc., ‘Meshing workshop’
- [18] Szechenyi University, Audi Department of Vehicle Engineering, ‘Computational Fluid Dynamics’
- [19] Andre Bakker, ‘Applied Computational Fluid Dynamics’: <http://www.bakker.org>.
- [20] PADT Lunch & Learn series, ‘ANSYS Meshing Advanced Techniques.’
- [21] Milovan Peric and Stephen Ferguson, ‘The advantage of polyhedral meshes’ CD-adapco.
- [22] ANSYS Fluent Theory guide.
- [23] Turbulence Models and their applications to Complex Flows, ANSYS Inc.
- [24] Turbulence Modeling for engineering flows, ANSYS Inc.
- [25] Hermann and Gersten, ‘Boundary Layer Theory’, 9th Edition, Springer.
- [26] Chimielewski and Giers, ‘Three zonal wall functions for K-Epsilon Turbulence models’, Warsaw University of Technology, Institute of Heat Engineering.
- [27] ANSYS Fluent 2019 R1 Theory Guide.
- [28] ANSYS Fluent 2019 R1 User’s Guide.
- [29] John Brandt, UIUC MS Thesis, Propeller Database, Volume 1.